
**DRUG DISCOVERY AND SEARCH FOR
NEW THERAPEUTIC TARGETS:
STRATEGIES TO COUNTERACT HUMAN
PATHOGENS USING *CAENORHABDITIS
ELEGANS* AND COLD-ADAPTED
MICROORGANISMS**

Pietro Tedesco

Dottorato in Scienze Biotecnologiche – XXVIII ciclo
Indirizzo Biotecnologie Molecolari e Industriali
Università di Napoli Federico II



Dottorato in Scienze Biotecnologiche – XXVIII ciclo
Indirizzo Biotecnologie Molecolari e Industriali
Università di Napoli Federico II



**DRUG DISCOVERY AND SEARCH FOR
NEW THERAPEUTIC TARGETS:
STRATEGIES TO COUNTERACT HUMAN
PATHOGENS USING *CAENORHABDITIS
ELEGANS* AND COLD-ADAPTED
MICROORGANISMS**

Pietro Tedesco

Dottorando: Pietro Tedesco

Relatore: Prof. Giovanni Sannia

Correlatore: Dott. Donatella de Pascale

Coordinatore: Prof. Giovanni Sannia

I leave Sisyphus at the foot of the mountain! One always finds one's burden again. But Sisyphus teaches the higher fidelity that negates the gods and raises rocks. He too concludes that all is well. This universe henceforth without a master seems to him neither sterile nor futile. Each atom of that stone, each mineral flake of that night filled mountain, in itself forms a world. The struggle itself toward the heights is enough to fill a man's heart. One must imagine Sisyphus happy.

Albert Camus.

INDEX

SUMMARY	pag.	1
RIASSUNTO	pag.	3
General Introduction	pag.	9
1. The rise of Multi-drug Resistance Pathogens	pag.	10
2. Strategies to fight MDR pathogens	pag.	12
3. <i>Caenorhabditis elegans</i> : a versatile model host and tool for antimicrobial drug discovery	pag.	15
4. The <i>Burkholderia cepacia</i> complex	pag.	18
5. Aims of the project	pag.	19
6. References	pag.	20
Chapter 1: Investigating the role of the host multidrug resistance associated protein transporter family in <i>Burkholderia cepacia</i> complex pathogenicity using a <i>Caenorhabditis elegans</i> infection model	pag.	25
Abstract	pag.	27
1.1 Introduction	pag.	28
1.2 Materials and methods	pag.	29
1.3. Results and Discussion	pag.	30
1.4 Conclusions	pag.	40
1.5. References	pag.	41
1.6 Supplementary Material	pag.	45
Chapter 2: Antimicrobial activity of monoramnholipids produced by bacterial strains isolated from Ross sea (Antarctica)	pag.	47
Abstract	pag.	49
2.1 Introduction	pag.	50
2.2 Materials and methods	pag.	50
2.3 Results and Discussion	pag.	53
2.4 Conclusions	pag.	62
2.5 References	pag.	62
2.6 Supplementary Material	pag.	66

Chapter 3: Bioprospecting for novel bioactive compounds exploiting cold-adapted bacteria isolated from Tibetan glaciers	pag.	75
Abstract	pag.	77
3.1 Introduction	pag.	78
3.2 Materials and methods	pag.	78
3.3 Results and Discussion	pag.	82
3.4 Conclusions	pag.	89
3.5 References	pag.	90
PUBLICATIONS	pag.	92
COMMUNICATIONS	pag.	93
EXPERIENCES IN FOREIGN LABORATORIES	pag.	94

Summary

The alarming diffusion of multidrug-resistant pathogens represents a serious threat to human health and economy. To counteract this phenomenon two main strategies have been pursued: the research of novel therapeutic targets and the identification of novel drugs exploiting natural products. The first strategy is focused principally on the identification of genes involved in bacterial virulence mechanism, to “disarm” pathogens. Dissecting and validating the pathogenicity determinants of human pathogens have been facilitated by the use of non-vertebrate host models such as *Caenorhabditis elegans*. The second strategy aims at the utilization of the huge potential of secondary metabolites produced by microorganisms focusing on bacteria living in extreme environments such as the oceans, the poles and the deserts.

In this research project we applied these two approaches with special emphasis on pathogens belonging to the *Burkholderia cepacia* complex Bcc and parasite nematodes. To this aim we exploited the versatility of *C. elegans* as versatile model system and the potential of psychrophilic microorganisms as source of novel bioactive compounds. The first part of the project was focused on establishing an infection model between a selected panel of strains belonging to Bcc and the nematode *C. elegans*. With this aim, two different toxicity tests were performed to monitor host mortality by accumulation in the intestine or by toxins production. A Virulence Ranking scheme was defined based on the percentage of surviving worms. Our results suggested that only the cystic fibrosis isolated strains possessed profound nematode killing ability to accumulate in worms' intestines. We also investigated the role of host transporter during the infection. For this analysis a complete set of isogenic nematode single Multidrug Resistance associated Protein efflux mutants and a number of efflux inhibitors were interrogated in the host toxicity assays. We demonstrated that disabling host transporters genetically (*C. elegans* knock out mutants) or chemically (efflux inhibitors) enhanced nematodes mortality, suggesting a role in toxin-substrate recognition for some of the tested transporters. The work performed has provided useful information on Bcc pathogenicity and it achieved the development of a suitable platform for dissecting Bcc virulence factors and for drug discovery and validation of anti-Bcc molecules. The second part of the project was focused on the identification of new bioactive compounds targeting Bcc strains and parasite nematodes. To achieve this goal a biodiversity pipeline was developed starting with isolation of cold-adapted bacteria from sediments collected from Antarctica and Tibet. The isolates were first evaluated for their antimicrobial and anthelmintic activity with cell-based assays. Antimicrobial capability was evaluated using the cross-streaking experiments targeting human pathogens, while for the anthelmintic activity, we assayed isolates ability to survive and kill the nematodes *C. elegans* that was used as model helminth. Positive isolates to primary screening were grown in liquid cultures to produce crude extracts in order to perform secondary assays. Positive extracts were then fractionated using Solid Phase Extraction, and HPLC, and pure bioactive compounds were identified with LC-MS and NMR. With this strategy, we achieved the isolation of 3 Rhamnolipids, two of which were new, embedded with high (MIC < 1 µg/mL) antimicrobial activity against Bcc strains. We found also one positive extract able to kill the nematodes and a second one that completely inhibits the growth of *Francisella tularensis* an opportunistic human pathogen, at the concentration of 25 µg/mL. LC-MS analysis of this fraction revealed the presence of 16 β -hydroxycrambescidin, a known alkaloid with unreported antimicrobial activity.

Riassunto

Negli ultimi decenni la problematica dei patogeni Multi-Drug Resistant (MDR) ha raggiunto un livello di rischio drammatico. Attualmente, diversi antibiotici usati di routine, sono diventati totalmente inefficaci per combattere questo tipo di infezioni, aumentando i costi per la sanità pubblica e soprattutto il numero di decessi. Esiste un elevatissimo numero di batteri MDR, soprattutto in ambienti ospedalieri (le cosiddette infezioni nosocomiali) che rendono difficili da eradicare anche le più comuni infezioni. Il problema ha proporzioni mondiali e non è limitato ai soli batteri, ma anche a funghi, virus e parassiti. Tra questi ultimi, sono prominenti i nematodi parassiti, che causano gravissimi danni a popolazioni umani e bestiame, soprattutto in paesi del terzo mondo, e per questo motivo la ricerca antielmintica è tristemente molto limitata. Attualmente gli studiosi stanno percorrendo due differenti strategie per risolvere questo problema: la prima è la ricerca di nuove target terapeutici; la seconda riguarda l'identificazione di nuovi farmaci sfruttando il potenziale delle "sostanze naturali".

La ricerca di nuovi target terapeutici è mirata alla ricerca di bersagli molecolari, che non vadano ad inibire funzioni vitali dei patogeni come i normali antibiotici (replicazione DNA, sintesi della parete cellulare), in quanto questa strategia aumenta la pressione selettiva e stimola l'evoluzione dei patogeni MDR. Da questo punto di vista, i geni coinvolti nei meccanismi di patogenesi rappresentano una valida alternativa. Inibire i meccanismi di virulenza renderebbe i patogeni incapaci di creare danni all'organismo e di essere poi eliminati dal sistema immunitario del paziente. Un altro vantaggio di questo approccio è la possibilità di identificare e validare direttamente geni che agiscono *in vivo*. Per questi motivi la ricerca di nuovi fattori di virulenza dipende strettamente dall'impiego di sistemi modello di infezione *in vivo*, utilizzando organismi semplici e non vertebrati, come ad esempio il nematode *Caenorhabditis elegans*.

La ricerca di nuove "sostanze naturali" prevede invece lo sfruttamento dell'immenso potenziale biosintetico dei microorganismi presenti in Natura. I prodotti da sostanze naturali sono ancora oggi la principale fonte di nuovi farmaci, rappresentando i due terzi degli antibatterici messi in commercio o in clinical trial, degli ultimi 20 anni. Oggi, l'interesse scientifico è concentrato sui batteri definiti "estremofili", che abitano gli ambienti con le più estreme condizioni ambientali (gli oceani, i poli e le aree fredde, i deserti). Per sopravvivere in questi ambienti i microorganismi hanno sviluppato diverse strategie, tra cui la produzione di metaboliti secondari con attività antimicrobica, pertanto questi batteri hanno un altissimo valore biotecnologico.

L'obiettivo di questo progetto di ricerca è stata l'applicazione di approcci biotecnologici per contrastare il fenomeno dei patogeni MDR, con particolare enfasi per batteri appartenenti al *Burkholderia cepacia* complex (Bcc), un gruppo di patogeni verso il quale l'interesse è cresciuto notevolmente negli ultimi anni, e verso i nematodi parassiti. In questo progetto un ruolo fondamentale è stato acquisito dal nematode *C. elegans*, sistema modello estremamente versatile grazie alle sue caratteristiche peculiari (sistema molto semplice, ciclo vitale veloce, possibilità di screening su larga scala) e da batteri "cold-adapted" che sono stati utilizzati come fonte di nuovi composti bioattivi. Il progetto è stato quindi diviso in due principali sezioni: una riguardante l'utilizzo di *C. elegans* come sistema di infezione modello utilizzando batteri appartenenti al Bcc al fine di creare una piattaforma per screening e target validation; la seconda concentrata sul "drug discovery" utilizzando batteri

isolati da ambienti estremi come l'Antartide e ghiacciai tibetani, utilizzando in questo caso *C. elegans* come bersaglio e sistema di valutazione.

Parte 1: Utilizzo di *C. elegans* come sistema di infezione modello per batteri appartenenti al Bcc e studio del ruolo degli "host transporter" nell'infezione

Per mettere a punto il modello di infezione, sono stati selezionati 18 ceppi appartenenti al Bcc, che rappresentano i ceppi di riferimento di ognuna delle 18 specie che compongono il complex. Questi ceppi provengono da pazienti affetti da fibrosi cistica (CF) oppure da fonti ambientali (suolo, radici). Per testare la loro patogenicità verso il nematode *C. elegans*, sono stati utilizzati due differenti test di tossicità definiti "Slow killing Assay" (SKA) e "Fast killing Assay" (FKA). I test si basano sul differente mezzo di coltura utilizzato per la crescita dei patogeni. Lo SKA viene effettuato utilizzando, come terreno, il Nematode Growth Medium (NGM), e permette di osservare la morte dei nematodi a causa di una colonizzazione intestinale da parte delle *Burkholderie*. Il FKA viene invece eseguito su un terreno ad alta osmolarità definito PGS (Peptone, Glucosio, Sorbitolo), che causa un elevato assorbimento di molecole dal mezzo di coltura e permette di osservare la morte dei vermi a causa della produzione di tossine prodotte dai patogeni. Per confermare che la virulenza delle Bcc verso i nematodi dipendesse effettivamente dalla colonizzazione intestinale o dalla produzione di tossine, sono stati eseguiti degli appositi esperimenti, utilizzando osservazioni al microscopio e test su piastra. Una volta messo a punto il modello di patogenicità questo è stato utilizzato per effettuare uno studio sul ruolo degli "host transporter", cioè delle pompe di flusso dell'ospite, durante il processo infettivo. A questo scopo, sono stati selezionati 7 ceppi di *C. elegans*, ognuno dei quali singolo mutante per una specifica pompa di membrana appartenente alla famiglia delle Multi-Drug Resistance Protein (MRPs), della superfamiglia dei trasportatori ATP-Binding-Cassette (ABC). Per confermare poi il coinvolgimento delle MRP durante l'infezione da Bcc, sono stati effettuati esperimenti di tossicità tra le Bcc e i nematodi wild type aggiungendo al mezzo di coltura inibitori dei trasportatori di membrana, per osservare l'effetto di una inibizione chimica degli inibitori sulla sopravvivenza dei nematodi.

Risultati conseguiti

La patogenicità dei ceppi di Bcc è stata valutata attraverso i due test di patogenicità (SKA e FKA). Per entrambi i test, i nematodi sono stati sincronizzati allo stadio larvale L4 e poi posti su piastre contenenti NGM o PGS su cui erano stati cresciuti per 24 ore a 37°C vari ceppi di Bcc. Le piastre sono state poi incubate a 20°C e la conta dei nematodi vivi è stata effettuata ogni 24 ore. Per definire la virulenza dei ceppi, è stata stabilita una scala di patogenicità basata sulla percentuale dei nematodi sopravvissuti dopo 3 e 2 giorni di incubazione, per SKA e FKA rispettivamente. In base ai risultati ottenuti i nematodi sono stati divisi in quattro differenti gruppi. Un ceppo di Bcc è stato considerato non virulento ("Virulence Ranking" VR=0), quando la percentuale dei vermi sopravvissuti variava da 100 a 80%; VR=1 corrispondeva ad una percentuale di vermi morti tra il 79 e il 50%; VR= 2

tra 49 e 6%; infine il VR è stato considerato 3 quando la percentuale di vermi sopravvissuti era inferiore al 5%.

Lo SKA ha mostrato una elevata variabilità nella patogenicità. Solamente due ceppi (*B. metallica* e *B. stabilis*) sono stati in grado di eliminare completamente tutti i nematodi dopo 3 giorni di incubazione. Circa la metà delle Bcc ha invece mostrato una patogenicità intermedia, mentre ben 7 ceppi su 18, si sono rivelati totalmente innocui verso *C. elegans*. Riguardo il FKA, 5 ceppi di Bcc hanno ottenuto un VR=3 risultando effettivi nell'uccidere il 100% dei nematodi in 2 giorni, mentre solamente 2 ceppi non hanno mostrato alcuna virulenza. Il confronto tra i due test ci rivela che i ceppi isolati da pazienti affetti da FC sono mediamente più infettivi su SKA rispetto ai ceppi di origine ambientale. In particolare tre ceppi di Bcc (*B. ambifaria*, *B. cepacia* and *B. pyrrocinia*) hanno ottenuto VR=3 su FKA e VR=0 su SKA. Questa evidenza suggerisce che la produzione di tossine (osservata su FKA) sia un meccanismo di patogenicità piuttosto diffuso tra le varie *Burkholderie*, mentre solo i ceppi FC hanno sviluppato diversi tratti che gli consentono di infettare e colonizzare l'ospite.

Per valutare la colonizzazione intestinale i due ceppi con VR=3 per lo SKA (*B. metallica* e *B. stabilis*) sono stati utilizzati per infettare *C. elegans*, dopodiché i nematodi sono stati ispezionati al microscopio. Ceppi di Bcc non infettivi (*B. pseudomultivorans*, VR=0) ed *E. coli* OP50 sono stati utilizzati come controlli. Dopo solo 24 ore, gli intestini dei nematodi infettati da ceppi virulenti apparivano totalmente deformati e colonizzati dai patogeni rispetto a quelli dei nematodi cresciuti sui controlli. Osservazioni a vari intervalli di tempo hanno dimostrato che l'accumulo aumenta col passare del tempo fino a provocare la morte dei nematodi.

Per confermare la produzione di tossine è stato invece effettuato il "Toxin diffusion assay". In questi esperimenti, i ceppi di Bcc col massimo punteggio per il FKA (*B. contaminans*, *B. cepacia*, *B. ambifaria*, *B. metallica* and *B. stabilis*) sono stati cresciuti su filtri di carta con un cut-off di 0,22 µm su piastre PGS. Dopo 24 ore di incubazione i filtri sono stati rimossi e i nematodi sono stati posti sul solo agar condizionato. I risultati hanno mostrato che già dopo solo 4 ore di incubazione, più del 50% dei nematodi esposti all' agar condizionato apparivano paralizzati e incapaci di muoversi sulla piastra. Dopo 24 ore, per la maggioranza dei ceppi testati, circa il 70% dei nematodi era morto. Al contrario, vermi posti su piastre condizionate da *E. coli*, non presentavano alcuna paralisi.

È stato poi valutato il ruolo dei trasportatori MRP nell'infezione da Bcc, utilizzando ceppi di *C. elegans* knock-out per sette specifici MRP. I sette mutanti sono stati quindi ritestati contro tutte i 18 ceppi di Bcc, utilizzando nuovamente il FKA e lo SKA, al fine di osservare differenze di patogenicità tra questi mutanti e il ceppo wild-type di *C. elegans*. Sono state riscontrate alcune differenze suggerendo un effetto specifico per ogni *Burkholderia*. Sono stati identificati però alcuni dati significativi: i mutanti *mrp-5* e *mrp-2* hanno mostrato un elevato aumento della mortalità da parte di almeno 8 ceppi di Bcc su 18, indicando un'importante ruolo dei rispettivi trasportatori MRP nell'infezione. Al contrario, i mutanti *mrp3* e *mrp-4* non hanno mostrato alcun aumento della mortalità suggerendo una diversa specificità di substrato tra i vari trasportatori. Sono stati poi effettuati esperimenti di tossicità con inibitori delle MRP, al fine di dimostrare un aumento della mortalità dei nematodi inibendo le pompe MRP sia geneticamente (mutanti knock-out) che con composti chimici. I 5 ceppi di Bcc che hanno mostrato aumento della mortalità contro i mutanti (*B. ambifaria*, *B. arboris*, *B. cepacia*, *B. dolosa*, *B. pyrrocinia*) sono stati testati nuovamente contro il ceppo wild-type di *C. elegans* in presenza di 3 inibitori (Lasalocid, Mometasone e Verapamil). I risultati hanno indicato un aumento della mortalità dei nematodi in presenza degli

inibitori, validando l'importanza di questi MDR nel processo infettivo. È quindi probabile che queste proteine abbiano un ruolo attivo pompando all'esterno delle cellule tossine o altre molecole tossiche prodotte dai ceppi di Bcc. È importante notare che i trasportatori MDR utilizzati hanno omologhi nell'uomo e soprattutto condividono meccanismi di attivazione con il Cystic Fibrosis Transmembrane conductance Regulator (CFTR), pompa di membrana la cui mutazione è la causa della FC. Quindi, l'identificazione di molecole effettori di virulenza, che siano substrati delle pompe MRP potrebbe essere un promettente punto di partenza per lo sviluppo di nuove terapie. In questa prima parte sono stati quindi ottenuti promettenti risultati e informazioni sulla patogenicità del Bcc ed inoltre è stata messa a punto una piattaforma per identificare fattori di virulenza e validare nuovi farmaci contro questi patogeni.

Parte 2: Identificazione di nuove molecole bioattive contro batteri patogeni e nematodi parassiti, da batteri cold-adapted.

La seconda parte di questo progetto è stata focalizzata sulla ricerca di nuove molecole bioattive contro batteri patogeni e nematodi parassiti. Per raggiungere gli obiettivi preposti è stata sviluppata una "biodiscovery pipeline" in sei diverse fasi a partire dalla raccolta di campioni ambientali fino alla purificazione e validazione dei nuovi composti. La prima fase ha riguardato la raccolta di campioni da ambienti estremi e freddi del pianeta quali l'Antartide e ghiacciai tibetani. Questi sedimenti sono stati utilizzati per la seconda fase, ovvero l'isolamento di batteri cold-adapted. Per isolare questi batteri estremofili sono stati utilizzati due appositi mezzi di coltura: il Marine Broth, per i sedimenti Antartici prelevati a -46m di profondità nel Mare di Ross; e il terreno PYG (Peptone, estratto di lievito, Glucosio) per i sedimenti tibetani, isolati dai ghiacciai Karuola e Midui a 5200 e 4800 metri di altitudine. I sedimenti sono stati aggiunti a una soluzione salina, mescolati per creare una miscela omogenea, successivamente diluita e piastrata sui differenti terreni. Per selezionare batteri "cold-adapted", le piastre sono state incubate a 4°C per circa due settimane, dopodiché le colonie presenti sono state selezionate e conservate. Gli isolati batterici così ottenuti sono stati utilizzati per la terza fase, ovvero gli screening primari per identificare batteri in grado di avere un effetto antagonista nei confronti di batteri patogeni o di *C. elegans*, che è stato utilizzato come sistema modello per i nematodi parassiti. A questo scopo sono stati utilizzati vari saggi: il "cross-streaking assay" per determinare potenziale attività antimicrobica utilizzando ceppi appartenenti al Bcc; il "nematode grazing assay" e il FKA e il SKA sono stati invece effettuati per identificare potenziale attività antielmintica. Una volta identificati potenziali isolati produttori di molecole bioattive, questi batteri sono stati cresciuti in liquido variando il mezzo di coltura e altre condizioni di crescita per stimolare la produzione di metaboliti secondari. I mezzi di coltura esausti sono stati poi estratti con solventi organici o specifiche resine al fine di creare una libreria di estratti da testare attraverso appositi saggi contro i target stabiliti (quarta fase). Per valutare l'attività antimicrobica si è utilizzato il test della concentrazione minima inibente (MIC), mentre per l'attività antielmintica è stato messo a punto un saggio di tossicità crescendo i nematodi in liquido. Gli estratti positivi per l'attività antimicrobica o elmintica sono stati poi prodotti in larga scala per effettuare una purificazione guidata da attività biologica (quinta fase). Gli estratti sono stati quindi frazionati inizialmente utilizzando la procedura della estrazione in fase solida (SPE) e le frazioni sono state poi

saggiate per la loro attività. Le frazioni attive così identificate sono state poi ulteriormente purificate tramite HPLC, al fine di ottenere composti puri e identificare le molecole biologicamente attive. L'ultimo step ha riguardato la determinazione della struttura dei composti tramite l'utilizzo di NMR e spettrometria di massa. Infine, i composti attivi contro le *Burkholderie* sono stati testati *in vivo*, utilizzando il modello di infezione, Bcc-*C. elegans* sviluppato nella prima parte di questo progetto.

Risultati conseguiti

Le procedure di isolamento utilizzate hanno permesso l'isolamento di 24 ceppi batterici cold-adapted dai sedimenti antartici (definiti BTN) e 11 ceppi da quelli tibetani (ceppi MD e KRL). I batteri sono stati inizialmente caratterizzati da un punto di vista filogenetico per determinare il genere, dopodiché sono stati utilizzati per identificare composti ad attività antimicrobica ed antielmintica.

Antimicrobici.

Per la determinazione dell'attività antimicrobica è stato utilizzato il "cross-streaking assay". Questo saggio permette di osservare attività antagonista su piastra tra un batterio "tester" (gli isolati cold-adapted) e dei batteri "target" (ceppi del Bcc isolati da pazienti CF). I ceppi tester sono stati fatti crescere sulla metà di una capsula Petri e sono stati incubati per diversi giorni per permettere la crescita dei batteri e la produzione di metaboliti secondari. I batteri target sono stati poi strisciati perpendicolarmente allo striscio dei target e il sistema è stato incubato nuovamente. La mancata crescita dei patogeni implica la produzione di molecole antimicrobiche da parte dei batteri "cold-adapted". Con questa tecnica sono stati individuati diversi ceppi potenzialmente produttori di antimicrobici. La maggior parte dei ceppi antartici si è mostrata in grado di inibire la crescita delle *Burkholderie*, mentre solo 5 ceppi tibetani hanno dato risultati positivi al test.

Tutti i batteri selezionati sono stati poi utilizzati per produrre estratti al fine di effettuare i saggi MIC in liquido contro ceppi Bcc e altri patogeni. Per questi saggi, i batteri sono stati incubati in piastre multiwell da 96 pozzetti in presenza dei vari estratti a diverse concentrazioni e la loro crescita è stata valutata misurando l'assorbanza a 600 nm dopo 24 ore di incubazione a 37°C. Gli estratti prodotti dai batteri tibetani non hanno mostrato significativa attività antimicrobica, con l'unica eccezione dell'estratto del ceppo MD3 che ha inibito la crescita del batterio patogeno *Francisella tularensis*, alla concentrazione di 0,1 mg/mL. Gli estratti ottenuti dai ceppi antartici invece hanno mostrato una discreta inibizione contro i batteri patogeni, ma solo l'estratto del ceppo BTN1 è riuscito a inibire quasi totalmente tutti i ceppi Bcc testati alla concentrazione di 1 mg/mL.

I ceppi MD3 e BTN1 sono stati quindi selezionati per la purificazione dei composti bioattivi. Il frazionamento del ceppo MD3 tramite SPE utilizzando un gel di silice (normal phase) ha permesso di individuare diverse frazioni biologicamente attive. L'analisi di queste frazioni utilizzando la spettrometria di massa ha permesso di identificare un composto maggioritario presente in tutte le frazioni attive. Questo composto è stato individuato come 16 β -hydroxycrambescidin 359, molecola già isolata ma la cui attività antimicrobica contro *F. tularensis* non era mai stata descritta in precedenza. Ulteriori studi (la purificazione e identificazione tramite NMR dei singoli composti presenti nelle frazioni) permetteranno di confermare questi dati. La purificazione dell'estratto del ceppo BNT1 ha portato all'identificazione di 3 mono-

ramnolipidi (di cui 2 descritti per la prima volta) con una promettente attività battericida contro ceppi del Bcc, con valore di MIC minori di 10 µg/mL contro *B. cenocepacia*. Questi composti sono stati testati *in vivo*, sfruttando il modello di infezione Bcc-*C. elegans*. I nematodi sono stati posti a contatto con i ceppi Bcc per 24 ore, dopodiché i vermi così infettati sono stati posti nei pozzetti di piastre multiwell contenenti terreno di coltura e i composti isolati dal ceppo BTN1. I vermi sono stati incubati per 48 ore a 20°C per osservare la capacità dei ramnolipidi di curare i nematodi infettati ed aumentare la percentuale di sopravvivenza rispetto a nematodi infettati a cui non erano stati aggiunti i ramnolipidi. I risultati hanno mostrato che i ramnolipidi non sono tossici per *C. elegans* ma non sono stati in grado di curare l'infezione dai ceppi di Bcc *in vivo*. L'utilizzo dell'antibiotico Trimetoprim, ha invece aumentato la percentuale di nematodi sopravvissuti confermando ad ogni modo la validità del sistema messo a punto per testare i molecole anti-Bcc.

Antielmintici

Per identificare attività antielmintica, gli isolati "cold-adapted" sono stati sottoposti inizialmente al "nematode grazing assay". I vari isolati sono stati cresciuti su piastre NGM come singole colonie e sono stati incubati in presenza di *C. elegans*. Le colonie di cui i nematodi non si sono nutriti (colonie "not-grazed") sono state individuate come potenziali produttori di composti antielmintici. I due ceppi così individuati (isolati tibetani MD4 e KRL4) sono stati poi sottoposti ai tox test sviluppati nella prima parte di questo progetto di ricerca (FKA e SKA). Da questi test è risultato che la morte dei nematodi in presenza dei due ceppi avveniva sul FKA ma non con lo SKA, quindi dipendeva dalla produzione di composti antielmintici.

Gli estratti dei due batteri sono stati testati in liquido incubando larve L4 di *C. elegans* ai vari pozzetti di piastre multiwell contenenti terreno di coltura e i vari estratti a diverse concentrazioni per 3 giorni a 20°C. La conta dei nematodi sopravvissuti è stata quindi effettuata ogni giorno. L'estratto intracellulare prodotto dal batterio KRL4 ha mostrato promettente attività nematocida uccidendo circa l'80% dei nematodi dopo 3 giorni alla concentrazione di 5 mg/mL. L'estratto è stato quindi sottoposto a frazionamento una procedura SPE con una resina C18 (reverse phase) utilizzando un sistema acqua/metanolo come fase mobile. La frazione di KRL4 eluita al 25% di concentrazione di metanolo si è rivelata in grado di eliminare completamente i nematodi alla concentrazione di 1 mg/mL. L'analisi chimica effettuata su questa frazione suggerisce che l'attività possa dipendere da peptidi, ma ulteriori studi saranno necessari per purificare il composto bioattivo e confermare la sua natura chimica.

In conclusione, in questa seconda parte di progetto è stata utilizzata con successo una valida procedura di Bioprospecting per l'identificazione di composti bioattivi. Grazie a questa procedura sono stati individuati diversi composti e estratti attivi contro patogeni e *C. elegans*, sottolineando quindi l'importanza dei batteri cold-adapted come promettente fonte di nuovi molecole attive.

General Introduction

1. The rise of Multi-drug resistance pathogens

In the last decades, humanity has experienced the hazardous phenomenon of multidrug-resistant (MDR) pathogens. Commonly used antibiotics gradually became ineffective to cure infections in community and hospital setting, increasing mortality and morbidity, causing longer hospitalization period and rising social health costs [1, 2]. There are high percentages of antibiotic resistance in bacteria that cause common infections (e.g. urinary tract infections, pneumonia, bloodstream infections) in all regions of the world. MDR in bacteria is defined as non-susceptibility to one or more antimicrobials on three or more antimicrobial classes, while strains that are non-susceptible to all antimicrobials, are classified as extreme drug-resistant strains [3]. A high number of hospital-acquired infections are caused by highly resistant bacteria such as methicillin-resistant *Staphylococcus aureus* (MRSA) and other gram-negative strains like ESKAPE pathogens group (*Enterococcus faecium*, *Staphylococcus aureus*, *Klebsiella pneumoniae*, *Acinetobacter baumannii*, *Pseudomonas aeruginosa*, and enterobacteriaceae), so called to emphasize their capability to “escape” from common antibacterial treatments [4]. It is estimated that, in the only USA every years, MRSA infections cause more than 10,000 deaths, with an annual cost of 3-4 USD Billion (14,000 \$ per patient). MDR issue is worldwide and is considered a major healthcare problem in the 21st century [5]. Keeping in view the seriousness of this problem, the World Health Organization (WHO) has recently held the **World Antibiotic Awareness Week** (16-22 November 2015) as a way to attract the public opinion interest.

The explanation of this dramatic situation relies on the combination of different factors. One reason relies on the incredible evolutionary capability of pathogens to adopt new strategies to survive and to spread these strategies through genetic material exchange. Even though the evolution of resistant strains is a natural phenomenon, the use and misuse of antimicrobial drugs has significantly accelerated the emergence of MDR strains. Poor infection control practices, inadequate sanitary conditions and inappropriate food handling encouraged the further spread of antimicrobial resistance.

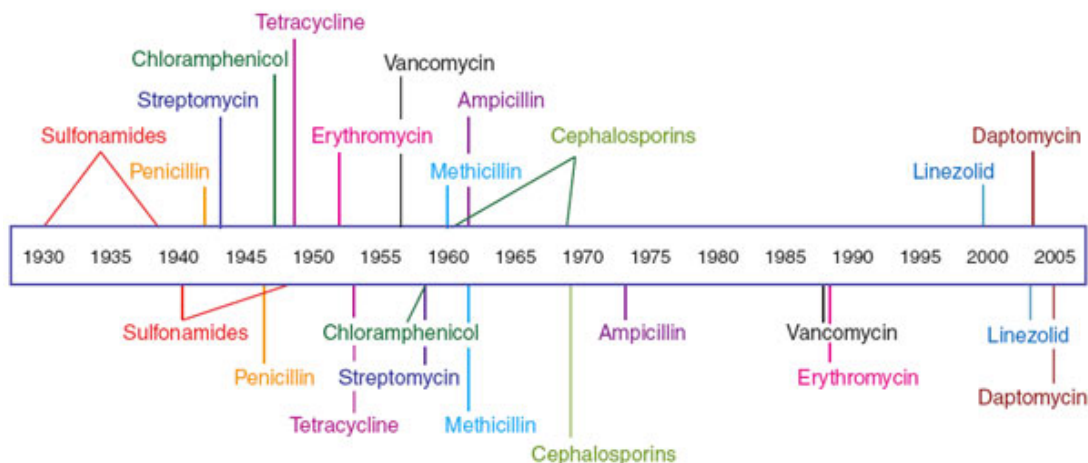
To quote Dr. Charles Penn, chairman of WHO's Guidelines Review Committee:
“Antibiotics are very often prescribed for no useful purpose. Too many antibiotics are prescribed for viral infections such as colds, flu and diarrhea. Unfortunately, these public misconceptions are often perpetuated by media and. For example, through the use of generic terms such as 'germs' and 'bugs.’”[6]

Anyway, one primary reason for MDR's rise is the astonishing decline in antibiotic discovery. Antibiotic innovation has experienced between the 40s and the 50s of the last century its golden age. These 20 years were extremely productive and led to the discovery and marketing of almost all the antibiotic classes used nowadays. Surprisingly no new classes of antimicrobials were developed in the thirty-seven years between the introduction of nalidixic acid (1962) and linezolid (2000) and all antimicrobials that entered the market during this time period were modifications of the existing molecules. “Innovation gap” is the expression that has been used to describe the lack of novel structural classes introduced to the antibacterial armamentarium since 1962 (**Figure 1**) [7].

After 1962, we assisted to a disengagement of the big pharma industries from pursuing antibiotics research for motivation mainly non-scientific and not health-related, but purely economical. The development of new antimicrobial agent had become a more complex, costly and lengthy process. On an average, research and

development of anti-infective drugs takes around 15-20 years and can cost more than \$1 billion dollars [8]. The politics of the regulatory authorities, like the US Food and Drug Administration (FDA) have also contributed to the problem by failing to approve drugs endowed with non-inferior properties.

Antibiotic deployment



Antibiotic resistance observed

Figure 1. Antibiotic development in the XX century[9]. The upper panel report the introduction of the antibiotics in the market while in the lower panel is reported the year when antibiotic resistance was first observed.

Numerous agencies and professional societies have tried to draw attention to the lack of new antibiotics, especially for MDR Gram-negative pathogens. Since 2004 repeated calls for reinvigorating pharmaceutical investments in antibiotic research and development have been made by the Infectious Diseases Society of America (IDSA) and several other distinguished societies [10].

Resistance to common drugs is not limited to bacteria but also to fungi, viruses and especially parasites. Among parasites a prominent role is played by nematodes. The nematodes, or roundworms, comprise a large number of human and domestic animals pathogens. Gastrointestinal nematodes, such as the blood-sucking *Haemonchus contortus*, are major parasites of ruminants that cause substantial economic losses to livestock production worldwide. Anthelmintic chemotherapy is limited to three major chemical classes: **the benzimidazoles, imidazothiazoles and macrocyclic lactones**. Inevitably, drug resistance has emerged in human and livestock pathogenic helminths against each class [11, 12]. No new anthelmintic class has reached the market during the past 25 years with the exception of the cyclodepsipeptides represented by emodepside, which is indicated for livestock use only. Despite the huge threat of parasitic worms, anthelmintic drug discovery is the poor relation of the pharmaceutical industry [13]. The simple truth is that these diseases are common in underprivileged tropical countries, which have no resources or infrastructures to invest in research. Most of the diseases linked to parasite are called “neglected diseases”, and pharmaceutical industry is not very interested in. This situation has been exacerbated by the incredible success of ivermectine as drug over the last 20 years [14]. Nonetheless, the rising of the anthelmintic resistance in

human and animals has underlined the huge necessity of regenerating antiparasites drug discovery [15].

The MDR situation has posed a serious challenge to our society. If proper and resolute measures will not be applied, humanity may fall in a pre-antibiotic era. In the last decade, scientists have been following two strategies to counteract MDR: **i) the research of novel therapeutic targets** and **ii) the identification of novel drugs exploiting natural products**.

2. Strategies to fight MDR pathogens

Research of novel therapeutic targets

Antibiotics have generally been discovered for their ability of inhibiting bacterial growth (bacteriostatic) or killing them (bactericidal). In any case, they inhibit vital function of bacteria, such as DNA replication, cell wall synthesis and protein synthesis. Although antibiotics targeting cellular viability are very effective, they impose a high and specific selective pressure promoting MDR strains evolution. Thus, there is the need to develop drugs with novel mechanisms of action, exploiting novel targets [9]. A possible solution may be targeting genes involved in pathogenesis. For decades, researchers have studied pathogenesis mechanisms and they have discovered and elucidated many involved genes. Targeting bacterial virulence or disrupting the interaction between the host and the pathogen are attractive options that are increasingly being explored. Thus, efforts to develop anti-virulence therapies are geared at “disarming” the pathogen by inhibiting virulence factors that can cause direct harm to the host. The bacteria are eventually cleared by the host immune response. The interest on this field has grown in the last years and some promising targets have already been identified. One is related to the inhibition of toxic function. Many pathogens produce toxins, which are proteins that perturb host cell functions and may ultimately result in host cell death. Much effort has been concentrated on inhibiting the effects of the three proteins that comprise anthrax toxin: lethal factor (LF), edema actor (EF) and protective antigen (PA). Merck has identified a compound, called hydroxymate that inhibits LF protease activity and promotes cellular survival in a macrophage cytotoxicity assay [16]. Interfering with toxin delivery mechanisms appeared as well to be a potential way to inhibit virulence. This principle has already been applied for treatment of the disease caused by *Clostridium difficile* using Cholestyramine, which binds the clostridial toxins, preventing their delivery and blunting their toxic effects [17]. A more recent application of this principle is prevention of toxins delivery by inhibiting bacterial secretion systems. There has been interest in targeting the type III secretion system (T3SS) common to *Yersinia spp.*, *Pseudomonas aeruginosa*, *pathogenic Escherichia coli*, *Shigella spp.*, *Salmonella spp.* and *Chlamydia spp.* The T3SS is a syringe-like apparatus that facilitates the injection of bacterial effectors from these species directly into the host cytosol [18]. Chemical screening for inhibitors of the T3SS in *Yersinia pseudotuberculosis* identified acylated hydrazones of different salicylaldehydes [19, 20]. Disrupting the mechanisms regulating virulence expression is also a very attractive target. Decades of studies on virulence regulation have identified many different regulatory steps that could be targeted. Most efforts have focused on interfering with quorum sensing (QS) a mode of bacterial communication used by multiple bacterial species to regulate secondary metabolites processes such as bioluminescence, antibiotic synthesis, biofilm formation and virulence factor

expression, as a function of population density [21]. In many Gram-negative bacteria, QS is mediated by acylhomoserine lactone molecules (AHLs) synthesized and recognized by quorum sensing circuits composed of LuxI and LuxR [21]. Thus, one could prevent AHL-mediated quorum sensing by inhibiting the enzymes that synthesize QS molecules. Alternatively, one could inhibit quorum sensing by interfering with the concentration of the AHL signalling molecules through degradation. For example, Gram-positive *Bacillus* species produce acylhomoserine lactonase, an enzyme that hydrolyses the lactone ring of AHLs, thereby rendering them unable to mediate signalling [22, 23]. Tobacco plants engineered to express AHL-lactonase show an enhanced resistance to *Erwinia carotovora* proving the effectiveness of this system.

It is still soon to know if these targets can be used as therapeutic target to develop drugs. So far, the exact therapeutic role of antimicrobials that target virulence is yet unclear. Anyway, this system can offer different advantages. A potential (though yet unproven) benefit of this approach is that new antimicrobials aimed at inhibiting virulence rather than growth may impose weaker selective pressure for the development of antibiotic resistance relative to current antibiotics. Another principal benefit is the possibility of targeting genes acting *in vivo*, rather than *in vitro*. It is known that *in vitro* and *in vivo* bacterial gene functions are distinct [9]. The environment within a host is unlikely to be the same as the artificial ones induced in a laboratory, and therefore the genes required for viability will likely differ [24]. Instead, targeting virulence genes requires the use of whole-organism infection models, using *in vivo* conditions. Dissecting and validating the pathogenicity determinants of human pathogens have been facilitated by the use of non-vertebrate host models *Drosophila melanogaster*, *Galleria melonella*, and especially *Caenorhabditis elegans*.

Identification of novel drugs exploiting natural products

Drug discovery is defined as the process in which new candidate medications are discovered. Natural products remain the best sources of drugs and drug leads, and this remains true today despite the fact that during the past 2 decades pharmaceutical companies have deemphasized natural products research in favour of High Throughput Screening (HTS) of combinatorial libraries. Nevertheless, Natural products represent the largest source of new antibiotic molecules, representing about two-thirds of new antibacterial therapies approved between 1980 and 2010 [25, 26].

Natural products represent the richest source of novel molecular scaffolds and chemistry. No one can predict, in advance, the details of how a small molecule will interact with the myriad of targets that we now know drive fundamental biological processes. Microbial natural products have several advantages favouring their consideration in drug discovery and development as they can be produced by large-scale fermentation and the producer microorganisms can be engineered to overproduce the desired natural products hence to solving the supply bottleneck. Also, metabolic pathways engineering can easily produce natural product analogues. The vast, untapped, ecological biodiversity of microbes holds great promise for the discovery of novel natural products, thereby improving the odds of finding novel drug leads. It is estimated that only 1% of the microbial community has been cultivated in laboratories, implying that the majority of microbial natural products still remains hidden [27].

Today, the discovery of novel natural products is a hot spot in biotechnology and it has become a multidisciplinary field that bring together biologists, microbiologists, geologists and chemists. The development of new cultivating techniques, the

expression of gene clusters in model heterologous hosts, and a serious effort and innovative approaches in novel microbial strain collection, identification, and classification, will be pivotal for the uncovering and exploitation of this Nature's treasure.

Bioprospecting of extreme environments

The methodical search in nature for novel bioactive compounds is defined bioprospecting. The term "bioprospecting" was coined by Thomas Eisner, a chemical ecologist who wrote an article in 1989 entitled "Prospecting for nature's chemical riches" [28]. Later on, the Convention on Biological Diversity (CBD) Secretariat defines bioprospecting as "the exploration of biodiversity for commercially valuable genetic and biochemical resources" [29].

A prospecting program includes collection of the material, screening to protect intellectual property interests and the eventual development of a commercial process or new products, which may include modification of the chemical structure to increase efficacy. Bioprospecting may also include downstream testing and the development of other substances derived from the initial discovery.

Bioprospecting has been applied with great success to extreme environments. There are some areas of the planet, once thought of as insurmountable physical and chemical barriers to life, which are now known to be niche habitats populated by 'extremophiles', organisms that require extreme environmental conditions for survival. Extreme environments have "environmental parameters showing values permanently close to lower or upper limits known for life in its various forms". Such environments range from terrestrial and marine hot springs (temperatures >100°C), polar environments (high latitudes; low temperatures), the deep-sea (depths >1000m; high pressures) to the deep biosphere (sub-seafloor; extremely low in nutrients). Explorations to these extreme environments have discovered a myriad of bacterial communities that have evolved novel bioactive compounds through their physiological adaptations to environmental stressors. In recent years, bioprospecting applied to marine environment has led to the development of a wide variety of marine-derived compounds, especially secondary metabolites with unique biological activities [30] and high potential for biotechnological and pharmaceutical applications. So far, several antibacterial [31], antifungal [32] and antiviral [33] compounds have been isolated from marine organisms. One of the best examples is anthracimycin, a new broad-spectrum antineoplastic antibiotic produced by a marine-derived actinomycete [34]. This molecule shows significant activity against *Bacillus anthracis*, the causative agent of anthrax, and several Gram-negative bacteria.

Natural products from cold-adapted microorganisms

Cold environments are arguably the most widespread on our planet and in our solar system. Due to their location and characteristics, extremophilic organisms are difficult and expensive to access and study. The significant expenses involved have led to a number of public/private partnerships in which private companies finance public research expeditions, which then pass samples to the companies for commercial research.

Many microorganisms populate Arctic and Antarctic regions (and the bacteria that can survive in these environments are known as cold-adapted bacteria [35]. Cold-adapted bacteria can be classified into two groups based on their temperature tolerance: (i) psychrophiles, which can grow at temperatures not exceeding approx. 20°C, and (ii) psychrotrophs (or psychrotolerants), that tolerate a broader range of

temperatures—between 0 and 30°C [36]. The diversity, biology and ecology of psychrophilic or psychrotolerant bacteria have been extensively studied in recent years. Both groups of microorganisms share basic molecular and physiological characteristics, which permit their survival in extremely cold environments: (i) increased fluidity of cellular membranes, (ii) the ability to accumulate compatible solutes (e.g. glycine, betaine and trehalose), (iii) the expression of cold shock, antifreeze and ice-nucleating proteins, as well as (iv) the production of cold-active enzymes [35, 37]. So far, cold-adapted organisms have received little attention both in basic and applied research and only recently their large potential for biotechnological applications has been recognized, but these studies are mainly focused on the cold-adapted enzymes [38]. Anyway, recent studies have proven that psychrophilic bacteria may be a promising source of bioactive compounds useful against MDR pathogens. These researches have shown that bacteria from Antarctica belonging to genus *Pseudoalteromonas*, produce a variety of bioactive compounds, able to inhibit the growth of different strains belonging to the Bcc [39, 40]. These strains demonstrated also interesting anti-biofilm activity against various pathogens including, *S. aureus* and *P. aeruginosa* [41, 42]. These results, despite preliminary, emphasise the importance of cold environments as source of new drugs, and certainly, encourage scientific and economic interests in those areas.

3. *Caenorhabditis elegans*: a versatile model host and tool for antimicrobial drug discovery

The nematode *Caenorhabditis elegans* is a widespread multicellular organism, a self-fertilizing hermaphrodite with a rapid generation time. Adults can reach the maximum length of 1 mm, and in optimal condition, they can produce about 300 genetically identical progeny in 3 days, allowing the cultivation of nematodes and the rapid establishment of homogenous populations. In laboratory conditions *C. elegans* can be easily propagated on agar plates or liquid media using the *E. coli* strains OP50. At 20°C, the development proceeds from embryo through four distinct larval stages (L1-L4) to gravid adults hermaphrodites in approximately 72 hours (**Figure 2**). Because they are transparent, the internal development of all *C. elegans* cells and organs can be easily monitored using light microscopy [43, 44]. The nematode has been the subject of intense study for more than four decades. Nowadays *C. elegans* is probably the most diffused host model in science. The availability of a fully sequenced genome [45], the well-developed tools for genetic manipulation and the rapid development of techniques (RNA interference, microarray, robotic machinery for HTS) made *C. elegans* an optimal candidate for all sort of scientific application. Moreover, because of their small size, *C. elegans* nematodes can be placed in 96- or 384-well plates for high-throughput screenings and there are decreased ethical concerns involved in their use compared to mammals.

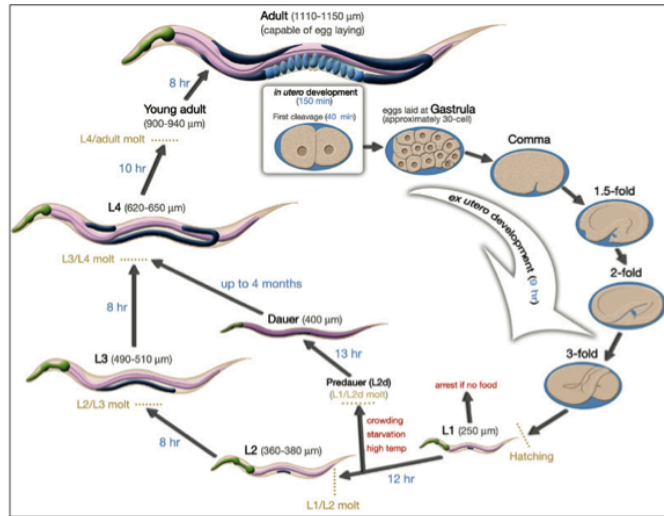


Figure 2. Life cycle of *C. elegans*

***C. elegans* as host model of infection**

In the last years, it has been observed that *C. elegans* can be infected and killed by many human pathogens, many of which of clinical relevance [46]. A prominent example is the human opportunistic pathogen *Pseudomonas aeruginosa*, which was the first microorganism shown to be able to infect and kill *C. elegans*. In a groundbreaking work, the Ausubel laboratory showed that many of the bacterial genes required for full virulence in the nematode were also important in other model systems [47, 48]. This first work has led to numerous *in vivo* large-scale screens for bacterial virulence factors. There are copious examples for the usefulness of the nematode to model virulence and antimicrobial efficacy in *S. aureus* [49], *E. coli* [50] and a variety of Gram-negative bacteria including the biological pathogens *B. pseudomallei* and *Burkholderia cenocepacia* [51, 52]. In many cases, these studies have demonstrated that virulence factors involved in the killing of *C. elegans* are also required for pathogenesis in mammals. These findings, combined with the peculiar useful features of the nematode (ease of culture and the possibility of automated handling) opens up new avenues for the development of novel therapies that target specific virulence mechanisms.

***C. elegans* in Drug Discovery**

The set-up of an infection system model between *C. elegans* and a pathogen has significant implication for the discovery and validation of new bioactive antimicrobial compounds. The nematode system can help in detecting compounds, which act by blocking virulence factors of pathogens, and compounds that have an immune modulator effect on the host.

The use of the nematode system is especially precious as it also allows detection of molecules that enhance immune defences *in vivo*. This sort of drug candidate has been found in compound library screenings assaying the effect of drugs on *C. elegans* survival after a bacterial infection. In the first pioneering screening, a liquid-based assay in 96-well microtiter plates was developed to test the effect of synthetic compounds and natural extracts to cure *C. elegans* following *Enterococcus faecalis* infection [53]. In this screen, 16 compounds and nine extracts were shown to promote *C. elegans* survival. The most important finding was that several of this

compounds had essentially no effect on bacterial growth *in vitro*, so they would not have been identified using a classical approach. This assay has been improved, miniaturized and fully automated (**Figure 3**). An important improvement involved the application of a fluorescent dye that simplify the discrimination between live and dead worms. With this newer high-throughput screen, close to 40,000 compounds and extracts were tested, allowing the identification of 28 novel antimicrobials [54]. Interestingly, the *in vivo* effective dose of many of the compounds identified was significantly lower than the minimum inhibitory concentration (MIC) needed to inhibit *E. faecalis in vitro*. The system has then been exploited against other bacteria, and especially against fungi, such as *Candida albicans*. In a first screening, more than one thousand compounds with known bioactivity were assayed, leading to the identification of 15 compounds able to prolong worms survival after *C. albicans* infection. Among the compounds identified in the screen, caffeic acid phenethyl ester and the fluoroquinolone agent enoxacin also exhibited marked antifungal activity in a mouse model of candidiasis, demonstrating the relevance of these approaches [55].

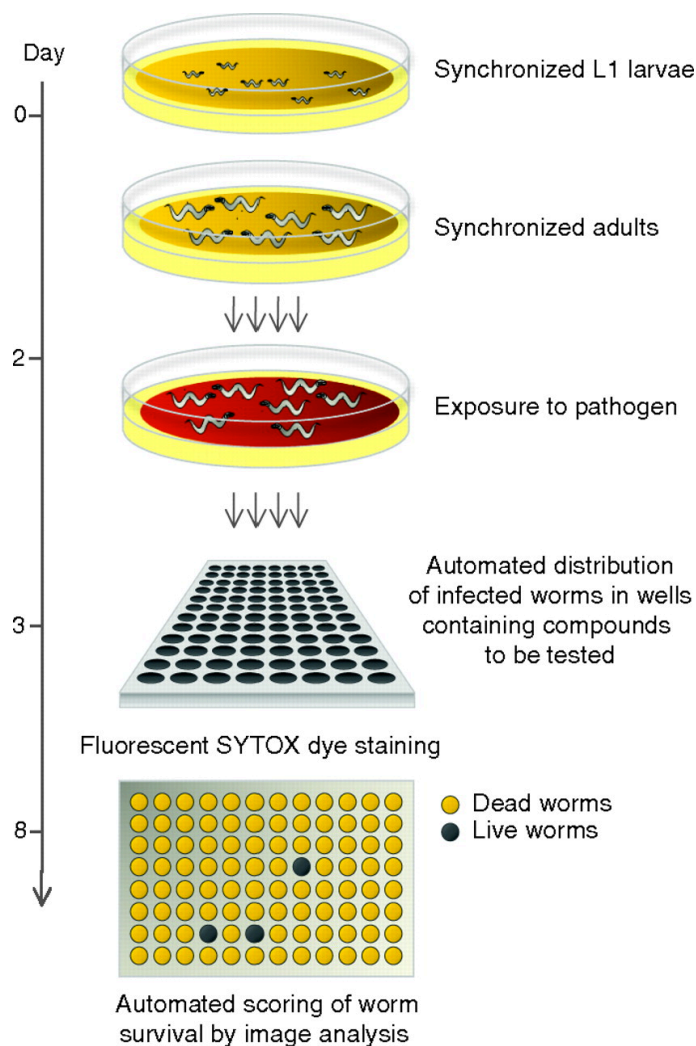


Figure 3. Automatized HTS system for the detection of antimicrobial compounds using *C. elegans*.

The *C. elegans* host system may be also used for the discovery of new anthelmintics. Parasitic nematodes are very hazardous and complex to manipulate in laboratory condition (especially because they cannot live without their host). In fact, *C. elegans* is sensitive to the majority of anthelmintic drugs that are used against parasitic worm infections of humans and livestock. *C. elegans*, in this case represent a valid alternative as “lab-friendly” model, despite the many differences with parasites, especially from a genomic point of view. Anyway, it is probably safe to conclude that *C. elegans* is no more dissimilar to parasitic nematodes than each individual species of parasite is to another [56]. The use of *C. elegans* allows the application of powerful molecular genetic approaches and it has been extensively, and successfully, exploited as a model system to define molecular components of signalling pathways that underpin nematode physiology [57]. There is a large body of literature describing the study of bioactive compounds in *C. elegans* and the proposal to use it for the study of anthelmintics precedes the publication of the *C. elegans* genome sequence by nearly 20 years [58, 59]. These studies generally hinge on the ability of a drug to elicit a significant, ideally quantifiable, change in the worm's growth, development, metabolism, and/or behaviour. Pharmacokinetic considerations include the method and duration of drug exposure. A recent study published in Nature, seems to have finally proved the usefulness of the *C. elegans* as model system for anthelmintic discovery. In this paper more than 67,000 compounds were subjected to a primary high-throughput automatized screening against *C. elegans* to find molecules with anthelmintic activity. The 267 positive hits were then tested against due parasites: *Cooperia onchophora* and *Haemonchus contortus*. This second test performed on a small scale, revealed that 103 compounds out of 267 (38%) were able to kill the two parasites, demonstrating the value of *C. elegans* as a model system for the discovery of useful nematocide molecules [60].

In conclusion, *C. elegans* characteristics made it a unique and incredible model for the antimicrobial drug discovery, as well as to untangle the molecular mechanisms that control resistance and susceptibility to disease.

4. The *Burkholderia cepacia* complex

In the last decades, bacteria belonging to *Burkholderia cepacia* complex (Bcc) have been acquired relevance as emerging Multihost MDR Pathogens.

The Bcc occupies a critical position among Gram-negative multi-drug resistant bacteria. It consists of at least, 20 closely related species inhabiting different ecological niches, including plants and animals [61-65]. Bcc multi drug and pandrug-resistant opportunistic human pathogens cause problematic lung infections in immune-compromised individuals, including cystic fibrosis (CF) patients. The two most clinically relevant species are *B. cenocepacia* and *B. multivorans*, accounting for >85% of all Bcc infections in CF patients [66-68]. Bcc members are naturally resistant to antibiotics including cephalosporins, β -lactams, polymyxins and aminoglycosides, rendering Bcc infections challenging to eradicate [69, 70].

Although, Bcc had a low rate infection in CF patients worldwide, the clinical outcome of these infections is highly variable and so far unpredictable. After colonization with a Bcc strain, few patients experience an asymptomatic carriage, while the majority experiences an increased decline of pulmonary function, associated with chronic

infection and exacerbation episodes. During the interaction with the CF host, several virulence factors such extracellular lipases, metalloproteases and serine proteases are thought to play critical roles for the success of the pathogen [71]. Another important feature of Bcc is their ability to form biofilms. A recent study has proven Bcc bacteria in biofilms appeared to be more resistant to antibiotics than planktonic cells, contributing to persistence in the CF lung [72]. Currently, the eradication of infections caused by Bcc bacteria is very difficult and often impossible, due to their intrinsic resistance to the vast majority of clinically available antimicrobials. A study about the characterization of antimicrobial resistance profiles of Bcc isolates, revealed that 55% of the isolates were MDR [73].

Despite the tremendous progresses on Bcc taxonomy, knowledge of their virulence pathogenicity mechanisms remains far to be elucidated. The knowledge of those aspects will be critical for the development of new strategies. Multidisciplinary approaches using genomics and proteomics, together with genetics and models of infection, will certainly reveal, in the near future, novel and interesting targets for the development of new strategies to fight Bcc and closely related bacteria.

5. Aims of the project

The aim of this project was to apply biotechnological strategies to counteract the rising phenomenon of MDR pathogens, with special emphasis against Bcc and parasite nematodes, exploiting the versatility of *C. elegans* as model system and the potential of psychrophilic microorganisms as source of novel bioactive compounds.

The project is divided into two principal sections:

Section 1:

This part (**Chapter 1**) was focused on establishing an infection model between a selected panel of strains belonging to Bcc and the nematode *C. elegans*. The pathogenicity of these strains has been evaluated using different toxicity tests and principal infection mechanism of Bcc strains has been observed. Moreover, Bcc strain virulence has been profiled exploiting a panel of *C. elegans* mutants with impaired ABC transporters. The work performed has provided useful information on Bcc virulence and it achieved the development of a suitable platform for dissecting Bcc virulence factors and for drug discovery and validation of anti-Bcc molecules.

Section 2:

The second part of the project (**Chapters 2-3**) was focused on the identification of new bioactive compounds targeting Bcc strains and parasite nematodes.

Psychrophilic strains isolated from Antarctica and Tibet, were initially evaluated for their potential as drug producers against Bcc and the nematode *C. elegans*. Positive strains to primary screening were grown in liquid media, which were used for extraction with organic solvents. Then, pure compounds were obtained using bioassay-guided purification. Finally pure compounds were tested against the respective targets and evaluated *in vivo* against *C. elegans*.

6. References

1. Giske, C.G., et al., *Clinical and economic impact of common multidrug-resistant gram-negative bacilli*. Antimicrob Agents Chemother, 2008. **52**(3): p. 813-21.
2. Pendleton, J.N., S.P. Gorman, and B.F. Gilmore, *Clinical relevance of the ESKAPE pathogens*. Expert Rev Anti Infect Ther, 2013. **11**(3): p. 297-308.
3. Kallen, A.J. and A. Srinivasan, *Current epidemiology of multidrug-resistant gram-negative bacilli in the United States*. Infect Control Hosp Epidemiol, 2010. **31 Suppl 1**: p. S51-4.
4. Boucher, H.W., et al., *Bad bugs, no drugs: no ESKAPE! An update from the Infectious Diseases Society of America*. Clin Infect Dis, 2009. **48**(1): p. 1-12.
5. Organization, W.H., *Antimicrobial resistance: global report on surveillance*. 2015.
6. Whiteman, H., *Antibiotic resistance: how has it become a global threat to public health?*, in *Medical News Story*. 2014.
7. Spellberg, B., et al., *The epidemic of antibiotic-resistant infections: a call to action for the medical community from the Infectious Diseases Society of America*. Clin Infect Dis, 2008. **46**(2): p. 155-64.
8. Birkett, D., et al., *Clinical pharmacology in research, teaching and health care: Considerations by IUPHAR, the International Union of Basic and Clinical Pharmacology*. Basic Clin Pharmacol Toxicol, 2010. **107**(1): p. 531-59.
9. Clatworthy, A.E., E. Pierson, and D.T. Hung, *Targeting virulence: a new paradigm for antimicrobial therapy*. Nat Chem Biol, 2007. **3**(9): p. 541-8.
10. Piddock, L.J., *The crisis of no new antibiotics--what is the way forward?* Lancet Infect Dis, 2012. **12**(3): p. 249-53.
11. Awadzi, K., et al., *An investigation of persistent microfilaridermias despite multiple treatments with ivermectin, in two onchocerciasis-endemic foci in Ghana*. Ann Trop Med Parasitol, 2004. **98**(3): p. 231-49.
12. Osei-Atweneboana, M.Y., et al., *Prevalence and intensity of Onchocerca volvulus infection and efficacy of ivermectin in endemic communities in Ghana: a two-phase epidemiological study*. Lancet, 2007. **369**(9578): p. 2021-9.
13. Holden-Dye, L. and R.J. Walker, *Anthelmintic drugs*. WormBook, 2007: p. 1-13.
14. Geary, T.G., *Ivermectin 20 years on: maturation of a wonder drug*. Trends Parasitol, 2005. **21**(11): p. 530-2.
15. Besier, B., *New anthelmintics for livestock: the time is right*. Trends Parasitol, 2007. **23**(1): p. 21-4.
16. Rainey, G.J. and J.A. Young, *Antitoxins: novel strategies to target agents of bioterrorism*. Nat Rev Microbiol, 2004. **2**(9): p. 721-6.
17. King, C.Y. and S.L. Barriere, *Analysis of the in vitro interaction between vancomycin and cholestyramine*. Antimicrob Agents Chemother, 1981. **19**(2): p. 326-7.
18. Galan, J.E. and H. Wolf-Watz, *Protein delivery into eukaryotic cells by type III secretion machines*. Nature, 2006. **444**(7119): p. 567-73.
19. Kauppi, A.M., et al., *Targeting bacterial virulence: inhibitors of type III secretion in Yersinia*. Chem Biol, 2003. **10**(3): p. 241-9.
20. Nordfelth, R., et al., *Small-molecule inhibitors specifically targeting type III secretion*. Infect Immun, 2005. **73**(5): p. 3104-14.

21. Miller, M.B. and B.L. Bassler, *Quorum sensing in bacteria*. Annu Rev Microbiol, 2001. **55**: p. 165-99.
22. Dong, Y.H., et al., *AiiA, an enzyme that inactivates the acylhomoserine lactone quorum-sensing signal and attenuates the virulence of Erwinia carotovora*. Proc Natl Acad Sci U S A, 2000. **97**(7): p. 3526-31.
23. Dong, Y.H., et al., *Quenching quorum-sensing-dependent bacterial infection by an N-acyl homoserine lactonase*. Nature, 2001. **411**(6839): p. 813-7.
24. Sassetti, C.M. and E.J. Rubin, *Genetic requirements for mycobacterial survival during infection*. Proc Natl Acad Sci U S A, 2003. **100**(22): p. 12989-94.
25. Newman, D.J. and G.M. Cragg, *Natural products as sources of new drugs over the 30 years from 1981 to 2010*. J Nat Prod, 2012. **75**(3): p. 311-35.
26. Bologna, C.G., et al., *Emerging trends in the discovery of natural product antibacterials*. Curr Opin Pharmacol, 2013. **13**(5): p. 678-87.
27. Pham, V.H. and J. Kim, *Cultivation of unculturable soil bacteria*. Trends Biotechnol, 2012. **30**(9): p. 475-84.
28. Eisner, T., *Prospecting for nature's chemical riches*. CHEMOECOLOGY, 1990. **1**(1): p. 38-40.
29. Nicol, D., *Balancing access to pharmaceuticals with patent rights*. Monash Bioeth Rev, 2003. **22**(2): p. 50-62.
30. Imhoff, J.F., A. Labes, and J. Wiese, *Bio-mining the microbial treasures of the ocean: new natural products*. Biotechnol Adv, 2011. **29**(5): p. 468-82.
31. Teasdale, M.E., et al., *Secondary metabolites produced by the marine bacterium Halobacillus salinus that inhibit quorum sensing-controlled phenotypes in gram-negative bacteria*. Appl Environ Microbiol, 2009. **75**(3): p. 567-72.
32. Nishimura, S., et al., *Marine antifungal theonellamides target 3beta-hydroxysterol to activate Rho1 signaling*. Nat Chem Biol, 2010. **6**(7): p. 519-26.
33. Cheng, S.Y., et al., *Antiviral and anti-inflammatory diterpenoids from the soft coral Sinularia gyrosa*. J Nat Prod, 2010. **73**(6): p. 1184-7.
34. Jang, K.H., et al., *Anthracimycin, a potent anthrax antibiotic from a marine-derived actinomycete*. Angew Chem Int Ed Engl, 2013. **52**(30): p. 7822-4.
35. de Pascale, D., et al., *The microbial diversity of Polar environments is a fertile ground for bioprospecting*. Mar Genomics, 2012. **8**: p. 15-22.
36. Helmke, E. and H. Weyland, *Psychrophilic versus psychrotolerant bacteria--occurrence and significance in polar and temperate marine habitats*. Cell Mol Biol (Noisy-le-grand), 2004. **50**(5): p. 553-61.
37. Russell, N.J., *Molecular adaptations in psychrophilic bacteria: potential for biotechnological applications*. Adv Biochem Eng Biotechnol, 1998. **61**: p. 1-21.
38. Cavicchioli, R., et al., *Biotechnological uses of enzymes from psychrophiles*. Microb Biotechnol, 2011. **4**(4): p. 449-60.
39. Papaleo, M.C., et al., *Bioactive volatile organic compounds from Antarctic (sponges) bacteria*. N Biotechnol, 2013. **30**(6): p. 824-38.
40. Maida, I., et al., *Phenotypic and genomic characterization of the Antarctic bacterium Gillisia sp. CAL575, a producer of antimicrobial compounds*. Extremophiles, 2013.
41. Papa, R., et al., *Anti-Biofilm Activities from Marine Cold Adapted Bacteria Against Staphylococci and Pseudomonas aeruginosa*. Front Microbiol, 2015. **6**: p. 1333.

42. Papa, R., et al., *Anti-biofilm activity of the Antarctic marine bacterium Pseudoalteromonas haloplanktis TAC125*. Res Microbiol, 2013. **164**(5): p. 450-6.
43. Brenner, S., *The genetics of Caenorhabditis elegans*. Genetics, 1974. **77**: p. 71-94.
44. Stiernagle, T., *Maintenance of C. elegans* WormBook, The C. elegans Research Community, 2006.
45. *Genome sequence of the nematode C. elegans: a platform for investigating biology*. Science, 1998. **282**(5396): p. 2012-8.
46. Powell, J.R. and F.M. Ausubel, *Models of Caenorhabditis elegans infection by bacterial and fungal pathogens*. Methods Mol Biol, 2008. **415**: p. 403-27.
47. Tan, M.W., S. Mahajan-Miklos, and F.M. Ausubel, *Killing of Caenorhabditis elegans by Pseudomonas aeruginosa used to model mammalian bacterial pathogenesis*. Proc Natl Acad Sci U S A, 1999. **96**(2): p. 715-20.
48. Tan, M.W., et al., *Pseudomonas aeruginosa killing of Caenorhabditis elegans used to identify P. aeruginosa virulence factors*. Proc Natl Acad Sci U S A, 1999. **96**(5): p. 2408-13.
49. Wu, K., et al., *A correlative analysis of epidemiologic and molecular characteristics of methicillin-resistant Staphylococcus aureus clones from diverse geographic locations with virulence measured by a Caenorhabditis elegans host model*. Eur J Clin Microbiol Infect Dis, 2013. **32**(1): p. 33-42.
50. Bhatt, S., A. Anyanful, and D. Kalman, *CsrA and TnaB coregulate tryptophanase activity to promote exotoxin-induced killing of Caenorhabditis elegans by enteropathogenic Escherichia coli*. J Bacteriol, 2011. **193**(17): p. 4516-22.
51. Lee, S.H., et al., *Complete killing of Caenorhabditis elegans by Burkholderia pseudomallei is dependent on prolonged direct association with the viable pathogen*. PLoS One, 2011. **6**(3): p. e16707.
52. O'Quinn, A.L., E.M. Wiegand, and J.A. Jeddloh, *Burkholderia pseudomallei kills the nematode Caenorhabditis elegans using an endotoxin-mediated paralysis*. Cell Microbiol, 2001. **3**(6): p. 381-93.
53. Moy, T.I., et al., *Identification of novel antimicrobials using a live-animal infection model*. Proc Natl Acad Sci U S A, 2006. **103**(27): p. 10414-9.
54. Moy, T.I., et al., *High-throughput screen for novel antimicrobials using a whole animal infection model*. ACS Chem Biol, 2009. **4**(7): p. 527-33.
55. Breger, J., et al., *Antifungal chemical compounds identified using a C. elegans pathogenicity assay*. PLoS Pathog, 2007. **3**(2): p. e18.
56. Mitreva, M., et al., *Comparative genomics of nematodes*. Trends Genet, 2005. **21**(10): p. 573-81.
57. Angstadt, J.D., J.E. Donmoyer, and A.O. Stretton, *Retrovesicular ganglion of the nematode Ascaris*. J Comp Neurol, 1989. **284**(3): p. 374-88.
58. Rand, J.B. and C.D. Johnson, *Genetic pharmacology: interactions between drugs and gene products in Caenorhabditis elegans*. Methods Cell Biol, 1995. **48**: p. 187-204.
59. Nguyen, M., et al., *Caenorhabditis elegans mutants resistant to inhibitors of acetylcholinesterase*. Genetics, 1995. **140**(2): p. 527-35.
60. Burns, A.R., et al., *Caenorhabditis elegans is a useful model for anthelmintic discovery*. Nat Commun, 2015. **6**: p. 7485.

61. Compant S, N.J., Coenye T, Clement C, Ait Barka E, *Diversity and occurrence of Burkholderia spp. in the natural environment*. FEMS Microbiol Rev, 2008. **32(4)**: p. 607-626.
62. Coenye, T. and P. Vandamme, *Diversity and significance of Burkholderia species occupying diverse ecological niches*. Environ Microbiol, 2003. **5(9)**: p. 719-29.
63. Peeters, C., et al., *Burkholderia pseudomultivorans sp. nov., a novel Burkholderia cepacia complex species from human respiratory samples and the rhizosphere*. Syst Appl Microbiol, 2013. **36(7)**: p. 483-9.
64. Mahenthalingam, E., T.A. Urban, and J.B. Goldberg, *The multifarious, multireplicon Burkholderia cepacia complex*. Nat Rev Microbiol, 2005. **3(2)**: p. 144-56.
65. De Smet, B., et al., *Burkholderia stagnalis sp. nov. and Burkholderia territorii sp. nov., two novel Burkholderia cepacia complex species from environmental and human sources*. Int J Syst Evol Microbiol, 2015. **65(7)**: p. 2265-71.
66. Ramsay, K.A., et al., *Factors influencing acquisition of Burkholderia cepacia complex organisms in patients with cystic fibrosis*. J Clin Microbiol, 2013. **51(12)**: p. 3975-80.
67. Rose, H., et al., *Biocide susceptibility of the Burkholderia cepacia complex*. J Antimicrob Chemother, 2009. **63(3)**: p. 502-10.
68. Nash, E.F., et al., *"Cepacia syndrome" associated with Burkholderia cepacia (genomovar I) infection in an adolescent with cystic fibrosis*. Pediatr Pulmonol, 2010.
69. Bazzini, S., C. Udine, and G. Riccardi, *Molecular approaches to pathogenesis study of Burkholderia cenocepacia, an important cystic fibrosis opportunistic bacterium*. Appl Microbiol Biotechnol, 2011. **92(5)**: p. 887-95.
70. Drevinek, P. and E. Mahenthalingam, *Burkholderia cenocepacia in cystic fibrosis: epidemiology and molecular mechanisms of virulence*. Clin Microbiol Infect, 2010. **16(7)**: p. 821-30.
71. McClean, S. and M. Callaghan, *Burkholderia cepacia complex: epithelial cell-pathogen confrontations and potential for therapeutic intervention*. J Med Microbiol, 2009. **58(Pt 1)**: p. 1-12.
72. Caraher, E.M., et al., *The effect of recombinant human lactoferrin on growth and the antibiotic susceptibility of the cystic fibrosis pathogen Burkholderia cepacia complex when cultured planktonically or as biofilms*. J Antimicrob Chemother, 2007. **60(3)**: p. 546-54.
73. Leitao, J.H., et al., *Variation of the antimicrobial susceptibility profiles of Burkholderia cepacia complex clonal isolates obtained from chronically infected cystic fibrosis patients: a five-year survey in the major Portuguese treatment center*. Eur J Clin Microbiol Infect Dis, 2008. **27(11)**: p. 1101-11.

CHAPTER 1

Investigating the role of the host multidrug resistance associated protein transporter family in *Burkholderia cepacia* complex pathogenicity using a *Caenorhabditis elegans* infection model

Investigating the role of the host multidrug resistance associated protein transporter family in *Burkholderia cepacia* complex pathogenicity using a *Caenorhabditis elegans* infection model

ABSTRACT

This study investigated the relationship between host efflux system of the non-vertebrate nematode *Caenorhabditis elegans* and *Burkholderia cepacia* complex (Bcc) strain virulence. This is the first comprehensive effort to profile host-transporters within the context of Bcc infection. With this aim, two different toxicity tests were performed: a slow killing assay that monitors mortality of the host by intestinal colonization and a fast killing assay that assesses production of toxins. A Virulence Ranking scheme was defined, that expressed the toxicity of the Bcc panel members, based on the percentage of surviving worms. According to this ranking the 18 Bcc strains were divided in 4 distinct groups. Only the Cystic Fibrosis isolated strains possessed profound nematode killing ability to accumulate in worms' intestines. For the transporter analysis a complete set of isogenic nematode single Multidrug Resistance associated Protein (MRP) efflux mutants and a number of efflux inhibitors were interrogated in the host toxicity assays. The Bcc pathogenicity profile of the 7 isogenic *C. elegans* MRP knock-out strains functionality was classified in two distinct groups. Disabling host transporters enhanced nematode mortality more than 50% in 5 out of 7 mutants when compared to wild type. In particular *mrp-2* was the most susceptible phenotype with increased mortality for 13 out 18 Bcc strains, whereas *mrp-3* and *mrp-4* knock-outs had lower mortality rates, suggesting a different role in toxin-substrate recognition. The use of MRP efflux inhibitors in the assays resulted in substantially increased (>40% on average) mortality of wild-type worms.

Keywords: *Burkholderia cepacia* complex (Bcc), non-vertebrate hosts, *Caenorhabditis elegans* virulence, pathogenicity, multidrug resistance, ABC transporters

1.1 Introduction

The *Burkholderia cepacia* complex (Bcc) occupies a critical position among Gram-negative multi-drug resistant bacteria. It consists of at least 20 closely related species inhabiting different ecological niches, including plants and animals [1-5]. Bcc multi drug and pandrug-resistant opportunistic human pathogens cause problematic lung infections in immune-compromised individuals, including cystic fibrosis (CF) patients [6-8]. Bcc members are naturally resistant to antibiotics including cephalosporins, β -lactams, polymyxins and aminoglycosides, rendering Bcc infections challenging to eradicate [9,10]. There is an imminent need to develop new Bcc antimicrobial therapeutic strategies. Dissecting virulence and pathogenicity determinants as well as identifying novel therapeutic targets may be proven promising approaches. A major part of these tasks can be advanced by the exploitation of the non-vertebrate host models *Drosophila melanogaster*, *Galleria mellonella*, and *Caenorhabditis elegans*. Model hosts have been used to evaluate microbial virulence traits involved in mammalian infections and the efficacy of antimicrobial compounds [11-16]. The free-living nematode *C. elegans* is a widespread multicellular organism that is a self-fertilizing hermaphrodite with a rapid generation time. *C. elegans* has been proven cost-effective, ethical, reproducible and genetically powerful infection model despite the obvious reported technical limitations (nematodes have lower optimal growth temperatures when compared with human pathogens; occurrence of host specific virulence factors) [15,17-19]. In fact, there is an extensive body of literature for the utility of the nematode to model infection with a variety of Gram-negative bacteria including *Escherichia coli*, *Burkholderia pseudomallei*, *B. cepacia* complex and *Pseudomonas aeruginosa* [20-23]. The *C. elegans*-Bcc studies in the last decade have shed some light on the complex-nematode interaction, correlating genotypic characteristics of the pathogen with phenotypic changes in the host. These efforts have identified specific virulence factors: the auto inducer dependent Acyl-HomeSerineLactone (*aidA*), the phenazine biosynthesis regulator (*Pbr*), and the host factor phage Q, (*hfq*) [16,24-33].

Recent studies have underlined the importance of efflux systems in infection within the content of host-pathogen interaction [34-36]. The host efflux capability is considered part of a basic defence mechanism. For example the *B. pseudomallei* infection stimulates the overproduction of the ATP Binding Cassette (ABC) transporter *pgp-5* in *C. elegans* [37]. However, the partition of host transporters in the infection process has never been studied in depth. Bcc members produce a variety of metabolites and toxins, potential host efflux substrates. Furthermore, exploring the role of host transporters in pathogenicity may facilitate the design of appropriate tools for toxin identification. Multidrug Resistance associated Proteins (MRPs) are members of the ABC efflux transporter family with broad substrate specificity for the transport of endogenous and xenobiotic anionic substances found in Bacteria, Archaea and Eukarya [38-41]. MRPs play important roles in nematode physiology such as control resistance to anthelmintic (ivermectine) and heavy metals (arsenic) [42-44]. This study emphasizes the contribution of the host MRP efflux subfamily to Bcc virulence, employing a panel of 18 strains representing the up-to-date different acknowledged species and a fully functional seven single *C. elegans* mutant set impaired in MRPs. A Virulence-Ranking (VR) scheme based on comparing host survival rates in two different assays was developed. This scheme provides the tool

for a detailed study on the effect of the MRP transporter family on Bcc virulence using as well as selected efflux inhibitors.

1.2 Materials and Methods

Bacterial strains, nematode strains and growth conditions

C. elegans Wild-type (WT) Bristol N2, NL147 (*mrp-1(pk89)* X), RB1713 (*mrp-2(ok2157)* X), RB1028 (*mrp-3(ok955)* X), VC712 (*mrp-4(ok1095)* X), VC1599 (*mrp-5(ok2067)/szT1* X), RB1070 (*mrp-6(ok1027)* X) and RB1269 (*mrp-8(ok1360)* III) strains were obtained from the *Caenorhabditis* Genetic Centre (CGC). For strain VC1599, due to *ok2067* mutation lethality in homozygosis, all the experiments were performed assaying heterozygotes worms. All mutants presented identical phenotypic traits in respect to WT: normal larval development (eggs reaching adults state in 72 h as indicated on standard table (www.wormbook.org)), non-impaired reproduction, and survival rate at 100% when fed with *E. coli*. Mutant *mrp-5* in heterozygosis also aligned to those parameters. All strains were recovered from frozen stocks, and routinely kept on NGM (Nematode Growth Medium) plates seeded with *E. coli* OP50 as a food source [45]. The panel of Bcc strains used in this work belongs to the Bcc collection at the University of Gent, Belgium, and is listed in **Table 1**. Bcc and *E. coli* OP50 cells were routinely grown in Luria-Bertani broth (LB) (10 g/L Bacto-tryptone, 5 g/L Yeast extract, 10 g/L NaCl) at 37 °C.

Nematode Toxicity Assays

Slow Killing Assay (SKA) was performed against the *C. elegans* WT strain N and MRP-mutants. 2.5-cm-diameter plates containing 3 ml of NGM agar (Peptone 2.5 g/L, NaCl 2.9 g/L, Bacto-Agar 17 g/L, CaCl₂ 1 mM, Cholesterol 5 µg/mL, KH₂PO₄ 25 mM, MgSO₄ 1 mM) were seeded with 50 µl of the overnight Bcc cultures, normalized to an OD₆₀₀, of 1.7 and incubated for 24 h at 37 °C to allow the formation of a bacterial lawn. This was the standard bacterial growth condition unless otherwise stated. *C. elegans* WT strain and MRP-mutants were synchronized by bleaching treatment [46], and 30-40 worms at larval stage 4 (L4), were transferred to each plate and incubated at 20 °C for three days. The plates were scored for living worms every 24 h.

Fast Killing assay (FKA) was carried out in 2.5-cm-diameter plates containing 3 ml of Peptone Glucose Sorbitol (PGS) agar medium [25] (Peptone 12 g/L, Glucose 12 g/L, Sorbitol 27.25 g/L, NaCl 12 g/L, Bacto-Agar 17 g/L, CaCl₂ 1 mM, Cholesterol 5 µg/mL, KH₂PO₄ 25 mM, MgSO₄ 1 mM). Plates were prepared as described above for the SKA. Then, L4 worms from WT strain and MRP-mutants were collected from NGM plates, washed with M9 medium (Na₂HPO₄·7H₂O 12.8 g/L, Na₂HPO₄ (anhydrous) 6 g/L, KH₂PO₄ 3 g/L, NaCl 0.5 g/L, NH₄Cl 1 g/L) and 30-40 L4 worms were spotted onto the bacterial lawn. The plates were then incubated at 20 °C and scored for living worms every 24 h. In both assays, *E. coli* OP50 was used as a negative control. A worm was considered dead when it no longer responded to touch. For statistical purposes, 5 replicates per trial were carried out with a unique egg preparation. The incubation time was set at 2 days. A pathogenicity scheme (VR) was established by comparing the "infectivity" towards nematodes between *E. coli* OP50 and Bcc isolates.

Microscopy analysis

40-60 WT L4 worms were grown on NGM plates seeded with Bcc or *E. coli* OP50 propagated in standard growth conditions. Plates were incubated at 20 °C, and after 4 and 24 h, the nematodes were inspected using a Zeiss Axioskop microscope equipped with Differential Interference Contrast (DIC) employing 10x, 20x, 40x, 63x and 100x objectives and 10X eyepiece. Images were collected with a Zeiss AxioCam MR digital camera.

Toxin Diffusion assay

Bcc or *E. coli* OP50 cells were grown under standard growth conditions and spread on sterile 0.22 mm Millipore Nitrocellulose (Darmstadt, Germany) filter disk located onto 2.5-cm-diameter PGS plates [25]. After overnight incubation at 37 °C, the filter together with the bacterial lawn was removed and the plates were allowed to cool to room temperature. 30-40 hypochlorite-synchronised WT L4 nematodes were spotted onto the conditioned agar. Paralysis and mortality of the worms were detected at 4 and 24 h. The experiments were performed in triplicate, and data reported are mean values \pm SD.

Statistical analysis and clustering

All the Kaplan-Meier survival curves were analyzed using the Graph-pad Prism 5 software. Comparisons vs. control for both the *C. elegans* and inhibitor experiments were performed using Fisher's exact test to account for possible non-Normality in the data. In particular, as it was observed that replicate means of *C. elegans* percent mortality correlated extremely well to pooled percent mortality ($R^2 > 0.99$ in all cases), counts of *C. elegans* that were alive and dead after 72 h were used to populate the various 2x2 tables onto which the Fisher's exact test was applied. Bonferroni-Holm correction of p-values was used to account for the multiple comparisons performed.

Mutant clustering analysis was performed using hierarchical clustering via Ward's method. Clusters were fixed using a consistency threshold of 1.1, resulting in cophenetic coefficient (correlation between cluster and metric distance) of at least 0.80.

Transporter Inhibitor assays

The MRP transporter inhibitors mometasone furoate, lasalocid A sodium, verapamil hydrochloride were purchased from Sigma-Aldrich, Saint Louis, MO. Compounds were dissolved in DMSO and spread onto NGM plates in different concentration ranges: 25-100 μ M (mometasone and verapamil) and 125-500 nM (lasalocid). DMSO (0,5% w/v) was used as control. Subsequently, Bcc strains (grown in standard conditions) were spotted onto the plates that were incubated overnight at 37 °C. After the incubation 30-40 WT L4 worms were spotted onto the bacterial lawn. The plates were then incubated at 20 °C for 3 days and scored for living worms every 24 h. The experiments were performed in triplicate, and the data reported are mean values.

1.3 Results and Discussion

Killing of *C. elegans* by Bcc strains

To evaluate Bcc virulence determinants and properties, two different assays were performed: i) SKA, performed on a low osmolarity medium (NGM), assigned to

correlate worms mortality with intestinal bacterial accumulation/colonisation [24,25]; ii) FKA carried out on a high osmolarity medium (PGS) to demonstrate the secretion of bacterial toxins and evaluate their capacity to paralyse and kill the nematodes [24,25]. A VR was established for the Bcc strains under investigation by comparing the "infectivity" against nematodes between *E. coli* OP50 and Bcc isolates. The VR ranges from 0 to 3 (see **Fig. 1**) and was based on the percentage of surviving worms after the period of observation, which was set at 3 days. A Bcc strain was considered to be non-pathogenic (VR=0) when no symptom of disease was observed during the course of nematodes infection and the percentage of live worms at the conclusion of the period of observation ranged from 100 to 80%; VR=1 corresponded to a percentage of alive worms between 79 to 50%; VR=2 corresponded to a percentage of alive worms between 49 to 6%; finally, the VR was considered 3 when the percentage of surviving worms was $\leq 5\%$.

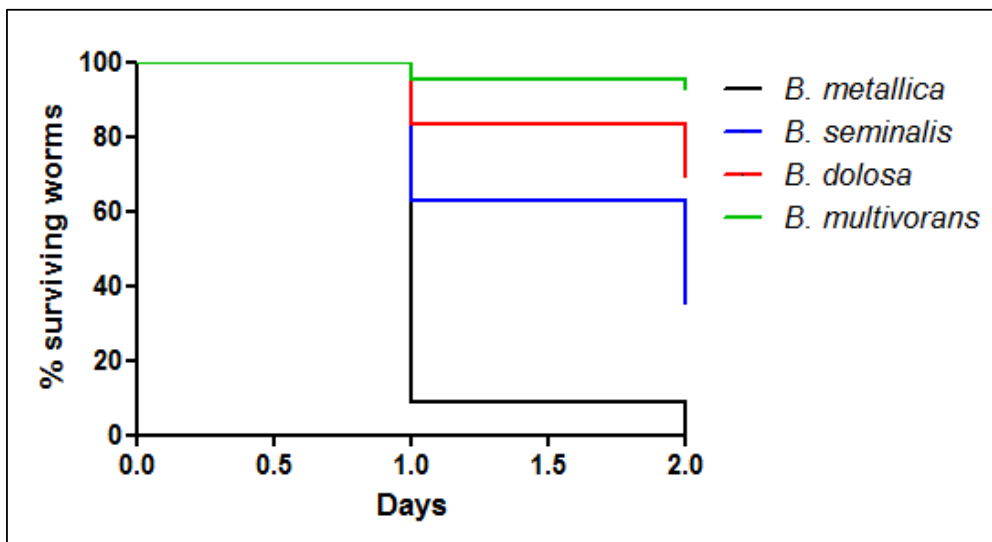


Figure 1: Kaplan-Meier survival plots for L4 N2 worms fed with exemplifying Bcc strains for different VR grown on PGS medium. Worms fed on: *B. metallica* (VR 3; black line; n = 113; 0% survival at day 2); *B. seminalis* (VR 2; blue line; n=150; 34% survival at day 2); *B. dolosa* (VR 1; redline; n=198; 69% survival at day 2); *B. multivorans* (VR 0; green line; n=120; 93% survival worms). n: Number of worms at day 0. All p-values, comparing each survival curve between them, resulted to be < 0.0001 , calculated with "Log-rank (Mantel-Cox) Test" with the Graph-pad Prism 5 software.

SKA performed against WT L4 worms revealed diverse pathogenicity capabilities among the 18 Bcc representatives **[Table 1]**:

- i) 2 Bcc strains (*B. metallica*, *B. stabilis*) displayed high nematocide activity (VR 3). No viable nematodes were detectable in the plates after 3 days of incubation at 20 °C.
- ii) Half of the Bcc strains exhibited VR between 1 and 2, showing an intermediate toxicity towards *C. elegans*.
- iii) Seven Bcc strains (*B. ambifaria*, *B. cepacia*, *B. dolosa*, *B. pseudomultivorans*, *B. pyrrocinia*, *B. lata* and *B. multivorans*) were unable to kill worms, and the whole population was viable (VR=0).

Nematodes killed in the lawn of bacteria took on a ghostly and hollow “shell-like” appearance about 48 h after the L4 were first introduced, and their shells induced by *B. ubonensis*, *B. metallica* and *B. stabilis* were defined as “chalk-mark ghosts”. This shape is characteristic of organisms lacking a discernible internal cell structures. Often the ghosts eroded to a mere outline.

Species	Strain	Source	SKA	FKA
<i>Burkholderia cepacia</i>	LMG 1222	Onion	0	3
<i>Burkholderia multivorans</i>	LMG 13010	CF	0	0
<i>Burkholderia cenocepacia</i>	LMG 16656	CF	2	2
<i>Burkholderia stabilis</i>	LMG 14294	CF	3	3
<i>Burkholderia vietnamiensis</i>	LMG 10929	Soil	1	0
<i>Burkholderia dolosa</i>	LMG 18943	CF	0	1
<i>Burkholderia ambifaria</i>	LMG 19182	Soil	0	3
<i>Burkholderia anthina</i>	LMG 20980	Soil	2	1
<i>Burkholderia pyrrocinia</i>	LMG 14191	Soil	0	2
<i>Burkholderia ubonensis</i>	LMG 20358	Soil	2	1
<i>Burkholderia latens</i>	LMG 24064	CF	1	1
<i>Burkholderia diffusa</i>	LMG 24065	CF	2	2
<i>Burkholderia arboris</i>	LMG 24066	Soil	1	1
<i>Burkholderia seminalis</i>	LMG 24067	CF	2	2
<i>Burkholderia metallica</i>	LMG 24068	CF	3	3
<i>Burkholderia lata</i>	LMG 22485	Soil	0	1
<i>Burkholderia contaminans</i>	LMG 23361	AI	1	3
<i>Burkholderia pseudomultivorans</i>	LMG 26883	CF	0	1

Table 1. *Burkholderia cepacia* complex used in this work and VR relative to the different killing assays. Abbreviations: Soil = Soil rhizosphere, AI = Animal Infections, CF = Cystic Fibrosis patients

VRs:

0 = 100 % > Survival worms > 80% (dark green)

1 = 79 % > Survival worms > 50% (pale green)

2 = 49% > Survival worms > 6% (yellow)

3 = 5 % > Survival worms > 0% (red)

The pathogenicity of the 18 Bcc strains was then assessed on FKA. Data obtained are summarised in **Table 1**. Nematodes death on FKA appeared to be a rapid process as they lose locomotor functions, as shown by the quick onset of lethargy. Motility visibly decreased after exposure for 4 h, and the rate of foraging was similarly affected in the same time frame. In FKA, five strains (*B. ambifaria*, *B. cepacia*, *B. contaminans*, *B. metallica*, *B. stabilis*) demonstrated deep killing ability (VR=3) against *C. elegans* and only two strains (*B. multivorans* and *B. vietnamiensis*) were completely ineffective in killing worms. For the highly active strains, almost 100 % mortality occurred in 24 h, while on SKA 3 days are required for complete killing (**Fig. 2**). Nine out of 18 Bcc strains have previously been characterized using SKA [30,47]. The VR of 7 strains (*B. anthina*, *B. ubonensis*, *B. vietnamiensis*, *B. cenocepacia*, *B. dolosa*, *B. ambifaria*, *B. cepacia*) are consistent with the previously reported SKA ranking. The same comparison revealed a variation for *B. pyrrocinia* and *B. stabilis*,

which were found as more and less virulent, respectively. This variability may be due to ranking differences, as the experimental conditions were very reproducible. This is the first report for an indicative pathogenicity ranking for 8 *Burkholderia* species, recently added to Bcc, (*B. latens*, *B. diffusa*, *B. arboris*, *B. seminalis*, *B. metallica*, *B. pseudomultivorans*, *B. lata*, *B. contaminans*). *B. metallica*, *B. stabilis* (both isolated from CF patients) were the most virulent in both assays (**Fig. 2B-C**). The comparison of data obtained in the FKA and SKA revealed that, on average, strains isolated from CF patients appeared more virulent than environmental isolates on SKA. In particular, three Bcc strains (*B. ambifaria*, *B. cepacia* and *B. pyrrocinia*) exhibited high nematocide activity in the FKA, whereas they were unable to kill the worms in the SKA (VR 0 and 1). Therefore we can assume that toxin production is a common virulence mechanism for Bcc members, while CF isolates might have acquired different pathogenic traits that allow them to infect and colonize hosts, as already proposed by Pirone et al. [48]. The only exception is represented by *B. multivorans*, and *B. pseudomultivorans*. These two strains are CF isolates, but were non-virulent towards nematodes. This evidence likely rely in the limitation of the nematode host model, once more indicating that virulence factors are not universal for all hosts [15].

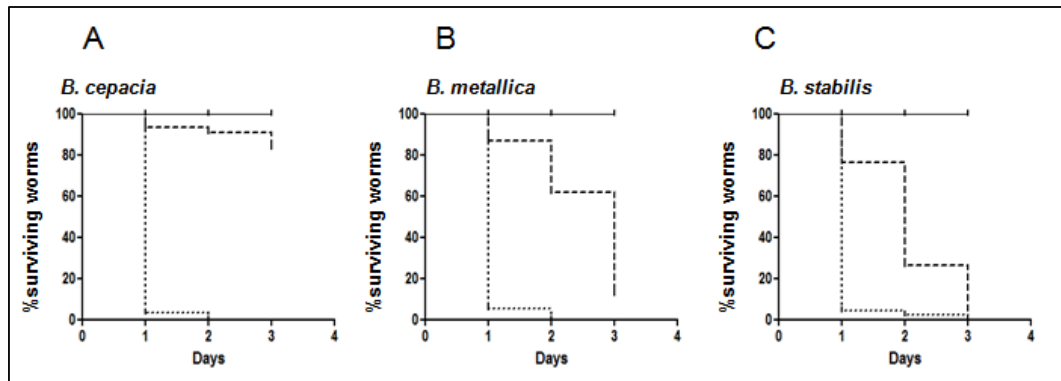


Figure 2: Kaplan-Meier survival plots for L4 stage WT worms fed with: *E. coli* OP50 (solid lines), *Bcc* strains on NGM (dashed lines), *Bcc* strains on PGS (dotted lines). n: Number of worms at day 0. **A)** The pathogenicity of *Bcc* strain *B. cepacia* on SKA (n = 93) was compared with the ability on FKA (n = 184). **B)** The pathogenicity of *Bcc* strain *B. metallica* on SKA (n = 80) was compared with the ability on FKA (n = 113). **C)** The pathogenicity of *Bcc* strain *B. stabilis* on SKA (n = 87) was compared with the ability on FKA (n = 161). p-values were calculated between survival curves on FKA and SKA of each bacteria, and resulted to be < 0.0001 calculated with "Log-rank (Mantel-Cox) Test" with the Graph-pad Prism 5 software.

Bacterial intestinal accumulation

The two *Bcc* strains with VR=3 in the SKA (*B. stabilis* and *B. metallica*) were then assessed for their ability to accumulate in the *C. elegans* intestine. Worms grown in standard condition were inspected using a compound microscope at different incubation times to evaluate the bacterial accumulation in the intestinal lumen.

Bcc colonization of nematode occurred rapidly. After 4 h of incubation, worms fed with *E. coli* OP50 showed a thin intestinal lumen (**Fig. 3A-B**), whereas, when spotted onto *B. metallica* layer, worms already presented deformed intestines (**Fig. 3E**). After 24 h nematodes displayed a full intestinal lumen packed with bacteria (**Fig. 3F**). These data confirmed that *Bcc* with high VR were able to accumulate within the entire nematode intestine and therefore slow-killing may resemble an infection-like process. On the contrary, nematodes exposed to the strain *B. pseudomultivorans*, which exhibited a low pathogenicity (VR=0 on SKA), under the same experimental

conditions presented a healthy intestine with the presence of bacterial cells only in the first part of the intestine (**Fig. 3C-D**). This finding may signify that: i) even non-pathogenic Bcc strains were able to pass intact through the pharynx and occupy the intestine; ii) the accumulation of the Bcc in the whole nematode gut, especially in the last part of the intestine, might be responsible for the worm's death [24].

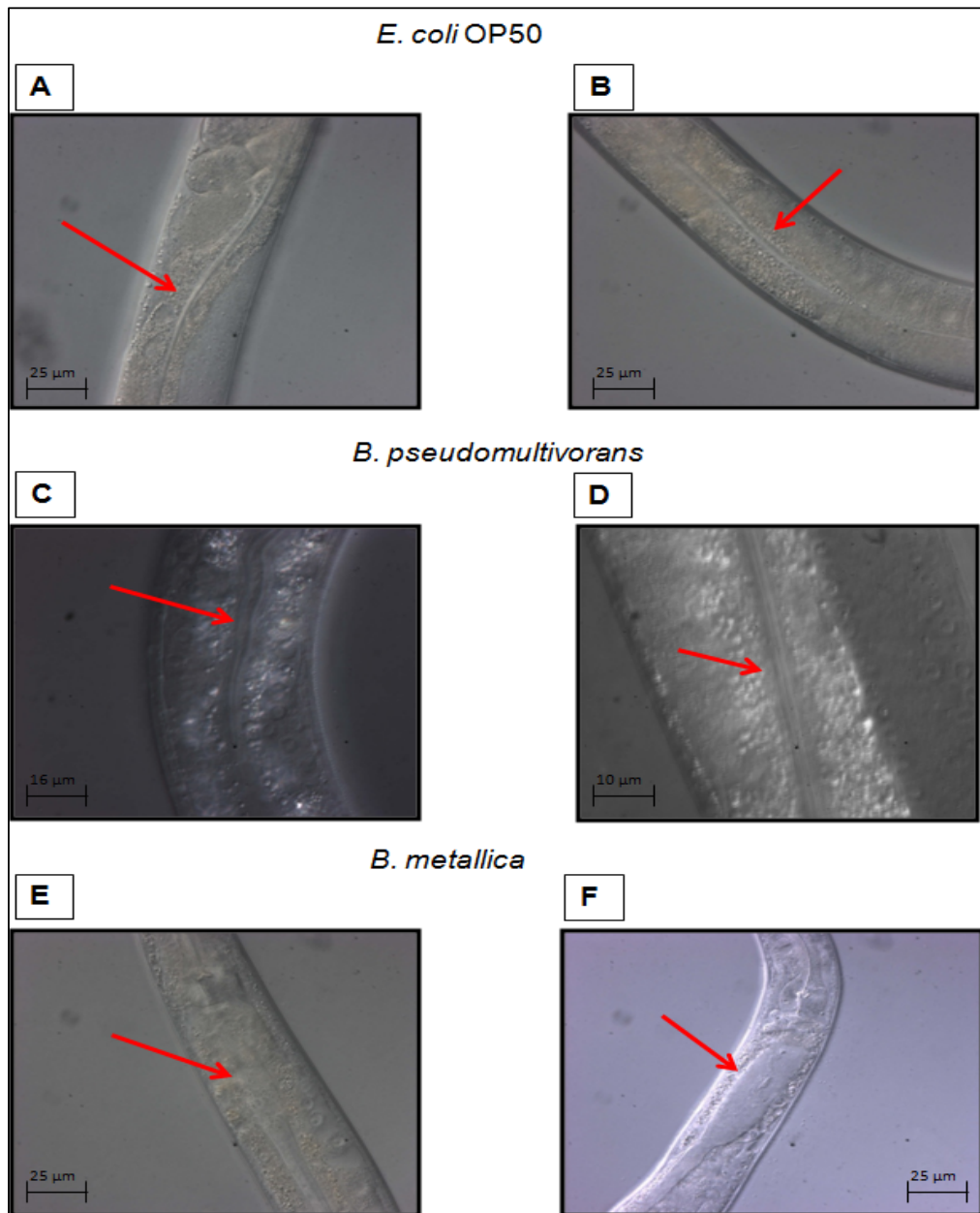


Figure 3: The ability of *Bcc* strains to accumulate in *C. elegans* intestinal lumen was evaluated with microscopy analysis. Red arrows indicate the nematodes intestine. **A)** Intestinal lumen of one L4 stage WT worm after 4 h of incubation on NGM plate spotted with *E. coli* OP50, and **B)** after 24 h of incubation on the same plate. **C)** Intestinal lumen of one L4 WT after 4 h of incubation on NGM plate spotted with *B. pseudomultivorans* (VR 0 on SKA, and **D)** after 24 h of incubation on the same plate. **E)** Intestinal lumen of one L4 WT after 4 h of incubation on NGM plate spotted with *B. metallica* (VR 3 on SKA, and **F)** after 24 h of incubation on the same plate.

Toxin Diffusion assay

To evaluate the contribution of diffusible secreted factors (toxins and/or other virulence chemical signalling molecules) to the rapid kinetics of killing on FKA, we performed the toxin diffusion assay [25]. These experiments were carried out on a reduced panel consisting of the five Bcc strains possessing the highest nematocide activity on FKA (*B. contaminans*, *B. cepacia*, *B. ambifaria*, *B. metallica* and *B. stabilis*). Results shown in **Fig. 4** revealed that a high percentage of worms were paralyzed after 4 h of incubation on plates, even if they were not in contact with the bacteria. In particular, only 30% of the worms placed on *B. ambifaria* plates were still mobile and active, whereas the remaining nematode population appeared paralysed. On the contrary, worms spotted on plates containing *E. coli* conditioned agar did not present any paralysis or mortality. Among the tested Bcc strains, *B. ambifaria* was the most active toxin producer. Indeed, after 24 h of incubation only 20% of the total number of nematodes was still moving on *B. ambifaria* plates (**Fig. 4**). In the case of *B. stabilis*, it was observed that paralyzed worms at 4 h were able to move again and survive. One plausible explanation for this variation might be related to low stability of the diffusible toxins/virulence determinants produced by those strains that require constant production.

Interestingly, when the toxin filter assay was performed on NGM medium, no paralysis or mortality was detected. This experiment confirms that FKA rapid killing kinetics revealed a role for diffusible toxins as a main component of the infectious process.

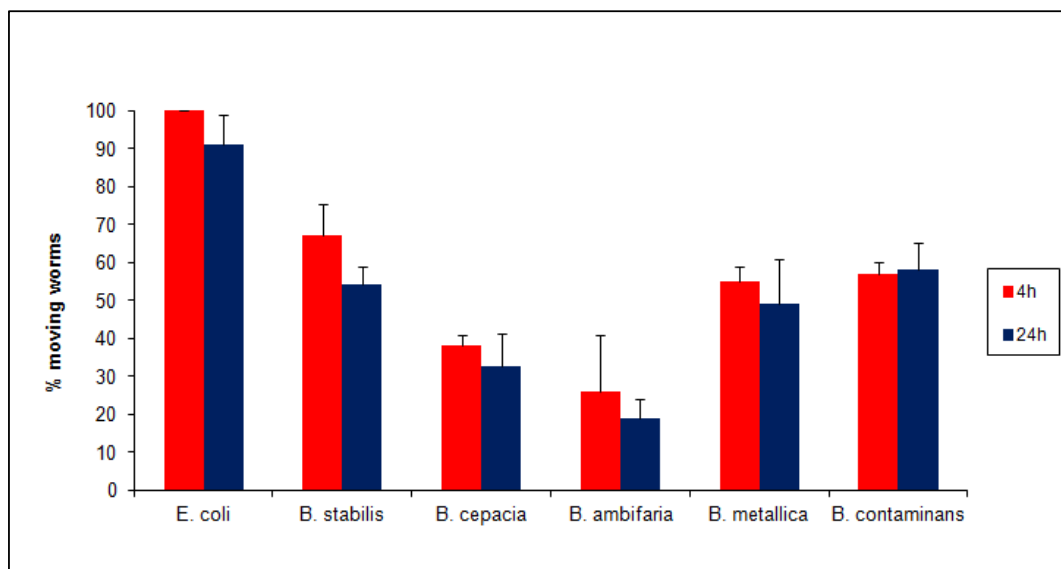


Fig. 4: Secreted compounds or toxins mediate fast killing. Data reports paralysis and mortality at 4 and 24 h of worms plated on PGS medium plates treated with Bcc strains or *E. coli* grown on a sterile disk. Data represent mean values of three independent experiments and SD values are reported. P-values were calculated between sample (Bcc) and control (OP50) at the corresponding time, and were always < 0.05.

Thomson and Dennis demonstrated the production by Bcc strains of a haemolytic toxin required for full virulence, synthesized by a non-ribosomal peptide synthase (NRPS) pathway, typical of a complex secondary metabolite [49]. They screened a panel of Bcc strains including *B. cenocepacia*, *B. stabilis*, *B. pyrrocinia* and *B. vietnamiensis* for the presence of this gene cluster. A NRPS cluster was identified in *B. pyrrocinia* and *B. stabilis* with VR=3 on FKA. Moreover, Bcc strains are known to produce toxins with demonstrated antifungal activity like the cyclic peptides occidiofungins (burkholdines) [50]. Therefore, we cannot *a priori* exclude the possibility that a peptide might represent the toxin active towards *C. elegans*.

Killing of MRPs knock-out *C. elegans* mutants by Bcc member strains

The nematode-Bcc pathogenicity ranking system developed was investigated for its ability to detect and map genotype-specific host responses. We obtained access to a complete, seven MRPs knock-out nematode mutant set, *mrp-1(pk89)*, *mrp-2(ok2157)*, *mrp-3(ok955)*, *mrp-4(ok1095)*, *mrp-5(ok2067)*, *mrp-6(ok1027)* and *mrp-8(ok1360)*, impaired in the corresponding ABC membrane transporters.

These knock-out mutants exhibited identical phenotypic attributes with the WT. The 18 Bcc representative strains were profiled against the 7 mutants in both SKA and FKA. Control mortality was calculated to be the number of dead worms divided by the number of total worms. Pooled mortality counts (alive vs. dead) for each mutant were tested against the WT using Fisher's Exact test. Statistically significant (Bonferroni-Holm corrected p-value < 0.05) differences from WT are shown in **Table 2**. The mortality rates calculated were highly variable suggesting a Bcc strain-specific effect towards the MRP *C. elegans* mutants. Some trends were detected: *mrp-5* and *mrp-2* had increased mortality rate for several Bcc strains in both SKA and FKA. Specifically, 8 Bcc strains in SKA and 9 in FKA showed increased killing towards *mrp-5*, while 8 strains in SKA and 8 in FKA appeared more virulent against *mrp-2*. *C. elegans* mutants *mrp-3* and *mrp-4* displayed lower killing rates when incubated with several Bcc strains. In particular, mutant *mrp-4* exhibited decreased mortality to 8 Bcc species in SKA and to 7 strains in FKA. Regarding the Bcc strains, on SKA *B. ambifaria* displayed increased virulence towards the whole mutant set, with mortality rate compared to the WT higher than 75% and 71% towards, *mrp-5* and *mrp-6* respectively. *B. arboris* demonstrated an increased pathogenic effect towards *mrp-1*, *mrp-2*, *mrp-6*, *mrp-8*, while *B. dolosa* was more lethal against *mrp-2*, *mrp-5*, *mrp-6*, *mrp-8* mutants. On FKA, *B. lata* and *B. multivorans* were the most pathogenic strains with increased mortality rate against all mutants, while *B. diffusa* was more virulent against 6 mutants, and *B. arboris* against 5 mutants.

Strain	WT Mortality FKA	Significant Changes in % Mortality						
		mrp-1	mrp-2	mrp-3	mrp-4	mrp-5	mrp-6	mrp-8
<i>B. ambifaria</i>	95	NS	-27	NS	NS	NS	NS	NS
<i>B. anthina</i>	42	45	50	NS	NS	58	NS	NS
<i>B. arboris</i>	28	70	72	21	NS	NS	72	72
<i>B. cenocepacia</i>	64	NS	31	NS	-45	NS	27	NS
<i>B. cepacia</i>	100	-19	NS	NS	-19	NS	-15	-18
<i>B. contaminans</i>	94	NS	NS	-17	-16	NS	NS	NS
<i>B. diffusa</i>	69	NS	NS	NS	NS	NS	NS	-26
<i>B. dolosa</i>	31	33	NS	59	NS	48	49	NS
<i>B. latens</i>	42	NS	NS	-34	NS	38	NS	-28
<i>B. metallica</i>	100	NS	NS	-13	-17	NS	NS	-10
<i>B. pseudomultivorans</i>	20	NS	NS	NS	NS	50	NS	NS
<i>B. pyrrocinia</i>	70	NS	21	-44	-35	26	NS	29
<i>B. seminalis</i>	64	NS	NS	-44	-31	NS	NS	NS
<i>B. stabilis</i>	100	-9	-47	NS	NS	-10	-63%	-77%
<i>B. ubonensis</i>	52	NS	41	NS	-24%	38	NS	32
<i>B. vietnamiensis</i>	14	NS	40	-12%	NS	57	61	35
<i>B. lata</i>	18	38	64	27	42	70	54	53
<i>B. multivorans</i>	7	33	22	21	34	62	28	45
Strain	WT Mortality SKA	mrp-1	mrp-2	mrp-3	mrp-4	mrp-5	mrp-6	mrp-8
<i>B. ambifaria</i>	6	61	67	30	28	75	71	58
<i>B. anthina</i>	91	9	NS	-27	-24	NS	NS	NS
<i>B. arboris</i>	46	53	54	-35	NS	NS	50	51
<i>B. cenocepacia</i>	81	NS	NS	NS	-77	-65	-24	-54
<i>B. cepacia</i>	9	81	75	NS	NS	78	62	45
<i>B. contaminans</i>	47	30	26	49	NS	NS	NS	NS
<i>B. diffusa</i>	88	NS	NS	NS	-25	NS	NS	NS
<i>B. dolosa</i>	13	NS	25	NS	NS	61	61	28
<i>B. latens</i>	22	NS	43	-19	-19	46	NS	42
<i>B. metallica</i>	100	NS	NS	-14%	-8%	NS	NS	NS
<i>B. pseudomultivorans</i>	11	NS	NS	NS	NS	30	NS	NS
<i>B. pyrrocinia</i>	5	53	61	NS	NS	64	57	46
<i>B. seminalis</i>	69	28	NS	-50	-67	NS	NS	NS
<i>B. stabilis</i>	100	-90	-58	NS	NS	-55	-60	-84
<i>B. ubonensis</i>	83	-60	NS	-28	-36	NS	NS	NS
<i>B. vietnamiensis</i>	46	-44	-39	-43	-44	-34	50	-41
<i>B. lata</i>	10	NS	NS	NS	NS	52	NS	NS
<i>B. multivorans</i>	3	NS	22	NS	NS	35	41	NS

Table 2. MRP knock-out *C. elegans* mutants mortality expressed as percentage of dead worms and comparison between the mutants and the WT. Mutant mrp-5 was tested as heterozygote, due to

lethality of the mutation in homozygosis. Statistical significant differences appear highlighted, with negative values (blue) indicating statistically significant reductions in mortality from WT, and with positive values (red) indicating statistically significant increases in mortality from WT. NS= Not significant difference.

The complete set of killing results for each Bcc strain generated a unique killing profile in each MRP mutant. To determine whether these profiles constitute a coherent mutant classification pattern, a hierarchical clustering of significant effect sizes vs. each strain (Ward's method, Consistency Threshold 1.1) was performed. This analysis showed different patterns for *mrp-3* and *mrp-4* when compared with the rest of MRP-phenotypes in both FKA and SKA. However, *mrp-3* and *mrp-4* share low sequence identity/similarity among them (data not shown), suggesting that these two transporters do not have similar substrate specificity or function. These MRP-phenotypes were grouped consistently and differentiated from the rest of single knock out strains (**Fig. 5**). This pattern could justify the diverse phenotypic response to Bcc of the MRP knock-out mutants, indicating variation in substrate profile specificity for the 7 MRP efflux systems. The clustering patterns of the other transporters suggest distinct substrate specificity, in agreement with the low degree of sequence identity/similarity shared among them (data not shown). Nevertheless, we can assume that toxins and small molecules are MRP-related substrates, and these transporters play a fundamental role in Bcc defence, with the exception of *mrp-3* and *mrp-4*.

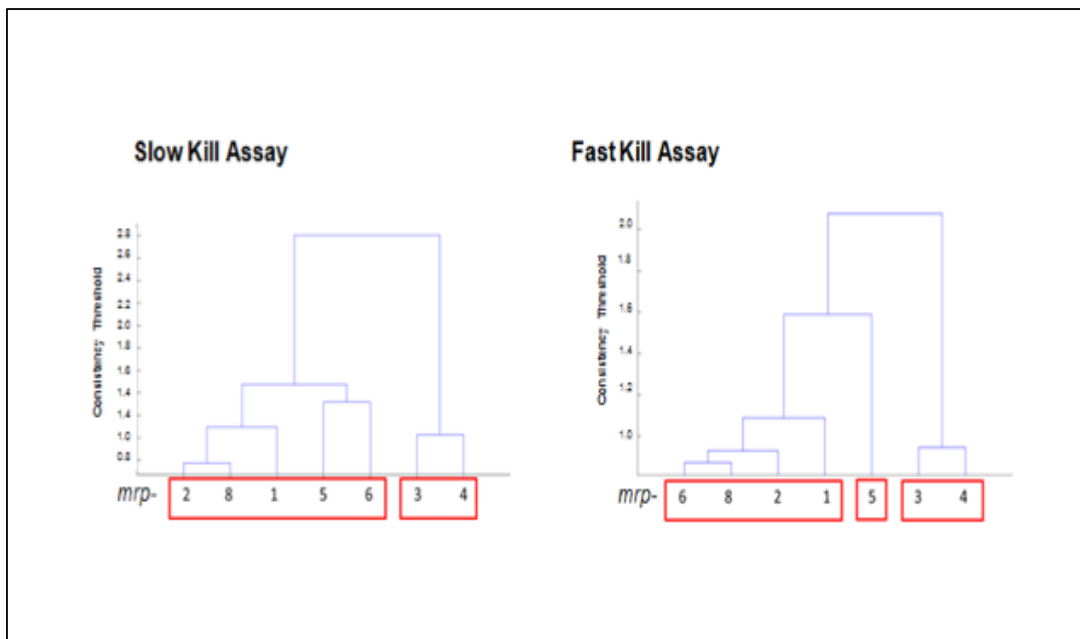


Figure 5: Hierarchical Clusterings. Ward's method with a consistency threshold 1.1 used to cluster mutants based on significant changes in pathogenicity.

Inhibitor experiments

The Bcc pathogenicity ranking system was used to facilitate testing for a distinct MRP-efflux system substrate profile within the content of infection. Disabling efflux pumps genetically (knock-outs) or chemically (small molecules-inhibitors) should have a similar toll on increasing nematode mortality. A pilot analysis was performed utilizing the Bcc strains that exhibited increased *C. elegans* susceptibility in numerous efflux knock-outs on SKA (*B. ambifaria*, *B. arboris*, *B. cepacia*, *B. dolosa*, *B. pyrrocinia*) and the well-characterized mammalian MRP-efflux inhibitors mometasone furoate, lasalocid A and verapamil [51]. All compounds did not affect Bcc or *C. elegans* viability at the concentration used for the assay (**Figure S1**). The compounds were spread in concentration ranges onto NGM plates to perform SKA and DMSO (0.5 %) was used as a growth control. Control mortality was calculated to be the number of dead worms divided by the number of total worms. Comparison to solvent control of pooled mortality counts was done using Fisher's Exact test; results were considered significant if Bonferroni-Holm corrected *p*-values were less than 0.05. Statistically significant differences from the WT are shown in **Table 3**. Reduction in mortality from the controls was not observed. The inhibitor use in the infection system, provided a statistically significant increase of mortality in the presence of at least one inhibitor compared to DMSO controls for 3 Bcc strains, whereas *B. pyrrocinia* and *B. ambifaria* killing rates were not affected.

In particular, the presence of mometasone (100 μ M), *B. arboris*, *B. cepacia* and *B. dolosa* enhanced virulence against nematodes with mortality rate of 40% higher than the control. Lasalocid (500 nM) caused an increase in the percentage of dead worms of 34% and 48 % with *B. cepacia* and *B. dolosa*, respectively. Verapamil (100 μ M) enhanced killing only for *B. arboris*, with a killing rate of 35% higher than the control. These results demonstrated that the inhibitor driven MRP transporter inactivation results in increased mortality at least for two inhibitors, of the nematodes to Bcc strains, supporting the role of these transporters in Bcc infection. Verapamil has been characterized as a competitive inhibitor in ABCB1 malignant cell overexpression [52] as well as a potent ABCC family inhibitor [53]. It is also involved in inhibiting *C. elegans* P-gp1, which is involved in nematode resistance to ivermectine [54]. The present experimental setup differs as it explores verapamil against a number of targets simultaneously not by isolating transporters of interest. This analysis suggests that verapamil very likely works, but the number of interactions leading to a weaker phenotype should be investigated further.

Strain	Control Mortality	Significant Changes in % Mortality								
		Verapamil			Mometasone			Lasalocid		
		100 μ M	50 μ M	25 μ M	100 μ M	50 μ M	25 μ M	500 nM	250 nM	125 nM
<i>B. cepacia</i>	17	NS	NS	NS	45	NS	NS	34	NS	NS
<i>B. arboris</i>	20	35	NS	27	45	NS	NS	NS	NS	NS
<i>B. dolosa</i>	32	NS	NS	NS	44	29	NS	48	38	NS

Table 3. Effect of ABC inhibitors during *C. elegans*- Bcc infection on SKA.Nematodes mortality expressed as percentage of dead worms and compared between samples with inhibitors and control with DMSO (0,5%). Statistical significant differences appear highlighted (red). NS= Not significant difference

1.4 Conclusions

The major aim of this work was to inquire the role of host transporters in the infection developing a nematode virulence ranking system focusing in well-recognized Bcc strains. It is common knowledge that every bacterial species includes member-strains with different pathogenic characteristics. However, the key purpose was to build the model using type strains of each of the 18 currently known Bcc species, a combination of two different killing assays (SKA and FKA), and a set of nematode mutants impaired in MRP efflux transporters. We focused on type strains due to the extensive information known, as many Bcc genomes have been completely sequenced and more will be soon become available. To define Bcc virulence we established a VR scheme, based on the percentage of surviving worms. Both nematocidal assays revealed different pathogenicity profiles for the Bcc species. Strains with high score in the VR system were able to accumulate in the nematodes intestine and produce virulence factors, on SKA and FKA, respectively. Only Bcc CF isolates accumulate within worms, an observation that correlates well with the apparent differences in virulence factors between environmental and CF isolates. This VR scheme was applied to profile Bcc pathogenesis in seven MRP impaired *C. elegans* mutants. MRPs are implicated in distinct nematode cellular processes: MRP1 is involved in heavy metal tolerance and ivermectine resistance [42,43]; MRP4 is central in early-stage differentiation [55]; MRP5 acts as a fundamental heme exporter into embryonic development [56]. Results showed increased nematode mortality for several *C. elegans* mutants grown in the presence of specific Bcc strains compared to WT nematodes. In particular *mrp-2* and *mrp-5* were the most susceptible mutants with increased mortality respectively in 13 and 11 different Bcc strains in the two assays, suggesting an active role of these two efflux transporters in host defense. However strain *mrp-5* was tested only in heterozygosis and this could have affected survival rate. Cluster analysis consistently grouped and separated *mrp-3* and *mrp-4* mutants in both assays from the other MRP-phenotypes. This pattern suggested different substrate specificity for these MRP transporters. To further explore the role of MRP transporters in host defense, inhibitor experiments were carried out on a selected panel of the five most "infectious" Bcc strains against the MRP knock-out mutants (*B. ambifaria*, *B. arboris*, *B. cepacia*, *B. dolosa*, *B. pyrrocinia*). These strains were tested against the WT nematodes in the presence of three well-characterized MRP-inhibitors, with a broad inhibitory activity against MRP transporters [51]. These results suggested that chemically disabling of the MRPs resulted in increased *C. elegans* susceptibility to Bcc strains. The use of mometasone and lasalocid in the infection system increased killing rate when incubated with *B. cepacia* and *B. dolosa*, while verapamil showed a mild effect for *B. arboris*. In conclusion, this study provided tools to correlate microbial pathogenicity with the host transporters, and highlighted specific efflux systems with a central role in Bcc virulence.

It is worth noting that MRPs share components of a conserved activation mechanism with the Cystic Fibrosis Transmembrane conductance Regulator (CFTR)[57,58]. Therefore, identification of bacterial signalling molecules with substrate specificity in recognizing MRPs CFRT-like efflux transporters involved in host response could be a starting point for the development of novel therapeutic strategies.

1.5 References:

1. Compant S, N.J., Coenye T, Clement C, Ait Barka E, *Diversity and occurrence of Burkholderia spp. in the natural environment*. FEMS Microbiol Rev, 2008. **32(4)**: p. 607-626.
2. Coenye, T. and P. Vandamme, *Diversity and significance of Burkholderia species occupying diverse ecological niches*. Environ Microbiol, 2003. **5(9)**: p. 719-29.
3. Peeters, C., et al., *Burkholderia pseudomultivorans sp. nov., a novel Burkholderia cepacia complex species from human respiratory samples and the rhizosphere*. Syst Appl Microbiol, 2013. **36(7)**: p. 483-9.
4. Mahenthiralingam, E., T.A. Urban, and J.B. Goldberg, *The multifarious, multireplicon Burkholderia cepacia complex*. Nat Rev Microbiol, 2005. **3(2)**: p. 144-56.
5. De Smet, B., et al., *Burkholderia stagnalis sp. nov. and Burkholderia territorii sp. nov., two novel Burkholderia cepacia complex species from environmental and human sources*. Int J Syst Evol Microbiol, 2015. **65(7)**: p. 2265-71.
6. Ramsay, K.A., et al., *Factors influencing acquisition of Burkholderia cepacia complex organisms in patients with cystic fibrosis*. J Clin Microbiol, 2013. **51(12)**: p. 3975-80.
7. Rose, H., et al., *Biocide susceptibility of the Burkholderia cepacia complex*. J Antimicrob Chemother, 2009. **63(3)**: p. 502-10.
8. Nash, E.F., et al., *"Cepacia syndrome" associated with Burkholderia cepacia (genomovar I) infection in an adolescent with cystic fibrosis*. Pediatr Pulmonol, 2010.
9. Bazzini, S., C. Udine, and G. Riccardi, *Molecular approaches to pathogenesis study of Burkholderia cenocepacia, an important cystic fibrosis opportunistic bacterium*. Appl Microbiol Biotechnol, 2011. **92(5)**: p. 887-95.
10. Drevinek, P. and E. Mahenthiralingam, *Burkholderia cenocepacia in cystic fibrosis: epidemiology and molecular mechanisms of virulence*. Clin Microbiol Infect, 2010. **16(7)**: p. 821-30.
11. Fallon, J.P., E.P. Reeves, and K. Kavanagh, *The Aspergillus fumigatus toxin fumagillin suppresses the immune response of Galleria mellonella larvae by inhibiting the action of haemocytes*. Microbiology, 2011. **157(Pt 5)**: p. 1481-8.
12. Lionakis, M.S., *Drosophila and Galleria insect model hosts: new tools for the study of fungal virulence, pharmacology and immunology*. Virulence, 2011. **2(6)**: p. 521-7.
13. Abebe, E., et al., *An insect pathogenic symbiosis between a Caenorhabditis and Serratia*. Virulence, 2011. **2(2)**: p. 158-61.
14. Olsen, R.J., et al., *Virulence of serotype M3 Group A Streptococcus strains in wax worms (Galleria mellonella larvae)*. Virulence, 2011. **2(2)**: p. 111-9.
15. Uehlinger, S., et al., *Identification of specific and universal virulence factors in Burkholderia cenocepacia strains by using multiple infection hosts*. Infect Immun, 2009. **77(9)**: p. 4102-10.
16. Schwager, S., et al., *Identification of Burkholderia cenocepacia strain H111 virulence factors using nonmammalian infection hosts*. Infect Immun, 2013. **81(1)**: p. 143-53.
17. Kurz, C.L., et al., *Virulence factors of the human opportunistic pathogen Serratia marcescens identified by in vivo screening*. EMBO J, 2003. **22(7)**: p. 1451-60.

18. Mylonakis, E., et al., *The art of serendipity: killing of Caenorhabditis elegans by human pathogens as a model of bacterial and fungal pathogenesis*. Expert Rev Anti Infect Ther, 2003. **1**(1): p. 167-73.
19. Tan, M.W. and F.M. Ausubel, *Caenorhabditis elegans: a model genetic host to study Pseudomonas aeruginosa pathogenesis*. Curr Opin Microbiol, 2000. **3**(1): p. 29-34.
20. Bhatt, S., A. Anyanful, and D. Kalman, *CsrA and TnaB coregulate tryptophanase activity to promote exotoxin-induced killing of Caenorhabditis elegans by enteropathogenic Escherichia coli*. J Bacteriol, 2011. **193**(17): p. 4516-22.
21. Lee, S.H., et al., *Complete killing of Caenorhabditis elegans by Burkholderia pseudomallei is dependent on prolonged direct association with the viable pathogen*. PLoS One, 2011. **6**(3): p. e16707.
22. O'Quinn, A.L., E.M. Wiegand, and J.A. Jeddelloh, *Burkholderia pseudomallei kills the nematode Caenorhabditis elegans using an endotoxin-mediated paralysis*. Cell Microbiol, 2001. **3**(6): p. 381-93.
23. Lee, S.H., et al., *Burkholderia pseudomallei suppresses Caenorhabditis elegans immunity by specific degradation of a GATA transcription factor*. Proc Natl Acad Sci U S A, 2013.
24. Huber, B., et al., *Identification of a novel virulence factor in Burkholderia cenocepacia H111 required for efficient slow killing of Caenorhabditis elegans*. Infect Immun, 2004. **72**(12): p. 7220-30.
25. Kothe, M., et al., *Killing of Caenorhabditis elegans by Burkholderia cepacia is controlled by the cep quorum-sensing system*. Cell Microbiol, 2003. **5**(5): p. 343-51.
26. Sousa, S.A., C.G. Ramos, and J.H. Leitao, *Burkholderia cepacia Complex: Emerging Multihost Pathogens Equipped with a Wide Range of Virulence Factors and Determinants*. Int J Microbiol, 2011. **2011**.
27. Tegos, G.P., M.K. Haynes, and H.P. Schweizer, *Dissecting novel virulent determinants in the Burkholderia cepacia complex*. Virulence, 2012. **3**(3): p. 234-7.
28. O'Grady, E.P., D.F. Viteri, and P.A. Sokol, *A unique regulator contributes to quorum sensing and virulence in Burkholderia cenocepacia*. PLoS One, 2012. **7**(5): p. e37611.
29. Cooper, V.S., W.A. Carlson, and J.J. Lipuma, *Susceptibility of Caenorhabditis elegans to Burkholderia infection depends on prior diet and secreted bacterial attractants*. PLoS One, 2009. **4**(11): p. e7961.
30. Cardona, S.T., et al., *Diverse pathogenicity of Burkholderia cepacia complex strains in the Caenorhabditis elegans host model*. FEMS Microbiol Lett, 2005. **250**(1): p. 97-104.
31. Springman, A.C., et al., *Genetic diversity and multihost pathogenicity of clinical and environmental strains of Burkholderia cenocepacia*. Appl Environ Microbiol, 2009. **75**(16): p. 5250-60.
32. Sousa, S.A., et al., *The hfq gene is required for stress resistance and full virulence of Burkholderia cepacia to the nematode Caenorhabditis elegans*. Microbiology, 2010. **156**(Pt 3): p. 896-908.
33. Markey, K.M., et al., *Caenorhabditis elegans killing assay as an infection model to study the role of type III secretion in Burkholderia cenocepacia*. J Med Microbiol, 2006. **55**(Pt 7): p. 967-9.

34. Martinez, J.L., et al., *Functional role of bacterial multidrug efflux pumps in microbial natural ecosystems*. FEMS Microbiol Rev, 2009. **33**(2): p. 430-49.
35. Buroni, S., et al., *Assessment of three Resistance-Nodulation-Cell Division drug efflux transporters of Burkholderia cenocepacia in intrinsic antibiotic resistance*. BMC Microbiol, 2009. **9**: p. 200.
36. Feinbaum, R.L., et al., *Genome-wide identification of Pseudomonas aeruginosa virulence-related genes using a Caenorhabditis elegans infection model*. PLoS Pathog, 2012. **8**(7): p. e1002813.
37. Ooi, S.K., et al., *Burkholderia pseudomallei kills Caenorhabditis elegans through virulence mechanisms distinct from intestinal lumen colonization*. Virulence, 2012. **3**(6): p. 485-96.
38. Harland, D.N., et al., *ATP-binding cassette systems in Burkholderia pseudomallei and Burkholderia mallei*. BMC Genomics, 2007. **8**: p. 83.
39. Dean, M., A. Rzhetsky, and R. Allikmets, *The human ATP-binding cassette (ABC) transporter superfamily*. Genome Res, 2001. **11**(7): p. 1156-66.
40. Sheps, J.A., et al., *The ABC transporter gene family of Caenorhabditis elegans has implications for the evolutionary dynamics of multidrug resistance in eukaryotes*. Genome Biol, 2004. **5**(3): p. R15.
41. Rees, D., Johnson, E, Lewinson, O *ABC transporters: the power to change*. Nat Rev Mol Cell Biol, 2009. **10**: p. 218-227.
42. James, C.E. and M.W. Davey, *Increased expression of ABC transport proteins is associated with ivermectin resistance in the model nematode Caenorhabditis elegans*. Int J Parasitol, 2009. **39**(2): p. 213-20.
43. Yan, R., et al., *The role of several ABC transporter genes in ivermectin resistance in Caenorhabditis elegans*. Vet Parasitol, 2012. **190**(3-4): p. 519-29.
44. Kurz, C.L., et al., *Caenorhabditis elegans pgp-5 is involved in resistance to bacterial infection and heavy metal and its regulation requires TIR-1 and a p38 map kinase cascade*. Biochem Biophys Res Commun, 2007. **363**(2): p. 438-43.
45. Brenner, S., *The genetics of Caenorhabditis elegans*. Genetics, 1974. **77**: p. 71-94.
46. Stiernagle, T., *Maintenance of C. elegans* WormBook, The C. elegans Research Community, 2006.
47. Wopperer, J., et al., *A quorum-quenching approach to investigate the conservation of quorum-sensing-regulated functions within the Burkholderia cepacia complex*. Appl Environ Microbiol, 2006. **72**(2): p. 1579-87.
48. Pirone, L., et al., *Burkholderia cenocepacia strains isolated from cystic fibrosis patients are apparently more invasive and more virulent than rhizosphere strains*. Environ Microbiol, 2008. **10**(10): p. 2773-84.
49. Thomson, E.L. and J.J. Dennis, *A Burkholderia cepacia complex non-ribosomal peptide-synthesized toxin is hemolytic and required for full virulence*. Virulence, 2012. **3**(3): p. 286-98.
50. Lu, S.E., et al., *Occidiofungin, a unique antifungal glycopeptide produced by a strain of Burkholderia contaminans*. Biochemistry, 2009. **48**(35): p. 8312-21.
51. Strouse, J.J., et al., *Fluorescent substrates for flow cytometric evaluation of efflux inhibition in ABCB1, ABCC1, and ABCG2 transporters*. Anal Biochem, 2013. **437**(1): p. 77-87.

52. Horger, K.S., et al., *Hydrogel-assisted functional reconstitution of human P-glycoprotein (ABCB1) in giant liposomes*. *Biochim Biophys Acta*, 2015. **1848**(2): p. 643-53.
53. Eilers, M., U. Roy, and D. Mondal, *MRP (ABCC) transporters-mediated efflux of anti-HIV drugs, saquinavir and zidovudine, from human endothelial cells*. *Exp Biol Med (Maywood)*, 2008. **233**(9): p. 1149-60.
54. Ardelli, B.F. and R.K. Prichard, *Inhibition of P-glycoprotein enhances sensitivity of Caenorhabditis elegans to ivermectin*. *Vet Parasitol*, 2013. **191**(3-4): p. 264-75.
55. Currie, E., et al., *Role of the Caenorhabditis elegans multidrug resistance gene, mrp-4, in gut granule differentiation*. *Genetics*, 2007. **177**(3): p. 1569-82.
56. Korolnek, T., et al., *Control of metazoan heme homeostasis by a conserved multidrug resistance protein*. *Cell Metab*, 2014. **19**(6): p. 1008-19.
57. Wei, S., et al., *Conserved allosteric hot spots in the transmembrane domains of cystic fibrosis transmembrane conductance regulator (CFTR) channels and multidrug resistance protein (MRP) pumps*. *J Biol Chem*, 2014. **289**(29): p. 19942-57.
58. Keppler, D., *Multidrug resistance proteins (MRPs, ABCs): importance for pathophysiology and drug therapy*. *Handb Exp Pharmacol*, 2011(201): p. 299-323.

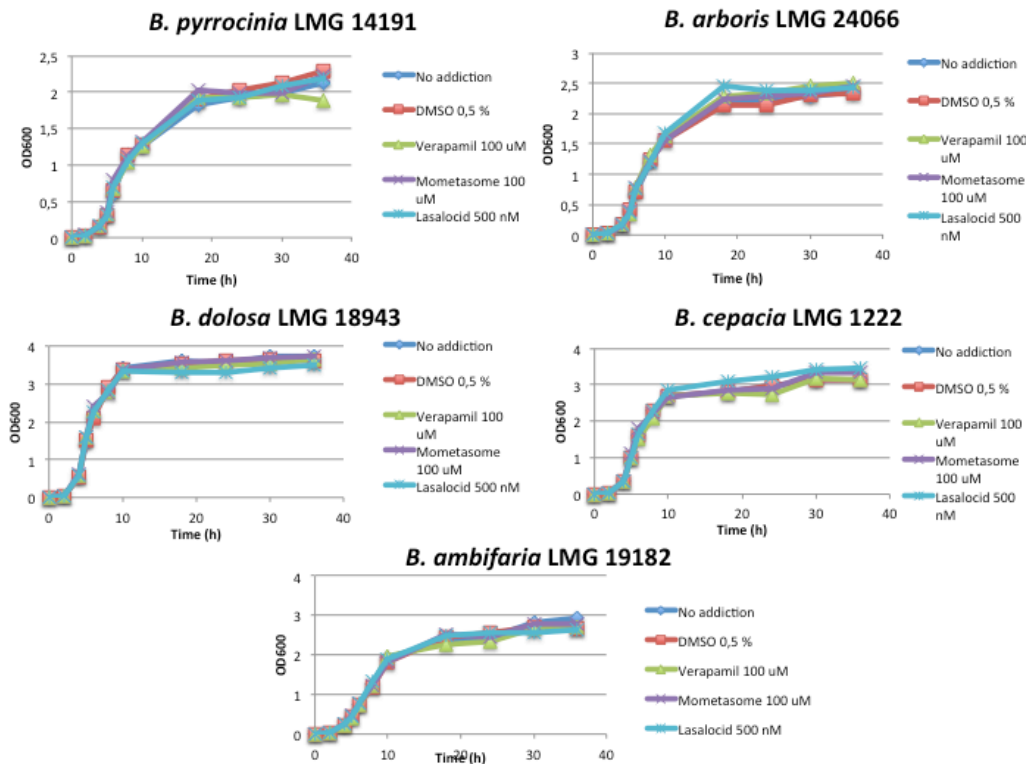
1.6 Supplementary material

S1 Figure. Bcc strain growth in the presence of inhibitors.

For the Bcc strain growth curves in the presence of inhibitors, one single colony of each Bcc strain was placed in a tube containing 3 mL of LB broth. The tubes were then incubated at 37°C overnight in agitation. The overnight cultures were used to inoculate 250 mL flasks containing 50 mL of LB broth plus the inhibitors at an initial concentration of 0.01 OD₆₀₀/mL. For each strain, a set of 5 flasks was employed: 1) Verapamile 100 µM; 2) Mometasone 100 µM; 3) Lasalocid 500 nM; 4) DMSO 0.5% v/v; 5) control (no inhibitor or DMSO). The flasks were incubated at 37°C in agitation at 220 rpm.

Bacterial growth was monitored following OD₆₀₀ for 36 hours every 2 hours. The experiments were performed in duplicate and the data reported represent mean values. Error bars were omitted for clarity.

Results proved that the inhibitors did not interfere with Bcc growth at the concentration used in our assays. as The growth curves obtained for each strain are very similar with no viable effect in growth by any inhibitor.



CHAPTER 2

**Antimicrobial activity of
monoramnholipids produced by
bacterial strains isolated from
Ross sea (Antarctica)**

Antimicrobial activity of monoramnholipids produced by bacterial strains isolated from Ross sea (Antarctica)

Abstract

Microorganisms living in extreme environments represent a huge reservoir of novel antimicrobial compounds and possibly of novel chemical families. Antarctica is one of the most extraordinary places on Earth and exhibits many distinctive features. Antarctic microorganisms are well known producers of valuable secondary metabolites. Specifically, several Antarctic strains have been reported to inhibit opportunistic human pathogens strains belonging to *Burkholderia cepacia* complex (Bcc). Herein, we applied a biodiscovery pipeline for the identification of anti-Bcc compounds. Antarctic sub-sea sediments were collected from the Ross Sea, and used to isolate 25 microorganisms, which were phylogenetically affiliated to three bacterial genera (*Psychrobacter*, *Arthrobacter*, and *Pseudomonas*) via sequencing and analysis of 16S rRNA genes. They were then subjected to a primary cell-based screening to determine their bioactivity against Bcc strains. Positive isolates were used to produce crude extracts from microbial spent culture media, to perform the secondary screening. Strain *Pseudomonas* BNT1 was then selected for bioassay-guided purification employing SPE and HPLC. Finally, LC-MS and NMR structurally resolved the purified bioactive compounds. With this strategy, we achieved the isolation of 3 Rhamnolipids, two of which were new, embedded with high (MIC < 1 µg/mL) and unreported antimicrobial activity against Bcc strains.

Keywords: Antimicrobials; rhamnolipids; cold-adapted bacteria, bioprospecting, *Burkholderia cepacia* complex

2.1 Introduction

The alarming rise of Multi-Drug Resistance (MDR) bacteria in the last decades has highlighted the need for novel antimicrobial compounds and for effective drug discovery approaches [1, 2]. Natural products are the largest source of new antibiotic molecules, representing about two-thirds of new antibacterial therapies approved between 1980 and 2010 [3, 4]. Bioprospecting for natural products from unexplored natural environments, such as the marine environment is considered a promising strategy to identify novel compounds. It is increasingly recognized that a huge number of natural products and novel chemical entities exist in these environments, but the overwhelming biological diversity of these environments has so far only been explored to a very limited extent [5, 6]. The Antarctic environment, as well as having incredibly low temperatures, possesses other diverse traits that may have helped to shape the unique way in which Antarctic bacteria have evolved. This extreme environment contains hyper-salinity that exists in sea ice brine channels, a lack of free water due to freezing temperatures, as well as low nutrient availability. Unique light conditions also exist due to the high latitude of the region. Several studies have shown that Antarctic bacteria harvested from Antarctic corals and sponges are promising source of new antimicrobial compounds [7-14]. Specifically, several Antarctic strains belonging to the genus *Pseudoalteromonas*, *Psychrobacter*, *Pseudomonas*, and *Arthrobacter*, were able to inhibit the growth of several strains belonging to the *Burkholderia cepacia* complex (Bcc) [11, 14]. Further studies demonstrated that the antimicrobial activity relies (at least in part) on the production of Volatile Organic Compounds (VOCs)[12, 13, 15]. The Bcc consists of at least 20 closely related species inhabiting different ecological niches such as water, soil, plants rizosphere, and plants and animals [16-18]. Bcc are also opportunistic human pathogens that cause lung infections in immune-compromised individuals, including cystic fibrosis (CF) patients [19]. In one-third of infected individuals it causes the “cepacia syndrome” – a form of septic shock, which involves the lungs essentially shutting down resulting in fatality [20-22]. Bcc bacteria have showed to be very resilient and incredibly difficult to combat as they are resistant to almost all known antimicrobial agents and can survive under the most extreme conditions [23]. In this publication we report a complete biodiscovery pipeline aiming at the identification of novel anti-Bcc compounds, starting from the isolation of bacteria from Antarctic sub-sea sediments. Bacteria were tested for their antimicrobial potential and a bioassay-guided purification was performed that yielded 3 bioactive compounds active against Bcc. Structures were then elucidated and 2 compounds have not been reported previously.

2.2 Materials and methods

Isolation of bacterial strains

The Antarctic bacterial strains used in this study were isolated from environmental samples collected at -20 m of depth (sub-sea sediments) near the Mario Zucchelli Station, Baia Terranova, Ross sea, Antarctica (74.6936° S, 164.1117° E). 1 gr of sediments was mixed with 20 mL of M9 salts solution (KH₂PO₄ 3.0 g/L, Na₂HPO₄ 6.0 g/L, NaCl 0.5 g/L, NH₄Cl 1.0 g/L) in a 50 mL Falcon tube and gently mixed; the supernatant was serially diluted in sterile M9 buffer and plated on PYG medium (Peptone 5.0 g/L, Yeast extract 4.0 g/L, Glucose 1.0 g/L, CaCl₂ 0.2 g/L, MgSO₄·7H₂O 0.4 g/L, K₂HPO₄ 1.0 g/L, KH₂PO₄ 1.0 g/L, NaHCO₃ 10.0 g/L NaCl 2.0 g/L and 17 g/L).

After 15 days of incubation 24 visible colonies were picked, grown in liquid PYG and stored at -80°C.

Target strains and growth conditions

Bcc strains used in this work are listed in **Table 2** and **Table S1**. Bcc and *S. aureus* 6538P were routinely grown on Luria-Bertani broth (LB) (Tryptone 10 g/L, Yeast extract 5 g/L, NaCl 10 g/L) at 37 °C. BTN isolated Antarctic strains were routinely grown in TYP medium (Bacto-tryptone 16 g/L, 16 g/L Yeast extract, 10 g/L NaCl) and Marine Broth (MB) at 21 °C. To allow bacterial growth on solid media, 17 g/L of bacteriological agar were added to each medium.

RAPD analysis

Typing of bacterial isolates was performed using the Random Amplified Polymorphic DNA (RAPD) technique performed on cell lysates [24-26]; to this purpose, Antarctic bacterial colonies grown overnight at 21°C on MA plates were suspended in 25 µl of sterile distilled water, heated to 95°C for 10 min, and cooled on ice for 5min. RAPD analysis was carried out in a total volume of 25µl containing 1X Reaction Buffer, 300 µM MgCl₂, 200 µM of each deoxynucleoside triphosphate, 0.5 U of Polytaq DNA polymerase (Polymed, Florence, Italy), 10 µM of primer 1253 (5' GTTCCGCC 3') or primer AP5 (5' TCACGCTGCG 3') and 2 µl of lysate cell suspension [26]. PCR were performed using MasterCycle Personal Thermal Cycler (Eppendorf, Hamburg, Germany). After incubation at 90°C for 1 min and 95°C for 1.5 min, the reaction mixtures were cycled 45 times through the following temperature profile: 95°C for 30 s, 36°C for 1 min, and 75°C for 1 min. Samples were then incubated at 60°C for 10 min, and finally at 5° C for 10 min. Amplification products were then stored at -20°C. Reaction products were analyzed by agarose (2.5 % w/v) gel electrophoresis in TAE buffer containing 0.5 µg/ml (w/v) of ethidium bromide.

Phylogenetic affiliation of BTN strains

Two µl of each cell lysate were used for the amplification *via* PCR of 16S rRNA genes. PCR were carried out in a total volume of 50 µl containing 1X Reaction Buffer, 150 µM MgCl₂, 250 µM of each deoxynucleoside triphosphate, and 2.0 U of Polytaq DNA polymerase and 0.6 µM of primer P0 (5' GAGAGTTTGATCCTGGCTCAG) and P6 (5' CTACGGCTACCTTGTACGA)[27]. The reaction conditions used were: 1 cycle (95° C for 90 s), 30 cycles (95° C 30 s, 50° C 30 s, and 72° C 1 min), with a final extension of 10 min at 72 °C. Amplicons corresponding to the 16S rRNA genes (observed under UV light, 312 nm) were excised from the gel and purified using the "QIAquick" gel extraction kit (QiAgen, Chatsworth, CA) according to manufacturer's instructions. Direct sequencing was performed on both DNA strands using an ABI PRISM 310 Genetic Analyzer (Applied Biosystems, Forster City, CA) and the chemical dye terminator [28]. Each 16S rRNA gene sequence was submitted to GenBank and assigned the accession number shown in Table 1. BLAST probing of DNA databases was performed with the BLASTn option of the BLAST program using default parameters [29]. Nucleotide sequences were retrieved from RDP databases. The ClustalW program was used to align the 16S rRNA gene sequences obtained with the most similar ones retrieved from the databases [30]. Each alignment was checked manually, corrected, and then analysed. The evolutionary history was inferred using the Neighbor-Joining method according to the model of Kimura 2-parameter distances [31, 32]. The percentage of replicate trees where the associated

taxa clustered together in the bootstrap test (1000 replicates) is shown next to the branches [33].

Cross streaking

Cross-streaking experiments were carried out as previously described [11]. Petri dishes with or without a septum separating two hemi-cycles were used. Plates with a central septum allowed the growth of tester and target strains without any physical contact. Antarctic strains (tester strains) were grown on MA for four days at 21°C; then they were streaked on TYP and incubated at 21°C for four days. Bcc strains (target strains) were perpendicularly streaked to the initial streak and plates were further incubated at 21°C for two days and at 37°C for two additional days. The experiments were conducted in parallel with a positive control to verify the viability of Bcc cells.

Extract preparation

A single colony of a bacterial isolate was used to inoculate 3 mL of liquid TYP media in sterile bacteriological tube. After 48 h of incubation at 21°C at 200 rpm the pre-inoculum was used to inoculate 100 mL of TYP medium in a 500 mL flask, at an initial cell concentration of 0.01-OD₆₀₀/mL. The flasks were incubated up to 5 days at 21°C at 200 rpm. The cultures were then centrifuged at 6800 x g at 4°C for 30', and the exhausted culture broths were collected and stored at -20°C. The exhausted culture broths were subjected to organic extraction using 3 volume of ethyl acetate in a 500 mL separatory funnel. The organic phase collected was evaporated using a Laborota 4000 rotary evaporator (Heidolph, Schwabach, Germany), and the extracts were weight, dissolved in 100% DMSO at 50 or 100 mg/mL and stored at -20°C.

Minimal inhibitory concentration assay (MIC)

To evaluate the antimicrobial potential of Antarctic extracts, samples were placed into each well of a 96-well microtiter plate at an initial concentration of 2% (v/v) and serially diluted using LB medium. Wells containing no compound represented the negative control. DMSO was used as control to determine the effect of solvent on cell growth. A single colony of a Bcc strain was used to inoculate 3 mL of liquid LB media in sterile bacteriological tube. After 6-8 h of incubation, growth was measured by monitoring the absorbance at 600 nm and about 40000 CFU were dispensed in each well of the prepared plate. Plates were incubated at 37°C for 24h and growth was measured with a Cytation3 Plate Reader (Biotek, Winoosky, VT) by monitoring the absorbance at 600 nm.

Minimal bactericidal concentration (MBC) assay

To determine the MBC, the dilution representing the MIC and two of the more concentrated test product dilutions were plated on LB agar plates and enumerated to determine CFU/ml. An aliquot of the positive control was plated and used to establish a baseline concentration of the microorganism used.

Purification of ethyl-acetate crude extract

Crude extract of 3L BTN1 fermentation, prepared as described above, was subjected to fractionation using Chromabond SPE C18 column cartridges (Macherey-Nagel, Duren, Germany) The sample was dissolved in methanol and loaded on the top of the column. Elution was performed at step increasing methanol concentration (25%-50%-100%-100%+TFA). HPLC separations were carried out using a VP 250/10

Nucleodur C18 HTec, 5 μm , (Macherey-Nagel Duren, Germany) connected to a Ultimate 3000 HPLC Chromatograph with a Ultimate 3000 Diode Array detector and in-line degasser (Dionex, Sunnyvale, CA). Detection was achieved on-line through a scan of wavelengths from 200 to 400 nm.

NMR- LCMS experiments

NMR data, both 1D and 2D were recorded on a spectrometer (Bruker, Billerica, MA) at 600 and 150 MHz for ^1H and ^{13}C respectively using an ID cryoprobe in methanol- d_4 as solvent. Chemical shifts are reported in parts per million (δ/ppm) downfield relative to residual CD_3OD at 3.31 ppm for protons and 49.0 ppm for carbons. High-resolution mass spectrometry and fragmentation data were recorded using a LTQ Orbitrap system (ThermoScientific, Whaltman, MA) coupled to an 1290 Infinity HPLC system (Agilent, Santa Clara, CA). The following conditions were used: capillary voltage 45 V, capillary temperature 320°C, auxiliary gas flow rate 10-20 arbitrary units, sheath gas flow rate 40-50 arbitrary units, spray voltage 4.5 kV, mass range 100-2000 amu (maximum resolution 30,000). Optical rotation measurements were recorded using a Perkin Elmer, Model 343 Polarimeter at 589 nm (Perkin Elmer, Whaltman, MA). The UV spectrum was recorded on a UV-Vis spectrophotometer model S10 (Spectromlab, Barcelona, Spain). The IR was recorded on a PerkinElmer FTIR Spectrum Two instrument (Perkin Elmer, Whaltman, MA).

Worms rescue experiments

In order to evaluate the antimicrobial effects of the isolated rhamnolipids *in vivo*, a procedure was set-up using the nematode *Caenorhabditis elegans*. *C. elegans* strain KU25 *pmk-1(km25)* was chosen for its susceptibility to pathogens [34]. This mutant was obtained from the *Caenorhabditis* Genetic Centre (CGC), and routinely kept on Nematode Growth Medium (NGM Peptone 2.5 g/L, NaCl 2.9 g/L, Bacto-Agar 17 g/L, CaCl_2 1 mM, Cholesterol 5 $\mu\text{g}/\text{mL}$, KH_2PO_4 25 mM, MgSO_4 1 mM) plates seeded with *E. coli* OP50 as a food source [35]. Nematodes were infected by two Bcc strains using Slow Killing Assay developed in a previous work [36]. 2.5-cm-diameter plates containing 3 ml of NGM agar were seeded with 50 μl of the overnight Bcc cultures, normalized to an OD_{600} of 1.5 and incubated for 24 h at 37 °C to allow the formation of a bacterial lawn. *C. elegans* worms were synchronized by bleaching treatment [37], and 30-40 worms at larval stage 4 (L4), were transferred to each plate and incubated at 20 °C for 24 h. The infected worms were then collected from the plates and washed three times with M9 buffer supplemented with the antibiotic Trimetoprim 50 $\mu\text{g}/\text{mL}$ to kill Bcc strain in solution. The worms were then transferred into a 24-multiwell plate containing M9 buffer, *E. coli* as a food source and **Compound 2** (the novel rhamnolipid with the lowest MIC against *B. cenocepacia* and *B. metallica*) at concentration of 50 $\mu\text{g}/\text{mL}$ to evaluate its *in vivo* activity. Trimetoprim at 50 $\mu\text{g}/\text{mL}$ and wells without any addition were used as control. The worms were incubated at 20°C for 2 days and survival count was performed daily. The experiments were performed in triplicate, and data reported are mean values \pm SD.

2.3 Results and Discussion

Isolation of bacteria, typing and phylogenetic analysis

Psychrophilic Antarctic bacteria were isolated from sediments on PYG minimal medium. After 15 days of incubation at 4°C, 25 visible colonies were picked and grown in liquid PYG at 15 °C for 48 hours in agitation, and glycerol stab were stored

at -80°C. In order to check whether the 25 bacterial isolates represented either the same or different strains, a RAPD analysis was carried out using the primers 1253 (5'-GTTTCCGCC-3') and AP5 (5'-TCACGCTGCG-3'). AP5.

Genus	Strains	RAPD profile	Accession number	
<i>Pseudomonas</i>	BTN1		KT989002	
	BTN6		KT989003	
	BTN7	1	KT989004	
	BTN8		KT989005	
	BTN9		KT989006	
	BTN10		KT989007	
	BTN3	2	KT989009	
	BTN19	3	KT989019	
	BTN20B		KT989021	
	BTN24	4	KT989022	
	BTN21	5	KT989025	
	BTN23	6	KT989024	
	BTN2	7	KT989008	
	BTN11	8	KT989011	
	BTN5	9	KT989010	
	BTN20A	4	KT989020	
	<i>Psychrobacter</i>	BTN15	10	KT989015
BTN13		11	KT989012	
BTN14		12	KT989013	
BTN17		13	KT989017	
BTN16		14	KT989016	
BTN18		15	KT989018	
BTN12		16	KT989014	
BTN22		17	KT989023	
<i>Arthrobacter</i>		BTN4	18	KT989001

Table 1. List of the strains used in this work, for each strain are reported the genus and the RAPD haplotype.

The RAPD profiles obtained were then compared among them; the comparative analysis obtained with primer 1253 revealed that the 25 Antarctic isolates were split into 18 different RAPD group (hereinafter RAPD haplotypes), most of which represented by just 1 bacterial isolate as summarized in **Table 1**. Two groups embedding more than one isolate were identified: group 1 (RAPD haplotype 1) including strains BTN1, BTN6, BTN 7, BTN8, BTN9 and BTN10 and group 4 (embedding isolates BTN20A, BTN20B, and BTN24). These data were completely confirmed by the RAPD analysis performed with primer. The phylogenetic affiliation of bacterial isolates was performed through the 16S rRNA genes amplification and analysis. To this purpose the 16S rRNA genes were PCR amplified and the nucleotide sequence of the amplicons determined. Each sequence was used as a query in a BLAST search to retrieve the most similar ones. Sequences were then aligned using the program ClustalW and the alignment was used to construct the phylogenetic trees shown in **Figure S1**, revealing that:

- i) As expected on the basis of the sharing of RAPD profiles, the six strains exhibiting the same RAPD profile (RAPD haplotype 1) share the same 16S rRNA gene sequence and clustered together joining the species *Pseudomonas azotoformans*.
- ii) Strain BTN4 was affiliated to the genus *Arthrobacter*.
- iii) All the other strains were affiliated to the genus *Psychrobacter* and, according to the different RAPD profile they exhibited, joined different *Psychrobacter* clades. The three strains (BTN20A, BTN24 and BTN 20B) sharing the same RAPD profile (RAPD haplotype 4), joined the same *Psychrobacter* cluster.

Cross-streaking experiments

In order to check the ability of Antarctic bacteria to inhibit the growth of Bcc strains, cross-streaking experiments were performed using representative of each RAPD haplotype as test strain. We used as targets a panel of 84 different Bcc strains belonging to 17 known species (see **Table S1**). Most of the strains had a clinical origin. Data obtained are summarized in **Table S1**, revealing that all BTN strains are able to completely inhibit the growth of Bcc strains. In order to check whether this anti-Bcc activity was due VOCs synthesis, a further cross-streaking experiment was performed using Petri dishes with a central septum, which physically separates the tester (Antarctic) from the target strains. To perform this analysis we selected the 17 Bcc type strains listed in **Table S2**, which are highlighted in red. Data obtained are reported in **Table 2** and revealed that the inhibitory power of the BTN strains decreased in the presence of the central septum. This finding suggested that BTN strains synthesize a combination of volatile and soluble molecules and that the Bcc-inhibitory activity likely might rely principally on the soluble fraction. Thus, we decided to concentrate our efforts on the soluble molecules for this study.

Bcc Strain	S	BTN strain																						
		1	2	3	5	11	13	14	4	12	15	16	17	18	19	20 a	20 b	21	22	23	C+			
<i>B. ambifaria</i> LMG 19182	W	-	-	-	-	-	-	-	-	-	-	-	-	-	-	-	-	-	-	-	-	+		
	N	-	-	-	-	-	-	-	-	-	-	-	-	-	-	-	-	-	-	-	-	-	+	
<i>B. anthina</i> LMG 20980	W	-	-	-	-	-	-	-	-	-	-	-	-	-	-	-	-	-	-	-	-	+		
	N	-	-	-	-	-	-	-	-	-	-	-	-	-	-	-	-	-	-	-	-	-	+	
<i>B. vietnamensis</i> LMG10929	W	-	-	-	-	-	-	-	-	-	-	-	-	-	-	-	±	-	-	-	-	+		
	N	-	-	-	-	-	-	-	-	-	-	-	-	-	-	-	-	-	-	-	-	-	+	
<i>B. cenocepacia</i> LMG 16656	W	±	-	±	±	-	±	-	-	-	-	±	±	-	±	±	-	-	-	-	-	+		
	N	-	-	-	-	-	-	-	-	-	-	-	-	-	-	-	-	-	-	-	-	-	+	
<i>B. cepacia</i> LMG 1222	W	±	±	±	±	±	±	±	±	±	±	±	±	±	±	±	±	±	±	±	±	±	+	
	N	-	-	-	-	-	-	-	-	-	-	-	-	-	-	-	-	-	-	-	-	-	+	
<i>B. contaminans</i> LMG 23361	W	±	±	±	±	±	±	±	±	±	±	±	±	±	±	±	±	±	±	±	±	±	+	
	N	-	-	-	-	-	-	-	-	-	-	-	-	-	-	-	-	-	-	-	-	-	+	
<i>B. diffusa</i> LMG 24065	W	±	±	±	±	±	±	±	±	±	±	±	±	±	±	±	±	±	±	±	±	±	+	
	N	-	-	-	-	-	-	-	-	-	-	-	-	-	-	-	-	-	-	-	-	-	+	
<i>B. dolosa</i> LMG 18943	W	±	±	±	±	±	±	±	±	±	±	±	±	±	±	±	±	±	±	±	±	±	+	
	N	-	-	-	-	-	-	-	-	-	-	-	-	-	-	-	-	-	-	-	-	-	+	
<i>B. lata</i> LMG 22485	W	±	±	±	±	±	±	±	-	±	±	±	±	±	±	±	±	±	±	±	±	±	+	
	N	-	-	-	-	-	-	-	-	-	-	-	-	-	-	-	-	-	-	-	-	-	+	
<i>B. latens</i> LMG 24064	W	-	-	±	±	±	-	-	-	±	±	±	±	±	-	±	±	-	-	±	-	±	+	
	N	-	-	-	-	-	-	-	-	-	-	-	-	-	-	-	-	-	-	-	-	-	+	
<i>B. metallica</i> LMG 24068	W	±	±	±	±	±	±	±	±	±	±	±	±	±	±	±	±	±	±	±	±	±	+	
	N	-	-	-	-	-	-	-	-	-	-	-	-	-	-	-	-	-	-	-	-	-	+	
<i>B. multivorans</i> LMG 13010	W	-	±	±	±	±	±	±	-	±	±	±	±	±	±	±	±	±	±	±	±	±	+	
	N	-	-	-	-	-	-	-	-	-	-	-	-	-	-	-	-	-	-	-	-	-	+	
<i>B. pseudomultivorans</i> LMG 26883	W	±	±	±	±	±	±	±	±	±	±	±	±	±	±	±	±	±	±	±	±	±	+	
	N	-	-	-	-	-	-	-	-	-	-	-	-	-	-	-	-	-	-	-	-	-	+	
<i>B. pyrrocinia</i> LMG 14191	W	±	±	±	±	±	±	±	±	±	±	±	±	±	±	±	±	±	±	±	±	±	+	
	N	-	-	-	-	-	-	-	-	-	-	-	-	-	-	-	-	-	-	-	-	-	+	
<i>B. seminalis</i> LMG 24067	W	-	±	±	±	±	±	±	-	±	-	±	±	±	±	±	±	-	±	±	±	±	+	
	N	-	-	-	-	-	-	-	-	-	-	-	-	-	-	-	-	-	-	-	-	-	+	
<i>B. stabilis</i> LMG 14294	W	±	±	±	±	±	±	±	±	±	±	±	±	±	±	±	±	-	±	±	±	±	+	
	N	-	-	-	-	-	-	-	-	-	-	-	-	-	-	-	-	-	-	-	-	-	+	
<i>B. uborrensis</i> LMG 20358	W	-	-	±	±	±	±	±	-	±	±	±	±	±	-	±	±	±	±	±	±	±	+	
	N	-	-	-	-	-	-	-	-	-	-	-	-	-	-	-	-	-	-	-	-	-	+	

Table 2: Growth of Bcc strains in cross-streaking experiment carried out using Petri dishes either with (W) or without (N) a central septum (S). Symbols: +, growth; ±, reduced growth; -, no growth.

Extracts antimicrobial assay

Eight of the most active Antarctic strains belonging to the three different genera (*Pseudomonas*, *Psychrobacter*, and *Arthrobacter*) were selected and used to produce extracts, which were then tested against a reduced panel of Bcc type-strains isolated from CF patients. The MIC assays were carried out as described in Materials and Methods. **Table 3** reports the antimicrobial activity as percentage of Bcc growth inhibition in the presence of each extract at a concentration of 1 mg/mL.

Species	Strain	<i>Pseudomonas</i>	<i>Psychrobacter</i>						<i>Arthrobacter</i>
		BTN 1	BTN 2	BTN 15	BTN 3	BTN 19	BTN 21	BTN 5	BTN 4
<i>B. diffusa</i>	LMG 24065	100 ± 0	75 ± 3	77 ± 3	43 ± 7	45 ± 11	70 ± 4	77 ± 9	63 ± 3
<i>B. metallica</i>	LMG 24068	92 ± 4	70 ± 5	71 ± 3	32 ± 2	30 ± 3	53 ± 5	77 ± 4	64 ± 9
<i>B. cenocepacia</i>	LMG 16656	100 ± 0	78 ± 2	87 ± 1	84 ± 6	64 ± 4	45 ± 1	84 ± 2	57 ± 1
<i>B. latens</i>	LMG 24064	100 ± 0	53 ± 11	75 ± 2	55 ± 6	43 ± 3	65 ± 2	56 ± 3	41 ± 2
<i>B. seminalis</i>	LMG 24067	100 ± 0	43 ± 6	67 ± 5	73 ± 8	45 ± 6	78 ± 11	40 ± 3	56 ± 3

Table 3: Antimicrobial activity of BTN cell extracts reported as % of inhibition of Bcc strains treated with 1 mg/mL of BTN extracts. .

Data obtained revealed that the extracts were differentially active against the selected Bcc strains. Three Antarctic bacterial strains, i.e. BTN2, BTN15, and BTN5, were able to inhibit at least three of the five Bcc strains more than 70 % of growth. However, the extract from *Pseudomonas* BTN1 exhibited the best anti-Bcc activity; indeed, it was able to almost completely inhibit the growth of all the target strains at the concentration used. For this reason, this strain was selected for further scale-up and extract purification.

Bioassay-guided purification of BTN1 extract

Pseudomonas sp. BTN1 strain was grown in 3L TYP medium for 5 days at 20°C, then the culture broth was extracted with ethyl acetate. Subsequently, the crude extract (1 g) was fractionated with a SPE C18 Cartridge. Elution was performed stepwise with an increasing methanol concentration. The 4 eluted fractions were collected, dried and dissolved in DMSO to perform bioassay at a stock concentration of 50 mg/mL. The fraction eluted at 100% methanol was shown to be the most active one against *B. cenocepacia* LMG 16656 with a MIC of 50 µg/mL and was subjected to HPLC separation. HPLC chromatograms extracted from 200 to 400 nm presented 11 different peaks, which were separated, dried and dissolved in DMSO at a stock concentration of 10 mg/mL to perform MIC assay. Data obtained revealed promising inhibitory activity against *B. cenocepacia* strain LMG 16656 of three compounds, hereinafter referred to as Compound **1**, **2** and **3**, respectively.

Compound structure elucidation

The molecular formula of compound **1** was established as C₂₈H₅₂O₉ by HRESIMS (555.35141 Δ 0.92 ppm [M+Na]⁺). Dereplication of this compound based on 1D, 2D NMR and LCMS data indicated that the primary structure of **1** was similar to a known rhamnolipid [38], but differed in terms of the relative configuration of the sugar moiety. The relative configuration of the sugar unit of compound **1** was identified as

β -L-rhamnopyranose as compared to α -L-rhamnopyranose for the known compound based on analysis of coupling constants and proton chemical shifts and by comparing with literature values [39].

The molecular formula of Compound **2** was established as $C_{28}H_{50}O_9$ by high-resolution electrospray ionization mass spectrometry (HRESIMS) ($553.33429 \Delta -0.75$ ppm $[M+Na]^+$) and subsequent dereplication suggested it was new. The molecular formula suggested 4 degrees of unsaturation. The 1H , ^{13}C NMR data (Table 1) in CD_3OD of **2** revealed one ester (δ_C 173.4 ppm), one carboxylic acid group (δ_C 171.40) ppm, two olefinic carbons (δ_C 132.8, 123.7 ppm), and an anomeric carbon (δ_C 98.47 ppm) of a sugar unit. This analysis accounted for 3 of the double bond equivalents, suggesting that the sugar unit was present as a ring. The structure was elucidated based on 2D NMR correlation experiments. Data clearly showed three distinctive spin systems. There were COSY correlations observed between the anomeric proton and the adjacent protons of the sugar unit. There was a strong observed COSY correlation between the methyl group at δ_H 1.27 ppm and the proton at δ_H 3.38 ppm placing the methyl group at position C5. The proposed structure was fully supported by HMBC correlations (Table 4) indicating that compound **2** is a rhamnolipid with the A and B chains having 10 and 12 carbons respectively, and a single unsaturation at position B5. The sugar moiety in compound **2** was identified as β -L-rhamnopyranose based on the chemical shift of the anomeric proton, δ_H 4.86 ppm as compared to δ_H 5.11 ppm for α -L-rhamnopyranose sugars, and similarities of proton chemical shifts with β -L-rhamnopyranose sugars (Ref). Because of overlap of the water peak and the anomeric proton in the 1H NMR spectrum of **2** in CD_3OD it was remeasured in DMSO- d_6 . It showed the anomeric proton as a broad singlet suggesting that the sugar was linked in an equatorial position to the lipid chain giving rise to a very small coupling constant with H-2 ($^3J(1,2)$). All the other coupling constants ($^3J(2,3)$, 3.5 Hz), ($^3J(3,4)$, 9.5 Hz), ($^3J(4,5)$, 9.8 Hz) agreed with the published data for β -L-rhamnopyranose sugars [39].

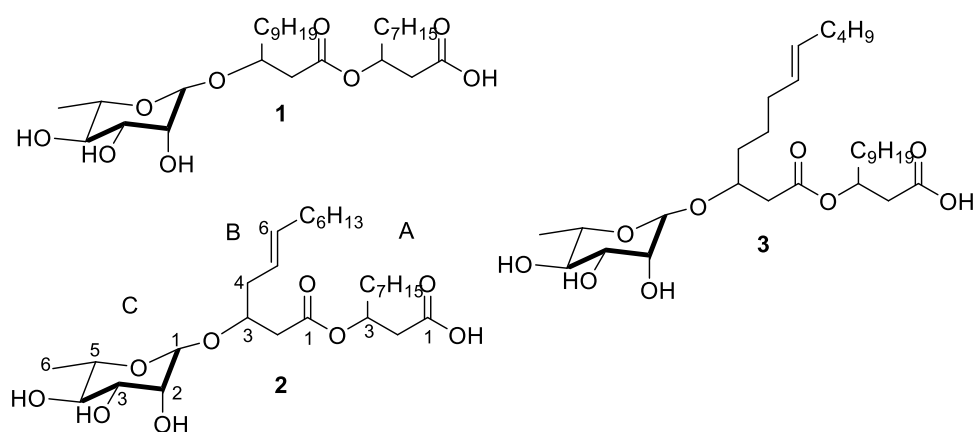


Figure 1. Structures of the 3 rhamnolipids isolated from *Pseudomonas* BTN1.

The molecular formula of compound **3** was established as C₃₀H₅₄O₉ by HRESIMS 581.36490 Δ 1.72 ppm [M+Na]⁺. Based on 1D and 2D NMR data compound **3** was similar to **2**, the difference being an additional C₂H₄ unit. However, careful interpretation of the data indicated that both the lipid chains A and B were C12 carbons with a single unsaturation at position B7 instead of C10 and C12 carbons and an unsaturation position at B5 in **2**. The relative configuration of the sugar unit was similar to that of compound **2** based on analysis of chemical shifts and proton coupling constants.

		2				3			
	Position	d _C /ppm	d _H /ppm (m, J in Hz)	COSY ¹ H- ¹ H	HMBC H@C	d _C /ppm	d _H /ppm (m, J in Hz)	COSY ¹ H- ¹ H	HMBC H@C
A	1	173.4				175.5			
	2	38.9	2.58, dd, 7.1, 6.0	A3	A1	40.9	2.55, m; 2.53, m	A3	A1
	3	71.1	5.27, quintet, 6.70	A2, A3	A1, A2	72.7	5.29, quintet	A2, A4	A1, A2
	4	33.8	1.64, m	A3	A3	34.9	1.63, bm	A3	A3
	5	24.9	1.35, overlap			26.0	1.35, overlap		
	6	29.3	1.31, overlap			30.5	1.37, overlap		
	7	29.3	1.31, overlap			30.1	1.32, overlap		
	8	31.6	1.31, overlap			29.8	1.33, overlap		
	9	22.3	1.33, overlap	A10	A10	30.2	1.36, overlap	A10	A10
	10	13.1	0.92, m	A9	A9	32.7	1.31, overlap	A9	A9
	11					23.4	1.33, overlap		
	12					14.1	0.92, m		
B	1	171.4				172.3			
	2	39.5	2.53, dd, 8.0, 7.09	B3	B1	41.0	2.59, m; 2.50, m	B3	B1
	3	72.9	4.16, quintet, 5.76	B2, B4	B1, B5	74.8	4.10, quintet, 5.87	B2, B4	B1, B5
	4	30.4	2.39, m	B3, B5	B3, B5	33.5	1.58, bm	B3, B5	B3, B5
	5	123.7	5.40, m	B4, B6	B3, B4, B6, B7	25.7	1.43, overlap	B4, B6	
	6	132.8	5.55, m	B5, B7	B5, B8	27.8	2.08, overlap	B5, B7	
	7	27.1	2.08, quartet	B6	B5, B6	130.0	5.37, m	B6, B8	B8, B9
	8	29.3	1.31, overlap			131.2	5.39, m	B7	B7
	9	28.9	1.33, overlap	B7		32.7	1.31, overlap	B8	
	10	31.6	1.31, overlap			32.7	1.31, overlap		
	11	22.3	1.33, overlap		B12	23.4	1.33, overlap	B12	
	12	13.1	0.92, m		B11	14.1	0.92, m	B11	
C	1	98.5	4.86, overlap	C2	B3, C2	100.0	4.80, d, 1.44	C2	B3, C2
	2	71.2	3.77, dd, 3.45, 1.70	C1, C3	C3, C4	72.4	3.76, dd, 3.42, 1.66	C1, C3	C3, C4
	3	70.9	3.64, dd, 9.46, 3.46	C2, C4	C5	71.9	3.66, dd, 9.70, 3.46	C2, C4	C5
	4	72.7	3.38, dd, 9.81, 9.78	C3, C5	C3	73.8	3.35, dd, 9.94, 8.84	C3, C5	C3
	5	68.7	3.67, m	C4, C6	C4, C6	69.8	3.68, m	C4, C6	C4, C6
	6	16.7	1.27, d, 6.22	C5	C5	17.6	1.27, d, 6.33	C5	C5

Table 4. NMR data of **2** and **3** in CD₃OD. ^a150 MHz; ^b600 MHz

Compound 2. $[\alpha]_D -53.4^\circ$ (c 0.001 MeOH; UV(MeOH) λ_{max} (log ϵ) 202 (3.55) nm; IR (film) ν_{max} 3361, 2925, 2855, 1735, 1671, 1575, 1455, 1380, 1314, 1207, 1161, 1126, 1037, 983, cm^{-1} ; 1H , ^{13}C , HMBC NMR data see Table 1; HRESIMS m/z 553.33429 Δ -0.75 ppm $[M+Na]^+$ calculated for $C_{28}H_{50}O_9$.

Compound 3. $[\alpha]_D +49.3^\circ$ (c 0.001 MeOH. UV(MeOH) λ_{max} (log ϵ) 202 (3.78) nm; IR (film) ν_{max} 3387, 2926, 2855, 1667, 1587, 1402, 1316, 1204, 1130, 1072, 1049, 983 cm^{-1} ; 1H , ^{13}C , HMBC NMR data see Table 1; HRESIMS m/z 581.36490 Δ 1.72 ppm $[M+Na]^+$ calculated for $C_{30}H_{54}O_9$.

Antimicrobial activity of BTN1 pure compounds

The three monorhamnolipids isolated from strain BTN1 were tested against a selected panel of Bcc strains isolated from CF patients and *S. aureus*. MIC and MBC values are reported in Table 5. It is worth noticing that the 3 compounds have identical MIC and MBC values indicating a bactericidal effect against the target bacteria, as reported for several natural biosurfactants [40, 41]. Compounds 2 and 1 were the most active compounds as they were effective against all the tested stains, with the only exception of *B. diffusa*. Specifically, compounds 2 and 1 had the lowest MBC values against *B. cenocepacia* (3.12 $\mu g/mL$) and *S. aureus* (respectively 3.12 and 1.56 $\mu g/mL$). Compound 3 had antimicrobial effect only against *S. aureus* with a MBC value of 100 $\mu g/mL$, while resulted to ineffective towards Bcc strains. Rhamnolipids (RLs) are well-known secondary metabolites synthesized by members of different Gram-negative species, particularly from bacteria belonging to the genus *Pseudomonas*. They perform several potential functions in bacteria: as powerful biosurfactants they are involved in the uptake and biodegradation of poorly soluble substrates and are essential for surface motility and biofilm development [42]. Recently, they have emerged as potential antimicrobials against a broad range of pathogens such as *Staphylococcus*, *Mycobacterium*, and *Bacillus*, and significant activity against a number of Gram-negative species, including *Serratia marcescens*, *Enterobacter aerogenes*, and *Klebsiella pneumoniae* [43-45]. RLs act like synthetic surfactants and their proposed mechanism of action consists of intercalation into biological membranes and destruction by their permeabilising effect leading to cell death [46].

Antimicrobial activity ($\mu g/mL$)												
	<i>B. cenocepacia</i> LMG 16656		<i>B. metallica</i> LMG 24068		<i>B. seminalis</i> LMG 24067		<i>B. diffusa</i> LMG 24065		<i>B. latens</i> LMG 24064		<i>S. aureus</i> 6538P	
	MIC	MBC	MIC	MBC	MIC	MBC	MIC	MBC	MIC	MBC	MIC	MBC
C1	3.12	3.12	50	50	12.5	12.5	>200	>200	12.5	12.5	1.56	1.56
C2	3.12	3.12	25	25	3.12	3.12	200	200	12.5	12.5	3.12	3.12
C3	200	200	>200	>200	>200	>200	>200	>200	>200	>200	100	100

Table 5. MIC and MBC values of the 3 mono-rhamnolipids isolated in this study.

In vivo evaluation of RLs

In order to evaluate the *in vivo* antimicrobial activity of the isolated RLs, a “rescue procedure” was set-up using the nematode *C. elegans*. The worms were infected using *B. cenocepacia* LMG 16656 and *B. metallica* LMG 24068, whose colonization of worms had been previously observed [36]. The infected worms were then placed in the presence of **Compound 2** or the antibiotic trimethoprim as a control, in a 24-multiwell plate. Worms placed into wells containing DMSO 0.5% were used as a comparison. Toxicity of **Compound 2** towards *C. elegans* was evaluated incubating Compound 1 (50 µg/mL) with KU25 not-infected worms. The plate was incubated for 2 days and count of the surviving worms was performed. Results proved that the antibiotic treatment of Trimetoprim is able to increase the percentage of surviving worms after the infection compared to DMSO control. Specifically, the percentage of surviving worms in the presence of Trimentoprim is 40% for *B. metallica* and 25% for *B. cenocepacia*, higher than the DMSO controls.

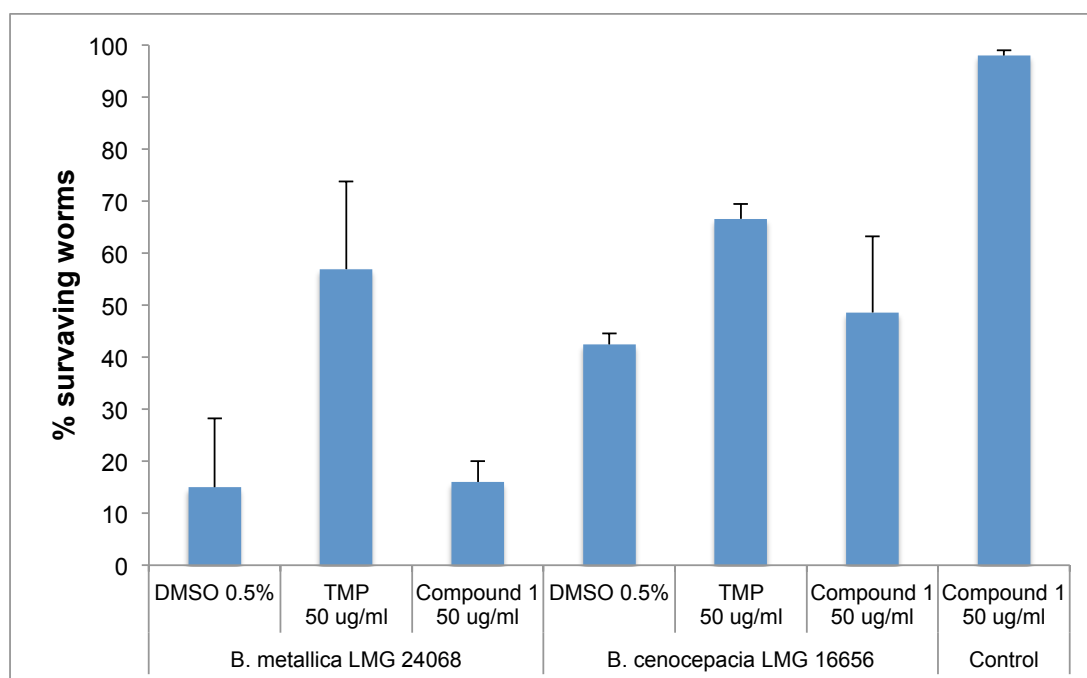


Figure 2. In vivo proof of activity of Compound 1 and Trimetoprim (TMP). Results are reported as percentage of surviving worms after two days of incubation. Experiments were performed in triplicate and results reported are mean valued and standard deviation.

The treatment with **Compound 2**, instead, did not result into an increase of nematode survival rate, as the percentage of surviving worms after 2 days of incubation in the presence of **Compound 2** are comparable with the DMSO control. However, results also proved that the compounds are not toxic to the nematodes. There are different explanations that can explain the lack of *in vivo* activity, related to RLs uptake buffer/solvent effects and interfering with the mechanism of action. Another reason may be also due to the poor RLs solubility in water system, which can results in a reduced availability of the compounds. Generally, the lethal dose of compound may be also 10-20 times higher than the *in vitro* calculated values.

Chemical synthesis experiments aimed at increasing the solubility of these compounds may be a solution to increase their *in vivo* activity.

2.4 Conclusions

Exploiting a bioassay-driven purification approach, 3 RLs (one of which was novel) with antimicrobial activity against Bcc strains, were isolated from *Pseudomonas* sp. BTN1, recovered from Antarctic sediments. RLs represent a promising class of biosurfactants as antimicrobials or in combination with antibiotics. A recent study suggested the use of RLs as an additive in the formulation of antibiotic and other antimicrobial agents for enhancing the effectiveness of chemotherapeutics [47]. Moreover, the possibility of RLs production by the fermentation of organic waste (such as waste oils), make this products economically appealing [48]. To the best of our knowledge, this is the first report of antimicrobial activity of RLs against Bcc strains, and it prompts future studies aimed at RLs exploitation as drugs to counteract these hazardous opportunistic human pathogens.

2.5 References

1. Berdy, J., *Thoughts and facts about antibiotics: where we are now and where we are heading*. J Antibiot (Tokyo), 2012. **65**(8): p. 385-95.
2. Tegos, G.P. and M.R. Hamblin, *Disruptive innovations: new anti-infectives in the age of resistance*. Curr Opin Pharmacol, 2013. **13**(5): p. 673-7.
3. Newman, D.J. and G.M. Cragg, *Natural products as sources of new drugs over the 30 years from 1981 to 2010*. J Nat Prod, 2012. **75**(3): p. 311-35.
4. Bologna, C.G., et al., *Emerging trends in the discovery of natural product antibacterials*. Curr Opin Pharmacol, 2013. **13**(5): p. 678-87.
5. Zhu, F., et al., *Drug discovery prospect from untapped species: indications from approved natural product drugs*. PLoS One, 2012. **7**(7): p. e39782.
6. Jaspars, M. and G. Challis, *Microbiology: a talented genus*. Nature, 2014. **506**(7486): p. 38-9.
7. von Salm, J.L., et al., *Shagenes A and B, new tricyclic sesquiterpenes produced by an undescribed Antarctic octocoral*. Org Lett, 2014. **16**(10): p. 2630-3.
8. Godinho, V.M., et al., *Diversity and bioprospection of fungal community present in oligotrophic soil of continental Antarctica*. Extremophiles, 2015. **19**(3): p. 585-96.
9. Lee, L.H., et al., *Analysis of Antarctic proteobacteria by PCR fingerprinting and screening for antimicrobial secondary metabolites*. Genet Mol Res, 2012. **11**(2): p. 1627-41.
10. Papa, R., et al., *Anti-biofilm activity of the Antarctic marine bacterium *Pseudoalteromonas haloplanktis* TAC125*. Res Microbiol, 2013. **164**(5): p. 450-6.
11. Papaleo, M.C., et al., *Sponge-associated microbial Antarctic communities exhibiting antimicrobial activity against *Burkholderia cepacia* complex bacteria*. Biotechnol Adv, 2012. **30**(1): p. 272-93.
12. Papaleo, M.C., et al., *Bioactive volatile organic compounds from Antarctic (sponges) bacteria*. N Biotechnol, 2013.

13. Romoli, R., et al., *Characterization of the volatile profile of Antarctic bacteria by using solid-phase microextraction-gas chromatography-mass spectrometry*. J Mass Spectrom, 2011. **46**(10): p. 1051-9.
14. Maida I., B.E., Fondi M., Perrin E., Orlandini V., Papaleo M.C., Mengoni A., de Pascale D., Tutino M.L., Michaud L., Lo Giudice A. and Fani R., *Antimicrobial activity of Pseudoalteromonas strains isolated from the Ross Sea (Antarctica) vs Cystic Fibrosis opportunistic pathogens*. Hydrobiologia, 2015. **Accepted for publication**.
15. Romoli, R., et al., *GC-MS Volatolomic Approach to Study the Antimicrobial Activity of the Antarctic Bacterium Pseudoalteromonas sp. TB41*. Metabolomics, 2013. **10**: p. 42-51.
16. Coenye, T. and P. Vandamme, *Diversity and significance of Burkholderia species occupying diverse ecological niches*. Environ Microbiol, 2003. **5**(9): p. 719-29.
17. Compant S, N.J., Coenye T, Clement C, Ait Barka E, *Diversity and occurrence of Burkholderia spp. in the natural environment*. FEMS Microbiol Rev, 2008. **32**(4): p. 607-626.
18. De Smet, B., et al., *Burkholderia stagnalis sp. nov. and Burkholderia territorii sp. nov., two novel Burkholderia cepacia complex species from environmental and human sources*. Int J Syst Evol Microbiol, 2015. **65**(7): p. 2265-71.
19. Drevinek, P. and E. Mahenthiralingam, *Burkholderia cenocepacia in cystic fibrosis: epidemiology and molecular mechanisms of virulence*. Clin Microbiol Infect, 2010. **16**(7): p. 821-30.
20. Ramsay, K.A., et al., *Factors influencing acquisition of Burkholderia cepacia complex organisms in patients with cystic fibrosis*. J Clin Microbiol, 2013. **51**(12): p. 3975-80.
21. Rose, H., et al., *Biocide susceptibility of the Burkholderia cepacia complex*. J Antimicrob Chemother, 2009. **63**(3): p. 502-10.
22. Nash, E.F., et al., *"Cepacia syndrome" associated with Burkholderia cepacia (genomovar I) infection in an adolescent with cystic fibrosis*. Pediatr Pulmonol, 2010.
23. Tegos, G.P., M.K. Haynes, and H.P. Schweizer, *Dissecting novel virulent determinants in the Burkholderia cepacia complex*. Virulence, 2012. **3**(3): p. 234-7.
24. Williams, J.G., et al., *DNA polymorphisms amplified by arbitrary primers are useful as genetic markers*. Nucleic Acids Res, 1990. **18**(22): p. 6531-5.
25. Welsh, J. and M. McClelland, *Fingerprinting genomes using PCR with arbitrary primers*. Nucleic Acids Res, 1990. **18**(24): p. 7213-8.
26. Mori, E., et al., *Molecular nature of RAPD markers from Haemophilus influenzae Rd genome*. Res Microbiol, 1999. **150**(2): p. 83-93.
27. Grifoni, A., et al., *Identification of Azospirillum strains by restriction fragment length polymorphism of the 16S rDNA and of the histidine operon*. FEMS Microbiol Lett, 1995. **127**(1-2): p. 85-91.
28. Sanger, F., S. Nicklen, and A.R. Coulson, *DNA sequencing with chain-terminating inhibitors*. Proc Natl Acad Sci U S A, 1977. **74**(12): p. 5463-7.
29. Altschul, S.F., et al., *Gapped BLAST and PSI-BLAST: a new generation of protein database search programs*. Nucleic Acids Res, 1997. **25**(17): p. 3389-402.
30. Thompson, J.D., D.G. Higgins, and T.J. Gibson, *CLUSTAL W: improving the sensitivity of progressive multiple sequence alignment through sequence*

- weighting, position-specific gap penalties and weight matrix choice. *Nucleic Acids Res*, 1994. **22**(22): p. 4673-80.
31. Saitou, N. and M. Nei, *The neighbor-joining method: a new method for reconstructing phylogenetic trees*. *Mol Biol Evol*, 1987. **4**(4): p. 406-25.
 32. Kimura, M., *A simple method for estimating evolutionary rates of base substitutions through comparative studies of nucleotide sequences*. *J Mol Evol*, 1980. **16**(2): p. 111-20.
 33. Felsenstein, J., *Confidence Limits on Phylogenies: An Approach Using the Bootstrap*. *Evolution*, 1985. **39**(4): p. 783-791.
 34. Bolz, D.D., J.L. Tenor, and A. Aballay, *A conserved PMK-1/p38 MAPK is required in caenorhabditis elegans tissue-specific immune response to Yersinia pestis infection*. *J Biol Chem*, 2010. **285**(14): p. 10832-40.
 35. Brenner, S., *The genetics of Caenorhabditis elegans*. *Genetics*, 1974. **77**: p. 71-94.
 36. Tedesco, P., et al., *Investigating the Role of the Host Multidrug Resistance Associated Protein Transporter Family in Burkholderia cepacia Complex Pathogenicity Using a Caenorhabditis elegans Infection Model*. *PLoS One*, 2015. **10**(11): p. e0142883.
 37. Stiernagle, T., *Maintenance of C. elegans WormBook*, The C. elegans Research Community, 2006.
 38. Sharma, A., et al., *Rhamnolipids from the rhizosphere bacterium Pseudomonas sp. GRP(3) that reduces damping-off disease in Chilli and tomato nurseries*. *J Nat Prod*, 2007. **70**(6): p. 941-7.
 39. De Bruyn, A. and M. Anteunis, *1H-N.m.r. study of L-rhamnose, methyl alpha-L-rhamnopyranoside, and 4-o-beta-D-galactopranosyl-L-rhamnose in deuterium oxide*. *Carbohydr Res*, 1976. **47**(1): p. 158-63.
 40. Das, P., S. Mukherjee, and R. Sen, *Antimicrobial potential of a lipopeptide biosurfactant derived from a marine Bacillus circulans*. *J Appl Microbiol*, 2008. **104**(6): p. 1675-84.
 41. Das, P., X.P. Yang, and L.Z. Ma, *Analysis of biosurfactants from industrially viable Pseudomonas strain isolated from crude oil suggests how rhamnolipids congeners affect emulsification property and antimicrobial activity*. *Front Microbiol*, 2014. **5**: p. 696.
 42. Abdel-Mawgoud, A.M., F. Lepine, and E. Deziel, *Rhamnolipids: diversity of structures, microbial origins and roles*. *Appl Microbiol Biotechnol*, 2010. **86**(5): p. 1323-36.
 43. Haba, E., et al., *Physicochemical characterization and antimicrobial properties of rhamnolipids produced by Pseudomonas aeruginosa 47T2 NCBIM 40044*. *Biotechnol Bioeng*, 2003. **81**(3): p. 316-22.
 44. Benincasa, M., et al., *Chemical structure, surface properties and biological activities of the biosurfactant produced by Pseudomonas aeruginosa LBI from soapstock*. *Antonie Van Leeuwenhoek*, 2004. **85**(1): p. 1-8.
 45. Haba, E., et al., *Rhamnolipids as emulsifying agents for essential oil formulations: antimicrobial effect against Candida albicans and methicillin-resistant Staphylococcus aureus*. *Int J Pharm*, 2014. **476**(1-2): p. 134-41.
 46. Sotirova, A.V., et al., *Rhamnolipid-biosurfactant permeabilizing effects on gram-positive and gram-negative bacterial strains*. *Curr Microbiol*, 2008. **56**(6): p. 639-44.

47. Bharali, P., et al., *Rhamnolipid (RL) from Pseudomonas aeruginosa OBP1: a novel chemotaxis and antibacterial agent*. Colloids Surf B Biointerfaces, 2013. **103**: p. 502-9.
48. Dobler, L., et al., *Rhamnolipids in perspective: gene regulatory pathways, metabolic engineering, production and technological forecasting*. N Biotechnol, 2016. **33**(1): p. 123-35.

Figure S2. Edited-HSQC NMR spectrum of compound 2 in CD₃OD

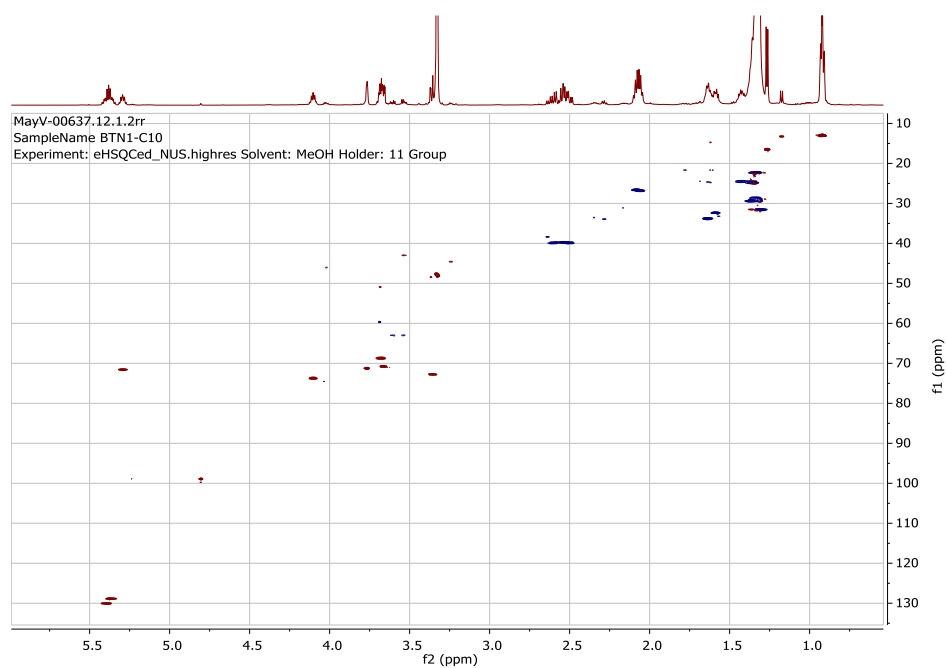


Figure S3. COSY NMR spectrum of compound 2 in CD₃OD

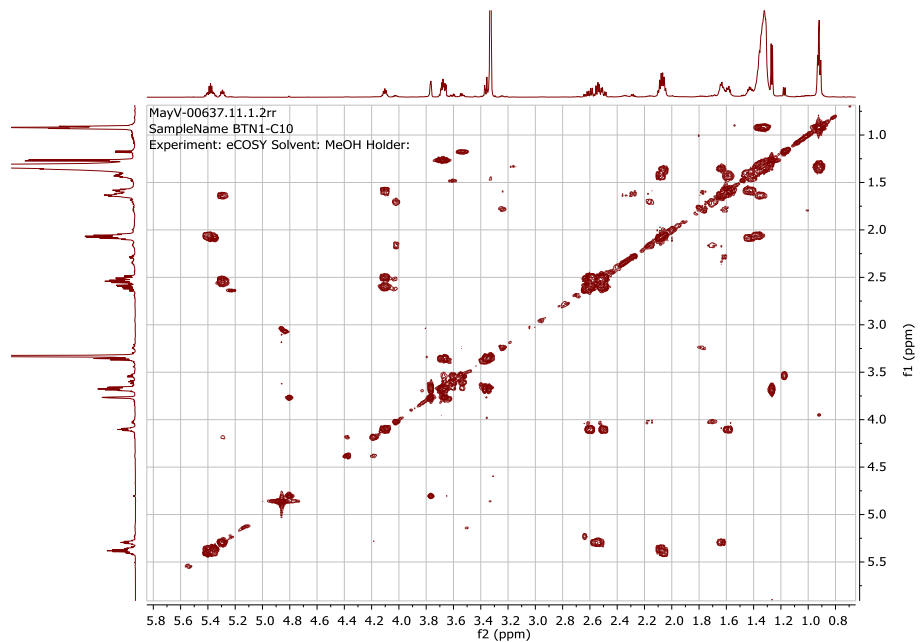


Figure S4. ^1H NMR spectrum of compound **2** in DMSO- d_6 at 400 MHz

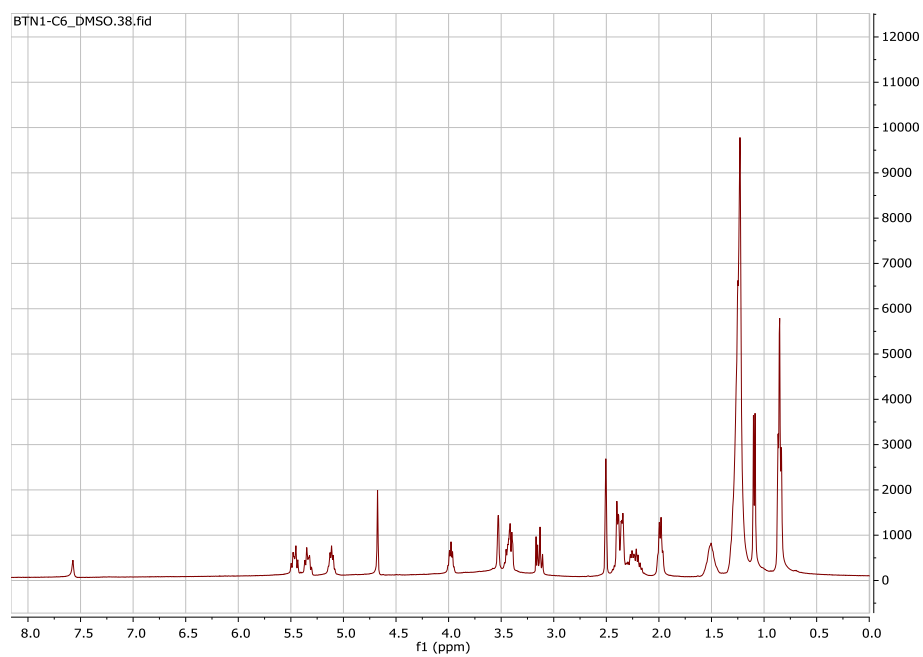


Figure S5. Edited-HSQC spectrum of compound **3** in CD_3OD at 600 MHz

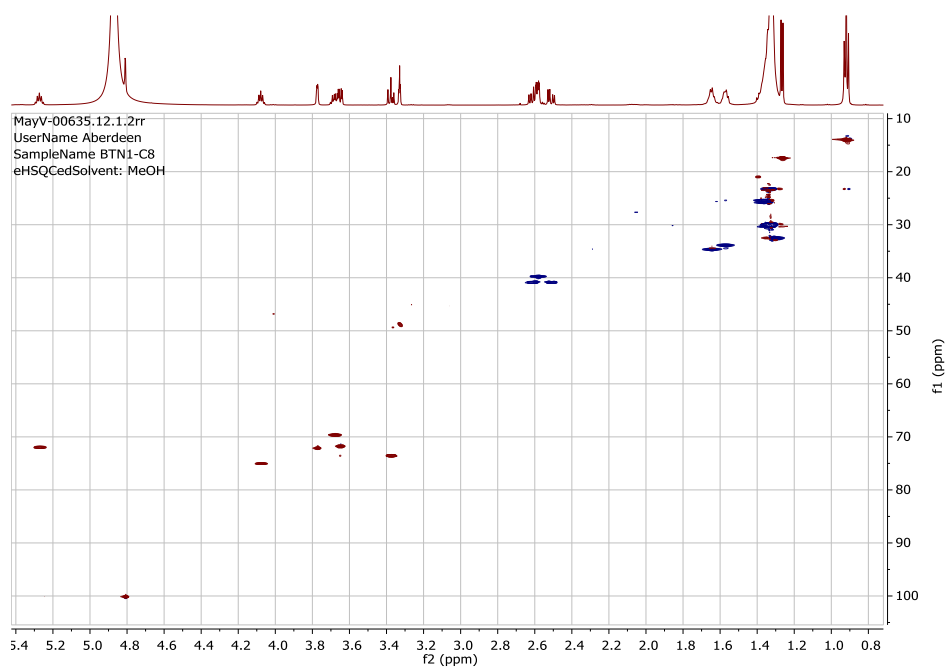
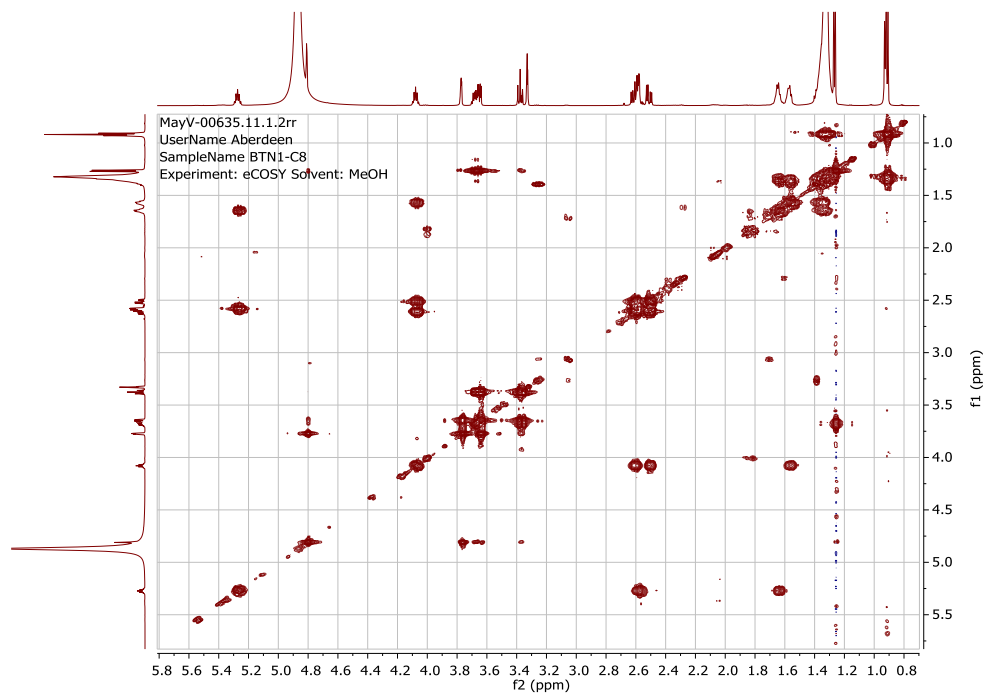


Figure S6. COSY NMR spectrum of compound 3 in CD₃OD at 600 MHz



Bcc Species	Source	Strain	C	Ps Psychrobacter																Ar			
				BTN1	BTN2	BTN15	BTN3	BTN19	BTN20B	BTN21	BTN24	BTN23	BTN5	BTN12	BTN14	BTN17	BTN16	BTN18	BTN11		BTN13	BTN22	BTN4
<i>B. cepacia</i>	CF	FCF 1	+	-	-	-	-	-	-	-	-	-	-	-	-	-	-	-	-	-	-	-	
	CF	FCF 2	+	-	-	-	-	-	-	-	-	-	-	-	-	-	-	-	-	-	-	-	
	CF	FCF3	+	-	-	-	-	-	-	-	-	-	-	-	-	-	-	-	-	-	-	-	
	Env	LMG 2161	+	-	-	-	-	+	-	-	-	-	-	-	-	-	-	-	-	-	-	-	
<i>B. multivorans</i>	CF	FCF 5	+	-	-	-	-	-	-	-	-	-	-	-	-	-	-	-	-	-	-	-	
	CF	FCF 6	+	-	-	-	-	+	-	-	-	-	-	-	-	-	-	-	-	-	-	-	
	CF	FCF 7	+	-	-	-	-	+	-	-	-	-	-	-	-	-	-	-	-	-	-	-	
	CF	FCF 8	+	-	-	-	-	+	-	-	-	-	-	-	-	-	-	-	-	-	-	-	
	CF	FCF 9	+	-	-	-	-	-	-	-	-	-	-	-	-	-	-	-	-	-	-	-	
	CF	FCF 10	+	-	-	-	-	-	-	-	-	-	-	-	-	-	-	-	-	-	-	-	
	CF	FCF 11	+	-	-	-	-	-	-	-	-	-	-	-	-	-	-	-	-	-	-	-	
	CF	LMG 18822	+	-	-	-	-	-	-	-	-	-	-	-	-	-	-	-	-	-	-	-	
	Env	LMG 17588	+	-	-	-	-	-	-	-	-	-	-	-	-	-	-	-	-	-	-	-	
<i>B. cenocepacia</i>	CF	FCF 12	+	-	-	-	-	-	-	-	-	-	-	-	-	-	-	-	-	-	-	-	
	CF	FCF 13	+	-	-	-	-	-	-	-	-	-	-	-	-	-	-	-	-	-	-	-	
	CF	FCF 14	+	-	-	-	-	-	-	-	-	-	-	-	-	-	-	-	-	-	-	-	
	CF	FCF 15	+	-	-	-	-	-	-	-	-	-	-	-	-	-	-	-	-	-	-	-	
	CF	FCF 16	+	-	-	-	-	-	-	-	-	-	-	-	-	-	-	-	-	-	-	-	
	CF	FCF 17	+	-	-	-	-	-	-	-	-	-	-	-	-	-	-	-	-	-	-	-	
	CF	FCF 18	+	-	-	-	-	-	-	-	-	-	-	-	-	-	-	-	-	-	-	-	
	CF	FCF 19	+	+	-	-	+	-	-	-	-	+	-	+	+	-	+	-	+	-	-	+	
	CF	FCF 20	+	-	-	-	-	-	-	-	-	-	-	-	-	-	-	-	-	-	-	-	
	CF	FCF 21	+	-	-	-	-	-	-	-	-	-	-	-	-	-	-	-	-	-	-	-	
	CF	FCF 22	+	-	-	+	-	-	+	+	-	-	+	-	-	-	-	-	-	-	-	-	
	CF	FCF 23	+	-	-	-	-	-	-	-	-	-	-	-	-	-	-	-	-	-	-	-	
	CF	FCF 24	+	-	-	-	-	-	-	-	-	-	-	-	-	-	-	-	-	-	-	-	
	CF	FCF 25	+	+	-	-	-	-	-	-	-	-	-	-	-	-	-	-	-	-	+	-	

	CF	FCF 26	+	-	-	-	-	-	-	-	-	-	-	-	-	-	-	-	-	-
	CF	FCF 27	+	-	-	-	-	-	-	-	-	-	-	-	-	-	-	-	-	-
	CF	FCF 28	+	-	-	-	-	-	-	-	-	-	-	-	-	-	-	-	-	-
	CF	FCF 29	+	-	-	-	-	-	-	-	-	-	-	-	-	-	-	-	-	-
	CF	FCF 30	+	-	-	-	-	-	-	-	-	-	-	-	-	-	-	-	-	-
	CF	FCF 31	+	-	-	-	-	-	-	-	-	-	-	-	-	-	-	-	-	-
	CF	LMG 16654	+	-	-	-	-	-	-	-	-	-	-	-	-	-	-	-	-	-
	CF	C 5424	+	-	-	-	-	-	-	-	-	-	-	-	-	-	-	-	-	-
	CF	CEP 511	+	-	-	-	-	-	-	-	-	-	-	-	-	-	-	-	-	-
	Env	MVP C 1/16	+	-	-	-	-	-	-	-	-	-	-	-	-	-	-	-	-	-
	Env	MVP C 1/73	+	-	-	-	-	-	-	±	-	-	-	-	-	-	-	-	-	-
	CF	LMG 24506	+	-	-	-	-	-	-	-	-	-	-	-	-	-	-	-	-	-
	Env	LMG 19230	+	-	-	-	-	-	-	-	-	-	-	-	-	-	-	-	-	-
	Env	LMG 19240	+	-	-	-	-	-	-	-	-	-	-	-	-	-	-	-	-	-
	CF	FCF 32	+	-	-	-	-	-	-	-	-	-	-	-	-	-	-	-	-	-
	CF	FCF 33	+	-	-	-	-	-	-	-	-	-	-	-	-	-	-	-	-	-
	CF	FCF 34	+	-	-	-	-	-	-	-	-	-	-	-	-	-	-	-	-	-
	CF	FCF 36	+	-	-	-	-	-	-	-	-	-	-	-	-	-	-	-	-	-
	CF	FCF 37	+	-	-	-	-	-	-	-	-	-	-	-	-	-	-	-	-	-
	CF	FCF 38	+	-	-	-	-	-	-	-	-	-	-	-	-	-	-	-	-	-
	CF	FCF 39	+	-	-	-	-	-	-	-	-	-	-	-	-	-	-	-	-	-
	CF	LMG 21462	+	-	-	-	-	-	-	-	-	-	-	-	-	-	-	-	-	-
<i>B. stabilis</i>	CF	FCF 40	+	-	-	-	-	-	-	-	-	-	-	-	-	-	-	-	-	-
	CF	FCF 41	+	-	-	-	-	-	-	-	-	-	-	-	-	-	-	-	-	-
<i>B. vietnamensis</i>	CF	FCF 42	+	-	-	-	-	-	-	-	-	-	-	-	-	-	-	-	-	-
<i>B. dolosa</i>	CF	LMG 18941	+	-	-	-	-	-	-	-	-	-	-	-	-	-	-	-	-	-
	CF	LMG 18942	+	-	-	-	-	-	-	-	-	-	-	-	-	-	-	-	-	-
<i>B. ambifaria</i>	Env	MCI 7	+	-	-	-	-	-	-	-	-	-	-	-	-	-	-	-	-	-
	CF	LMG 19467	+	-	-	-	-	-	-	-	-	-	-	-	-	-	-	-	-	-
<i>B. anthina</i>	Env	LMG 16670	+	-	-	-	-	-	-	-	-	-	-	-	-	-	-	-	-	-
	CF	LMG 20983	+	-	-	-	-	-	-	-	-	-	-	-	-	-	-	-	-	-
<i>B. pyrrocinia</i>	CF	FCF 43	+	-	-	-	-	-	-	-	-	-	-	-	-	-	-	-	-	-
	CF	FCF 44	+	-	-	-	-	-	-	-	-	-	-	-	-	-	-	-	-	-

	CF	FCF 45	+	-	-	-	-	-	-	-	-	-	-	-	-	-	-	-	-	-
	CF	FCF 46	+	-	-	-	-	-	-	-	-	-	-	-	-	-	-	-	-	-
	Env	MVP C 1/26	+	-	-	-	-	-	-	-	-	-	-	-	-	-	-	-	-	±
	Env	MVP C 2/77	+	-	-	-	-	-	-	±	-	-	-	-	-	-	-	-	-	-
	CF	LMG 21824	+	-	-	-	-	±	±	-	±	-	-	-	-	-	-	±	-	±
<i>B. lata</i>	CF	LSED 4	+	-	-	-	-	-	-	-	-	-	-	-	-	-	-	-	-	-
	Env	LMG 6991	+	-	-	-	-	±	±	±	-	±	-	-	-	-	±	-	-	±
<i>B. ambifaria</i>	Env	LMG 19182	+	-	-	-	-	-	-	-	-	-	-	-	-	-	-	±	-	-
<i>B. anthina</i>	Env	LMG 20980	+	-	-	-	-	-	-	-	-	-	-	-	-	-	-	-	-	-
<i>B. cenocepacia</i>	CF	LMG 16656	+	-	-	-	-	-	-	-	-	-	-	-	-	-	-	-	-	-
<i>B. cepacia</i>	Env	LMG 1222	+	-	-	-	-	-	-	-	-	-	-	-	-	-	-	-	-	-
<i>B. contaminans</i>	AI	LMG 23361	+	-	-	-	-	-	-	-	-	-	-	-	-	-	-	-	-	-
<i>B. diffusa</i>	CF	LMG 24065	+	-	-	-	-	-	-	-	-	-	-	-	-	-	-	-	-	-
<i>B. dolosa</i>	CF	LMG 18943	+	-	-	-	-	-	-	-	-	-	-	-	-	-	-	-	-	-
<i>B. lata</i>	Env	LMG 22485	+	-	-	-	-	-	-	-	-	-	-	-	-	-	-	-	-	-
<i>B. latens</i>	CF	LMG 24064	+	-	-	-	-	-	-	-	-	-	-	-	-	-	-	-	-	-
<i>B. metallica</i>	CF	LMG 24068	+	-	-	+	-	-	±	±	±	±	±	+	-	-	-	-	-	-
<i>B. multivorans</i>	CF	LMG 13010	+	-	-	±	-	-	-	-	-	-	-	-	-	-	-	-	-	-
<i>B. pseudomultivorans</i>	CF	LMG 26883	+	-	-	±	-	-	-	-	-	-	-	-	-	-	-	-	-	-
<i>B. pyrrocinia</i>	Env	LMG 14191	+	-	-	+	-	-	-	±	±	-	+	-	-	-	-	-	-	-
<i>B. seminalis</i>	CF	LMG 24067	+	-	-	-	-	-	-	-	-	-	-	-	-	-	-	-	-	-
<i>B. stabilis</i>	CF	LMG 14294	+	-	-	-	-	-	-	-	-	-	-	-	-	-	-	-	-	-
<i>B. uborrensis</i>	Env	LMG 20358	+	-	-	±	-	-	-	-	-	-	-	-	-	-	-	-	-	-
<i>B. vietnamensis</i>	Env	LMG 10929	+	-	-	-	-	-	-	-	-	-	-	-	-	-	-	-	-	-

Table S1. Cross- streaking experiments of BTN isolates against a wide panel of Bcc strains. The Bcc strains highlighted in red correspond to type strains. Symbols: +, growth; ±, reduced growth; -, no growth; C+, positive controls, i.e. Bcc strains grown in the absence of the tester strain(s). Abbreviations: *Ps*, *Pseudomonas*; *Ar*, *Arthrobacter*; CF, Cystic Fibrosis; Env, environmental

CHAPTER 3

Bioprospecting for novel bioactive compounds exploiting cold-adapted bacteria isolated from Tibetan glaciers

Bioprospecting for novel bioactive compounds exploiting cold-adapted bacteria isolated from Tibetan glaciers

Abstract

The alarming rise of multidrug resistance pathogens led to scientific community to search for novel drug. Extreme environments hide an extraordinary microbial community, whose biotechnological potential still need to be fully evaluated. In this work we explored the capability of microorganisms isolated from Tibet as drug producers. 11 cold-adapted isolates were isolated using sediments collected from two different glaciers. The strains were evaluated for their anthelmintic and antimicrobial activity. For the anthelmintic activity, we assayed strains ability to survive and kill the nematode *Caenorhabditis elegans* that was used as model helmint. Antimicrobial capability was evaluated using the cross-streaking experiments targeting human pathogens. Positive isolates to primary screening were used to produce crude extracts to perform secondary assays in liquid experiments. We found one positive extract able to kill the nematodes and a second one that completely inhibit the growth of *Francisella tularensis*, an opportunistic human pathogen. Positive extracts were subjected to a preliminary fractionation and active fractions were identified used to perform chemical profiling. The most active antimicrobial fractions (MIC against *F. tularensis*: 25 µg/mL) revealed the presence of dikepiperazines, and especially of 16 β -hydroxycrambescidin, an alkaloid first with unreported antimicrobial activity compound.

Keywords: Antimicrobials; anthelmintic; Tibetan glaciers, cold-adapted microorganism.

3.1 Introduction

Multi-Drug Resistance (MDR) pathogens represent a huge threat to human being [1]. This problem has been worsened because of the recent antibiotic crisis. The number of the antibiotic released has dramatically decreased since 1962 [2]. Resistance to common drugs is not limited to bacteria but is now common also to parasites [3, 4]. No new anthelmintic class has reached the market during the past 25 years, but the principal problem is that anthelmintic drug discovery is not a priority of pharmaceutical industry as third-world country are mainly endangered by these pathogens [5]. Scientific community is deeply focused on the discovery of new drugs to counteract this threat. The bioprospecting of natural products is considered the richest source of novel molecular scaffolds and chemistry. This approach has led to the exploitation of the most extreme places on Earth. The reasons of this choice relies in the evidence that microorganisms inhabiting those places, face with harsh conditions and this high selective pressure may have led to the synthesis of potential bioactive compound. Cold adapted bacteria have proven their potentiality as potential antimicrobial producers against MDR human pathogens [6-9]. However, the majority of these studies are principally focused on bacteria isolated from the Poles. Bioprospecting for antimicrobials from Alpine environments has been investigated so far to a very limited extend [10, 11]. Nonetheless, glaciers are known to be a reservoir of microbial life where biomolecules and microorganism can be preserved for long term under extreme constant environmental conditions [12]. The Qinghai-Tibet Plateau, often called the 'world's roof' or 'the third pole', is located in the southwest of China and is the highest and largest region with permafrost in the world. These conditions make these are a unique alpine ecosystem, sensitive to changes in climate and surface conditions [13]. Here we explore the antimicrobial and anthelmintic potential of cold-adapted bacteria isolated from Tibetan Glaciers in the Qinghai-Tibet Plateau. Bacteria were isolated from environmental soil and screened for antagonistic activity against a panel of MDR pathogens and for their capability to kill *C. elegans* in appropriated assay. Positive strains were further processed, and a bioassay-guided strategy was performed to purify the active compounds.

3.2 Materials and methods

Isolation of Tibetan psychrophilic strains

Tibetan strains used in this work were isolated from Midui Glacier and Karuola glaciers located on the Qinghai-Tibet Plateau China at 5000 meters above sea level, and are listed in Table 1. For the isolation, 1 gr of sediments was mixed with 20 mL of M9 salts solution (KH_2PO_4 3.0 g/L, Na_2HPO_4 6.0 g/L, NaCl 0.5 g/L, NH_4Cl 1.0 g/L) in a 50 mL Falcon tube and gently mixed; the supernatant was serially diluted in sterile M9 buffer and plated on PYG medium (Peptone 5.0 g/L, Yeast extract 4.0 g/L, Glucose 1.0 g/L, CaCl_2 0.2 g/L, $\text{MgSO}_4 \cdot 7\text{H}_2\text{O}$ 0.4 g/L, K_2HPO_4 1.0 g/L, KH_2PO_4 1.0 g/L, NaHCO_3 10.0 g/L NaCl 2.0 g/L and 17 g/L agar). After 15 days of incubation 13 visible colonies were picked, grown in liquid PYG or LB and stored at -80°C .

Bacterial strains and growth conditions

Bcc strains used in this work are listed in **Table 1**. Bcc strains, *B. pseudomallei* Bp82, *E. coli* K12 and *E. coli* OP50 were routinely grown on Luria-Bertani broth (LB) (Tryptone 10 g/L, Yeast extract 5 g/L, NaCl 10 g/L) at 37°C . *Francisella tularensis*

strains LVS toIC was propagated on Chocolate agar plates (BD, Rutherford, NJ), and grown in liquid MH, modified as described before at 37 °C [14, 15]. Tibetan strains were routinely grown in liquid PYG or TYP medium (Tryptone 10 g/L, Yeast extract 5 g/L, NaCl 10 g/L) at 20°C.

Maintenance of nematodes

The *C. elegans* strain N2 Bristol (wild type) was purchased from the *Caenorhabditis* Genetic Center (CGC), University of Michigan, USA. The nematodes were propagated on Nematode Growth Medium (NGM, 2,5 g/L Peptone, 2,9 g/L NaCl, 17 g/L Bacto-Agar, 1 mM CaCl₂, 5 µg/mL Cholesterol, 25 mM KH₂PO₄ and 1 mM MgSO₄) or PGS (12 g/L Peptone, 12 g/L Glucose, 27,25 g/L Sorbitol, 12 g/L NaCl, 17 g/L Bacto-Agar, 1 mM CaCl₂, 5 µg/mL Cholesterol, 25 mM KH₂PO₄ and 1 mM MgSO₄) agar plates, supplemented with *E. coli* OP50 as carbon source, and incubated at 20°C [16].

Nematodes Grazing assay

The nematodes grazing assay was performed modifying an existing protocol [17]. Briefly, the psychrophilic strains, were picked from agar plates and spotted on 10 cm squared-plates containing agar NMG and allowed to grow for 5 days at 20°C. At day 5, two hundreds L4-stage nematodes were added in different point of the plate next to each colony with a multichannel pipette. The plates were stored at room temperature and checked every 24 h. A clone was considered positive if the colony was not grazed after 5 days of incubation with *C. elegans*.

Nematode Toxicity Assays

Positive isolates from grazing assay were further investigated singularly for their ability to kill the nematodes. Slow Killing Assay (SKA) in 2.5-cm-diameter plates containing 3 ml of NGM agar, while Fast Killing assay (FKA) was carried out in 2.5-cm-diameter plates containing 3 ml of PGS agar medium [18]. For both assays, the plates were seeded with 50 µl of the cold-adapted bacteria liquid cultures, and then incubated for 48 h at 20 °C to allow the formation of a bacterial lawn. *C. elegans* was synchronized by bleaching treatment [16], and 30-40 worms at larval stage 4 (L4), were transferred to each plate and incubated at 20 °C for seven days. The plates were scored for living worms every 48 h. *E. coli* OP50 was used as a negative control. A worm was considered dead when it no longer responded to touch. For statistical purposes, 5 replicates per trial were carried out with a unique egg preparation.

Cross streaking

Cross-streaking experiments were carried out as previously described [6, 19]. Petri dishes with or without a septum separating two hemi-cycles were used. Plates with a central septum allowed the growth of tester and target strains without any physical contact. Tibetan strains were grown on PYG for four days at 20°C; then they were streaked on PYG and incubated at 20°C for four days. Bcc strains (target strains) were perpendicularly streaked to the initial streak and plates were further incubated at 20°C for two days and at 37°C for two additional days. The experiments were conducted in parallel with a positive control to verify the viability of Bcc cells.

Preparation of crude extracts

A single colony of a bacterial isolate was used to inoculate 3 mL of liquid media in sterile bacteriological tube. After 48 h of incubation at 21°C at 200 rpm the pre-inoculum was used to inoculate 100 mL of TYP medium or PYG in a 500 mL flask, at an initial cell concentration of 0.01-OD₆₀₀/mL. The flasks were incubated up to 5 days at 20°C at 220 rpm. The cultures were then centrifuged at 6800 x g at 4°C for 30', and the exhausted culture broths were collected and stored at -20°C. The exhausted culture broths were subjected to organic extraction. Organic extractions were performed using 3 volume of ethyl acetate in a 500 mL separator funnel. In alternative, extractions with 3 different resins (XAD7, XAD16, HP20) were performed. For the resin extractions, samples were incubated with the resin (5g resin/ 100mL broth), which was then collected after 4 hours of incubation at room temperature, washed with distilled water and eluted with methanol. The organic phase collected was evaporated using a Laborota 4000 rotary evaporator (Heidolph, Schwabach, Germany), and the extracts were weight, dissolved in 100% DMSO at 50 or 10 mg/mL and stored at -20°C.

Nematode Liquid toxicity assay

To test the effect of crude extracts or compounds on *C. elegans* viability a liquid toxicity assay has been set-up. The assay has been performed in 24-well plates. Each well contained a 400 µL solution of M9 buffer, 5 µg/mL Cholesterol, and *E. coli* OP50 at the concentration of 0.5 OD/mL as carbon source. Extracts or compounds at different concentration were then added to each well. 1% DMSO was also added as control to evaluate solvent effects on nematodes. *C. elegans* was synchronized by bleaching treatment [16], and 30-40 L4 worms were transferred to each well and incubated at 20 °C up to seven days. The wells were scored for living worms every 24 h. A worm was considered dead when it no longer responded to touch. For statistical purposes, 3 replicates per trial were carried out with a unique egg preparation.

Minimal inhibitory concentration assay (MIC)

To evaluate the antimicrobial potential of Antarctic extracts, samples were placed into each well of a 96-well microtiter plate at an initial concentration of 2% (v/v) and serially diluted using LB medium. Wells containing no compound represented the negative control. DMSO was used as control to determine the effect of solvent on cell growth. A single colony of a Bcc strain was used to inoculate 3 mL of liquid LB media in sterile bacteriological tube. After 6-8 h of incubation, growth was measured by monitoring the absorbance at 600 nm and about 40000 CFU were dispensed in each well of the prepared plate. Plates were incubated at 37°C for 24h and growth was measured with a Cytation3 Plate Reader (Biotek, Winoosky, VT) by monitoring the absorbance at 600 nm.

Chemical purification

Crude extracts of 3L fermentation of selected strains, prepared as described above, were subjected to fractionation using Chromabond SPE C18 column cartridges (Macherey-Nagel, Duren, Germany). Samples were dissolved in water and loaded on the top of the column. Elution was performed at step increasing methanol concentration (25%-50%-100%-100%+TFA). In alternative, fractionation was performed using Chromabond SPE Silica column cartridges (Macherey-Nagel,

Duren, Germany), with a normal phase protocol. Samples were dissolved in chloroform and loaded on the top of the column. The elution was performed increasing methanol concentration. HPLC separations were carried out using a VP 250/10 Nucleodur C18 HTec, 5 µm, (Macherey-Nagel Duren, Germany) connected to an Ultimate 3000 HPLC Chromatograph with a Ultimate 3000 Diode Array detector and in-line degasser (Dionex, Sunnyvale, CA). Detection was achieved on-line through a scan of wavelengths from 200 to 400 nm.

Chemical profiling

High-resolution mass spectrometry and fragmentation data were recorded using a LTQ Orbitrap system (ThermoScientific, Waltman, MA) coupled to a 1290 Infinity HPLC system (Agilent, Santa Clara, CA). The following conditions were used: capillary voltage 45 V, capillary temperature 320°C, auxiliary gas flow rate 10-20 arbitrary units, sheath gas flow rate 40-50 arbitrary units, spray voltage 4.5 kV, mass range 100-2000 amu (maximum resolution 30,000). Optical rotation measurements were recorded using a Perkin Elmer, Model 343 Polarimeter at 589 nm (Perkin Elmer, Waltman, MA). The UV spectrum was recorded on a UV-Vis spectrophotometer model S10 (Spectromlab, Barcelona, Spain). The IR was recorded on a PerkinElmer FTIR Spectrum Two instrument (Perkin Elmer, Waltman, MA).

Phylogenetic analysis

Psychrophilic bacteria colonies grown overnight at 20°C on MA or LB plates were suspended in 25 µl of sterile distilled water, heated to 95°C for 10 min, and cooled on ice for 5min. Two µl of each cell lysate were used for the amplification *via* PCR of 16S rRNA genes. PCR were carried out in a total volume of 50 µl containing 1X Reaction Buffer, 150 µM MgCl₂, 250 µM of each deoxynucleoside triphosphate, and 2.0 U of Polytaq DNA polymerase and 0.6 µM of primer P0 (5' GAGAGTTTGATCCTGGCTCAG) and P6 (5' CTACGGCTACCTTGTTACGA)[20]. The reaction conditions used were: 1 cycle (95° C for 90 s), 30 cycles (95° C 30 s, 55° C 30 s, and 72° C 2 min), with a final extension of 10 min at 72 °C. Amplicons corresponding to the 16S rRNA genes (observed under UV light, 312 nm) were excised from the gel and purified using the "QIAquick" gel extraction kit (QiAgen, Chatsworth, CA) according to manufacturer's instructions. Direct sequencing was performed on both DNA strands using an ABI PRISM 310 Genetic Analyzer (Applied Biosystems, Foster City, CA) and the chemical dye terminator. BLAST probing of DNA databases was performed with the BLASTn option of the BLAST program using default parameters [21]. Nucleotide sequences were retrieved from RDP databases. The ClustalW program was used to align the 16S rRNA gene sequences obtained with the most similar ones retrieved from the databases [22]. Each alignment was checked manually, corrected, and then analysed.

3.3 Results and discussion

Identification of potential anthelmintic producers bacteria

The 11 Tibetan strains isolated from the two Tibetan glaciers (**Table 1**) were evaluated for their ability as anthelmintic producers.

Strain code	Tibetan Glacier
MD 1	Midui Glacier (4800 m above sea level)
MD2	Midui Glacier (4800 m above sea level)
MD3	Midui Glacier (4800 m above sea level)
MD4	Midui Glacier (4800 m above sea level)
MD5	Midui Glacier (4800 m above sea level)
KRL1	Karuola Glacier (5200 m above sea level)
KRL2	Karuola Glacier (5200 m above sea level)
KRL3	Karuola Glacier (5200 m above sea level)
KRL4	Karuola Glacier (5200 m above sea level)
KRL5	Karuola Glacier (5200 m above sea level)
KRL5	Karuola Glacier (5200 m above sea level)

Table 1. List of the Tibetan isolates from the two Tibetan glaciers

To this aim, the 11 isolates were spotted on a NGM agar plates and allow to grow as colony. After the incubation, L4 worms were spotted on the plates, which was further incubated to allow the worms graze the colonies. After 5 days we observed that only two colonies were not grazed by worms, as shown in **Figure 1**.

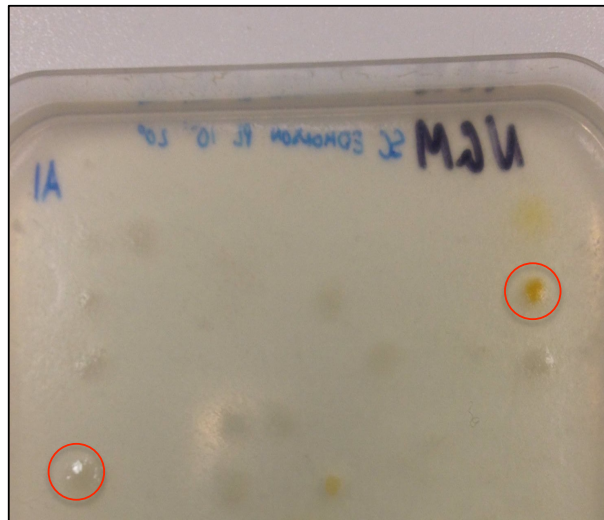


Figure 1. Nematode grazing assay. After five days of incubation only 2 colonies remain untouched. The two colonies are highlighted by a red circle and are MD4 (white colony, left) and KRL4 (yellow colony, right).

These colonies corresponded to isolate MD4, from Midui glaciers sediments and isolate KRL4 from Karuola glaciers. Apparently those two strains produced some secondary metabolites that prevented them from being grazed by the nematodes.

Strains KRL4 and MD4 were then selected for further investigation performing SKA and FKA. The two Tibetan strains were grown on two different media (NGM and PGS) and incubated at 20°C. After two days of incubation L4 worms were spotted on the plates and surviving count was performed. As shown in **Figure 2**, nematodes were able to survive when placed on bacteria grown on NGM plates. On the contrary, when spotted on PGS plates, nematodes are slowly killed. On MD4, only 10% of the worms are still alive after 100 hours (**FIG. 2A**). Nematodes placed on KRL4 present a similar surviving curve, but with a lower killing rate than MD4. In fact, worms population is reduced to 10% after 11 days (**Fig 2B**). PGS medium is considered a high osmolarity medium, which causes the absorption of compounds from agar including potential secondary metabolites produced by the Tibetan strains.

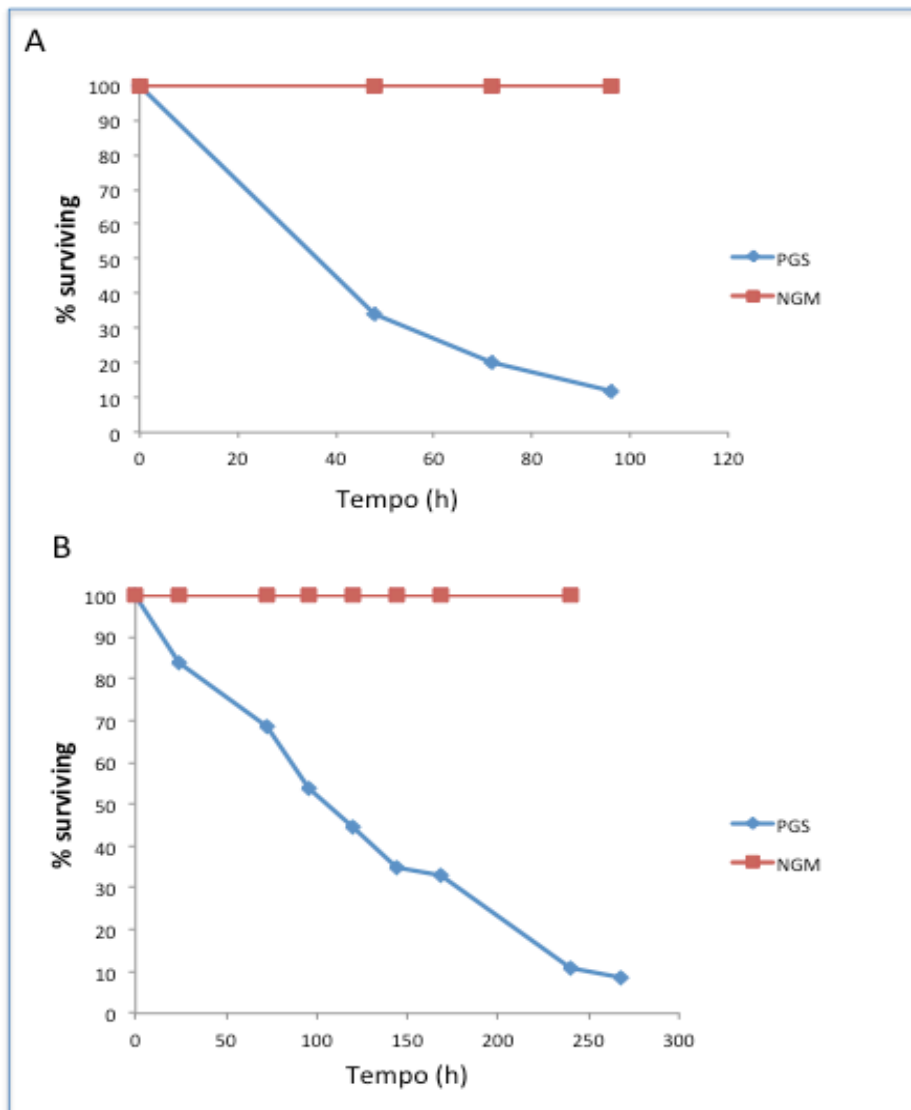


Figure 2. Surviving curves on N2 worms on MD4 (A) and on KRL4 (B)

Cross-streaking experiments

In order to check the ability of Tibetan also as potential antimicrobial producers, cross-streaking experiments were performed to evaluate their ability to inhibit pathogens growth. We used as targets a panel different Bcc strains with clinical origin. Data obtained are summarized in **Table 2**, revealing that some of the Tibetan strains were able to inhibit the growth of Bcc strains. Strains MD3 and KRL4 were the most active strains and were able to inhibit all the Bcc tested, while MD1, MD4, and KRL4 prevented the growth of 6,4 and 6 strains respectively. In order to check if this anti-Bcc activity was due to volatile organic compounds synthesis (VOCs), a further cross-streaking experiment was performed using Petri dishes with a central septum, which physically separates the tester (Tibetan) from the target strains. Data obtained are reported in **Table 2** and revealed that Tibetan strains inhibitory capabilities decreased in the presence of the central septum. This finding suggested that active Tibetan strains synthesize a combination of volatile and soluble molecules and that the Bcc-inhibitory activity likely relies principally on the soluble fraction. Thus, we decided to concentrate our efforts on the soluble molecules for this study.

	Septum	B. <i>metallica</i> LMG 24068	B. <i>seminalis</i> LMG 24067	B. <i>arboris</i> LMG 24066	B. <i>diffusa</i> LMG 24065	B. <i>ambifaria</i> LMG 19182	B. <i>contaminans</i> LMG 23361	B. <i>latens</i> LMG 24064	B. <i>cenocepacia</i> LMG 16656
MD1	Y	+	-	+	+	-	+	+	+
	N	+/-	-	+	+/-	-	-	-	+
MD2	Y	+	+	+	+	+	+	+	+
	N	+	+	+	+	-	+	+	+
MD3	Y	+	-	+	+	-	+	+	+
	N	+/-	-	-	-	-	-	+/-	-
MD4	Y	+	+	-	+	+	+	+	+
	N	+	+	+/-	-	-	-	+	+
MD5	Y	+	+	+	+	+/-	+	+	+
	N	+	+	+	+	+	+	+	+
KRL1	Y	+	+	+	+	+	+	+	+
	N	+	+	+	-	+	+	+	+
KRL2	Y	+	+	+	+	+	+	+	+
	N	+	+	+	+	+	-	+/-	+
KRL3	Y	+	-	+	+	-	+	+	+
	N	+/-	+/-	+/-	+/-	-	-	+/-	-
KRL4	Y	+	-	+	+	+	-	+	+
	N	+/-	+/-	+/-	+	+	-	-	-
KRL5	Y	+	+	+	+	+	+	+	+
	N	+	+	+	-	+	+	+	+
KRL6	Y	+	+	+	+	+	+	+	+
	N	+	+	+	+	+	+	+	+

Table 2. Inhibitory activity of Tibetan strains against Bcc strains. Y: plate with septum; N: plate without septum; +: growth of Bcc strains; -: inhibition of Bcc growth; +/-: partial inhibition of Bcc strains.

Anthelmintic activity of Tibetan bacteria extracts

Once established the anthelmintic potential of the Tibetan strains MD4 and KRL4, crude extracts were produced from these strains. Initially, we focused our attention on the exhausted culture broths, which were processed using ethyl acetate and the resin HP20. Crude extracts were weighted, dissolved in DMSO and tested for the ability of killing nematodes using a liquid assay. L4 synchronized worms were deployed into the wells of a 24-well plates containing M9 medium supplemented with cholesterol and OP50 and the extracts. DMSO at 1% was used as control to verify the effect of the solvents on nematodes growth. Surprisingly, no extract showed significant anthelmintic effect after 3 days of incubation. We then decided to analyze the extracellular content of the Tibetan strains. To this aim, bacterial pellets of the strains were collected and subjected to sonication. Then, this lysate was centrifuged and the supernatant was extracted with ethyl acetate and HP20 resin to generate crude extracts. The intracellular extracts were then tested in liquid assay. Results are shown in **Figure 3**.

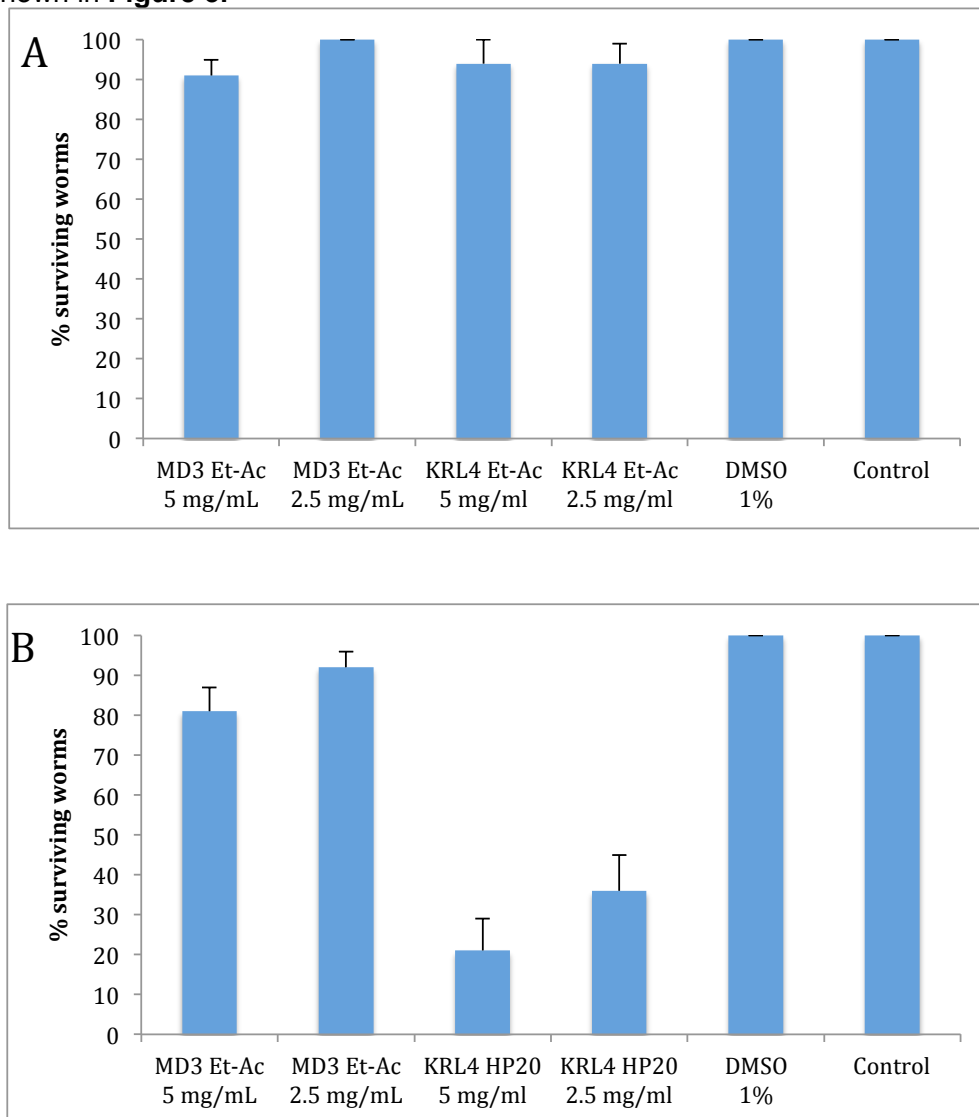


Figure 3. Anthelmintic activity of extracellular (**A**) and intracellular (**B**) extracts of strains MD4 and KRL4. Activity is expressed as the percentage of surviving worms after 3 days of incubation in the presence of extracts.

Concerning MD4, we did not find extracts showing anthelmintic activity compared to controls (1% DMSO and No addition wells), at any concentration assayed after 3 days, as shown in **Figure 3A**. Instead, we observed a significant effect on nematodes viability of the HP20 extract of strains KRL4, compared to controls (**Fig. 3B**). Specifically, at 5 mg/mL concentration only 20% of worms population were still alive after 3 days, while 37% of nematodes survived at 2.5 mg/mL suggesting a dose-response effect. Surprisingly, active extract was obtained only with HP20 resin and not with ethyl acetate, denoting a polar nature of the anthelmintic compound.

Antimicrobial activity of Tibetan extract

The 5 Tibetan strains (KRL3, KRL4, MD1, MD3 and MD4) displaying antimicrobial activity against Bcc strains, were used to produce crude extracts. Bacteria were grown in small-scale volume (100 mL) in TYP medium and after the fermentation, exhausted culture broths were extracted with ethyl-acetate (specific for organic compounds), XAD7 resin (specific for peptides) and XAD16 resin (broad range of polarity). This small extracts library was tested against a panel of human pathogens in Liquid MIC experiments. Results are summarized in **Table 3**, and were reported as percentage of inhibition of the strains in the presence of extracts at 100 µg/mL.

		<i>F. tularensis</i> LVS tol-C	<i>B. pseudomallei</i> BP82	<i>B. cenocepacia</i> LMG 16656	<i>B. metallica</i> LMG 24068	<i>E. coli</i> K12
KRL3	Et. Ac	15	9	35	0	1
	XAD7	10	6	21	9	0
	XAD16	16	5	27	10	0
KRL4	Et. Ac	15	0	34	0	5
	XAD7	9	17	29	8	0
	XAD16	14	1	28	10	0
MD1	Et. Ac	19	5	33	0	6
	XAD7	13	8	28	9	0
	XAD16	17	0	25	8	0
MD4	Et. Ac	22	2	10	6	0
	XAD7	10	5	25	13	0
	XAD16	17	6	20	1	0
MD3	Et. Ac	100	2	21	5	1
	XAD7	8	5	18	0	0
	XAD16	5	1	0	0	0

Table 3. Antimicrobial activity of tibetan extracts library, expressed as percentage of target growth inhibition in the presence of extracts at 100 µg/mL.

The extracts did not show significant antimicrobial activity against all the targets, with the only exception of the Ethyl Acetate extract from strain MD3, which was able to completely inhibit the growth of *F. tularensis* LVS tol-C strain. The absence of

significant inhibition in the presence of MD3 XAD7 and MD3 XAD16 extracts suggests that the active compound is a small organic compound.

Fractionation of KRL4 and MD3 active extracts

Active strains KRL4 and MD3, for anthelmintic and antimicrobial activity, respectively, were then selected for further analysis. The bacteria were grown in large scale (3 L) and processed to generate crude extracts. The extracts were then fractionated in order to attempt a preliminary purification of the bioactive compounds. Intracellular extracts from strain KRL4 was fractionated using a C18 column Cartridge with a water/methanol system. The extract was dissolved in water and loaded on the top of the column. Elution was performed at step, increasing the methanol concentration (25%-50%-100%). Fractions were collected, dried and dissolved in DMSO to perform liquid assay against L4 nematodes. As shown in **Figure 4**, fraction 25% Methanol, was the most active fraction with no nematodes alive at 1 mg/mL and only 22% of surviving worms at 0.5 mg/mL after 3 days of incubation. Fractions eluted at 50 and 100% of methanol, have a lower effect on nematodes viability (60% and 80% of surviving worms, respectively), thus confirming the polar nature of the bioactive anthelmintic compound produced by strains KRL4.

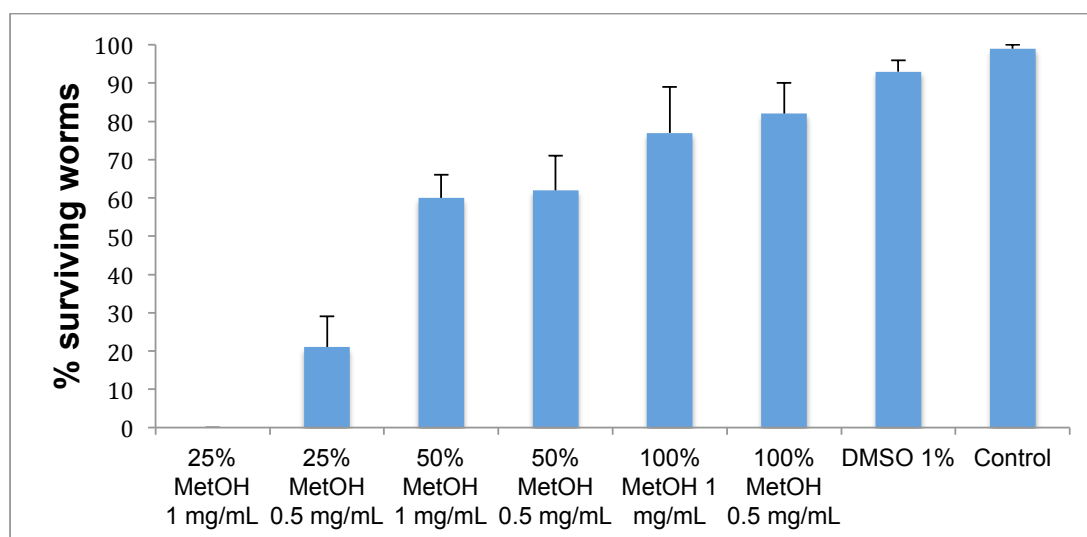


Figure 4. Anthelmintic activity of KRL4 SPE fractions. Data report percentage of surviving worms in the presence of the different fractions after 3 days of incubation at 20°C.

Ethyl Acetate extracts of strains MD3 was instead fractionated performing a flash column chromatography with silica (normal phase) with a methanol/chloroform system. The sample was dissolved with chloroform and loaded onto the column and the elution was performed at step increasing the methanol concentration up to 15% of methanol, then a final wash with 100% methanol was performed. Eluted fraction were then dried and dissolved in DMSO to perform antimicrobial assay against *F. tularensis*. Results are summarized in **Table 4** and report antimicrobial activity as the percentage of inhibition of the target with the different fractions at different concentration. It is possible to observe a clear peak of inhibition from fraction #2 to fraction #6, eluted between 0 and 6% methanol. Fraction #3 was eluted at 3% methanol and was the most active fraction with a MIC between 50 and 25 µg/mL.

Fraction	% Methanol	100 µg/mL	50 µg/mL	25 µg/mL	12.5 µg/mL	6.25 µg/mL	3.12 µg/mL
#1	Flow through	90	48	40	48	46	32
#2	0 %-2%	100	95	56	22	24	25
#3	3%	100	100	88	28	0	4
#4	4%	100	100	34	0	0	0
#5	5%	100	100	57	42	32	22
#6	5.5%	100	66	54	52	47	33
#7	6%-7%	67	48	44	39	37	28
#8	7%-11%	76	31	14	0	-6	0
#9	11%-14%	56	9	0	0	0	0
#10	100% wash	21	17	20	23	26	15

Table 4. Antimicrobial activity of MD3 fractions expressed as percentage of growth inhibition of *F. tularensis* when incubated the different fraction at different concentrations.

Chemical profiling of strain MD3 active fractions

The most active fractions produced from flash silica chromatography were submitted for a chemical profiling using LC-MS. This analysis revealed the presence of different compounds, especially diketopiperazines. Nonetheless, a major compound present in all the active fractions had $m/z = 375.2125$ and from MS^2 fragmentation pattern was tentatively identified as 16 β -hydroxycrambescidin 359. This compound is Batzelladine alkaloid and was first isolated from a caribbean sponge [23]. This compound has been reported for antiviral activity but not for antimicrobial. However, further purification and NMR experiments are required to confirm these results.

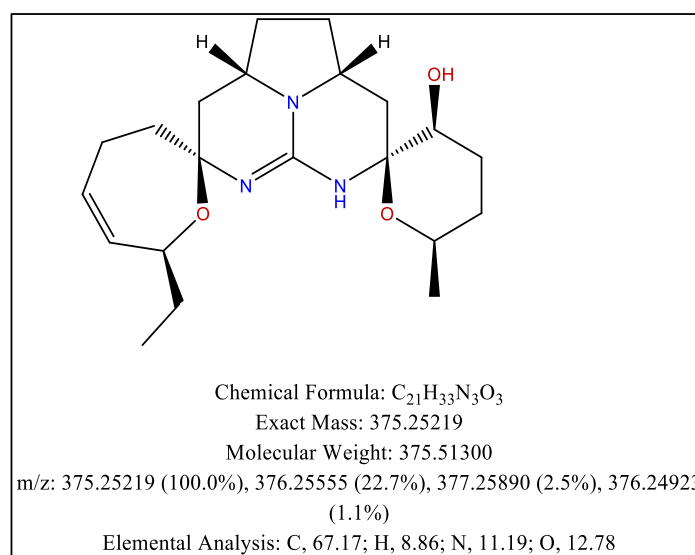


Figure 5. Molecular formula and chemical properties of 16 β -hydroxycrambescidin 359.

Phylogenetic analysis

The phylogenetic affiliation of bioactive producers strains MD3 and KRL4 was performed through the 16S rRNA genes amplification and analysis. To this purpose the 16S rRNA genes were PCR amplified and the nucleotide sequence of the amplicons determined. Each sequence was used as a query in a BLAST search to retrieve the most similar ones. This analysis proved that strain MD3 belongs to the genus *Pseudomonas*, and to the *mandelii* species. Bacteria belonging to this species are psychrophiles and are well-studied for their biotechnological potential [24-26]. Strain KRL4 was instead assigned to the *Exiguobacterium* genus, gram-positive psychrophilic bacteria. The strain has a low (less than 94%) sequence similarity with species *E. antarcticum* and *E. soli* and it is probably a new species. Bacteria belonging to this genus have already been observed as antimicrobial producers [27].

3.4 Conclusions

The aim of this work was to evaluate the potential of cold-adapted bacteria isolated from Tibetan glaciers as source of bioactive compounds. Applying an assay-based biodiscovery pipeline, we found two strains producing active metabolites against *C. elegans* and *F. tularensis*. Extracts from these two strains were purified and active fractions were identified and subjected to chemical profiling. The analyses performed on strain KRL4 (anthelmintic producer) active fractions, revealed the presence of peptides, but further analysis will be needed to identify the active molecule. Concerning strain MD3, its purified fraction was able to inhibit *F. tularensis* with a MIC between 50 and 25 µg/mL. This bacterium is a hazardous human pathogen causing tularemia, endemic in North America [28]. LC-MS analysis of the active fraction revealed the presence of diketopiperazines and of a batzellamine alkaloid: 16 β -hydroxycrambescidin 359. This compound was first isolated from a marine sponge, thus this finding is curious. We could explain that with the established evidence that several metabolites once attributed to sponges are actually produced by bacteria [29, 30], and this may be the case of 16 β -hydroxycrambescidin 359, but further studies are required to prove this hypothesis.

Nonetheless, this work confirms the promising potential of alpine microorganisms and prompts future efforts aiming at a large-scale exploitation of this resource of natural products.

3.5 References

1. Organization, W.H., *Antimicrobial resistance: global report on surveillance*. 2015.
2. Spellberg, B., et al., *The epidemic of antibiotic-resistant infections: a call to action for the medical community from the Infectious Diseases Society of America*. Clin Infect Dis, 2008. **46**(2): p. 155-64.
3. Awadzi, K., et al., *An investigation of persistent microfilaridermias despite multiple treatments with ivermectin, in two onchocerciasis-endemic foci in Ghana*. Ann Trop Med Parasitol, 2004. **98**(3): p. 231-49.
4. Osei-Atweneboana, M.Y., et al., *Prevalence and intensity of Onchocerca volvulus infection and efficacy of ivermectin in endemic communities in Ghana: a two-phase epidemiological study*. Lancet, 2007. **369**(9578): p. 2021-9.
5. Holden-Dye, L. and R.J. Walker, *Anthelmintic drugs*. WormBook, 2007: p. 1-13.
6. Papaleo, M.C., et al., *Bioactive volatile organic compounds from Antarctic (sponges) bacteria*. N Biotechnol, 2013. **30**(6): p. 824-38.
7. Maida, I., et al., *Phenotypic and genomic characterization of the Antarctic bacterium Gillisia sp. CAL575, a producer of antimicrobial compounds*. Extremophiles, 2013.
8. Papa, R., et al., *Anti-Biofilm Activities from Marine Cold Adapted Bacteria Against Staphylococci and Pseudomonas aeruginosa*. Front Microbiol, 2015. **6**: p. 1333.
9. Papa, R., et al., *Anti-biofilm activity of the Antarctic marine bacterium Pseudoalteromonas haloplanktis TAC125*. Res Microbiol, 2013. **164**(5): p. 450-6.
10. Hemala, L., D. Zhang, and R. Margesin, *Cold-active antibacterial and antifungal activities and antibiotic resistance of bacteria isolated from an alpine hydrocarbon-contaminated industrial site*. Res Microbiol, 2014. **165**(6): p. 447-56.
11. Lv, Y.L., et al., *Diversity and antimicrobial activity of endophytic fungi associated with the alpine plant Saussurea involucreta*. Biol Pharm Bull, 2010. **33**(8): p. 1300-6.
12. Wei, S., et al., *Diversity and distribution of archaea community along a stratigraphic permafrost profile from Qinghai-Tibetan Plateau, China*. Archaea, 2014. **2014**: p. 240817.
13. CHENG, D.G., *Glaciology and Geocryology of China in the Past 40 Years: Progress and Prospect*. Journal of Glaciology and Geocryology, 1998. **20**(3): p. 213-226.
14. Gil, H., et al., *Deletion of TolC orthologs in Francisella tularensis identifies roles in multidrug resistance and virulence*. Proc Natl Acad Sci U S A, 2006. **103**(34): p. 12897-902.
15. Platz, G.J., et al., *A tolC mutant of Francisella tularensis is hypercytotoxic compared to the wild type and elicits increased proinflammatory responses from host cells*. Infect Immun, 2010. **78**(3): p. 1022-31.
16. Stiernagle, T., *Maintenance of C. elegans* WormBook, The C. elegans Research Community, 2006.
17. Ballestriero, F., et al., *Identification of compounds with bioactivity against the nematode Caenorhabditis elegans by a screen based on the functional*

- genomics of the marine bacterium Pseudoalteromonas tunicata D2*. Appl Environ Microbiol, 2010. **76**(17): p. 5710-7.
18. Kothe, M., et al., *Killing of Caenorhabditis elegans by Burkholderia cepacia is controlled by the cep quorum-sensing system*. Cell Microbiol, 2003. **5**(5): p. 343-51.
 19. Papaleo, M.C., et al., *Sponge-associated microbial Antarctic communities exhibiting antimicrobial activity against Burkholderia cepacia complex bacteria*. Biotechnol Adv, 2012. **30**(1): p. 272-93.
 20. Grifoni, A., et al., *Identification of Azospirillum strains by restriction fragment length polymorphism of the 16S rDNA and of the histidine operon*. FEMS Microbiol Lett, 1995. **127**(1-2): p. 85-91.
 21. Altschul, S.F., et al., *Gapped BLAST and PSI-BLAST: a new generation of protein database search programs*. Nucleic Acids Res, 1997. **25**(17): p. 3389-402.
 22. Thompson, J.D., D.G. Higgins, and T.J. Gibson, *CLUSTAL W: improving the sensitivity of progressive multiple sequence alignment through sequence weighting, position-specific gap penalties and weight matrix choice*. Nucleic Acids Res, 1994. **22**(22): p. 4673-80.
 23. Hui-Ming Hua, J.P., D. Chuck Dunbar, Raymond F. Schinazi, Arcadio G. Castro Andrews, Carmen Cuevas, Luis F. Garcia-Fernandez, Michelle Kelly, Mark T. Hamann, *Batzelladine alkaloids from the caribbean sponge Monanchora unguifera and the significant activities against HIV-1 and AIDS opportunistic infectious pathogens*. Tetrahedron, 2007. **63**(45).
 24. Li, R., et al., *Psychrotrophic Pseudomonas mandelii CBS-1 produces high levels of poly-beta-hydroxybutyrate*. Springerplus, 2013. **2**: p. 335.
 25. Mageswari, A., et al., *Synthesis and larvicidal activity of low-temperature stable silver nanoparticles from psychrotolerant Pseudomonas mandelii*. Environ Sci Pollut Res Int, 2015. **22**(7): p. 5383-94.
 26. Kim, J., S.H. Jang, and C. Lee, *An organic solvent-tolerant alkaline lipase from cold-adapted Pseudomonas mandelii: cloning, expression, and characterization*. Biosci Biotechnol Biochem, 2013. **77**(2): p. 320-3.
 27. Shanthakumar, S.P., et al., *Broad spectrum antimicrobial compounds from the bacterium Exiguobacterium mexicanum MSSRFS9*. Microbiol Res, 2015. **178**: p. 59-65.
 28. Rowe, H.M. and J.F. Huntley, *From the Outside-In: The Francisella tularensis Envelope and Virulence*. Front Cell Infect Microbiol, 2015. **5**: p. 94.
 29. Piel, J., *Metabolites from symbiotic bacteria*. Nat Prod Rep, 2009. **26**(3): p. 338-62.
 30. Hochmuth, T. and J. Piel, *Polyketide synthases of bacterial symbionts in sponges--evolution-based applications in natural products research*. Phytochemistry, 2009. **70**(15-16): p. 1841-9.

PUBLICATIONS

Investigating the Role of the Host Multidrug Resistance Associated Protein Transporter Family in Burkholderia cepacia Complex Pathogenicity Using a Caenorhabditis elegans Infection Model. Tedesco P, Visone M, Parrilli E, Tutino ML, Perrin E, Maida I, Fani R, Ballestriero F, Santos R, Pinilla C, Di Schiavi E, Tegos G, de Pascale D. **PLoS One**. 2015 Nov 20;10(11):e0142883. doi: 10.1371/journal.pone.0142883. eCollection 2015.

Identification and characterization of a novel salt-tolerant esterase from a Tibetan glacier metagenomic library. De Santi C, Ambrosino L, Tedesco P, Zhai L, Zhou C, Xue Y, Ma Y, de Pascale D. **Biotechnol Prog**. 2015 Jul-Aug;31(4):890-9. doi: 10.1002/btpr.2096. Epub 2015 May 15. Erratum in: *Biotechnol Prog*. 2015 Sep-Oct;31(5):1442.

Marine metagenomics, a valuable tool for enzymes and bioactive compounds discovery. Barone R, De Santi C, Palma Esposito F, Tedesco P, Visone M, Galati F, Di Scala A, de Pascale D. **Frontiers in Marine Science**, 04 September 2014 | doi: 10.3389/fmars.2014.00038

A new alkaliphilic cold-active esterase from the psychrophilic marine bacterium Rhodococcus sp.: functional and structural studies and biotechnological potential. De Santi C, Tedesco P, Ambrosino L, Altermark B, Willassen NP, de Pascale D. **Appl Biochem Biotechnol**. 2014 Mar;172(6):3054-68. doi: 10.1007/s12010-013-0713-1. Epub 2014 Feb 1.

α -rhamnosidase activity in the marine isolate Novosphingobium sp. PP1Y and its use in the bioconversion of flavonoids. Izzo V, Tedesco P, Notomista E, Pagnotta E, Di Donato A, Trincone A, Tramice A. *Journal of Molecular Catalysis B: Enzymatic* 105 (2014) 95–103

Submitted Manuscripts

Antimicrobial activity of monoramnholipids produced by bacterial strains isolated from Ross sea (Antarctica). Tedesco P, Maida I, Palma Esposito F, Tortorella E, Subko E, Ezeofor CC, Zhang Y, Tabudravu J, Jaspars M, Fani R, de Pascale D. **Marine Drugs**. Manuscript accepted with minor revisions.

The antimicrobial potential of algicolous marine fungi to counteract multidrug resistant bacteria: phylogenetic diversity and chemical profiling. Gnani G, Palma Esposito F, Festa C, Polia A, Tedesco P, Fani R, Monti MC, de Pascale D, D'Auria MV, Varese GC. **Research in Microbiology**. Manuscript accepted with minor revisions.

Book Chapter

High Throughput Flow Cytometry Screening of Multidrug Efflux Systems. Haynes MK, Garcia M, Peters R, Waller A, Tedesco P, Ursu O, Bologna CG, Santos R, Pinilla C, Wu TH, Lovchik J A, Oprea TI, Sklar LA, Tegos GP. Book Title: *Bacterial Multidrug Exporters in Methods in Molecular Biology*, Springer. To be published in

May 2016.

COMMUNICATION

Oral communication

Pietro Tedesco

Antimicrobial activity of monoramnholipids produced by bacterial strains isolated from Ross sea (Antarctica)

Conference: Pharmasea Project General Assembly meeting (Glasgow, Scotland 4-5 September 2015)

Pietro Tedesco

Exploiting the cold potential: psychrophilic bacteria as a promising source of novel bioactive compounds

Conference: "Biotechnology World Congress 2014 (Valencia, Spain, 25-27 June 2014)

Pietro Tedesco

Microorganisms from Tibetan Glaciers as source of novel drugs

Conference: "Cortona Procarioti 2014 (Cortona, Italy 15-17 May 2014)

Poster communication

Antimicrobial activity of Antarctic bacteria

Pietro Tedesco, Isabel Maida, Fortunato Palma Esposito, Emiliana Tortorella, Jioji Tabudravu, Marcel Jaspars, Renato Fani, Donatella de Pascale.

Conference: Bioprosp 2015 (Tromso, Norway 18-20 February 2015)

Analysis of virulence factors of Burkholderia cepacia complex strains in the Caenorhabditis elegans host model

Pietro Tedesco, Marco Visone, Ermenegilda Parrilli, Maria Luisa Tutino, Elena Perrin, Renato Fani, George Tegos, Elia Di Schiavi, Donatella de Pascale.

Conference: Biotechnology World Congress 2014 (Valencia, Spain, 25-27 June 2014)

Analysis of virulence factors of Burkholderia cepacia complex strains in the Caenorhabditis elegans host model. **Pietro Tedesco, Marco Visone, Ermenegilda Parrilli, Maria Luisa Tutino, Elena Perrin, Renato Fani, Donatella de Pascale.**

Conference: MICROBIOLOGY 2013 30th Meeting of the "Società Italiana di Microbiologia Generale e Biotecnologie Microbiche" SIMGBM, (Ischia, Italy 18-21 September 2013)

A high throughput flow cytometric platform targeting RND multidrug efflux systems in gram-negative bacteria.

Mark K. Haynes, Oleg Ursu, Anna Waller, Matthew Garcia, Ryan Peters, Pietro Tedesco, Julie Lovchik, Cristian Bologna, Larry A. Sklar¹, George P. Tegos.

Conference: SLAS 2014 - An exceptional array of answers. (San Diego, USA 18-22 January 2014).

EXPERIENCES IN FOREIGN LABORATORIES

During my PhD project I have spent 3 months of my first year (September 2013 - December 2013) at the University of New Mexico, Center for Molecular Discovery, under the supervision of the Prof. George Tegos. The research activities performed were focused on the creation and the screening of a library of natural extracts from psychrophilic bacteria against a panel of multi-drug resistance pathogens. A partial purification of one extract against the human pathogen *Francisella tularensis* was also carried out.

During my second year I have spent 2 months (July 2014 - September 2014) performing my research activities at the University of Aberdeen, Marine Biodiscovery Centre, under the supervision of the Prof. Marcel Jaspars. The research activities I have performed at the MBC were focused on the purification and identification of bioactive compounds from Antarctic bacteria targeting human pathogens, by using SPE and HPLC, as well as NMR and LC-MS instrumentation.

During my third year I have taken part to the PHARMADEEP mission funding by the Eurofleet consortium. The goal of the mission was to explore the pharmaceutical potential of organisms isolated from Antarctic deep Trench located near the South Shetlands Island, Antarctica. The mission was performed in December 2015 (11-30 December) on board the Spanish Scientific Vessel "Hesperides". My on-board activities were focused on the collected of deep-sea sediments and the isolation of bacteria.

A New Alkaliphilic Cold-Active Esterase from the Psychrophilic Marine Bacterium *Rhodococcus* sp.: Functional and Structural Studies and Biotechnological Potential

Concetta De Santi · Pietro Tedesco · Luca Ambrosino ·
Bjørn Altermark · Nils-Peder Willassen ·
Donatella de Pascale

Received: 25 October 2013 / Accepted: 25 December 2013
© Springer Science+Business Media New York 2014

Abstract The special features of cold-adapted lipolytic biocatalysts have made their use possible in several industrial applications. In fact, cold-active enzymes are known to be able to catalyze reactions at low temperatures, avoiding side reactions taking place at higher temperatures and preserving the integrity of products. A lipolytic gene was isolated from the Arctic marine bacterium *Rhodococcus* sp. AW25M09 and expressed in *Escherichia coli* as inclusion bodies. The recombinant enzyme (hereafter called *RhLip*) showed interesting cold-active esterase activity. The refolded purified enzyme displayed optimal activity at 30 °C and was cold-active with retention of 50 % activity at 10 °C. It is worth noting that the optimal pH was 11, and the low relative activity below pH 10 revealed that *RhLip* was an alkaliphilic esterase. The enzyme was active toward short-chain *p*-nitrophenyl esters (C2–C6), displaying optimal activity with the butyrate (C4) ester. In addition, the enzyme revealed a good organic solvent and salt tolerance. These features make this an interesting enzyme for exploitation in some industrial applications.

Keywords Esterase · Cold-active · Alkaliphilic · Biotechnological applications

Introduction

Esterases (EC 3.1.1.1) are hydrolytic enzymes that catalyze the hydrolysis of esters into alcohol and acid. They generally differ from lipases (EC 3.1.1.3) regarding the substrate

Concetta De Santi and Pietro Tedesco contributed equally to this work.

C. De Santi · P. Tedesco · L. Ambrosino · D. de Pascale (✉)
Institute of Protein Biochemistry, National Research Council, Via P. Castellino, 111, 80131 Naples, Italy
e-mail: d.depascale@ibp.cnr.it

B. Altermark · N.-P. Willassen
NorStruct, Department of Chemistry, Faculty of Science and Technology, University of Tromsø, Tromsø,
Norway

specificity. By now, it is well recognized that esterases catalyze the hydrolysis and the synthesis of short-chain esters (less than 10 carbon atoms), while lipases act on substrates with long chains of carbon atoms (more than 10) [1]. These enzymes belong to the α/β -hydrolase superfamily and possess a highly conserved catalytic triad formed by Ser, His, and Asp [2]. Lipolytic enzymes are employed in a wide range of industrial applications including the food industry and detergent production as well as biocatalysts for chemical synthesis [3]. In particular, cold-active lipolytic enzymes are extremely appealing for industrial uses. It is generally accepted that cold-active biocatalysts have a more flexible structure [4] compared to mesophilic and thermophilic counterparts, and this high flexibility enables increased complementarity between active site and substrates, resulting in high specific activity at low temperatures [5]. Thus, the use of cold-adapted biocatalysts can minimize undesirable side reactions taking place at higher temperatures and allow reactions involving heat-sensitive substrates [6]. These properties are important for exploitation in the food industry, where the preservation of the nutritional value and flavor of the food is fundamental. Furthermore, thanks to their relatively low thermostability, these enzymes can often easily be inactivated.

Therefore, bioprospecting, looking for cold-active lipolytic enzymes from Arctic regions, has become an active and expanding discipline. In fact, organisms living in an extremely cold habitat have adopted several strategies to survive and thrive in these challenging environments, and these include the expression of enzymes able to efficiently catalyze reactions at temperatures close to 0 °C [7].

In this paper, we present the purification and characterization of a cold-active esterase from the marine psychrophilic actinobacterium *Rhodococcus* sp. AW25M09. This bacterium was isolated from the intestines/stomach of an Atlantic hagfish (*Myxine glutinosa*) captured on the cold seafloor during sampling performed in Hadsel Fjord, North Norway. Its genome was recently published [8]. The *lip3* gene was selected for its unique amino acid sequence and its homology with other lipases/esterases. The gene was amplified by PCR then cloned and recombinantly expressed in *Escherichia coli*, and the protein, aggregated as inclusion bodies, was refolded and extensively characterized.

Materials and Methods

Isolation of a Lipolytic Gene

The genome of the cold-adapted *Rhodococcus* sp. AW25M09 has been sequenced and has been deposited at DDBJ/EMBL/GenBank under accession number CAPS00000000. The genome was analyzed using the Artemis [9] with the aim to identify new genes encoding for esterases and lipases to be expressed in *E. coli*. Sequence analysis revealed an open reading frame (ORF) of 1,056 bp, the *lipR* lipolytic gene that encodes for a protein of 352 amino acids.

lipR Gene Cloning

Rhodococcus sp. AW25M09 was grown in Marine 2216 broth (Difco, Sparks, USA) at 20 °C, and the genomic DNA was purified with Sigma's GenElute Bacterial Genomic Kit according to the manufacturer's instruction and was used as template for the *lipR* gene amplification by PCR.

Two primers containing NdeI and NotI restriction sites were designed: 5'-AATACATATG TACCGCAGCAACGACTCCAACG-3' and 5'-AATAGCGGCCGCGCAGTTGGACGGTG CAGGCACT-3'.

PCR was performed by using Mastercycler personal (Eppendorf, New York, USA). The reaction conditions used were as follows: 1 cycle (94 °C for 3 min), 30 cycles (94 °C for 30 s, 60 °C for 30 s, and 72 °C for 1 min), and a final cycle of 72 °C for 7 min. The amplified PCR product of 1,056 bp was cloned into pET-22b expression vector previously digested by NdeI and NotI restriction enzymes (New England BioLabs, Ipswich, MA, USA) including an in-frame C-terminal fusion purification 6×His-Tag. *E. coli* DH5- α competent cells were first transformed through the ligation reaction, and the construct was verified by bidirectional DNA sequencing. The isolated plasmid was then used to transform *E. coli* strain BL21(DE3) competent cells.

RhLip Recombinant Production in *E. coli* Cells

E. coli BL21(DE3) carrying pET-22b-*lipR* vector was grown in a shake flask containing Luria Bertani broth (LB) medium supplemented with 100 μ g/mL ampicillin at 37 °C for 16 h. Growing culture was diluted to a cell density of about 0.05 OD₆₀₀ in a 1-L shake flask containing 200 mL of LB medium supplemented with 100 μ g/mL ampicillin. *RhLip* induction was performed when the culture density reached 0.5–0.6 at OD₆₀₀ by the addition of filter-sterilized isopropyl- β -D-1-thiogalactopyranoside (IPTG) to a final concentration of 0.1 mM. Culture was carried out at constant agitation (220 rpm) at 20 °C for 16 h post-induction. Cells were then harvested by centrifugation at 6,000 rpm for 20 min at 4 °C, divided into 0.5-g aliquots, and frozen at –20 °C.

RhLip Purification and Refolding from Inclusion Bodies

The bacterial pellet (0.5 g) was frozen and thawed twice, and resuspended in 4 mL of Tris-EDTA (TE) buffer (20 mM Tris-HCl pH 8.0, 5 mM EDTA pH 8.0), and 0.6 mg of lysozyme and 0.75 g sucrose were added to the suspension; the suspension was incubated at 37 °C. After 30 min, 4 mL ice-cold TE buffer was added to the suspension and the suspension was incubated for 30 min at 37 °C; then, cells were subjected to sonication. Sonicated cells were centrifuged at 6,700 rcf for 20 min at 4 °C; then, the pellet was washed with 4 mL TE buffer and centrifuged and washed with 2 mL of 20 mM Tris-HCl pH 8.0. The extract was finally centrifuged for 10 min at 4 °C at 10,000 rcf. The pellet was resuspended in 10 mL of 6 M urea, 20 mM Tris-HCl pH 8.0, 15 mM β -mercaptoethanol, and 5 mM EDTA pH 8.0 at 4 °C with gentle shaking for 2 h. The insoluble material was removed by centrifugation at 15,000 rcf for 30 min at 4 °C. Renaturation of the supernatant containing the *RhLip* was achieved by a 30-fold dilution of the denaturant in 20 mM Tris-HCl pH 8.0, 500 mM arginine, 0.6 mM GSH, and 12 mM GSSG, and the solution was concentrated to about 10 mL using an Amicon ultrafiltration cell (Millipore, Billerica, USA) equipped with a 10-kDa membrane and abundantly dialyzed against 20 mM Tris-HCl pH 8.0. The protein was finally aliquoted and stored at –20 °C in the presence of 20 % glycerol.

Electrophoretic Analysis

Electrophoretic runs were performed with a Mini-Protean II cell (Bio-Rad, Hercules, CA) unit at room temperature. Twelve percent SDS-PAGE was made as described by Laemmli [10]. Marker XL-OPTI Protein 2.8 (ABM, Richmond, BC, Canada) was used as molecular weight standard.

RhLip Determination of pH and Temperature Optima

The esterase activity was monitored at 348 nm (the pH-independent isosbestic point of *p*-nitrophenol and *p*-nitrophenoxide ion) with *p*NP-pentanoate (100 μ M) as substrate. The kinetic measurements were performed at 25 °C, and the buffers used were 0.1 M Naphosphate over the pH range of 7.0–7.5, 0.1 M Tris-HCl over the pH range of 7.5–9.5, and 0.1 M CAPS over the pH range of 9.5–12.0. The assays were carried out in duplicate or triplicate, and the results were the means of two or three independent experiments. Due to the high self-degradation rate of the *p*NP-esters at high pH values, all further characterizations were performed at pH 10.0. The dependence of activity on temperature was studied over the range of 10–60 °C, with *p*NP-pentanoate (100 μ M) as substrate, in a reaction mixture 0.1 M CAPS pH 10.0, containing 3 % acetonitrile (standard conditions).

RhLip Thermostability

The thermal stability of *RhLip* was studied over the range of 5–50 °C. Pure enzyme (0.2 mg/mL in a 0.1 M CAPS buffer pH 10.0) was incubated in tubes at different temperatures. Aliquots were withdrawn after 30, 60, 90, and 120 min and assayed at 30 °C in standard condition described above, using *p*NP-pentanoate as substrate.

RhLip Esterase Activity

The time course of the esterase-catalyzed hydrolysis of *p*NP-esters was followed by monitoring of *p*-nitrophenoxide production at 405 nm, in 1-cm path-length cells with a Cary 100 spectrophotometer (Varian, Mulgrave, Australia). Initial rates were calculated by linear least-squares analysis of time courses comprising less than 10 % of the substrate turnover. Assays were performed at 30 °C in a mixture of 0.1 M CAPS pH 10, 3 % acetonitrile, containing *p*NP-esters (100 μ M). Stock solutions of *p*NP-butanoate (C4), *p*NP-pentanoate (C5), and *p*NP-hexanoate (C6) (Sigma-Aldrich, MO, USA) were prepared by dissolving substrates in pure acetonitrile. Assays were performed in duplicate, and the results were the mean of two independent experiments. One unit of enzymatic activity was defined as the amount of the protein releasing 1 μ M of *p*-nitrophenoxide/min from *p*NP-esters. The absorption coefficient used for *p*-nitrophenoxide was 19,000 at 30 °C and pH 10.

Kinetic Measurements and Analysis

Initial velocities versus substrate concentration data were fitted to the Michaelis-Menten equation using the software GraphPad Prism version 5.00 (GraphPad software, La Jolla, USA). The concentration of *p*NP-butanoate and *p*NP-pentanoate ranged from 0.05 to 2 mM, while *p*NP-hexanoate were varied from 0.1 to 1 mM. Assays were done in duplicate and the results were the mean of two independent experiments. The kinetic experiments were performed using acetonitrile as solvent.

Effect on Enzymatic Activity by Organic Solvents, Detergents, Metals, and NaCl

Enzyme activity was evaluated in the standard assay (0.1 M CAPS pH 10, 3 % acetonitrile, 30 °C) using *p*NP-pentanoate as substrate. The activity was measured using an increasing concentration of the solvents such as acetonitrile, dimethyl sulfoxide (DMSO), diethyl ether,

and dimethyl formamide (DMFA) from 0 to 20 % (v/v) in the assay mixture. Results were reported as relative activity with respect to the value measured without solvents.

The effect of detergents on enzymatic activity of *RhLip* was evaluated by incubating 0.1 mg/mL of pure protein in the presence of 5 mM Triton X-100, Tween-20, and Tween-80 at 5 °C for 1 h. The residual enzymatic activity was measured in the standard condition as described above. Preferences for metal cations were analyzed by adding them separately to 0.1 mg/mL of pure protein at a final concentration of 5 mM and equilibrate at 5 °C for 1 h. The residual enzymatic activity was then measured in the standard condition as described above. The effect of NaCl on enzymatic activity was evaluated by increasing the salt concentration in a range of 0–1 M at 30 °C in standard assay conditions.

Modeling of *RhLip*

The three-dimensional model of *RhLip* was performed by a comparative modeling strategy using the structure of *Candida antarctica* lipase A as template (CAL A, PDB code 3GUU). The sequence alignment was calculated by the CLUSTALW program [11]. The MODELLER 9v11 program [12] was used to build 100 full atom models of *RhLip* structure setting 4.0 Å as root mean square deviation (RMSD) among initial models and by full model optimization. Structure validation was carried out using the pictorial database PDBsum [13]. The structure of the generated model was uploaded to the PDBsum server, and structural analyses, including PROCHECK plots [14], were generated. Moreover, the *Z* score of the *RhLip* model and *C. antarctica* lipase A (CAL A) structure was calculated by the web server WhatIf [15]. The *Z* score expresses how well the backbone conformations of all residues correspond to the known allowed areas in the Ramachandran plot. Furthermore, the solvent-accessible surface areas (SASAs) of *RhLip* model and CAL A structure were calculated using the POPS algorithm [16].

Molecular Dynamics

Molecular dynamics (MD) simulations were performed with GROMACS software package (v4.5.5) [17]. The model was inserted in a dodecahedron box filled with SPC216 water molecules using GROMOS43a1 all-atom force field. Simulations were carried out at different pH values. Imposing different protonation states according to the number of titratable groups reproduced neutral and basic pH conditions. The simulations were carried out by adding 26 sodium ions to have a value of zero for the net electrostatic charge of the system. The systems were subjected to several cycles of energy minimizations and position restraints to equilibrate the protein and the water molecules around the protein. Particle mesh Ewald (PME) algorithm was used for the electrostatic interactions with the cutoff of 1 nm. The time step was 2 fs, and the temperature was kept constant at 300 K using a modified Berendsen thermostat with a time constant of 0.1 ps. The simulation time for each dynamic was 10 ns. GROMACS routines were used to analyze the trajectories in terms of RMSD, RMSF, and gyration radius.

Results and Discussion

Purification and Refolding from Inclusion Bodies

In this work, we present a biochemical characterization of a new alkaliphilic esterase from *Rhodococcus* sp. The *lip3* gene was cloned into a pET-22b expression vector, and the

construct was transferred into *E. coli* BL21(DE3) calcium competent cells. Several expression conditions were investigated, but IPTG induction of *E. coli* cells resulted in the accumulation of recombinant *RhLip* as inclusion bodies (IB). The induction at 20 °C was effective in producing the highest amount of *RhLip* compared to the other contaminant proteins. The IBs were purified and the protein refolded as described in the “Materials and Methods” section. According to the structural analysis, two disulfide bridges were detected, and the refolding protocol was optimized by adding GSSG (oxidized glutathione) and GSH (reduced glutathione) to the refolding solution. Using this protocol, about 8 mg of pure enzyme was obtained from 0.5 g of *E. coli* cell pellet.

Purity of the protein preparation was evaluated by SDS-PAGE analysis. As shown in Fig. 1, a single band was observed with an apparent mass of about 38 kDa.

RhLip Functional Characterization

The dependence of *RhLip* activity in the function of pH was estimated using *p*NP-pentanoate as substrate (Fig. 2a). The absorption of *p*-nitrophenol changes at different pH values because of variations in equilibrium between *p*-nitrophenol and *p*-nitrophenoxide. In this work, we monitored the release of *p*-nitrophenol at 348 nm, that is, the isosbestic point of *p*-nitrophenol and *p*-nitrophenoxide. The maximum activity of

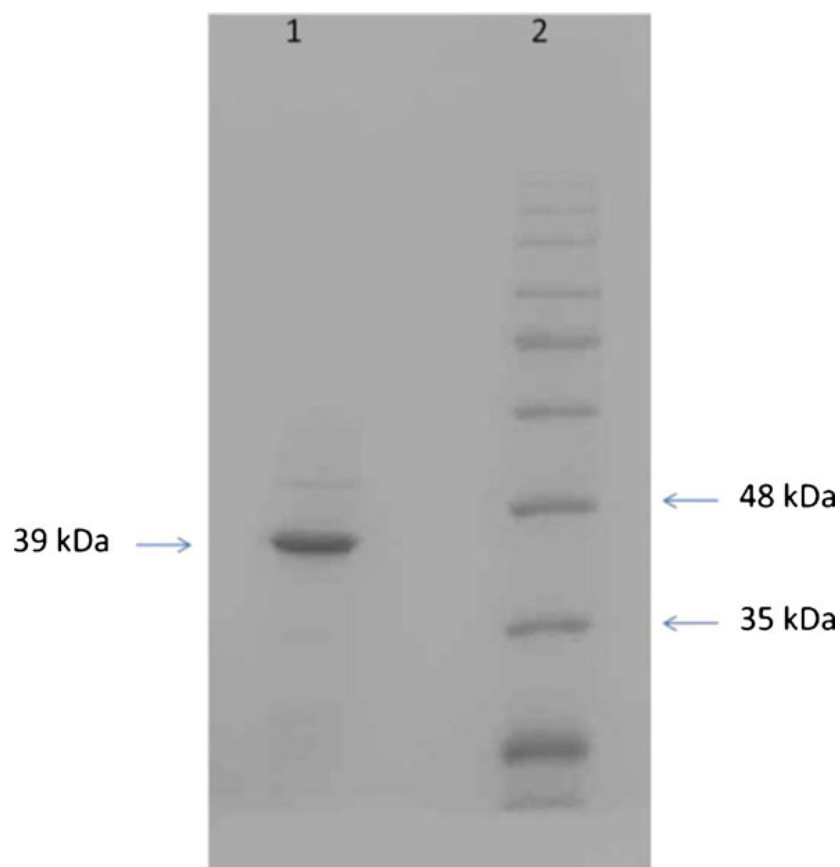


Fig. 1 SDS-PAGE (12 % acrylamide) of *RhLip* after the denaturation-refolding procedures. Lane 1, purified *RhLip*; lane 2, molecular weight marker

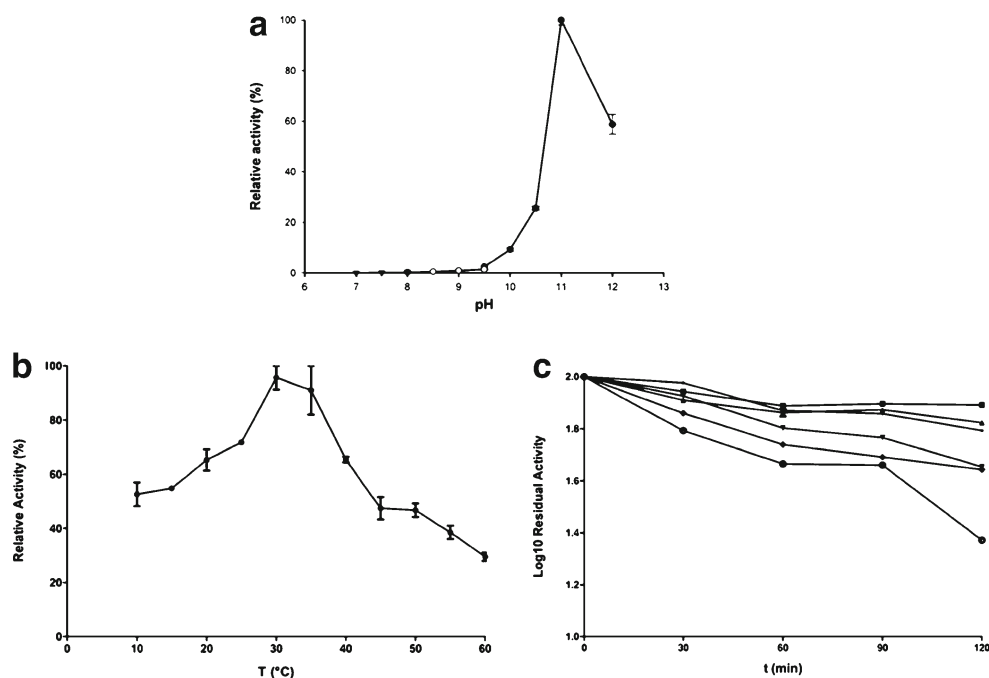


Fig. 2 **a** Effect of pH on the esterase activity. **b** Effect of temperature on the esterase activity. **c** Thermostability of *RhLip*, at various temperatures, such as 5 °C (black circles), 10 °C (black squares), 20 °C (black up-pointing triangles), 30 °C (black down-pointing triangles), 40 °C (black diamonds), and 50 °C (white circles). The enzyme was incubated in 0.1 M CAPS pH 10.0 at the indicated temperatures and times. The residual activity was measured at 30 °C using *p*NP-pentanoate as substrate

RhLip was recorded at pH 11 in 0.1 M CAPS, and the relatively low activity between pH 7 and pH 9 suggests that the enzyme was a highly alkaliphilic esterase. Other alkaliphilic esterases have been identified from genomic and metagenomic sources so far [18] including two other cold-active esterases with optimal pH >10 [19–21]. The relationship between *RhLip* activity and temperature was evaluated in the range of 10–60 °C using *p*NP-pentanoate as substrate (Fig. 2b). The apparent maximal activity was recorded at 30 °C, and the activity detected at 10 °C remained approximately the 50 % of the maximum activity.

The *RhLip* thermal stability was evaluated in the range of 5–50 °C. Enzyme samples were incubated at any given temperature for different lengths of time, and the residual activity was recorded at 30 °C. This study demonstrated that *RhLip* presented a typical behavior as other psychrophilic enzymes, showing a low kinetic stability at temperature higher than 30 °C [22, 23].

In fact, as shown in Fig. 2c, we observed a very low decrease in activity after 2 h of incubation at 5, 10, and 20 °C, while when the temperature increased up to 30 and 40 °C, we noted a significant decrease in activity. After 2 h of incubation at 50 °C, only 20 % of enzymatic activity was still recorded.

Kinetics Studies

We investigated the activity of *RhLip* toward different synthetic substrates by using several *p*NP-esters with different acyl chain lengths. Activity was assessed in the presence of 0.1 M CAPS pH 10 instead of the optimum pH buffer (0.1 M CAPS pH 11) due to the instability of

the various substrates at alkaline pH value. All the characterization was also performed at 30 °C and in the presence of 3 % acetonitrile. Concerning the affinity values, we observed that K_m values decrease when acyl chain length increases, and this suggests that *RhLip* possesses a high affinity with longer aliphatic chain substrates. Instead, the K_{cat} and K_{cat}/K_m values show the opposite behavior: in our standard conditions, the enzyme displays the highest K_{cat} and K_{cat}/K_m on *p*NP-butanoate with values of 1.63 s⁻¹ and 2.16 s⁻¹ mM⁻¹, respectively (Table 1). The biochemical characterization of the recombinant enzyme revealed *p*NP-butanoate (C4) as the preferred substrate, and the hydrolytic activity significantly decreased as the chain length increased above C8, with very little activity toward *p*NP-tetradecanoate (C14) (data not shown), suggesting that the enzyme was an esterase and not a lipase.

Effect on Enzymatic Activity by Organic Solvents, Detergents, Metals, and NaCl

The effect of the presence of water-miscible solvents on *RhLip* enzymatic activity on *p*NP-pentanoate at 30 °C in 0.1 M CAPS pH 10.0 was investigated. For all the solvents tested, except DMFA, we observed a similar behavior as shown in Fig. 3a. The increasing concentration of organic solvent in the assay mixture enlarged *RhLip* catalytic activity up to a critical concentration, and further addition of solvents led to a gradual protein inactivation. These results are coherent to what were observed for other esterases belonging to hormone-sensitive lipase protein family, as demonstrated by Mandrich and coworkers [24].

We reported the best enzymatic activation (more than 200 % of the relative activity) in the presence of 5 % diethyl ether. This behavior has been explained in literature as the ability of the organic solvents to stabilize ionic intermediates in the case of aprotic solvents [25]. *RhLip* was incubated in the presence of various denaturants or metal ions for 1 h, and the residual activity was measured using *p*NP-pentanoate as substrate at 30 °C. The resulting values are summarized in Table 2, which demonstrated that few tested compounds had an inhibitory effect on *RhLip* activity, although at various extents. The strongest inhibitory effect was observed in the presence of Ca²⁺ ions suggesting the absence of a Ca²⁺-binding motif sequence. A similar effect of enzymatic inactivation was detected in the presence of Tween-80. On the contrary, a strong activation was observed by incubating the *RhLip* in the presence of Tween-20 and EDTA. Tween 20 was more easily hydrolysed than Tween-80, indicating that the chain length may play an important role on substrate specificity [26].

The effect of the presence of NaCl on *RhLip* enzymatic activity was evaluated on *p*NP-pentanoate in 0.1 M CAPS pH 10.0 at 30 °C. We observed an improved activity with the highest concentration of 1 M NaCl (Fig. 3b). A similar behavior may be explained as the ability of salt to enhance the hydrophobic interaction between enzyme and substrate [27].

Table 1 Kinetic parameters

	K_m (mM)	K_{cat} (1/s)	K_{cat}/K_m (1/s*mM)
<i>p</i> NP-butanoate	0.753±0.098	1.63±0.19	2.16±0.25
<i>p</i> NP-valerate	0.691±0.090	0.69±0.09	0.99±0.11
<i>p</i> NP-caproate	0.276±0.036	0.14±0.01	0.45±0.04

All parameters were calculated at 30 °C, in 0.1 M CAPS pH 10.0, containing acetonitrile at a final concentration of 3 %

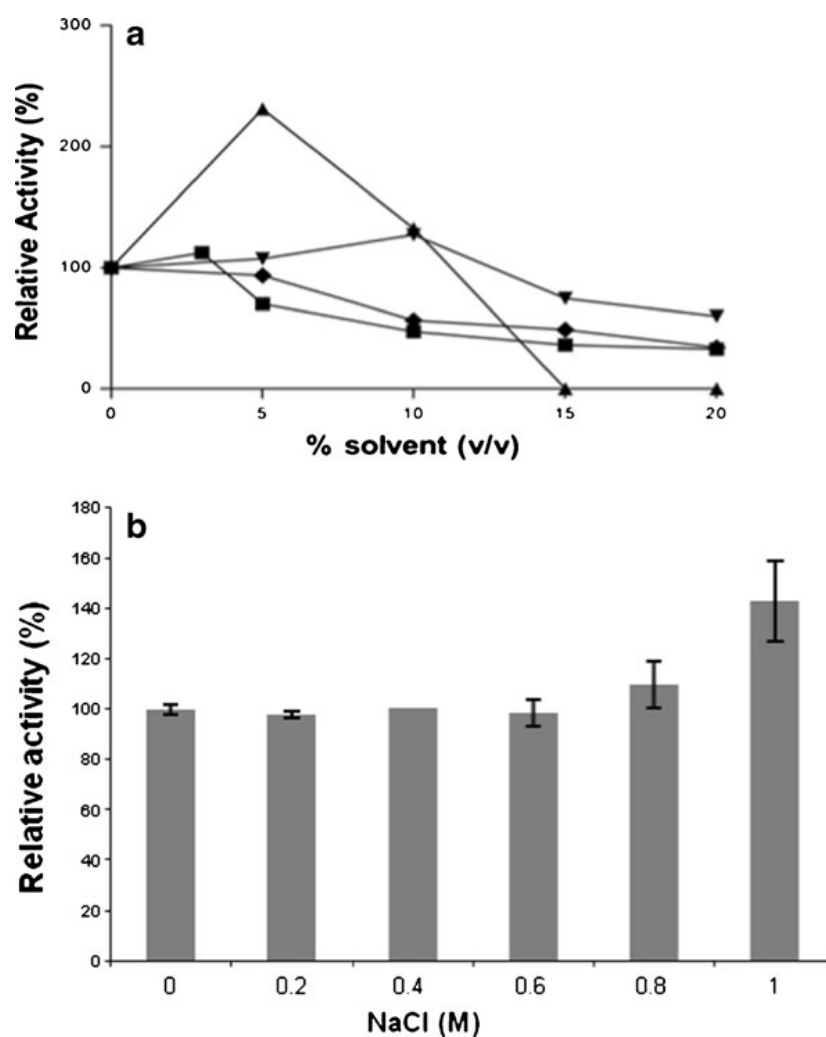


Fig. 3 **a** Effect of organic solvents on the esterase activity. Enzyme activity was evaluated in the presence of increasing concentration of acetonitrile (black squares), diethyl ether (black up-pointing triangles), DMSO (black down-pointing triangles), and DMFA (black diamonds). The relative activity was measured at 30 °C in 0.1 M CAPS pH 10.0 using *p*NP-pentanoate as substrate. **b** Effect of NaCl on the esterase activity. Enzyme activity was evaluated in the presence of increasing concentrations of NaCl. The relative activity was measured at 30 °C in 0.1 M CAPS pH 10.0 with *p*NP-pentanoate as substrate

RhLip Model

The three-dimensional modeling of *RhLip* was performed by a homology modeling approach using the *C. antarctica* lipase A (PDB ID: 3GUU) structure as template. The CAL A structure was chosen due to sequence identity of 30 % between the *RhLip* sequence and the template. The multiple alignments between *RhLip* and the best scoring templates are shown in Fig. 4. Starting from the alignment of *RhLip* sequence with the reference structure, a set of 100 all-atom models was generated. The best model (Fig. 5a) was selected in terms of energetic and stereochemical quality. In details, it had 89.2 % of

Table 2 Effect of various compounds on *RhLip* activity

Compounds (5 mM)	Relative activity (%)
No addition	100
CaCl ₂	40.77±2
CuCl ₂	101.94±9
MgCl ₂	124.27±17
LiCl ₂	130.10±1
EDTA	195.14±6
Tween-20	151.46±15
Tween-80	0
Triton X-100	98.06±10

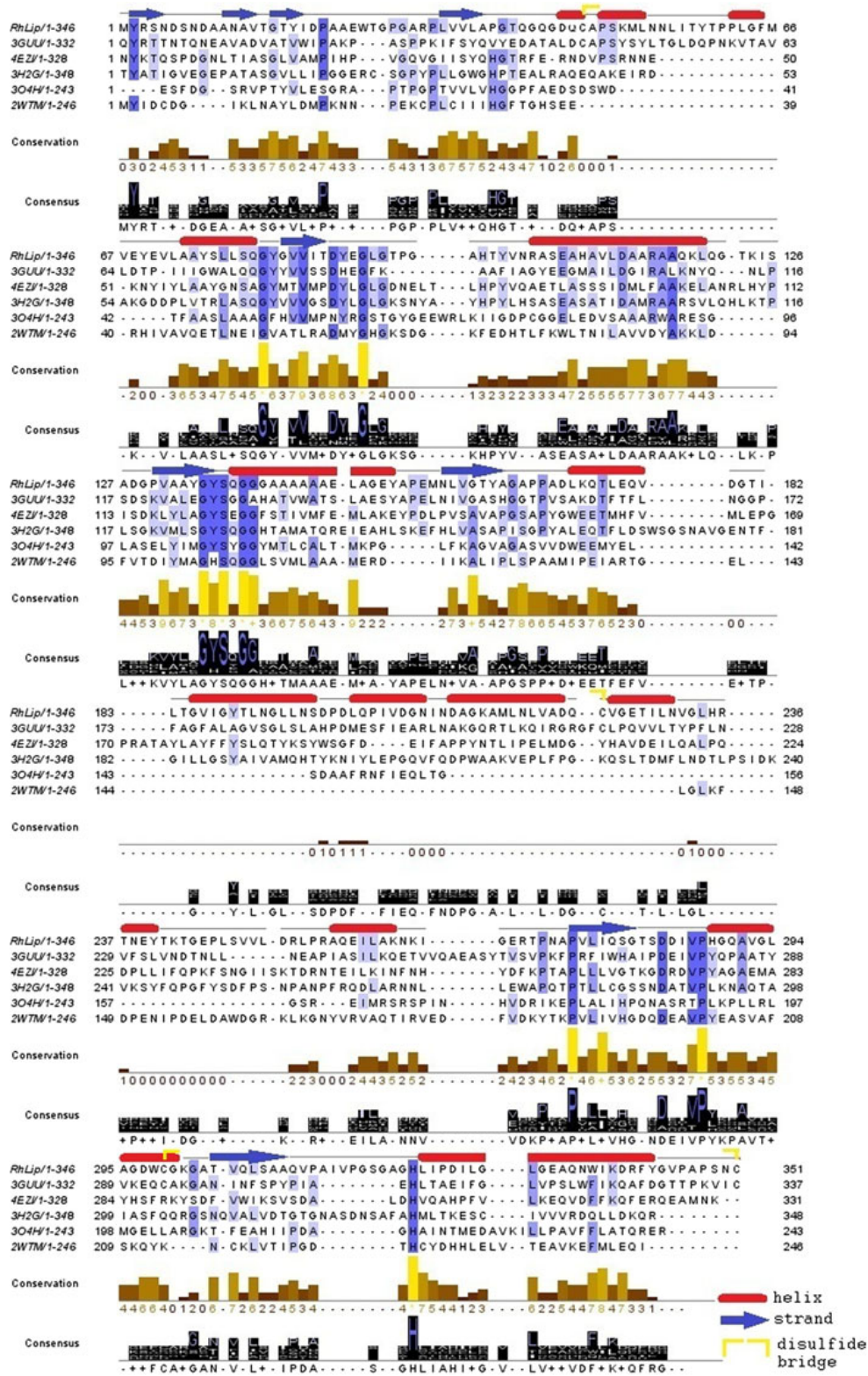
The residual activity was measured in 0.1 M CAPS pH 10.0 with *p*NP-pentanoate at 30 °C

residues in most favored regions of the Ramachandran plot according to PROCHECK program and a WhatIf *Z* score of 0.050. These values, compared with those of the template structure, i.e., *Z* score = -1.181 and 88.6 % of residues in most favored regions of the Ramachandran plot, indicated that the quality of the model was really high. The *RhLip* model showed an alpha-beta structure characterized by 13 α -helices (H3, H5–H16), three 3_{10} helices (H1, H2, and H4), and nine beta-strands (B1–B9), corresponding to 39.6 and 14.5 % of the sequence, respectively. *RhLip* secondary structures are represented in Fig. 6. *RhLip* was stabilized by two disulfide bonds as well as the template structure (Cys47–Cys224, Cys299–Cys351). The SASAs of *RhLip* model and CAL A structure calculated by POPS algorithm showed a hydrophobic area of 61.23 % and a hydrophilic area of 38.77 % for *RhLip*, while a hydrophobic area of 49.83 % and a hydrophilic area of 50.17 % for CAL A. Hydrophobicity of the surface exposed to the solvent is an important feature of lipases and esterases because these classes of enzymes work at the interface between a polar and an apolar phase. Structural analysis was carried out by analyzing the most conserved residues of *RhLip* multiple alignment (Fig. 7). Ser137, Asp283, and His323 form the catalytic triad of *RhLip* (Fig. 5b). These three amino acids are located in three different loops connecting three strands to three α -helices. In particular, Ser137 is within a conserved motif (GTSXGG), and the presence of the glycines gives some flexibility at this area. The side chain atoms NE2 and ND1 of H323 make two h-bonds (2.69 and 3.19 Å) with the side chain atom OG of S137 and the side chain atom OD2 of D283. These bonds hold together the members of the catalytic triad. Moreover, carbonyl oxygen of His323 makes a hydrogen bond (2.58 Å) with the hydroxyl group of Tyr136, another conserved residue located in a strand of beta-sheet B. This bond further helps this β -strand to keep close to the catalytic triad.

Molecular Dynamics

Since the three-dimensional model accurately described the structural organization of this protein, we tried to have a more dynamic view of its structure. We have subjected the best *RhLip* model to molecular dynamics simulations in order to evaluate its stability. These studies were made at neutral as well as at alkaline pH because the sequence of this protein

Fig. 4 Multiple sequence alignment among *RhLip* sequence and other four templates, which demonstrated to display the best score. The intensity of blue color is proportional to the identity percentage. The conservation level of residues and the consensus is also shown



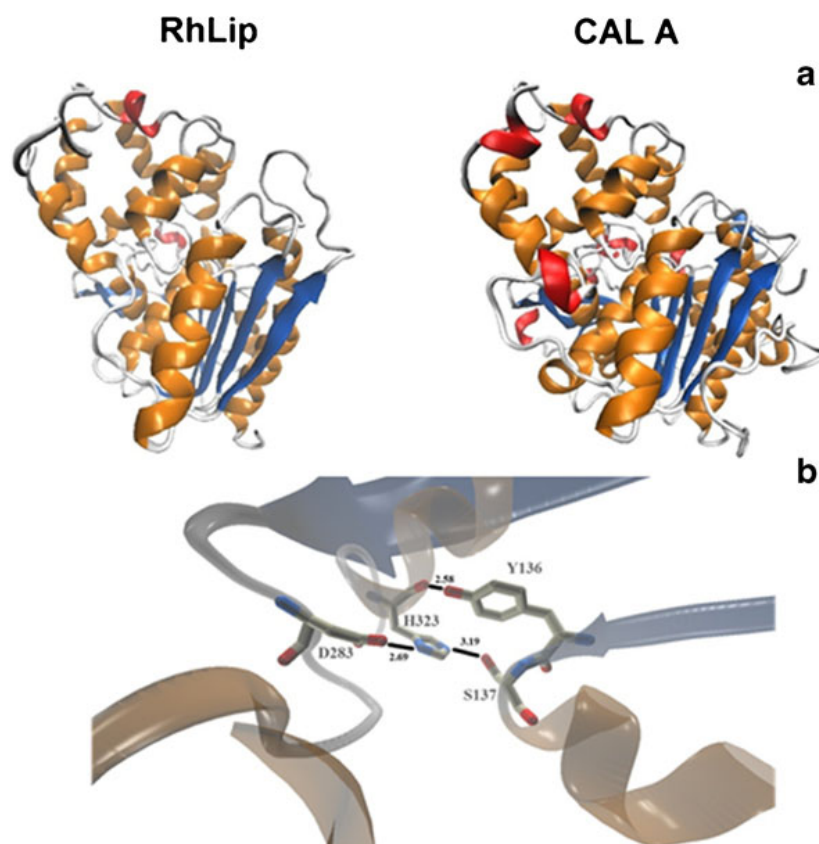


Fig. 5 **a** Graphical representation of *RhLip* and CAL A (PDB ID: 3GUU) structures. Alpha helices are shown in orange, 3–10 helices are shown in red, and beta-strands are shown in blue. **b** Graphical representation of *RhLip* catalytic triad. Hydrogen bond length is displayed in angstroms

shows many positively and negatively charged residues sensitive to pH changes. The *RhLip* model reached a stable equilibrated state after 6 ns simulation at both pH levels; in fact, the related RMSD values (Fig. 7a), computed by superposing the various structures obtained during the simulations and the initial structure at time zero, were almost constant in the remaining simulation time. However, we noted that the fluctuations observed at alkaline pH levels in the first 3–4 ns were slightly more severe in comparison with the simulation computed at neutral pH (Fig. 7b). This behavior highlighted a different way for the protein to reach an equilibrium state compared to the results at neutral pH. Then, in order to compare the overall size of the two systems at different pH levels, we computed the gyration radius concerning all atoms of 346 residues (Fig. 8). The gyration radius trend showed a quite similar evolution in the simulations, and practically, no variation in molecule compactness was observed.

Finally, the superposition of the RMS fluctuations at neutral and alkaline pH revealed that the residues with a high degree of flexibility fell in the loop region. This was due to the high presence of charged residues in these regions that, at neutral and alkaline pH, behaved differently. This suggests the important functional role played by these flexible loops in *RhLip* at structural as well as at functional levels.

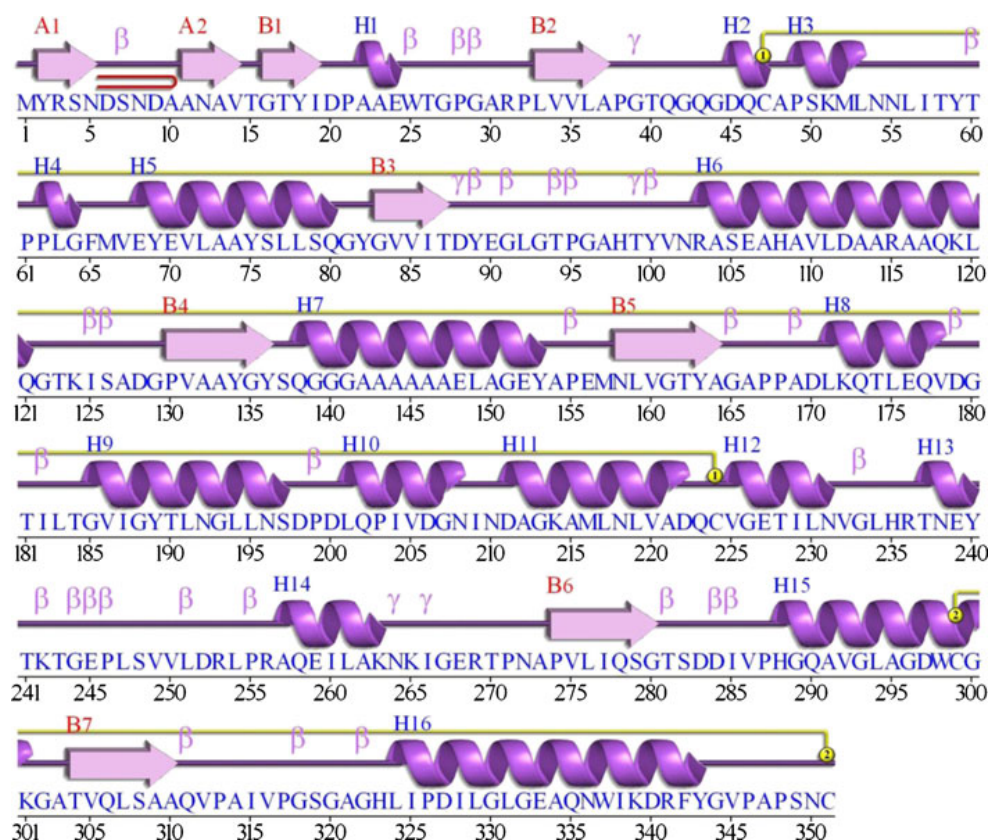


Fig. 6 *RhLip* secondary structure representation. Helices are labeled from H1 to H15. Beta-strands are labeled according to the beta-sheet they belong (a or b). Turns are labeled with β or γ . The disulfide bridge is represented in yellow

Conclusion

The present study shed light on a new lipolytic cold-adapted enzyme, which was demonstrated to possess interesting features and various potential applications, as additive for detergent production and biocatalyst for regio- and stereoselective reactions in chemical synthesis [6]. The recombinant enzyme was successfully purified from the inclusion body and characterized. *RhLip* was revealed to be an extremely alkaliphilic and cold-adapted esterase. As other psychrophilic enzymes, *RhLip* showed a low thermostability at temperature higher than 30 °C, and this heat lability can be exploited in several applications, especially in the food industry. In this case, an industrial process catalyzed by an esterase can be easily stopped by a little increase in temperature, preserving food integrity and flavor.

The enhanced catalytic activity in tested organic solvents could make it useful for some industrial purposes such as production of chemicals, biopolymers, and fuels [28]. *RhLip* also showed an improved activity in the presence of 1 M NaCl. This evidence could be useful for industrial application of food processing in the presence of a high concentration of salt. The analysis of the *RhLip* model revealed some structural features of the catalytic site of this enzyme, showing the three-dimensional arrangement and the interactions between residues of

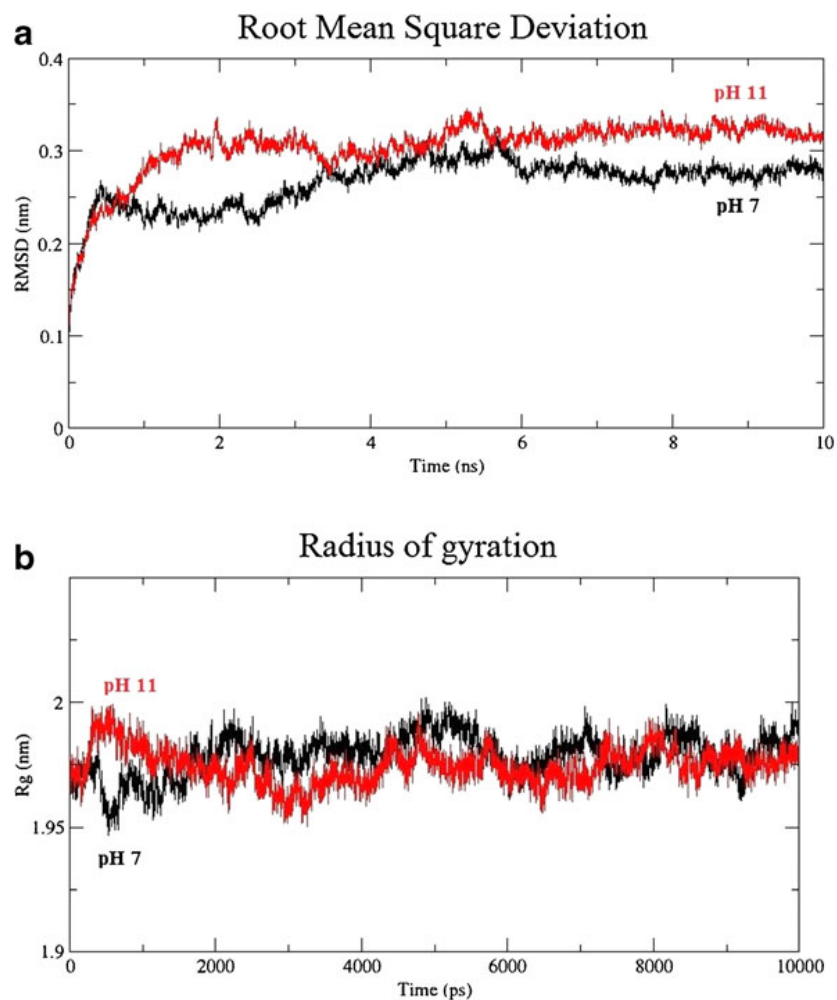


Fig. 7 **a** Trend of root-mean-square deviation (RMSD) for *RhLip* structure at pH 7 (*black*) and at pH 11 (*red*) during the molecular dynamic simulations. **b** Trend of gyration radius at pH 7 (*black*) and at pH 11 (*red*)

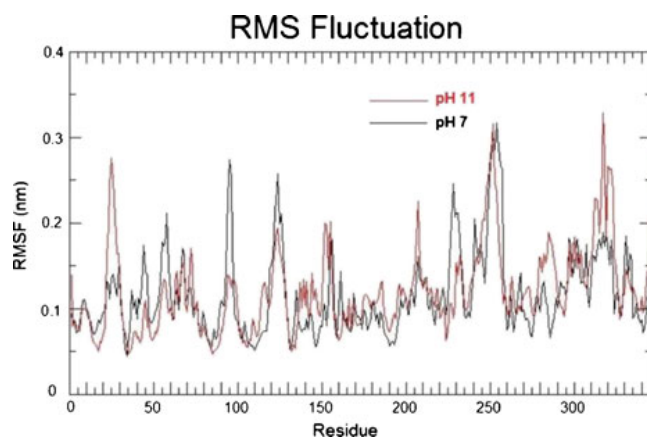


Fig. 8 Root mean square fluctuations at neutral (*black*) and alkaline (*red*) pH at the end of the molecular dynamic simulations

the catalytic triad. Moreover, results of MD simulations highlighted that the protein seems to be quite stable at neutral as well as at alkaline pH. Further developments of this study could be directed to identify potential targets for site-directed mutagenesis to improve protein stability and catalytic activity.

Acknowledgments This work was supported by P.N.R.A. (Italian National Antarctic Research Programme) 2009–2011. We also thank the Yggdrasil application grants 2011–2012 and 2012–2013, funded by the National Research Council of Norway, for supporting the research activities of Dr. Concetta De Santi.

References

1. Rhee, S. K., Liu, X., Wu, L., Chong, S. C., Wan, X., & Zhou, J. (2004). *Applied and Environmental Microbiology*, *70*, 4303–4317.
2. Gupta, R., Gupta, N., & Rathi, P. (2004). *Applied Microbiology and Biotechnology*, *64*, 763–781.
3. Aurilia, V., Parracino, A., & D'Auria, S. (2008). Microbial carbohydrate esterases in cold adapted environments. *Gene*, *410*, 234–240.
4. Paredes, D. I., Watters, K., Pitman, D. J., Bystroff, C., & Dordick, J. S. (2011). *BMC Structural Biology*, *11*, 42.
5. Cavicchioli, R., Charlton, T., Ertan, H., Mohd Omar, S., Siddiqui, K. S., & Williams, T. J. (2011). *Microbial Biotechnology*, *4*, 449–460.
6. Jeon, J. H., Kim, J. T., Kang, S. G., Lee, J. H., & Kim, S. J. (2009). *Marine Biotechnology (NY)*, *11*, 307–316.
7. de Pascale, D., De Santi, C., Fu, J., & Landfald, B. (2012). *Marine Genomics*, *8*, 15–22.
8. Hjerde, E., Pierechod, M. M., Williamson, A. K., et al. (2013). *Genome Announcements*, *7*(1). e0005513.
9. Rutherford, K., Parkhill, J., Crook, J., Horsnell, T., Rice, P., Rajandream, M. A., et al. (2000). *Bioinformatics*, *16*, 944–945.
10. Laemmli, U. K. (1970). *Nature*, *227*, 680–685.
11. Thompson, J. D., Higgins, D. G., & Gibson, T. J. (1994). *Nucleic Acids Research*, *22*, 4673–4680.
12. Sali, A., & Blundell, T. L. (1993). *Journal of Molecular Biology*, *234*, 779–815.
13. Laskowski, R. A. (2001). *Nucleic Acids Research*, *29*, 221–222.
14. Laskowski, R. A., MacArthur, M., Moss, D. S., & Thornton, J. M. (1993). *Journal Applied Crystallography*, *26*, 283–291.
15. Vriend, G. (1990). *Journal of Molecular Graphics*, *8*(29), 52–56.
16. Cavallo, L., Kleijnung, J., & Fraternali, F. (2003). *Nucleic Acids Research*, *31*, 3364–3366.
17. Hess, B., Kutzner, C., van der Spoel, D., & Lindhal, E. (2008). *Journal of Chemical Theory and Computation*, *4*, 435–447.
18. Kademi, A., Ait-Abdelkader, N., Fakhreddine, L., & Baratti, J. (2000). *Applied Microbiology and Biotechnology*, *54*, 173–179.
19. Park, H. J., Jeon, J. H., Kang, S. G., Lee, J. H., Lee, S. A., & Kim, H. K. (2007). *Protein Expression and Purification*, *52*, 340–347.
20. Hu, X. P., Heath, C., Taylor, M. P., Tuffin, M., & Cowan, D. (2012). *Extremophiles : Life Under Extreme Conditions*, *16*, 79–86.
21. Kim, Y. H., Kwon, E. J., Kim, S. K., Jeong, Y. S., Kim, J., Yun, H. D., et al. (2010). *Biochemical and Biophysical Research Communications*, *393*, 45–49.
22. De Santi, C., Tutino, M. L., Mandrich, L., Giuliani, M., Parrilli, E., Del Vecchio, P., et al. (2010). *Biochimie*, *92*, 949–957.
23. Wang, Q., Hou, Y., Ding, Y., & Yan, P. (2012). *Molecular Biology Reports*, *39*, 9233–9238.
24. Mandrich, L., De Santi, C., de Pascale, D., & Manco, G. (2012). *Journal of Molecular Catalysis B Enzymatic*, *83*, 46–52.
25. Peters, K. S. (2007). *Chemical Reviews*, *107*, 859–873.
26. Gandolfi, R., Marinelli, F., Lazzarini, A., & Molinari, F. (2000). *Journal of Applied Microbiology*, *89*, 870–875.
27. Morimoto, K., Furuta, E., Hashimoto, H., & Inouye, K. (2006). *Journal of Biochemistry*, *139*, 1065–1071.
28. Egorova, K., & Antranikian, G. (2005). *Current Opinion in Microbiology*, *8*, 649–655.



Contents lists available at ScienceDirect

Journal of Molecular Catalysis B: Enzymatic

journal homepage: www.elsevier.com/locate/molcatb

α -Rhamnosidase activity in the marine isolate *Novosphingobium* sp. PP1Y and its use in the bioconversion of flavonoids



Viviana Izzo^{a,c}, Pietro Tedesco^a, Eugenio Notomista^a, Eduardo Pagnotta^b,
Alberto Di Donato^a, Antonio Trincone^b, Annabella Tramice^{b,*}

^a Dipartimento di Biologia, Università di Napoli Federico II, Complesso Universitario di Monte S. Angelo, Via Cinthia 4, 80126 Naples, Italy

^b Istituto di Chimica Biomolecolare, Consiglio Nazionale delle Ricerche, Via Campi Flegrei 34, 80072 Pozzuoli, Naples, Italy

^c Dipartimento di Medicina e Chirurgia, Università degli Studi di Salerno, Via S. Allende, 84081 Baronissi, Salerno, Italy

ARTICLE INFO

Article history:

Received 3 January 2014

Received in revised form 6 March 2014

Accepted 5 April 2014

Available online 18 April 2014

Keywords:

 α -L-rhamnosidase*Novosphingobium* sp. PP1Y

Flavonoids bioconversion

ABSTRACT

Crude protein extracts of *Novosphingobium* sp. PP1Y, a microorganism isolated from polluted marine waters in Pozzuoli (Italy), were analyzed for the presence of glycosidase activities. Particular attention was devoted to a α -L-rhamnosidase activity able to hydrolyze several flavonoids of interest for the pharmaceutical and food industries. This activity had an alkaline pH optimum and a moderate tolerance to the presence of organic solvents, appealing features for its possible biotechnological uses. An increase of the α -L-rhamnosidase activity in PP1Y crude extracts was induced by adding naringin to the growth medium, suggesting the possibility to use material from *Citrus* industrial waste to induce the glycosidase activity expressed by strain PP1Y and produce simultaneously high-added-value molecules from the hydrolysis of their flavonoids. In order to investigate on the enzymatic mechanism of PP1Y α -L-rhamnosidase activity, hydrolysis products of PNP- α -L-rhamnopyranoside were analyzed by ¹H-NMR experiments. The kinetic behaviour clearly indicated an inverting mechanism of hydrolysis for this novel enzymatic activity.

© 2014 Elsevier B.V. All rights reserved.

1. Introduction

Biocatalysis represents nowadays a versatile and valuable tool for industrial biotechnologies. The use of enzymes as biocatalysts can have significant benefits compared to conventional chemical technologies, for achieving high reaction selectivity, higher reaction rate, improved product purity, and a significant decrease in chemical waste production. A wide variety of chemical substances is already produced in industrial processes through the use of enzymes [1,2].

Within this framework, α -L-rhamnosidases [E. C. 3.2.1.40] have attracted great attention in the last decade due to their application as biocatalysts in a variety of food, pharmaceutical and chemical industrial processes [3].

α -L-Rhamnosidases (from now on indicated as α -RHAs) are a class of glycosyl hydrolases that specifically cleave terminal α -L-rhamnose from a large number of natural products, which include flavonoids, some terpenyl glycosides [4,5] and many other natural glycosides containing a terminal rhamnose, such as glycopeptides antibiotics and glycolipids [6]. These enzymes have recently been

the focus of an increasing scientific interest. As an example, the use of α -RHAs to improve the bioavailability, and thus the biological activity, of flavonoids beneficial for human health as direct drugs or as nutritional supplements, has been reported [3].

Moreover, L-rhamnose has a central role in the organic synthesis as a chiral intermediate of pharmaceutically important compounds. Its production using the enzymatic activity of α -RHAs in hydrolysis reactions of glycosylated compounds that might be recovered from waste material of food processing industry (e.g. citrus peel), represents an interesting and useful biotechnological application these glycosidases [7].

Fungi are the main source of α -RHAs. However, these enzymes have been isolated also from animal tissues, such as the liver of both the marine gastropod *Turbo cornutus* [8] and pig [9], and from plants such as *Rhamnus daurica* [10] and *Fagopyrum esculentum* [11].

Bacteria represent a yet unexplored reservoir of α -RHAs, which might show novel interesting properties. An analysis of several α -RHAs isolated from various microbial sources reveals, for example, that one of the main differences found between fungal and bacterial enzymes is their optimal pH, with the fungal enzymes showing more acidic pH optima compared to bacterial counterparts, for which neutral and alkaline optimal pH values have generally been reported. This characteristic suggests different potential applications for fungal and bacterial enzymes, making bacterial α -RHAs

* Corresponding author. Tel.: +39 0818675070; fax: +39 0818041770.
E-mail address: atramice@icb.cnr.it (A. Tramice).

suitable in biotechnological processes requiring good activity in more basic solutions such as the production of L-rhamnose by hydrolysis of naringin or hesperidin, compounds whose solubility strongly increases at higher pH values [3,12].

Despite the very limited number of bacterial α -RHAs that has been described so far, data in literature suggest that this enzymatic activity is widely distributed over a diverse range of ecological niches. α -RHAs have been detected and characterized in the human intestinal bacterium *Bacteroides* JY-6 [13], in cold-adapted *Pseudomonas* species and *Ralstonia pickettii* isolated in the sea water of sub Antarctic environment [14], also in soil bacteria such as *Bacillus* sp. GL1 [15,16], *Sphingomonas paucimobilis* FP2001 [17] and *Sphingomonas* sp. R1 [18] and finally in wine strains of *Oenococcus oeni* [19].

α -RHAs from *Lactobacillus* species were identified and investigated for their potential biotechnological use to de-rhamnosylate flavonoids present in frequently consumed food commodities [20].

Moreover, α -RHAs genes have been cloned and expressed from thermophilic bacteria such as *Clostridium stercoararium* [21] and from the bacterium PRI-1686, which is a member of the phylum of Thermomicrobia [22].

Recently, the crystal structure of *Streptomyces avermitilis* α -L-rhamnosidase (SaCBM67) was reported [23]; its structure presented a novel catalytic carbohydrate-binding module and resulted different from the only two structures of α -L-rhamnosidases (GH78) previously reported: the BsRhaB isolated from *Bacillus* sp. GL1 [24] and the putative α -L-rhamnosidase BT1001 from *Bacteroides thetaiotaomicron* VPI-5482 [25].

It goes without saying that the biotechnological potential of bacterial α -RHAs, whose structural, functional and molecular biology aspects have not been sufficiently investigated, is strictly related to the acquisition of new information on the enzymatic systems isolated from new bacterial sources.

Recently, *Novosphingobium* sp. PP1Y, an organic solvent-resistant, biofilm-forming marine microorganism, was isolated from the surface waters of a docking bay in the harbour of Pozzuoli (Naples, Italy), an area heavily polluted with hydrocarbons [26]. The analysis of its genome, confirmed the presence of several genomic features of interest for the biotechnological potential of this microorganism, and more specifically for its exploitation as a source of enzymes active on carbohydrates. Strain PP1Y shows in fact a unique abundance among Sphingomonadales of genes encoding for glycosyl hydrolases (53 orfs) [27], which are distributed among 27 different families. This prompted our interest in investigating the presence of α -RHA activities in the crude protein extract of strain PP1Y.

In this work, cell extracts obtained from *Novosphingobium* sp. PP1Y cells grown in minimal medium were tested for the presence of glycosidase activities; in particular α -RHA and β -glucosidase activities were detected and partially characterized.

This α -RHA activity was successfully used in bioconversion studies of flavonoidic compounds, thus suggesting its potential use as an eco-friendly tool to modulate the biological and pharmacological properties of these molecules. It was further demonstrated by $^1\text{H-NMR}$ experiments that α -RHA activity from *Novosphingobium* sp. PP1Y functioned with an inverting mechanism, in agreement with the enzymatic mechanism already proposed for other α -RHAs previously described.

2. Materials and methods

2.1. General

Novosphingobium sp. PP1Y was isolated as previously reported [26]. All reagents were purchased from Sigma-Aldrich and used

without any further purification. Silica gel, reverse-phase silica gel C-18 and TLC silica gel plates were from E. Merck (Darmstadt, Germany). All other chemicals were of analytical grade. Compounds on TLC plates were visualized under UV light or charring with α -naphthol reagent.

TLC solvent systems used were (A) EtOAc:MeOH:H₂O, 70:20:10 and (B) EtOAc:AcOH:2-Propanol:HCOOH:H₂O, 25:10:5:1:15.

^1H -, ^{13}C - and 2D-NMR spectra were acquired by the NMR Service of the Istituto di Chimica Biomolecolare of the National Research Council of Italy (C.N.R.-Pozzuoli, Naples, Italy) and recorded on a Bruker DRX-600 spectrometer, equipped with a TCI CryoProbeTM, fitted with a gradient along the Z-axis, and on other Bruker instruments with fields at 400 and/or 300 MHz. Samples for NMR analysis were dissolved in the appropriate solvent; spectra in D₂O were referenced to internal sodium 3-(trimethyl-silyl)-(2,2,3,3-²H₄) propionate (Aldrich, Milwaukee, WI); for other solvents downfield shift of the signal of the solvent was used as internal standard.

In the bioconversion studies followed by $^1\text{H-NMR}$ experiments, reported in paragraph 2.8 and 2.9, the selected signals integral values of products and reagents resulted affected by an error in integration (<5%) which depended upon instrument optimization.

Protein concentration was routinely estimated using the Bio-Rad Protein System [28]; bovine serum albumin was used as standard.

2.2. Bacterial growth

Novosphingobium sp. PP1Y was routinely grown in minimal medium. Potassium phosphate minimal medium (PPMM) contained 20 mM potassium phosphate pH 6.9, 1 g/L NH₄Cl and 100 mM NaCl. After autoclaving, 5 mL of a trace element solution was added to each litre of cooled PPMM. The trace element solution contained in a 0.92% solution of HCl: 30.1 g/L MgSO₄, 4.75 g/L FeSO₄ × 7H₂O, 5.4 g/L MgO, 1.0 g/L CaCO₃, 0.72 g/L ZnSO₄ × 7 H₂O, 0.56 g/L MnSO₄ × H₂O, 0.125 g/L CuSO₄ × 5 H₂O, 0.14 g/L CoSO₄ × 7 H₂O, 0.03 g/L H₃BO₃, 0.004 g/L NiCl₂ × 6 H₂O, 0.006 g/L Na₂MoO₄ × 2H₂O. When using PPMM as growth medium, 0.4% (w/v) of glutamic acid, prepared in deionized water and sterilized by filtration with a 0.22 μm Millipore membrane, was used as unique carbon and energy source and added to the autoclaved media. Cultures were incubated at 30 °C with orbital shaking (220 rpm).

Bacterial growth was monitored by measuring the optical density at 600 nm (OD₆₀₀). A pre-inoculum in rich medium was prepared by transferring 50 μL from a glycerol stock stored at -80 °C to a 50 mL Falcon tube containing 12.5 mL of sterile LB medium. LB was prepared according to Sambrook et al. [29]. The pre-inoculum was allowed to grow at 30 °C for at least 14 h at 220 rpm and then used to inoculate 1 L of a preparative growth in PPMM medium at an initial cell concentration of 0.01–0.02 OD₆₀₀/mL. Cells were usually harvested after 24 h at a final optical density of ca. 1 OD₆₀₀/mL. It is worthy to note that, when following the growth for more than 24 h, the formation of flocks was observed, thus hampering a correct estimation of the turbidity of the cell suspension.

2.3. Preparation of *Novosphingobium* sp. PP1Y crude protein extract

Cell cultures were harvested by centrifugation at 5,524 × g for 30 min at 4 °C. Cell pellets were suspended in 25 mM MOPS at pH 7.0 and disrupted by sonication (30' total, 30 s ON and 30 s OFF) in an ice-water bath. Cell suspension was centrifuged at 17,418 × g at 4 °C for 60 min. The soluble fraction obtained after centrifugation was filtered on a 0.45 mm Millipore membrane, divided in aliquots and stored at -80 °C. When used for the screening of glycosidase

Table 1

Evaluation of different substrates bioconversion by using glycosidase activities in the crude extract of *Novosphingobium* sp. PP1Y cells.

Substrates ^a	Crude extract of PP1Y cells grown in PPMM medium			
	Hydrolysis ^b		Transglycosylation ^c	
	3 h	24 h	3 h	24 h
PNP- α -D-Glcp	+	+	–	+/-
PNP-β-D-Glcp	+	++	+	++
PNP- α -D-Galp	+/-	+	–	+/-
PNP-β-D-Galp	+	++	+	++
PNP- α -D-Manp	–	–	–	–
PNP- β -D-Manp	–	–	–	–
PNP- α -d-Xylp	–	–	–	–
PNP-β-D-Xylp	+	++	+/-	+
PNP- α -L-Fucp	–	–	–	–
PNP-β-D-Fucp	+	++	+	++
PNP α -D-NAGp	–	–	–	–
PNP β -D-NAGp	+/-	+	+/-	+/-
PNP-α-L-Rhap	++	+++	–	+/-
PNP- α -L-Araf	–	–	–	–

Note: +/-: percentage of products below 10%; +: 10–30% of products; ++: 30–70% of products; +++: percentage of products higher than 70%.

^a Araf, arabinofuranose; Fucp, fucopyranose; Galp, galactopyranose; Glcp, glucopyranose; Manp, mannopyranose; NAGp, N-acetylglucosaminopyranose; Rhap, Rhamnopyranose; Xylp, xylopyranose.

^b Hydrolysis products were analyzed by comparing Rf values with appropriate standards in TLC solvent system A.

^c Due to self-transglycosylation reactions, products showed positive UV absorbance and lower Rf than the corresponding aryl substrates in the selected TLC solvent system A.

activities (Section 2.4), the soluble fraction was dialyzed against 20 mM potassium phosphate at pH 7, and then divided in aliquots and stored at -80°C . PP1Y crude extracts were assayed for their total protein content.

Without any different indication, all experiments reported in the following sections, were performed using a crude extract obtained from a 2 L culture of PP1Y cells grown in PPMM medium and with a protein concentration of 3.72 mg total protein/mL. Cells were recovered after 24 h at an optical density of 1.02 OD₆₀₀/mL.

2.4. Glycosidase activities screening

PP1Y crude protein extract, prepared as described in the previous paragraph, was tested for the presence of glycosidase activities by using several pNP- α - and pNP- β -substrates (Table 1) at a 20 mM concentration in 0.6 mL of 50 mM Na-phosphate buffer pH 7, at 35°C and under magnetic stirring. All reactions were carried out using 4.42 mg of total protein/mmol of reagent. Reactions were monitored over time (0–24 h) by TLC analysis (system solvent A).

Moreover, hydrolysis reactions with maltose, lactose, cellobiose, sucrose, raffinose, laminaripentaose, laminarin, curdlan, β -glucan from barley, xylan from birch wood, pullulan, amylopectin and starch as substrates were carried out using crude extracts of PP1Y cells grown in PPMM. Each substrate (10 mg) was suspended in 1 mL of 50 mM Na-phosphate buffer pH 7, containing 41.6 μg of total protein/mL of reaction mixture. Reactions were performed at 35°C . Hydrolysis products were monitored by TLC analysis (system solvents A and B).

Flavonoidic substrates such as naringin, diosmin, rutin, hesperidin, neohesperidin dihydrochalcone, quercitrin, were tested. To this purpose, a 2 mM solution of each compound prepared in a final volume of 1 mL of 50 mM Na-phosphate buffer pH 7 was incubated at 35°C in the presence of 100 μL of PP1Y crude extract obtained from cells grown in PPMM (3.72 mg of total protein/mL) for 24 h. Reactions were checked over time by TLC analysis (solvent system A).

Rutinose hydrolysis was also investigated. In this case, 0.5 mL of a solution containing 6 mM rutinose, 0.25 mL of PP1Y crude extract in 50 mM of Tris/HCl buffer at pH 8.5 was incubated at 35°C under magnetic stirring and monitored by TLC analysis (solvent system A) for 24 h.

In all experiments, TLC standard solutions of pure reagents and products were used for comparison.

2.5. α -L-rhamnosidase activity assay

α -RHA activity was determined using *p*-nitrophenyl- α -L-rhamnopyranoside (pNPR) as substrate. The assay was performed in 0.5 mL of 50 mM potassium acetate buffer pH 5.5, containing a variable amount of PP1Y crude extract and pNPR at a final concentration of 0.28 mM. The assay mixture was incubated for 30 min at room temperature; afterwards, 0.5 mL of a 1 M sodium carbonate solution were added and the sample absorbance was recorded spectrophotometrically at 405 nm ($\epsilon_{405} = 0.0182 \mu\text{M}^{-1}\text{cm}^{-1}$). One milliunit of enzymatic activity was defined as the amount of enzyme that releases 1 nmol of *p*-nitrophenol per min.

2.6. Induction of α -L-rhamnosidase activity

To evaluate the possible influence of naringin on the expression of the intracellular α -rhamnosidase activity of the strain PP1Y, we compared the specific activity in cell extracts obtained from growths in PPMM to which increasing concentrations of naringin were added. To this purpose, four 250 mL-Erlenmeyer flasks were prepared, each containing 250 mL of PPMM medium and 0.4% glutamic acid as unique carbon and energy source. Variable amounts of naringin were added to autoclaved media, in order to have final concentrations of 0.1–0.2–0.3 mM. The four flasks were inoculated with an overnight culture of PP1Y in LB, as described in paragraph 2.2. The initial cell concentrations in the flasks were comparable and in the range 0.02–0.04 OD₆₀₀/mL.

2.7. Influence of pH and organic solvents on α -L-rhamnosidase and β -glucosidase activities

In experiments of pH monitoring, 2 mM solutions of naringin were prepared in HCl/KCl, Na-acetate, Na-phosphate, Tris/HCl, Na-carbonate buffers, in order to cover the pH range between 2.2 and 10.9 (Table 2). 100 μL of PP1Y crude extract were added to 0.5 mL of each solution and incubated at 35°C under magnetic stirring. Reactions were checked every 20 min by TLC analyses (solvent system A) and naringin consumption was evaluated by using solutions of pure naringin, narigenin, rhamnose and glucose as chromatographic standards. Blank reactions at different pHs were performed to evaluate the chemical degradation of the flavanone glycoside, occurring preferentially in strongly basic conditions.

Similarly, solutions of 2 mM naringin in 50 mM Tris/HCl buffer pH 8.5 containing 1, 10 and 50% v/v of DMSO or CH₃CN (Table 2) were placed under constant agitation at 35°C in the presence of 200 μL of PP1Y crude enzymatic extract (0.74 mg total protein)/mL of reaction. As previously reported, reactions were monitored by TLC analysis (solvent system A).

2.8. Stereochemical course of α -L-rhamnosidase activity in hydrolysis reactions

To the purpose, 800 μL of a 6 mM pNPR solution prepared in 50 mM Tris/HCl buffer pH 7 was freeze-dried, re-suspended three times in D₂O and re-freeze-dried to exchange the ¹H atoms involved in labile linkages for ²H ones. A similar procedure of proton isotope exchange was applied to 200 μL of PP1Y crude extract. Just prior to the ¹H-NMR experiment, the previously exchanged pNPR

Table 2
The influence of pH and organic solvents presence on naringin hydrolysis by α -RHA activity in PP1Y crude protein extract.

pH values	Naringin hydrolysis			
	Time (min)			
	60	120	140	180
2.2	–	–	–	–
3.6	–	–	–	–
5.4	–	–	–	–
5.9	–	–	–	–/+
6.1	–	–/+	–/+	+
7.2	–/+	+	++	++
8.1	–	++	++	++
8.3	+	++	+++	+++
8.5	+	+++	+++	+++
8.8	+	+++	+++	+++
9.1 ^a	–	–	+	+
9.9 ^a	–	–	+	+
10.9 ^a	–	–	+	+
% of organic solvent				
DMSO 1%	+	++	++	+++
DMSO 10%	+	+	++	+++
DMSO 50%	–	–	–	–
CH ₃ CN 1%	–	–	–	–/+
CH ₃ CN 10%	–	–	–	–
CH ₃ CN 50%	–	–	–	–

Note: – no hydrolysis; –/+ : percentage of hydrolysis below 10%; +: 10–30% of hydrolysis; ++: 30–70% of hydrolysis; +++: percentage of hydrolysis higher than 70%.

^a In these conditions a partial chemical degradation of naringin was observed which was suggested by the presence on TLC, along with the disappearance of the substrate, of a product more polar than naringin and the absence of rhamnose and glucose spots, thus confirming the absence of an enzymatic hydrolysis.

solution was dissolved in 0.75 mL of D₂O, equilibrated at 35 °C in a NMR tube inside the spectrometer probe, and an initial spectrum of solution without enzyme was recorded (T_0). The aliquot of freeze-dried crude extract was suspended in 50 μ L of D₂O and added to the solution. Starting from that moment (T_0 with enzyme), the stereochemical course of hydrolysis was followed by recording ¹H-NMR spectra at close intervals during the incubation time (from 0 to 60 min).

A 6 mM solution of free rhamnose dissolved in 50 mM Tris/HCl buffer pH 7 was treated and monitored by ¹H-NMR experiments as previously reported.

2.9. Bioconversion studies followed by ¹H-NMR analyses

pNPR, naringin, rutin and neohesperidin dihydrochalcone bioconversions were performed and compared by ¹H-NMR spectroscopic analyses.

In particular, 11.4 μ mol of each substrate were dissolved in 1.9 mL of Na-phosphate buffer (50 mM, pH 8.5 or pH 7) containing 1 mL of PP1Y crude extract. Reactions were incubated at 35 °C, under constant magnetic stirring for 3 h. Aliquots of 380 μ L were withdrawn from each reaction at different time intervals from 0 to 173 min. Enzymatic reactions were stopped by boiling at 100 °C for 2 min and samples were freeze-dried. Collected aliquots were dissolved in MeOD or D₂O, as for pNPR, and analyzed by ¹H-NMR experiments. These reactions were also monitored by TLC analysis (system solvent A). These reactions were also monitored by TLC analysis (system solvent A).

2.10. Prunin production

The reaction was performed using 2 mL of PP1Y crude extract which were previously lyophilized and then resuspended in a 1 mL solution of Na-phosphate buffer (50 mM, pH 8.5) containing 10% of DMSO. 72.5 mg of naringin (0.125 mmol) were added and the

sample was incubated at 35 °C, under magnetic stirring. Reaction was stopped after 72 h by heating the sample at 100 °C for 2 min and prunin was isolated by silica gel purification with EtOAc:MeOH 9:1 (v/v) as mobile phase. 1D and 2D NMR analyses confirmed its structure.

3. Results and Discussion

3.1. Glycosidase activities screening

Glycosidase activities in crude protein extract of *Novosphingobium* sp. PP1Y cells collected after a 24 h growth in PPMM medium (Section 2.2) were preliminary investigated for their hydrolytic and transglycosylation potentials, as described in Section 2.4. Reaction products were analyzed over time by TLC analysis using solvent system A Section 2.1, and the results were reported in Table 1. Data indicated that α -L-rhamnosidase and β -glucosyl hydrolases activities resulted the most abundant ones. After 3 h, 30–70% of PNP- α -L-Rhap and 10–30% of PNP- β -D-Glcp, PNP- β -D-Galp, and PNP- β -D-Xylp were hydrolyzed. Hydrolysis reactions were allowed to proceed for 24 h. At this time, an almost complete conversion of PNP- α -L-Rhap was observed.

Transglycosylation reactions resulted more interesting by using PNP- β -glucosides as substrates, suggesting a better attitude of β -glucosyl hydrolases to transfer monosaccharidic units in self-condensation reactions than the α -L-rhamnosidase activity; aryl- β -oligosaccharides were present in the reaction media up to 24 h.

Polysaccharides and oligosaccharides were also tested as possible substrates for the enzymatic activities present in PP1Y crude extracts. Products formation was monitored by TLC analysis (system solvents A and B, Section 2.1), using pure compounds as chromatographic standards. After 24 h of reaction, curdlan and laminarin were only slightly consumed whereas laminaripentaose resulted the best hydrolyzed oligosaccharide, resulting in the major production of glucose; cellobiose, instead, was not a good substrate (data not shown).

α -glucans like pullulan, amylopectin, starch and maltose were partially or almost totally hydrolyzed to glucose, maltose or larger oligosaccharides, suggesting the possible presence of α -glucanase activities (data not shown).

These preliminary data confirmed the biotechnological potential of PP1Y strain as a source of a wide array of enzymatic activities that can be used for the modification of carbohydrates and glycoconjugates.

3.2. Hydrolytic behaviour of PP1Y crude extract enzymes on flavonoids: description, pH dependence and tolerance to organic solvents

The simultaneous presence in PP1Y crude extract of α -RHA and β -glucosidase activities prompted us to investigate the possibility to hydrolyze selected flavonoidic compounds, having in their chemical structure both α -rhamnose and β -glucose units, such as naringin, diosmin, rutin, hesperidin, neohesperidin dihydrochalcone and quercitrin (Fig. 1). It is worth to note that chemical modification of these compounds, which are endowed with therapeutic potential [12] is important to modulate their biological activity.

In the reaction conditions reported in Section 2.4, after 3 h of incubation, complete conversion of naringin, rutin and neohesperidin dihydrochalcone was detected by TLC analysis (system solvent A, Fig. 2): spots of rhamnose, glucose and the corresponding aglycone were observed for each reaction.

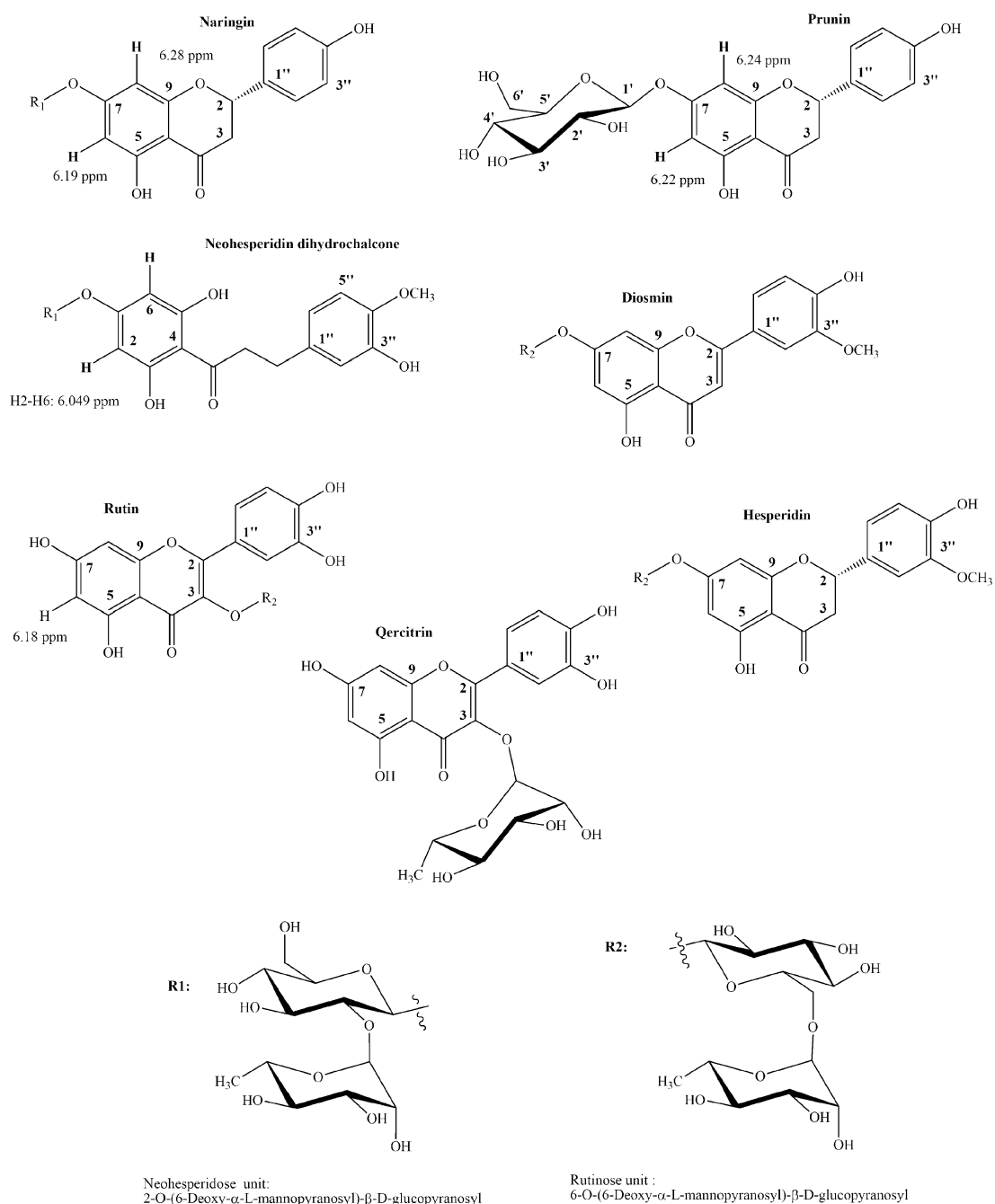


Fig. 1. Chemical structure of flavonoid compounds used as substrates. Chemical shift values of signals that are integrated in bioconversion reactions are reported.

On the other hand, diosmin, hesperidin and quercitrin were not hydrolyzed; after 24 h as observed by TLC investigations (system solvent A) rhamnose and glucose spots, at R_f 0.56 and 0.3 respectively, were absent on TLC plates of diosmin and hesperidin

reactions. Quercitrin was so poorly consumed (yield below 3%) that its hydrolysis was considered negligible; indeed, a very scarce presence of quercetin and rhamnose, at R_f 0.88 and 0.56 respectively, was observed.

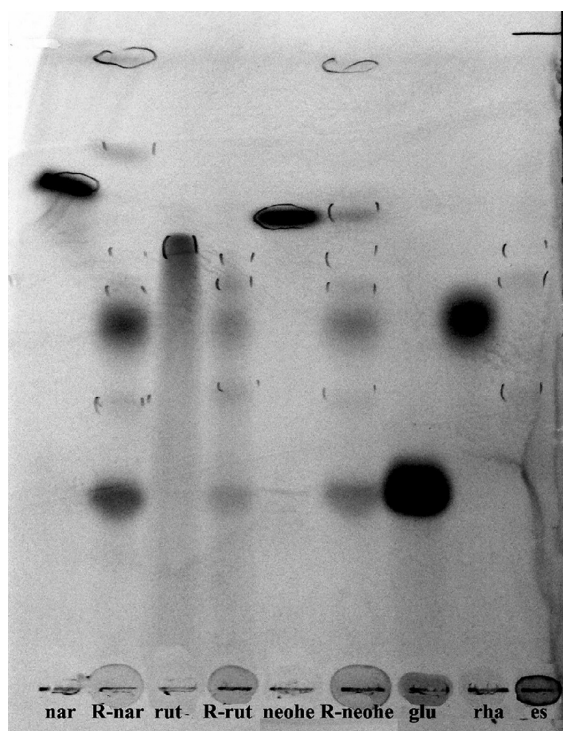


Fig. 2. Flavonoids hydrolysis followed by TLC (system solvent A). TLC standard solutions at a concentration of 2 mM were used. Nar: naringin, R-nar: naringin reaction; rut: rutin, R-rut: rutin reaction; neohe: neohesperidin dihydrochalcone; R-neohe: neohesperidin dihydrochalcone reaction; glu: glucose, rha: rhamnose; es: enzymatic solution.

These data gave some indication on the substrate preference of the α -RHA activity expressed by strain PP1Y under our experimental conditions.

Diosmin and hesperidin (Fig. 1), which contained the rutinose disaccharide (α -L-Rhamnopyranosyl-(1 \rightarrow 6)- β -D-glucopyranose) linked to the phenolic portion of the molecules, were not hydrolyzed. Rutin, whose rutinose portion was linked to the quercetin 3-enol position, was instead converted. Under similar reaction conditions, flavonoids with the neohesperidose disaccharide 2-O-(6-deoxy- α -L-mannopyranosyl)- β -D-glucopyranose linked to the phenolic portion (naringin and neohesperidin dihydrochalcone) were completely transformed.

These data suggested that the α -RHA activity was able to hydrolyze both α ,1-2 and α ,1-6 interglycosidic linkages. Most of the α -RHAs reported in literature are mainly active on α -1, 2 glycosidic linkages, to a smaller extent on α -1,6 linkages, and even less on other glycosidic bonds [30]. Interestingly, the enzymatic activity expressed by strain PP1Y was specific for α ,1-2 interglycosidic bonds when the disaccharide unit of rutinose was linked to the phenolic hydroxyl groups. In fact, diosmin and hesperidin, which shared the presence of a α ,1-6 interglycosidic bond in the disaccharide units linked to a phenolic site, were not hydrolyzed. The α ,1-6 interglycosidic bond was instead hydrolyzed when the rutinose unit was linked to 3-enol position of rutin. This hydrolytic behaviour might be a consequence of a different steric effect deriving from the attachment of the disaccharidic units to different sites of the aglycons [3].

Free rutinose disaccharide was also examined as a possible substrate, resulting in a very low yield of products (data not shown), thus suggesting the importance of the aromatic portion of the flavonoidic moiety in the recognition mechanism of the enzymes involved.

Moreover, quercitrin, the quercetin 3- α -L-rhamnoside, in which L-rhamnose is directly linked to the aglycon, was not hydrolyzed. It should be noted that a marked preference for the of PNP- α -L-Rhap (from now on indicated as pNPR) in comparison to quercitrin, robinin or rutin has been reported also for other characterized α -RHAs [3].

The solubility of flavonoids (typically polyphenols) is pH-dependent and generally increases in alkaline media, which are often not compatible with the enzymatic activities used in bioprocesses. Using naringin as the most water-soluble available flavonoid (0.5 g/L at 20 °C) [31], the influence of pH and organic solvents on the hydrolytic behaviour of the enzymes present in PP1Y crude extracts was investigated.

Results of these experiments were reported in Table 2. A higher yield of naringin hydrolysis products was obtained at alkaline pH values ranging from 7.2 to 8.8 (Na-phosphate and Tris/HCl buffers) and an optimum pH value of 8.5 was determined. In this case, after 3 h of reaction, substrate spots were absent on TLC plates, thus suggesting a substrate complete depletion.

Within a reaction time of 3 h, TLC analyses of reaction systems in the pH range 8.2–8.8 showed the presence of a product with an Rf value higher than that of naringin. Free glucose and the naringenin aglycone were almost absent.

These data suggested the occurrence at these basic pH values of a marked decrease of the β -glucosidase activity, which should be responsible for the production of free glucose and naringenin aglycone, and the permanence of the α -RHA activity. This hypothesis was confirmed by the concomitant accumulation of a compound which was identified as prunin (Fig. 1), the de-rhamnosylated product of naringin, a molecule of biotechnological importance endowed with anti-inflammatory and antiviral activity against DNA/RNA viruses [32,33].

It is worth to note that bacterial α -RHAs having a pH optimum value at 8–8.5 have not been often reported in literature [30].

Prunin structure (Fig. 1) was confirmed by a 2D NMR spectroscopic investigation. The presence of the β -glucose residue was established by the value of the anomeric position signal in 13 C NMR spectrum (in MeOD) at 101.25 ppm which resulted correlated in HSQC spectrum to the diastereoisomeric anomeric protons H-1' at 5.01 ($J=6.90$ Hz), and 4.99 ($J=6.90$ Hz) ppm. The following signals (in ppm): C-2' 74.66 (H-2': 3.48), C-3' 77.82 (H-3': 3.47), C-4' 71.16 (H-4': 3.41), C-5' 78.28 (H-5': 3.42), C-6' 62.34 (H-6'-H-6'': 3.90, 3.72) confirmed the glucose structure of prunin saccharidic portion. Aglycone structure was confirmed by the 13 C spectrum signals at 80.69 ppm (C-2), 44.19 ppm (C-3), 166.98 and 167.05 ppm (C-7, the glycosylation site), 129.12 ppm (C-2''-C6''), 116.33 ppm (C-3''-C5'') and in 1 H-NMR spectrum by the proton signals at 7.35 ppm (H-2''-H6'') and 6.85 ppm (H-3''-H5''). The other signals in the spectra were in agreement with data previously reported [34]. The increase of the α -RHA activity present in PP1Y protein extracts observed at alkaline pH values was also confirmed by the pNPR bioconversion study followed by NMR analysis reported in Section 3.3.

The pH variation is not the unique strategy that has been used to overcome the poor hydrosolubility of flavonoids; the use of water-miscible organic co-solvents, in fact, has also been suggested [31]. However, it should be noted that this strategy has several drawbacks, such as toxicity problems derived from the use of an organic solvent in a bioprocess, and the possible decrease in the enzymatic activities employed [35].

In this study, the influence of the presence of organic solvents on the hydrolysis of naringin was evaluated by TLC analysis of

reaction mixtures containing from 1 to 50% v/v DMSO or CH₃CN (Table 2). After 90 min, in the presence of 1% and 10% of DMSO, naringin was almost totally consumed and traces of prunin were detected, suggesting a tolerance of the α -RHA activity to the presence of organic solvents along with a detrimental effect of DMSO on the β -glucosidase activity, as free glucose was almost absent in the reaction mixtures.

Finally, in the presence of either 50% DMSO or any concentration of CH₃CN, de-rhamnosylation and de-glucosylation reactions did not proceed even after 10 h.

Using the apparent best experimental conditions reported in Table 2 (pH value of 8.5 and 10% DMSO), and starting from a 125 mM naringin solution (Section 2.10), prunin was produced with a yield of 32.1%, corresponding to a final concentration of 0.02 M and an amount of 17.4 mg of recovered product.

Furthermore, free L-rhamnose was produced as a secondary product at a concentration of 6 g/L. The yield of products obtained in this experiment was comparable to that reported for a recombinant α -RHA from *Clostridium stercoararium* used for the hydrolysis of citrus peel waste naringin [7] and to other similar processes [30].

3.3. Bioconversion experiments followed by NMR

To confirm and better detail the observations on the substrate preference of the α -RHA activity in *Novosphingobium* sp. PP1Y crude protein extracts described in the previous paragraph, bioconversion reactions of pNPR, naringin, rutin and neohesperidin dihydrochalcone were performed using PP1Y cell extracts (Section 2.9), and monitored over time by ¹H-NMR.

Based on diagnostic signals of reagents and products for each reaction, substrate conversions were calculated by measuring the percentage ratio between the integrals of diagnostic signals of the products and the sum of the integration values of selected signals of reagents and final products. Results were reported in Fig. 3.

The highest yield of bioconversion in a shortest time was obtained with rutin. After 20 min 76.2% of the substrate was consumed. At the same time, 30–35% of pNPR, 26% of naringin, and 7% of neohesperidin dihydrochalcone were transformed.

After 173 min, naringin and neohesperidin dihydrochalcone reached bioconversions yields (95.6 and 86%, respectively) similar to rutin (89.4%). Under these conditions, 3.1–3.3 g/L of flavonoids were converted to products and, although the flavonoidic substrates were not totally hydrolyzed to aglycone, free L-rhamnose was released into the reaction media at a concentration of about 0.77–0.86 g/L.

It should be added that pNPR bioconversion was performed not only at pH 8.5 but also at pH 7, looking for a possible pH influence on PP1Y α -RHA activity (see Section 3.2). In the experiment in which naringin was used as a substrate, the reaction course was evaluated by comparing in ¹H-NMR spectra the integral values of two aromatic protons singlets (Fig. 1) H6–H8 in ring B at 6.19 ppm and 6.28 ppm, which were attributed a value of 2, to the integration of the corresponding protons of the final product narigenin (aglycon) at 5.78 and 5.8 ppm. ¹H-NMR spectra in MeOD of naringin, narigenin and prunin (H6–H8 signals at 6.22–6.24, respectively) of pure solutions confirmed the identity of narigenin integrated signals.

When rutin was used as substrate, aromatic proton signal H6 of the reagent at 6.18 ppm was selected as reference for the integration (Fig. 1). As for the reaction products, an aromatic signal at 6.13 ppm, which increased over time, was selected for evaluating rutin bioconversion.

After 10 min of reaction, the anomeric proton of β -glucose in rutin at 5.07 ppm (d, $J = 7.61$ Hz) almost disappeared (72% of conversion) and an anomeric proton signal at 5.035 ppm (d, $J = 8.07$ Hz), possibly corresponding to the β -anomeric proton of quercetin 3- β -glucoside, appeared; anomeric signals of free glucose were absent.

On the other hand, in ¹H-NMR spectra at 173 min, anomeric protons region was more crowded with signals due to the presence of free glucose (α -proton at 5.13 ppm $J = 3.91$ Hz; β -proton at 4.50 ppm, $J = 7.8$ Hz) and a signal at 5.023 ppm of free rhamnose α -proton (with the β -anomeric proton overlapped by the solvent residual water signal).

These data suggested a fast hydrolysis of the interglycosidic linkage inside the rutinose unit (α -L-Rha-(1 \rightarrow 6)- β -D-Glu) with the production of free rhamnose at the beginning of the reaction, as confirmed by the presence of a further methyl signal at 1.27 ppm after 10 min of reaction, corresponding to protons at position 6 of free rhamnose, and the subsequent release of flavonol quercetin and glucose.

The Neohesperidin dihydrochalcone bioconversion was evaluated by ¹H-NMR using the aromatic signals at 6.049 ppm, corresponding to two overlapped aromatic protons H2 and H6 (Fig. 1) linked to the saccharidic portion, as the reagent reference signals, with a integral value of 1, and a signal at 6.077 ppm, belonging to the reaction product.

An evaluation of the anomeric signals in the range 4.45:5.2 ppm of ¹H-NMR experiment showed, after 173 min of reaction, the presence of the α -proton signal of linked rhamnose at 5.28 ppm and the anomeric signal of β -glucose at 5.065 ppm (d, $J = 7.63$ Hz) which belonged to the substrate, the α - and β -anomeric protons signals of free glucose at 5.13 ppm (d, $J = 3.81$ Hz) and 4.50 ppm (d, $J = 7.63$ Hz) respectively. Moreover, an intense signal at 5.03 ppm of the α -anomeric proton of free rhamnose, a signal at 4.95 ppm (d, $J = 7.31$ Hz) almost as intense as the previous signal, which was partially covered by residual H₂O signal in MeOD, corresponding to β -glucose H1 signal of neohesperidin dihydrochalcone without rhamnose were also observed. On the contrary, the free rhamnose β -anomeric signal was totally overlapped by residual H₂O signal in MeOD.

The high intensity of the α -anomeric proton of free rhamnose and the scarce presence of anomeric signals of free glucose, led us to suppose that the main reaction product was the de-rhamnosylated neohesperidin dihydrochalcone.

In experiments using pNPR as substrate, the integral value of aromatic proton signal at 7.23 ppm was set to 1 and the signal of *p*-nitrophenol at 6.69 ppm produced by the hydrolysis of glycosidic linkage was selected for the assessment of pNPR bioconversion. This bioconversion was performed at two pH values; as reported in Fig. 2, after 60 min, the conversion of pNPR was of about 61% at pH 7, whereas at higher pH it reached 97%, thus confirming the trend of the experiments in which naringin was used as substrate described in Section 3.2.

3.4. Induction of α -RHA activity in PP1Y cell extracts

α -RHA activity can be specifically induced by several flavonoids [36,37] among which naringin is of particular interest because this compound can be abundantly recovered in citrus solid wastes. These wastes are quite interesting because they can be used either as an energetic source for growing microorganisms, due to their content in carbon and other nutrient components, and/or as a specific inducer for the biosynthesis of glycosidases due to the presence of flavonoids. It goes without saying that the use of citrus waste as starting material in bioconversion processes is an advantage for industrial companies because, among others, it decreases the expenses for waste disposal. The possible role of naringin as an inducer of the α -RHA activity [37] in PP1Y protein extracts was investigated using PP1Y cells grown in PPMM medium supplemented with naringin at different initial concentrations up to 0.3 mM, as described in detail in Section 2.6.

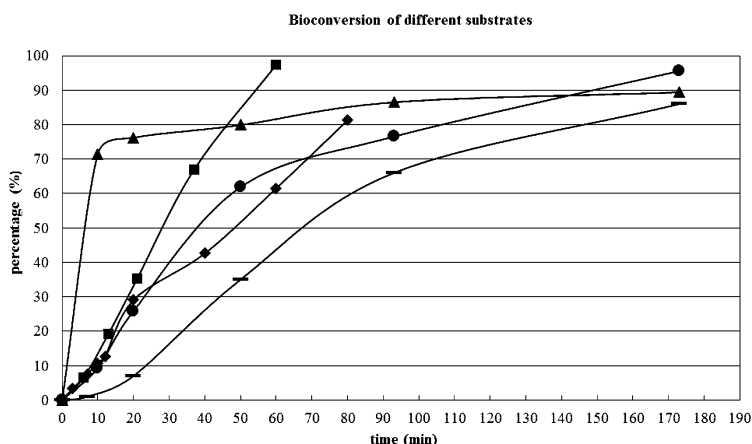


Fig. 3. Bioconversions of naringin ●, rutin ▲, neohesperidin dihydrochalcone —, *p*-nitrophenyl- α -L-rhamnopyranoside at pH 7 ◆ and 8.5 ■.

The effect of naringin could not be evaluated at concentrations higher than 0.3 mM due to its poor solubility under the experimental conditions used.

The effect of naringin could not be investigated at concentration values higher than 0.3 mM due to its poor solubility under the experimental conditions used. Results were reported in Fig. 4 and confirmed that naringin acts as an inducer leading, at a concentration of 0.3 mM, to a maximum 5-fold increase of the α -RHA activity (15.2 mU/mg) detected in the crude extract of PP1Y cells. These data encourage a future biotechnological use of PP1Y strain and of its α -RHA activity for the use of agro-industry vegetable residues.

3.5. Stereochemical course of α -RHA activity in hydrolysis reactions

To shed light on the type of enzymatic mechanism of PP1Y α -RHA activity, hydrolysis products of *p*NPR were analyzed by recording $^1\text{H-NMR}$ spectra over time. The integration of the anomeric proton signals of reagent and products was investigated; the analysis was performed taking into account that the anomeric proton of free rhamnose shows peaks at 5.06 ppm (α -anomeric form) and 4.83 ppm (β -anomeric form). Results were reported in Fig. 5, where the reaction time-dependent changes in amplitude of H-1 signals from substrate, α -1(S) (5.68 ppm), and products,

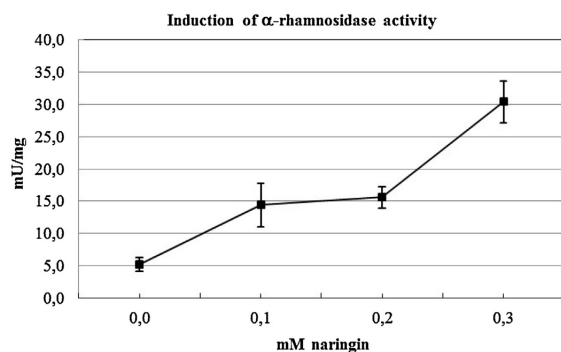


Fig. 4. α -RHA specific activity in the cell extract of strain PP1Y is expressed as mU/mg of total proteins (Y-axis). Specific activity is reported as a function of the concentration of naringin initially added to the growth medium.

α -1(P), and β -1(P), were plotted as % of total anomeric (H-1) signals. At t_0 , the only α -anomeric proton signal present was that of *p*NPR at 5.68 ppm (α -1(S)). During the first minutes of reaction a signal at 4.83 ppm, corresponding to the β -L-Rhap anomeric proton (β -1(P)), appeared only slightly earlier than the appearance of a further signal at 5.06 ppm, corresponding to the α -L-Rhap anomeric proton (α -1(P)).

These signals increased in intensity over time, while the anomeric signal of *p*NPR decreased concomitantly, as it is evident from Fig. 5. NMR analysis did not give evidence for the onset of mutarotation equilibration during the first minutes of reaction.

Later in the incubation, mutarotation of the initially released β -L-Rhap increased the ratio between the intensities of the α - and β -anomer protons signals. After 7 min, at a conversion percentage of 7.5%, the relative intensities of the α - and β -anomer resonances (calculated from peaks integration) were in a ratio of about 1:3 (25% of the α - and 75% for the β -anomer). After 20 min, at a conversion percentage of 29%, the α -/ β -anomer ratio was of about 1:2 (32% of the α - and 68% for the β -anomer). After 60 min, at a conversion percentage of 61.5%, the α / β ratio value increased to about 1:1. This ratio was kept constant also after 80 min, when the integration values showed that the yield of *p*NPR consumption was of

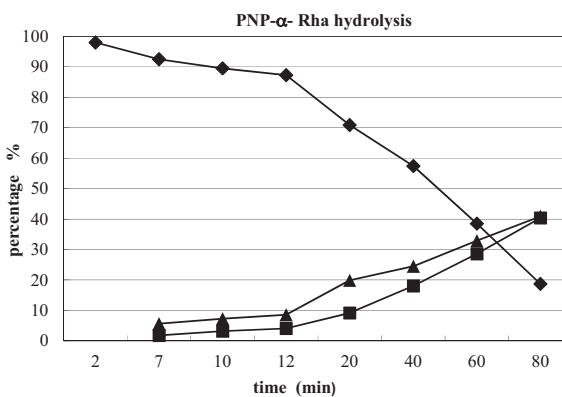


Fig. 5. % of total anomeric signals in *p*-nitrophenyl- α -L-rhamnopyranoside hydrolysis reaction: signals from substrate, α -1(S) ◆, and products, α -1(P) ■, and β -1(P) ▲, are plotted as % of total anomeric (H-1) signals.

about 86%, and was maintained up to 18 h, thus representing the equilibrium value of the ratio between both anomeric forms of L-rhamnopyranose. A solution of free rhamnose used in the same experimental conditions and monitored by $^1\text{H-NMR}$ reached the mutarotational equilibrium after 1–2 min and the concentrations ratio of α - and β -rhamnose was 1:1.

The kinetic behaviour suggested by these experiments for PP1Y α -RHA activity was an inverting mechanism of hydrolysis in which β -rhamnose was formed from the α -rhamnose via a single displacement mechanism and was then spontaneously converted by mutarotation to the α -anomeric form.

4. Conclusions

Bacterial glycosyl hydrolases are the focus of an increasing number of researches because of their key role in fundamental biological processes and their biotechnological applications. Here, the attention was focused on a novel α -RHA activity from *Novosphingobium* sp. PP1Y, which resulted interesting for its alkaline pH optimum and moderate tolerance to organic solvents.

This α -RHA was used, even without any further purification of PP1Y crude protein extract, for the bioconversion of flavonoids useful for the food and pharmaceutical industries. However, a future detailed biochemical characterization of this enzyme is now crucial for a better understanding of its effective biotechnological potential.

Acknowledgments

We thank D. Melck, E. Castelluccio and A. Esposito (NMR service of Istituto di Chimica Biomolecolare, CNR, Pozzuoli, Italy) for their skilful assistance.

References

- [1] A. Schmid, J.S. Dordick, B. Hauer, A. Kiener, M. Wubbolts, B. Witholt, *Nature* 409 (2001) 258–268.
- [2] U.T. Bornscheuer, G.W. Huisman, R.J. Kazlauskas, S. Lutz, J.C. Moore, K. Robins, *Nature* 485 (2012) 185–194.
- [3] P. Manzanares, S. Vallés, D. Ramón, M. Orejas, in: J. Polaina, A.P. MacCabe (Eds.), *Industrial Enzymes*, Springer, The Netherlands, 2007, pp. 117–140.
- [4] K. Habelt, F. Pittner, *Anal. Biochem.* 134 (1983) 393–397.
- [5] M. Roitner, T. Schalkhammer, F. Pittner, *Monatsh. Chem.* 115 (1984) 1255–1267.
- [6] N.L. Rojas, C.E. Voget, R.A. Hours, S.F. Cavalitto, *J. Ind. Microbiol. Biotechnol.* 38 (9) (2011) 1515–1522.
- [7] A. Kaur, S. Singh, R.S. Singh, W.H. Schwarz, M. Puri, *J. Chem. Technol. Biotechnol.* 85 (2010) 1419–1422.
- [8] Y. Kurosawa, K. Ikeda, F. Egami, *J. Biochem.* 73 (1973) 31–37.
- [9] S. Qian, H. Yu, C. Zhang, M. Lu, H. Wang, F. Jin, *Chem. Pharm. Bull.* 53 (2005) 911–914.
- [10] H. Suzuki, *Arch. Biochem. Biophys.* 99 (1962) 476–483.
- [11] R. Bourbouze, F. Pratiel-Sosa, F. Percheron, *Phytochemistry* 14 (1975) 1279–1282.
- [12] M. Puri, *Appl. Microbiol. Biotechnol.* 93 (2012) 49–60.
- [13] I.S. Jang, D.H. Kim, *Biol. Pharm. Bull.* 19 (1996) 1546–1549.
- [14] A.G. Orrillo, P. Ledesma, O.D. Delgado, G. Spagna, J.D. Breccia, *Enzyme Microb. Technol.* 40 (2007) 236–241.
- [15] W. Hashimoto, H. Nankai, N. Sato, S. Kawai, K. Murata, *Arch. Biochem. Biophys.* 368 (1999) 56–60.
- [16] W. Hashimoto, O. Miyake, H. Nankai, K. Murata, *Arch. Biochem. Biophys.* 15 (2003) 235–244.
- [17] T. Miyata, N. Kashige, T. Satho, T. Yamaguchi, Y. Aso, F. Miae, *Curr. Microbiol.* 51 (2005) 105–109.
- [18] W. Hashimoto, K. Murata, *Biosci. Biotechnol. Biochem.* 62 (1998) 1068–1074.
- [19] A. Grimaldi, E. Bartowsky, V. Jiranek, *Int. J. Food Microbiol.* 105 (2005) 233–244.
- [20] J. Beekwilder, D. Marozzi, S. Vecchi, R. de Vos, P. Janssen, C. Francke, R.D. Hall, *Appl. Environ. Microbiol.* 75 (2009) 3447–3454.
- [21] V.V. Zverlov, C. Hertel, K. Bronnenmeier, A. Hroch, J. Kellermann, W.H. Schwarz, *Mol. Microbiol.* 35 (2000) 173–179.
- [22] H. Birgisson, G.O. Hreggvidsson, O.H. Fridjónsson, A. Mort, J.K. Kristjánsson, B. Mattiasson, *Enzyme Microb. Technol.* 34 (2004) 561–571.
- [23] Z. Fujimoto, A. Jackson, M. Michikawa, T. Maehara, M. Momma, B. Henrissat, H.J. Gilbert, S. Kaneko, *J. Biol. Chem.* 288 (2013) 12376–12385.
- [24] Z. Cui, Y. Maruyama, B. Mikami, W. Hashimoto, K. Murata, *J. Mol. Biol.* 374 (2007) 384–398.
- [25] J.B. Bonanno, S.C. Almo, A. Bresnick, M.R. Chance, A. Fiser, S. Swaminathan, J. Jiang, F.W. Studier, L. Shapiro, C.D. Lima, T.M. Gaasterland, A. Sali, K. Bain, I. Feil, X. Gao, D. Lorimer, A. Ramos, J.M. Sauder, S.R. Wasserman, S. Emtage, K.L. D'Amico, S.K. Burley, *J. Struct. Funct. Genomics* 6 (2005) 225–232.
- [26] E. Notomista, F. Pennacchio, V. Cafaro, G. Smaldone, V. Izzo, L. Troncone, M. Varcamonti, A. Di Donato, *Microb. Ecol.* 61 (2011) 582–594.
- [27] V. D'Argenio, M. Petrillo, P. Cantiliello, B. Naso, L. Cozzuto, E. Notomista, G. Paolella, A. Di Donato, *F. Salvatore, J. Bacteriol.* 193 (2011) 4296.
- [28] M.M. Bradford, *Anal. Biochem.* 72 (1976) 248–254.
- [29] J. Sambrook, E.F. Fritsch, T. Maniatis, *Molecular Cloning, A Laboratory Manual*, 2nd ed., Cold Spring Harbor Laboratory Press, New York, 1989.
- [30] V. Yadav, P.K. Yadav, S. Yadav, K.D.S. Yadav, *Process Biochem.* 45 (2010) 1226–1235.
- [31] L. Chebil, C. Humeau, J. Anthoni, F. Dehez, J.-M. Engasser, M. Ghoul, *J. Chem. Eng. Data* 52 (2007) 1552–1556.
- [32] G. Celiz, M. Daz, M.C. Audisio, *J. Appl. Microbiol.* 111 (2011) 731–738.
- [33] T. Kaul, E. Middleton, P. Ogra, *J. Med. Virol.* 15 (1985) 71–79.
- [34] N.H. Tung, J.-H. Son, K. Cho, J.-A. Kim, J.-H. Hyun, H.-K. Kang, G.Y. Song, C.J. Park, Y.H. Kim, *Food Sci. Biotechnol.* 19 (1) (2010) 271–274.
- [35] L. Weignerova, P. Marhol, D. Gerstorferova, V. Kren, *Bioresource Technol.* 115 (2012) 222–227.
- [36] D. Monti, A. Pisvejcová, V. Kren, M. Lama, S. Riva, *Biotechnol. Bioeng.* 87 (6) (2004) 763–771.
- [37] V.V. Kumar, *Afr. J. Biotechnol.* 9 (45) (2010) 7683–7686.



Marine metagenomics, a valuable tool for enzymes and bioactive compounds discovery

Rosalba Barone[†], Concetta De Santi[†], Fortunato Palma Esposito[†], Pietro Tedesco[†], Federica Galati, Marco Visone, Alessia Di Scala and Donatella De Pascale*

Institute of Protein Biochemistry, National Research Council, Naples, Italy

Edited by:

Conxita Avila, Universitat de Barcelona, Spain

Reviewed by:

Susanna López-Legentil, University of North Carolina Wilmington, USA
Ana Riesgo, University of Barcelona, Spain

*Correspondence:

Donatella De Pascale, Institute of Protein Biochemistry, National Research Council, Via P. Castellino, 111, Naples, I-80131, Italy
e-mail: d.depascale@ibp.cnr.it

[†]These authors have contributed equally to this work.

The enormous potential in diversity of the marine life is still not fully exploited due to the difficulty in culturing many of the microorganisms under laboratory conditions. In this mini-review we underlined the importance of using an omics technique, such as metagenomics, to access the uncultured majority of microbial communities. We report examples of several hydrolytic enzymes and natural products isolated by functional sequenced-based and function- screening strategies assisted by new high-throughput DNA sequencing technology and recent bioinformatics tools. This article ends with an overview of the potential future perspectives of the metagenomics in bioprospecting novel biocatalysts and bioactive compounds from marine sources.

Keywords: marine environments, metagenomics, biocatalysts, bioactive compounds, biotechnological applications

MARINE ENVIRONMENT

Marine environment is the largest aquatic ecosystem on the planet and it is estimated to be one of the most important sources of biodiversity in the world (Zhao, 2011; Felczykowska et al., 2012). Marine ecosystems have peculiar characteristics that result from the unique combination of several physical factors. These habitats allow the growth of a multitude of organisms, such as bacteria, algae, sponges, fungi, and fishes, which are able to face with these harsh conditions. In particular, certain microorganisms are able to live in the cold sea of Arctic and Antarctic regions, and these species growth under high pressure and low temperatures, at different pH and salinity, or in seas characterized by high level of pollutions (Norway, Red Sea). For their particular features, many of these microorganisms are used in a wide range of biotechnological applications, providing novel bioactive compounds (Faulkner, 2001) and biocatalysts for modern industries (Kennedy et al., 2011; De Pascale et al., 2012).

However, most of the marine biodiversity is still unexplored, because of the difficulties in reproducing marine microenvironment in laboratory. In fact, it has been estimated that less than 0.1% of all microbes in the oceans today has been discovered so far (Simon and Daniel, 2009) and therefore it is clear we have explored just a minimal part of the vast potential of the ocean in terms of natural product discovery.

For these reasons most of the marine bioma remained so far uncultured, therefore the marine treasure still remains in the abysses.

Metagenomics, with its culture-independent principle, offers novel opportunities for studying marine biodiversity and its biotechnological application.

Herein, we analyzed the state of the art of marine metagenomics, focusing on the discovery and application of novel enzymatic biocatalysts and bioactive compounds as well as the novel technological improvement in the field.

BIOPROSPECTING

Marine bioprospecting is aimed to search novel organisms or genes. Sediments and biota sampling is generally carried out in less explored regions, such as at extreme depths, on the high seas or on the deep seabed, specifically around sub-marine trenches, cold seeps, and hydrothermal vents. Bioprospecting in the oceans has been potentiated by the integration of high-throughput DNA sequencing methods to evaluate marine biodiversity. Such genomic data can provide a useful starting point to identify new enzymes involved in the biosynthesis of secondary metabolites (Arrieta et al., 2010; Abida et al., 2013). Genomics and biotechnology are examples of modern approaches to expand our knowledge of the processes influencing the diversity of life in the oceans (Huete-Perez and Quezada, 2013).

METAGENOMIC APPROACH

CULTURE-INDEPENDENT METHOD

Many organisms require special growth parameters (physical and chemical) that are hard or even impossible to reproduce in the laboratory (Pace, 2009). In addition the interdependence with other organisms in Nature is a crucial point to be considered when culturing microorganisms under unnatural conditions. This is the reason why more than 70 bacterial phyla have no cultured representatives.

Although the cultivation success rate certainly can be improved (Tyson and Banfield, 2005), there are recent

approaches that microbiologists are employing to convert currently unculturable bacteria into cultured isolates in laboratory, as the capillary-based system of cells culturing based on porous hollow-fiber membranes (Stewart, 2012). To explore this vast source of genetic diversity, omics techniques are currently used.

Metagenomics is an extremely powerful omics technique. It refers to genetic analysis of microorganisms by direct extraction method and cloning of DNA recovered from mixed combination of organisms collected from Nature (Handelsman, 2004). Metagenomics may be focused on gene clusters or genes encoding enzymes and on the discovery of biocatalysts for synthesis and production of secondary metabolites like bioactive compounds (Wong, 2010). Three categories of environments are often considered: (1) highly diverse environments (e.g., soil and seawater), (2) naturally or artificially enriched environments for the target gene/biocatalyst, or (3) extreme environments.

SCREENING, SEQUENCING, AND DATA ANALYSIS OF METAGENOMIC LIBRARIES

Screening of metagenomic libraries can be divided in sequence-based screening and function-based screening; in the sequence-based screening PCR amplifications are used to identify target genes from conserved regions of known genes, while the function-based screening is often carried out using robotic systems looking for a well-defined phenotype.

The screening may be often considered a drawback for a successful metagenomic approach due to the sensitivity of agar plate-based screening and faint signals. Furthermore, the expression of the target genes may be considered the major bottleneck due to the choice of an adequate expression vector and a suitable recombinant host.

However, over the last years some of these issues have been solved thanks to the continuous progresses in robotic machinery and sequencing technologies.

A crucial connection from the screening to the data analysis is represented by the development of new sequencing systems. This new platform concept consists on sequencing of a dense array of amplified DNA fragments through iterative cycles of enzymatic manipulation and imaging-based data collection (Shendure and Ji, 2008). More recent technologies, the so-called “third generation sequencing technologies,” involve sequencing of individual molecules, the single-cell sequencing (Xu et al., 2009). Third generation sequencing technologies, based on fluorescence detection, have already been launched (Xu et al., 2009; Metzker, 2010).

One example is the Next-generation Sequencing Simulator for Metagenomics (NeSSM), which is a fast simulation system for high-throughput metagenome sequencing (Jia et al., 2013). The large number of metagenomic information obtained by the sequencing platforms must be processed and suitable data-analysis tools are required. Bio-informatics software tools have been developed in order to manage enormous datasets (reads- or contigs-). Examples are the metagenome analyzer MEGAN, a recently software tool able to analyze the taxonomic content of large metagenomic datasets of short DNA fragments obtained through 454 sequencing (Huson et al., 2007). Another recent ultrafast program, named Kraken, is a highly accurate program to

assign taxonomic labels to metagenomic DNA sequences (Wood and Salzberg, 2014) and the newest Meta-QC-Chain provides an useful and high-performance QC (quality control) tool for metagenomic data (Zhou et al., 2014).

MARINE PRODUCTS

ENZYMES

Oceanic microorganisms have to face extreme environmental conditions such as low temperature, high salinity, and extreme pressures and they have evolved special metabolites to survive and proliferate during the evolution. Thus, the general life conditions are reflected into the enzymes that potentially may endow of unique properties.

Metagenomics resulted in being very effective in the discovery of novel extremozymes, isolated from extreme marine environments (Table 1). Cold-adapted enzymes represent a class of extremozymes and compared to their mesophilic or thermophilic homologs, can be up to 10 times more active at low and moderate temperatures (Cipolla et al., 2012; Karan et al., 2012).

These enzymes are already being used in many biotechnological applications providing economic benefits and energy savings. As a result of their high activity at mild temperatures or fast heat-inactivation, a lower concentration of the enzyme is required to reach a given activity reducing the costs of enzyme preparation. Also, they can minimize undesirable chemical reactions that can occur at higher temperatures (Cipolla et al., 2012). These properties are of particular relevance for the food and feed industry to avoid spoilage and change in nutritional value and flavor of the original heat-sensitive substrates and products (Cavicchioli et al., 2011; Florczak et al., 2013).

It has been demonstrated that cold-adapted enzymes possess peculiar structural features that confer them a flexible configuration. Comparative genome analyzes suggested that this typical

Table 1 | Extremozymes through marine metagenomic approach.

Enzymes	Source	References
Esterase	Seashore sediments	Jeon et al., 2009a
Lipase	Deep-sea	Jeon et al., 2009b
Esterase	Intertidal zone	Fu et al., 2013
Alkaline phospholipase	Tidal flat sediments	Lee et al., 2012
Glycoside hydrolase	Baltic sea	Wierzbička-Wos et al., 2013
Phospholipase	Hot spring	Tirawongsaroj et al., 2008
Esterase	Deep-sea hydrothermal field	Zhu et al., 2013
Glycoside hydrolases	Hydrothermal vent	Wang et al., 2011
Fumarase	Marine water	Jiang et al., 2010
β -glucosidase	Hydrothermal spring	Schroder et al., 2014
Laccase	Marine water	Fang et al., 2012
Esterase (salt-tolerant)	Tidal flat sediment	Jeon et al., 2012
Esterase	Red Sea brine pool	Mohamed et al., 2013
Mercuric reductase	Red Sea brine pool	Sayed et al., 2014

features of psychrophilic enzymes are most probably due to a combination of changes in the overall amino-acid composition, by which psychrophilic proteins lose their rigidity and gain increased structural flexibility enhancing catalytic function at low temperatures (Liszka et al., 2012; De Pascale et al., 2012).

Lipase and esterase are prominent industrial enzymes, being employed in the food, laundry, textile, pulp and paper industries, production of biodiesel, and in the synthesis of fine chemicals. Furthermore, they are very easy to detect from a functional agar screening by using synthetic substrates (Jeon et al., 2009a,b).

A metagenomic library screening of an Arctic intertidal zone allowed the isolation of a novel cold active esterase called Est97 (Fu et al., 2013). The recombinant enzyme demonstrated to retain almost the 60% of relative activity at 20°C and a very low thermostability, suggesting its utilization in cold biotransformation. Metagenomic techniques also allow the isolation of other classes of enzymes, in fact, a phospholipase A with lipase activity (after called MPLaG) is the first obtained from a metagenomic library from tidal flat sediments on the Korean west coast. It shown a maximum activity at 25°C and also presented specific catalytic properties against olive oil and phosphatidylcholine, which means that MPLaG is a lipid-preferred phospholipase (Lee et al., 2012).

A monomeric cold-active glycoside hydrolase family 1 enzyme, named BgLMK_g, was identified from metagenomic library of Baltic Sea water sample. This enzyme is characterized by a wide range of enzymatic activities including β-galactosidase, β-fucosidase, and β-glucosidase activities and, it demonstrated to be stable below 30°C, in the range from pH 6.0 to 8.0. The results of the kinetic studies revealed that BgLMK_g more efficiently hydrolyzed β-glucosidase substrates than β-galactosidase (Wierzbicka-Wos et al., 2013). The β-galactosidases are mainly implied in dairy industry because they are able to specifically hydrolyze the lactose into galactose and glucose.

Apart from the cold-adapted enzymes, the oceans host many other classes of microorganism (and therefore of enzymes) in specific and extreme ecological niches. Thermophilic and hyperthermophilic microorganisms, halophiles, and barophiles possess biocatalysts with relevant biotechnological applications (Bruins et al., 2001), showing stability and catalytic efficiency in the presence of high temperature, high salt concentration, and high pressure.

Novel thermostable biocatalysts have also been isolated through metagenomic approach. Several classes of enzymes have been identified and characterized: lipolytic enzymes (Tirawongsaroj et al., 2008; Zhu et al., 2013), glycoside hydrolases (Wang et al., 2011), fumarase (Jiang et al., 2010), and β-glucosidase (Schroder et al., 2014). Interesting, salt-tolerant enzymes have also been discovered. Fang and coworkers discovered a novel bacterial laccase, with alkaline activity, whose activity is enhanced by chloride addition (Fang et al., 2012). A group of Korean researcher was able to identify salt-tolerant esterases belonged to a new subfamily, through metagenomics (Jeon et al., 2012).

Bioprospecting in polluted and contaminated seas can lead to the isolation of enzymes that also display tolerance for high concentration of heavy metals. Mohamed et al. (2013) isolated a novel esterase from a metagenomic library from a Red Sea brine

pool. This esterase combined a thermophilic activity with high resistant to several heavy metals, making this enzymes appealing for applications in bioremediation (Mohamed et al., 2013). Similarly, a novel mercuric reductase was, again, discovered from samples collected from Red Sea. This enzyme showed enhanced catalytic activity in presence of high temperature, high salt, and heavy metals concentrations (Sayed et al., 2014).

BIOACTIVE COMPOUNDS

Compounds from marine environments

The oceans may be considered a vast “container” of natural products that could be exploited in medicine. Marine macro/micro organisms, during the evolution, acquired the capability to produce secondary metabolites with unique biological activity (Imhoff et al., 2011). These compounds have found a wide range of applications as antibacterial (Teasdale et al., 2009; Plaza et al., 2010), antifungal (Nishimura et al., 2010), antimalarial, antiprotozoa (Dos Santos et al., 2011), and antiviral (Cheng et al., 2010), as well as being active in diseases related to the cardiovascular, immune, and nervous systems (Asolkar et al., 2009; Sakurada et al., 2010; Mayer et al., 2013). Metagenomics revealed to be a very powerful tool also for the exploitation of bioactive compounds from marine bacterial communities, since it is extremely hard to isolate and cultivate symbiotic bacteria of marine macroorganisms, e.g., sponges that has been recently indicated as promising source of novel compounds, in particular as anticancer, by a large body of literature (Schirmer et al., 2005; Kennedy et al., 2007).

Compounds from sequence-based screening

The continuous progress in sequencing technology (e.g., pyrosequencing), the bioinformatic tools and the acquired information on bacterial gene clusters that produce natural compounds, such as the Non-Ribosomal Peptide Synthases (NRPS), and the Polyketide synthases (PKSs) (Fischbach and Walsh, 2006; Fieseler et al., 2007; Hochmuth and Piel, 2009) contributed in making the sequence-based screening a valid approach for the drug-discovery of novel bioactive compounds (Table 2). A first success of this approach was in 2002 by using beetles (Piel, 2002), and it gave the input to perform metagenomic on the marine sponges. The first work employing this strategy on sponges dates back 2004 and were performed again by Piel et al. (2004). They isolated and identified several putative PKS clusters from a highly complex metagenome of the marine sponge *Theonella swinhoei*. The total DNA was extracted, cloned in cosmids and the library was screened by using appropriate PCR primers. With this strategy, the authors isolated the PKS and NRPS clusters responsible for the production of onnamides and theopeperins, a group of polyketides with clear antitumoral activity. The isolated genes resulted belonging to bacterial symbionts, due to the absence of introns and the presence of Shine-Dalgarno sequences. Between 2004 and 2007 the Haygood research group was able to identify, through metagenomic approach, the putative bryostatin PKS gene cluster. In a previous work (Davidson et al., 2001), the researchers identified a 300 bp fragments of a β-ketoacyl-synthase (KSa) involved in the production of bryostatin, that was used as a probe for the screening of a metagenomic library enriched

Table 2 | Natural products discovered through metagenomic approach.

Compound	Source	Type of screening	References
Onnamide A	<i>Theonella swinhoei</i> , bacterial symbiont	Sequence-based screening	Piel et al., 2004
Bryostatin	<i>Bugula neritina</i> , bacterial Symbiont	Sequence-based screening	Hildebrand et al., 2004
Minimide	<i>Didemnum molle</i> , microbiome	Sequence-based screening	Donia et al., 2011
Apratoxin A	<i>Lyngbya bouillonii</i>	Sequence-based screening	Grindberg et al., 2011
Patellamides	<i>Lissoclinum patella</i>	Function-based screening	Long et al., 2005
Zn-coproporphyrin III	<i>Discodermia calyx</i>	Function-based screening	He et al., 2012

with DNA of *Candidatus Endobugula sertula*, a bacterial symbiont of the marine bryozoans *Bugula neritina*. This screening led to the identification of a 65 kb cluster responsible for the bryostatin production (Hildebrand et al., 2004; Sudek et al., 2007).

Donia and co-workers showed the validity of metagenomics also for ribosomal peptides. In their work (Donia et al., 2011), they described the isolation and identification of a novel cyanobactin peptide that was called “minimide” from environmental DNA extracted from dotting colonies of *Didemnum molle*, an ubiquitous ascidian that inhabits diverse tropical marine habitats. The biosynthetic pathway was isolated by PCR screening, identified, cloned and the optimization of the recombinant expression in *E. coli* was FINALLY performed.

The recent advances of the genomics contributed to provide novel tools for developing of new metagenomic strategies. The single cell-genomics helped to reduce the metagenomic complexity. A single cell can now be isolated from complex microbial mixtures and the genome amplified for sequencing or PCR screening (Kvist et al., 2007). This approach, combined with metagenomic screening, led the isolation *apr* gene cluster that proved to be responsible for the biosynthesis of the antitumor natural product apratoxin A (Grindberg et al., 2011).

Compounds from function-based screening

The principal advantage of the function-based screening is that it does not require information regarding the biosynthetic origin of the compounds.

The functional approach has proven its validity thank to the work of Long and collaborators in 2005 (Table 2). In this study, a metagenomic BAC library was obtained from bacterial DNA extracted from the ascidian *Lissoclinum patella*. The library was then screened searching for clones producing patellamides compounds. The authors identified the recombinant-producing clones and performed the optimization of the heterologous expression in *E. coli* (Long et al., 2005). In a similar way, a Japanese group in 2012 developed a rapid and efficient functional screening for the detection of natural compounds. The 250.000-fosmid library, prepared using microbiome DNA from marine sponge *Discodermia calyx*, was rapidly screened on agar plates using a color selection to identify red *E. coli* clones that indicated the production of porphyrin. These procedures led the isolation two positive clones that were then cultured in large scale and analyzed. The red pigments were then isolated and structurally elucidated (He et al., 2012). Despite these two successes, the functional screenings displayed several drawbacks, among the others the

poor expression of interesting genes in heterologous host strains. However, this problem was addressed by the use of more suitable bacterial strains belonging to *Streptomyces*, *Pseudomonas*, and *Bacillus* genera (Ekkers et al., 2012) or by setting up of specific heterologous expression systems in *E. coli* (Yuzawa et al., 2012). Other liability of this strategy regards the few number of positive clones obtained in a screening and the missing of an easy and quick screening techniques for analyzing a huge amount of samples. However, there is an incessant development of new screening strategies (Ballestrero et al., 2010; Owen et al., 2012) as well as new approaches to improve the effectiveness of screenings (Penesyan et al., 2013), that will make functional screening more feasible in the future.

CONCLUSION

In this paper, we highlighted the importance of metagenomics for marine bioprospecting. Metagenomics allows the study and the biotechnological implementation of the marine biodiversity, proved by the huge number of novel biocatalysts and compounds discovered in the last 10 years. It is expected that metagenomics will acquire further interest, despite improvements of culturing techniques. Our suggestion is validated by the rapid advancement in the methods and tools, especially in sequencing and bioinformatic analysis.

As evidence of the metagenomics strength and validity, currently new interdisciplinary projects, aiming at the marine ecosystem access from a biotechnology point of view, have been funded in the EU FP7. Many of these projects are focused on the identification of new marine microbial strains from extreme environments to discovery novel products in the following industry sectors: health, personal care and nutrition. So far, the interest in the exploitation of the marine environment is still growing, as demonstrated by the large number of EU calls recently launched over the EU Horizon 2020 Framework.

ACKNOWLEDGMENT

This work was supported by the EU FP7-KBBE 2012-2016 project PharmaSea: Increasing Value and Flow in the Marine Biodiscovery Pipeline, grant N° 312184.

REFERENCES

- Abida, H., Ruchaud, S., Rios, L., Humeau, A., Probert, I., De Vargas, C., et al. (2013). Bioprospecting marine plankton. *Mar. Drugs* 11, 4594–4611. doi: 10.3390/md11114594
- Arrieta, J. M., Arnaud-Haond, S., and Duarte, C. M. (2010). What lies underneath: conserving the oceans' genetic resources. *Proc. Natl. Acad. Sci. U.S.A.* 107, 18318–18324. doi: 10.1073/pnas.0911897107

- Asolkar, R. N., Freel, K. C., Jensen, P. R., Fenical, W., Kondratyuk, T. P., Park, E. J., et al. (2009). Arenamides A-C, cytotoxic NFKappaB inhibitors from the marine actinomycete *Salinispora arenicola*. *J. Nat. Prod.* 72, 396–402. doi: 10.1021/np800617a
- Ballestrero, E., Thomas, T., Burke, C., Egan, S., and Kjelleberg, S. (2010). Identification of compounds with bioactivity against the nematode *Caenorhabditis elegans* by a screen based on the functional genomics of the marine bacterium *Pseudoalteromonas tunicata* D2. *Appl. Environ. Microbiol.* 76, 5710–5717. doi: 10.1128/AEM.00695-10
- Bruins, M. E., Janssen, A. E., and Boom, R. M. (2001). Thermozyms and their applications: a review of recent literature and patents. *Appl. Biochem. Biotechnol.* 90, 155–186. doi: 10.1385/ABAB:90:2:155
- Cavicchioli, R., Charlton, T., Ertan, H., Mohd Omar, S., Siddiqui, K. S., and Williams, T. J. (2011). Biotechnological uses of enzymes from psychrophiles. *Microb. Biotechnol.* 4, 449–460. doi: 10.1111/j.1751-7915.2011.00258.x
- Cheng, S. Y., Hsue, C. S., Hwang, G. H., Tsai, L. C., and Pei, S. C. (2010). Hourly oral misoprostol administration for terminating midtrimester pregnancies: a pilot study. *Taiwan. J. Obstet. Gynecol.* 49, 438–441. doi: 10.1016/S1028-4559(10)60095-2
- Cipolla, A., Delbrassine, F., Da Lage, J. L., and Feller, G. (2012). Temperature adaptations in psychrophilic, mesophilic and thermophilic chloride-dependent alpha-amylases. *Biochimie* 94, 1943–1950. doi: 10.1016/j.biochi.2012.05.013
- Davidson, S. K., Allen, S. W., Lim, G. E., Anderson, C. M., and Haygood, M. G. (2001). Evidence for the biosynthesis of bryostatins by the bacterial symbiont “*Candidatus Endobugula sertula*” of the bryozoan *Bugula neritina*. *Appl. Environ. Microbiol.* 67, 4531–4537. doi: 10.1128/AEM.67.10.4531-4537.2001
- De Pascale, D., De Santi, C., Fu, J., and Landfald, B. (2012). The microbial diversity of Polar environments is a fertile ground for bioprospecting. *Mar. Genomics* 8, 15–22. doi: 10.1016/j.margen.2012.04.004
- Donia, M. S., Ruffner, D. E., Cao, S., and Schmidt, E. W. (2011). Accessing the hidden majority of marine natural products through metagenomics. *ChemBiochem* 12, 1230–1236. doi: 10.1002/cbic.201000780
- Dos Santos, A. O., Britta, E. A., Bianco, E. M., Ueda-Nakamura, T., Filho, B. P., Pereira, R. C., et al. (2011). 4-Acetoxydolastane diterpene from the Brazilian brown alga *Canistrocarpus cervicornis* as antileishmanial agent. *Mar. Drugs* 9, 2369–2383. doi: 10.3390/md9112369
- Ekkers, D. M., Cretoiu, M. S., Kielak, A. M., and Elsas, J. D. (2012). The great screen anomaly—a new frontier in product discovery through functional metagenomics. *Appl. Microbiol. Biotechnol.* 93, 1005–1020. doi: 10.1007/s00253-011-3804-3
- Fang, Z. M., Li, T. L., Chang, F., Zhou, P., Fang, W., Hong, Y. Z., et al. (2012). A new marine bacterial lactase with chloride-enhancing, alkaline-dependent activity and dye decolorization ability. *Bioresour. Technol.* 111, 36–41. doi: 10.1016/j.biortech.2012.01.172
- Faulkner, D. J. (2001). Marine natural products. *Nat. Prod. Rep.* 18, 1–49. doi: 10.1039/b006897g
- Felczykowska, A., Bloch, S. K., Nejman-Falenczyk, B., and Baranska, S. (2012). Metagenomic approach in the investigation of new bioactive compounds in the marine environment. *Acta Biochim. Pol.* 59, 501–505.
- Fieseler, L., Hentschel, U., Grozdanov, L., Schirmer, A., Wen, G., Platzer, M., et al. (2007). Widespread occurrence and genomic context of unusually small polyketide synthase genes in microbial consortia associated with marine sponges. *Appl. Environ. Microbiol.* 73, 2144–2155. doi: 10.1128/AEM.02260-06
- Fischbach, M. A., and Walsh, C. T. (2006). Assembly-line enzymology for polyketide and nonribosomal peptide antibiotics: logic, machinery, and mechanisms. *Chem. Rev.* 106, 3468–3496. doi: 10.1021/cr0503097
- Florczak, T., Daroch, M., Wilkinson, M. C., Bialkowska, A., Bates, A. D., Turkiewicz, M., et al. (2013). Purification, characterisation and expression in *Saccharomyces cerevisiae* of LipG7 an enantioselective, cold-adapted lipase from the Antarctic filamentous fungus *Geomyces* sp. P7 with unusual thermostability characteristics. *Enzyme Microb. Technol.* 53, 18–24. doi: 10.1016/j.enzmictec.2013.03.021
- Fu, J., Leiros, H. K., De Pascale, D., Johnson, K. A., Blencke, H. M., and Landfald, B. (2013). Functional and structural studies of a novel cold-adapted esterase from an Arctic intertidal metagenomic library. *Appl. Microbiol. Biotechnol.* 97, 3965–3978. doi: 10.1007/s00253-012-4276-9
- Grindberg, R. V., Ishoey, T., Brinza, D., Esquenazi, E., Coates, R. C., Liu, W. T., et al. (2011). Single cell genome amplification accelerates identification of the apratoxin biosynthetic pathway from a complex microbial assemblage. *PLoS ONE* 6:e18565. doi: 10.1371/journal.pone.0018565
- Handelsman, J. (2004). Metagenomics: application of genomics to uncultured microorganisms. *Microbiol. Mol. Biol. Rev.* 68, 669–685. doi: 10.1128/MMBR.68.4.669-685.2004
- He, R., Wakimoto, T., Takeshige, Y., Egami, Y., Kenmoku, H., Ito, T., et al. (2012). Porphyrins from a metagenomic library of the marine sponge *Discodermia calyx*. *Mol. Biosyst.* 8, 2334–2338. doi: 10.1039/c2mb25169h
- Hildebrand, M., Waggoner, L. E., Liu, H., Sudek, S., Allen, S., Anderson, C., et al. (2004). bryA: an unusual modular polyketide synthase gene from the uncultivated bacterial symbiont of the marine bryozoan *Bugula neritina*. *Chem. Biol.* 11, 1543–1552. doi: 10.1016/j.chembiol.2004.08.018
- Hochmuth, T., and Piel, J. (2009). Polyketide syntheses of bacterial symbionts in sponges—evolution-based applications in natural products research. *Phytochemistry* 70, 1841–1849. doi: 10.1016/j.phytochem.2009.04.010
- Huete-Perez, J. A., and Quezada, F. (2013). Genomic approaches in marine biodiversity and aquaculture. *Biol. Res.* 46, 353–361. doi: 10.4067/S0716-97602013000400007
- Huson, D. H., Auch, A. F., Qi, J., and Schuster, S. C. (2007). MEGAN analysis of metagenomic data. *Genome Res.* 17, 377–386. doi: 10.1101/gr.5969107
- Imhoff, J. E., Labes, A., and Wiese, J. (2011). Bio-mining the microbial treasures of the ocean: new natural products. *Biotechnol. Adv.* 29, 468–482. doi: 10.1016/j.biotechadv.2011.03.001
- Jeon, J. H., Kim, J. T., Kang, S. G., Lee, J. H., and Kim, S. J. (2009a). Characterization and its potential application of two esterases derived from the arctic sediment metagenome. *Mar. Biotechnol.* 11, 307–316. doi: 10.1007/s10126-008-9145-2
- Jeon, J. H., Kim, J. T., Kim, Y. J., Kim, H. K., Lee, H. S., Kang, S. G., et al. (2009b). Cloning and characterization of a new cold-active lipase from a deep-sea sediment metagenome. *Appl. Microbiol. Biotechnol.* 81, 865–874. doi: 10.1007/s00253-008-1656-2
- Jeon, J. H., Lee, H. S., Kim, J. T., Kim, S. J., Choi, S. H., Kang, S. G., et al. (2012). Identification of a new subfamily of salt-tolerant esterases from a metagenomic library of tidal flat sediment. *Appl. Microbiol. Biotechnol.* 93, 623–631. doi: 10.1007/s00253-011-3433-x
- Jia, B., Xuan, L., Cai, K., Hu, Z., Ma, L., and Wei, C. (2013). NeSSM: a next-generation sequencing simulator for metagenomics. *PLoS ONE* 8:e75448. doi: 10.1371/journal.pone.0075448
- Jiang, C., Wu, L. L., Zhao, G. C., Shen, P. H., Jin, K., Hao, Z. Y., et al. (2010). Identification and characterization of a novel fumarase gene by metagenome expression cloning from marine microorganisms. *Microb. Cell Fact.* 9, 91. doi: 10.1186/1475-2859-9-91
- Karan, R., Capes, M. D., and Dassarma, S. (2012). Function and biotechnology of extremophilic enzymes in low water activity. *Aquat. Biosyst.* 8, 4. doi: 10.1186/2046-9063-8-4
- Kennedy, J., Marchesi, J. R., and Dobson, A. D. (2007). Metagenomic approaches to exploit the biotechnological potential of the microbial consortia of marine sponges. *Appl. Microbiol. Biotechnol.* 75, 11–20. doi: 10.1007/s00253-007-0875-2
- Kennedy, J., O’Leary, N. D., Kiran, G. S., Morrissey, J. P., O’Gara, F., Selvin, J., et al. (2011). Functional metagenomic strategies for the discovery of novel enzymes and biosurfactants with biotechnological applications from marine ecosystems. *J. Appl. Microbiol.* 111, 787–799. doi: 10.1111/j.1365-2672.2011.05106.x
- Kvist, T., Ahring, B. K., Lasken, R. S., and Westermann, P. (2007). Specific single-cell isolation and genomic amplification of uncultured microorganisms. *Appl. Microbiol. Biotechnol.* 74, 926–935. doi: 10.1007/s00253-006-0725-7
- Lee, M. H., Oh, K. H., Kang, C. H., Kim, J. H., Oh, T. K., Ryu, C. M., et al. (2012). Novel metagenome-derived, cold-adapted alkaline phospholipase with superior lipase activity as an intermediate between phospholipase and lipase. *Appl. Environ. Microbiol.* 78, 4959–4966. doi: 10.1128/AEM.00260-12
- Liszka, M. J., Clark, M. E., Schneider, E., and Clark, D. S. (2012). Nature versus nurture: developing enzymes that function under extreme conditions. *Annu. Rev. Chem. Biomol. Eng.* 3, 77–102. doi: 10.1146/annurev-chembioeng-061010-114239
- Long, P. F., Dunlap, W. C., Battershill, C. N., and Jaspers, M. (2005). Shotgun cloning and heterologous expression of the patellamide gene cluster as a strategy to achieving sustained metabolite production. *ChemBiochem* 6, 1760–1765. doi: 10.1002/cbic.200500210
- Mayer, A. M., Rodriguez, A. D., Tagliatela-Scafati, O., and Fusetani, N. (2013). Marine pharmacology in 2009–2011: marine compounds with antibacterial, antidiabetic, antifungal, anti-inflammatory, antiprotozoal, antituberculous, and antiviral activities; affecting the immune and nervous systems, and

- other miscellaneous mechanisms of action. *Mar. Drugs* 11, 2510–2573. doi: 10.3390/md11072510
- Metzker, M. L. (2010). Sequencing technologies - the next generation. *Nat. Rev. Genet.* 11, 31–46. doi: 10.1038/nrg2626
- Mohamed, Y. M., Ghazy, M. A., Sayed, A., Ouf, A., El-Dorry, H., and Siam, R. (2013). Isolation and characterization of a heavy metal-resistant, thermophilic esterase from a Red Sea brine pool. *Sci. Rep.* 3:3358. doi: 10.1038/srep03358
- Nishimura, S., Arita, Y., Honda, M., Iwamoto, K., Matsuyama, A., Shirai, A., et al. (2010). Marine antifungal theonellamides target 3beta-hydroxysterol to activate Rho1 signaling. *Nat. Chem. Biol.* 6, 519–526. doi: 10.1038/nchembio.387
- Owen, J. G., Robins, K. J., Parachin, N. S., and Ackerley, D. F. (2012). A functional screen for recovery of 4'-phosphopantetheinyl transferase and associated natural product biosynthesis genes from metagenome libraries. *Environ. Microbiol.* 14, 1198–1209. doi: 10.1111/j.1462-2920.2012.02699.x
- Pace, N. R. (2009). Mapping the tree of life: progress and prospects. *Microbiol. Mol. Biol. Rev.* 73, 565–576. doi: 10.1128/MMBR.00033-09
- Penesyan, A., Ballestrero, F., Daim, M., Kjelleberg, S., Thomas, T., and Egan, S. (2013). Assessing the effectiveness of functional genetic screens for the identification of bioactive metabolites. *Mar. Drugs* 11, 40–49. doi: 10.3390/md11010040
- Piel, J. (2002). A polyketide synthase-peptide synthetase gene cluster from an uncultured bacterial symbiont of *Paederus* beetles. *Proc. Natl. Acad. Sci. U.S.A.* 99, 14002–14007. doi: 10.1073/pnas.222481399
- Piel, J., Hui, D., Wen, G., Butzke, D., Platzer, M., Fusetani, N., et al. (2004). Antitumor polyketide biosynthesis by an uncultivated bacterial symbiont of the marine sponge *Theonella swinhoei*. *Proc. Natl. Acad. Sci. U.S.A.* 101, 16222–16227. doi: 10.1073/pnas.0405976101
- Plaza, A., Keffer, J. L., Lloyd, J. R., Colin, P. L., and Bewley, C. A. (2010). Paltolides A–C, anabaenopeptin-type peptides from the palau sponge *Theonella swinhoei*. *J. Nat. Prod.* 73, 485–488. doi: 10.1021/np900728x
- Sakurada, T., Gill, M. B., Frausto, S., Copits, B., Noguchi, K., Shimamoto, K., et al. (2010). Novel N-methylated 8-oxoisoguanines from Pacific sponges with diverse neuroactivities. *J. Med. Chem.* 53, 6089–6099. doi: 10.1021/jm100490m
- Sayed, A., Ghazy, M. A., Ferreira, A. J., Setubal, J. C., Chamberg, F. S., Ouf, A., et al. (2014). A novel mercuric reductase from the unique deep brine environment of Atlantis II in the Red Sea. *J. Biol. Chem.* 289, 1675–1687. doi: 10.1074/jbc.M113.493429
- Schirmer, A., Gadkari, R., Reeves, C. D., Ibrahim, F., Delong, E. F., and Hutchinson, C. R. (2005). Metagenomic analysis reveals diverse polyketide synthase gene clusters in microorganisms associated with the marine sponge *Discodermia dissoluta*. *Appl. Environ. Microbiol.* 71, 4840–4849. doi: 10.1128/AEM.71.8.4840-4849.2005
- Schroder, C., Elleuche, S., Blank, S., and Antranikian, G. (2014). Characterization of a heat-active archaeal beta-glucosidase from a hydrothermal spring metagenome. *Enzyme Microb. Technol.* 57, 48–54. doi: 10.1016/j.enzmictec.2014.01.010
- Shendure, J., and Ji, H. (2008). Next-generation DNA sequencing. *Nat. Biotechnol.* 26, 1135–1145. doi: 10.1038/nbt1486
- Simon, C., and Daniel, R. (2009). Achievements and new knowledge unraveled by metagenomic approaches. *Appl. Microbiol. Biotechnol.* 85, 265–276. doi: 10.1007/s00253-009-2233-z
- Stewart, E. J. (2012). Growing unculturable bacteria. *J. Bacteriol.* 194, 4151–4160. doi: 10.1128/JB.00345-12
- Sudek, S., Lopanik, N. B., Waggoner, L. E., Hildebrand, M., Anderson, C., Liu, H., et al. (2007). Identification of the putative bryostatin polyketide synthase gene cluster from "*Candidatus Endobugula sertula*," the uncultivated microbial symbiont of the marine bryozoan *Bugula neritina*. *J. Nat. Prod.* 70, 67–74. doi: 10.1021/mp060361d
- Teasdale, M. E., Liu, J., Wallace, J., Akhlaghi, F., and Rowley, D. C. (2009). Secondary metabolites produced by the marine bacterium *Halobacillus salinus* that inhibit quorum sensing-controlled phenotypes in gram-negative bacteria. *Appl. Environ. Microbiol.* 75, 567–572. doi: 10.1128/AEM.00632-08
- Tirawongsaroj, P., Sriprang, R., Harnpicharnchai, P., Thongaram, T., Champreda, V., Tanapongpipat, S., et al. (2008). Novel thermophilic and thermostable lipolytic enzymes from a Thailand hot spring metagenomic library. *J. Biotechnol.* 133, 42–49. doi: 10.1016/j.jbiotec.2007.08.046
- Tyson, G. W., and Banfield, J. F. (2005). Cultivating the uncultivated: a community genomics perspective. *Trends Microbiol.* 13, 411–415. doi: 10.1016/j.tim.2005.07.003
- Wang, H., Gong, Y., Xie, W., Xiao, W., Wang, J., Zheng, Y., et al. (2011). Identification and characterization of a novel thermostable gh-57 gene from metagenomic fosmid library of the Juan de Fuca Ridge hydrothermal vent. *Appl. Biochem. Biotechnol.* 164, 1323–1338. doi: 10.1007/s12010-011-9215-1
- Wierzbicka-Wos, A., Bartasun, P., Cieslinski, H., and Kur, J. (2013). Cloning and characterization of a novel cold-active glycoside hydrolase family 1 enzyme with beta-glucosidase, beta-fucosidase and beta-galactosidase activities. *BMC Biotechnol.* 13:22. doi: 10.1186/1472-6750-13-22
- Wong, D. (2010). "Applications of metagenomics for industrial bioproducts," in *Metagenomics: Theory, Methods and Applications*. 1st Edn. ed D. Marco (Norwich, UK: Horizon Scientific Press), 141–158.
- Wood, D. E., and Salzberg, S. L. (2014). Kraken: ultrafast metagenomic sequence classification using exact alignments. *Genome Biol.* 15, R46. doi: 10.1186/gb-2014-15-3-r46
- Xu, M., Fujita, D., and Hanagata, N. (2009). Perspectives and challenges of emerging single-molecule DNA sequencing technologies. *Small* 5, 2638–2649. doi: 10.1002/smll.200900976
- Yuzawa, S., Kim, W., Katz, L., and Keasling, J. D. (2012). Heterologous production of polyketides by modular type I polyketide synthases in *Escherichia coli*. *Curr. Opin. Biotechnol.* 23, 727–735. doi: 10.1016/j.copbio.2011.12.029
- Zhao, X. Q. (2011). Genome-based studies of marine microorganisms to maximize the diversity of natural products discovery for medical treatments. *Evid. Based Complement. Alternat. Med.* 2011:384572. doi: 10.1155/2011/384572
- Zhou, Q., Su, X., Jing, G., and Ning, K. (2014). Meta-QC-Chain: comprehensive and fast quality control method for metagenomic data. *Genomics Proteomics Bioinformatics* 12, 52–56. doi: 10.1016/j.gpb.2014.01.002
- Zhu, Y., Li, J., Cai, H., Ni, H., Xiao, A., and Hou, L. (2013). Characterization of a new and thermostable esterase from a metagenomic library. *Microbiol. Res.* 168, 589–597. doi: 10.1016/j.micres.2013.04.004

Conflict of Interest Statement: The authors declare that the research was conducted in the absence of any commercial or financial relationships that could be construed as a potential conflict of interest.

Received: 28 April 2014; accepted: 20 August 2014; published online: 04 September 2014.

Citation: Barone R, De Santi C, Palma Esposito F, Tedesco P, Galati F, Visone M, Di Scala A and De Pascale D (2014) Marine metagenomics, a valuable tool for enzymes and bioactive compounds discovery. *Front. Mar. Sci.* 1:38. doi: 10.3389/fmars.2014.00038

This article was submitted to *Marine Biotechnology*, a section of the journal *Frontiers in Marine Science*.

Copyright © 2014 Barone, De Santi, Palma Esposito, Tedesco, Galati, Visone, Di Scala and De Pascale. This is an open-access article distributed under the terms of the Creative Commons Attribution License (CC BY). The use, distribution or reproduction in other forums is permitted, provided the original author(s) or licensor are credited and that the original publication in this journal is cited, in accordance with accepted academic practice. No use, distribution or reproduction is permitted which does not comply with these terms.

Identification and Characterization of a Novel Salt-Tolerant Esterase from a Tibetan Glacier Metagenomic Library

Concetta De Santi, Luca Ambrosino, Pietro Tedesco, and Donatella de Pascale

Inst. of Protein Biochemistry, National Research Council, Naples I-80131, Italy

Lei Zhai

State Key Laboratory of Microbial Resources and National Engineering Laboratory for Industrial Enzymes, Institute of Microbiology, CAS, Beijing 100101, China

Graduate School of the Chinese Academy of Sciences, Beijing, China

Cheng Zhou, Yanfen Xue, and Yanhe Ma

State Key Laboratory of Microbial Resources and National Engineering Laboratory for Industrial Enzymes, Inst. of Microbiology, CAS, Beijing 100101, China

DOI 10.1002/btpr.2096

Published online May 15, 2015 in Wiley Online Library (wileyonlinelibrary.com)

A salt-tolerant esterase, designated H9Est, was identified from a metagenomic library of the Karuola glacier. H9Est gene comprised 1071 bp and encoded a polypeptide of 357 amino acids with a molecular mass of 40 kDa. Sequence analysis revealed that H9Est belonged to the family IV of bacterial lipolytic enzyme. H9Est was overexpressed in Escherichia coli and the purified enzyme showed hydrolytic activity towards p-nitrophenyl esters with carbon chain from 2 to 8. The optimal esterase activity was at 40°C and pH 8.0 and the enzyme retained its activity towards some miscible organic solvents such as polyethylene glycol. A three-dimensional model of H9Est revealed that S200, D294, and H324 formed the H9Est catalytic triad. Circular Dichroism spectra and molecular dynamic simulation indicated that the esterase had a wide denaturation temperature range and flexible loops that would be beneficial for H9Est performance at low temperatures while retaining heat-resistant features. © 2015 American Institute of Chemical Engineers Biotechnol. Prog., 31:890–899, 2015

Keywords: metagenomic, esterase, salt-tolerant, cold-tolerant

Introduction

Lipolytic enzymes including esterases (EC 3.1.1.1) and lipases (EC 3.1.1.3) are carboxylic ester hydrolases that catalyze the cleavage and formation of ester bonds. Esterases hydrolyze small ester-containing molecules that are at least partly soluble in water, while lipases display maximal activity towards water-insoluble long-chain triglycerides.¹ Both esterases and lipases belong to the α/β hydrolase superfamily and have a common Ser-Asp/Glu-His catalytic triad or a catalytic Ser-His dyad.² Based on amino acid sequence homology and physiological functions, Arpigny and Jaeger classified all bacterial lipolytic enzymes into eight families.¹ Recently, new families (families IX–XV) that diverge from the original eight were established for the most newly discovered bacterial lipolytic enzymes.³

Esterases possess useful features such as stability in organic solvents, broad substrate specificity, stereoselectivity, regioselectivity, and no requirement for cofactors.^{4,5}

They are useful in organic chemical synthesis, for producing enantiopure pharmaceuticals and agrochemicals, and in the degradation of natural materials and industrial pollutants.^{6,7} Many efforts have been made to screen and isolate novel microbial lipolytic enzymes with different characteristics. Metagenomics is a new and rapidly developing field aimed at accessing novel genes and biocatalysts from environmental samples for biotechnological applications.⁸ Lipolytic enzymes have been identified from metagenomic DNA libraries⁹ prepared from environmental samples such as soils,^{10–12} activated sludge,¹³ marine sediments,^{14,15} marine sponges,^{16,17} pond water,¹⁸ lake water,^{19,20} and hot springs.²¹ Exploring extreme environments may be a promising strategy for the discovery of novel biocatalyst with unusual properties. Compared with mesophilic and thermophilic counterparts, the interest and advantage of the biotechnological use of cold-tolerant lipolytic enzymes reside in high specific activity at low temperatures and their rapid inactivation at higher temperatures.²²

In this study, we describe the construction of a metagenomic library from a glacier soil sample from Tibet, China. Glaciers are known to be a reservoir of microbial life where biomolecules and microorganism can be preserve for long term under extreme constant environmental conditions.

Conflict of Interest: Authors declare that they have no conflict of interest.

Correspondence concerning this article should be addressed to Donatella de Pascale at d.depascale@ibp.cnr.it.

A novel esterase gene was isolated from the library using a function-based screening method.

According to the sequence analysis, the esterase was similar to bacterial family IV esterases, with conserved sequence motifs, specifically an oxyanion hole formed by residues HGGG ahead of the catalytic serine.

We describe the biochemical characterization of the deduced esterase (hereafter called H9Est), which was expressed in *Escherichia coli* and characterized for substrate specificity, optimum pH and temperature, thermal stability, and effect of solvents and salts. The structure of H9Est was also described to better understand the structure-function relationships of this catalyst for industrial development.

Material and Methods

Bacterial strains, plasmids, and growth conditions

E. coli DH5 α , BL21 (DE3), and EPI300-T1^R (Epicentre, Madison, WI) were used as hosts and grown in Luria-Bertani (LB) medium at 37°C. The fosmid pCC2FOS (Epicentre), and pUC118 (Takara, Dalian, China) and pET28a (Novagen, Madison, WI) were used as vectors to construct the metagenomic library, subcloning library and expression plasmid with H9Est gene, respectively. Ampicillin (100 $\mu\text{g mL}^{-1}$), kanamycin (50 $\mu\text{g mL}^{-1}$), and chloramphenicol (12.5 $\mu\text{g mL}^{-1}$) were used to select for vectors pUC118, pET28a, and pCC2FOS, respectively.

Metagenomic library construction and screening for lipolytic activity

A soil sample was collected from the Karuola glacier (glacier natural landscape area 90°19.23' E, 28°90.71' N,) located on the Tibetan Plateau, China, 5200 m above sea level. No specific permission was required for taking a small amount of soil in this area for scientific research. We took about 50 g soil sample near the glacier and did not damage the glacier, nor the activity endanger any protected species. The sample was stored on ice during transport and at -80°C in our laboratory until DNA extraction. DNA was extracted using the sodium dodecyl sulfate (SDS) lysis method described by Zhou et al.²³ The crude DNA preparation contaminated with humic compounds was purified in 0.8% low-melting-point agarose gel. Electrophoresis was carried out twice at 30 V overnight at 4°C. Size-fractionated DNA was recovered by GELase enzyme (Epicentre) and purified by chloroform extraction and isopropanol precipitation.

The metagenomic library from Karuola glacier soil was constructed using the CopyControl Fosmid Library Production Kit (Epicentre) according to the manufacturer's instructions. Purified fragments of environmental DNA (36–48 kb) blunt ends were repaired and ligated to the CopyControl vector pCC2FOS to form recombinant fosmid mixtures that were then packaged with lambda packaging extracts and infected *E. coli* EPI300-T1R.

LB agar medium supplemented with 12.5 $\mu\text{g mL}^{-1}$ chloramphenicol was used to select for recombinant cells. *E. coli* recombinant clones were maintained in 96-well microtiter plates with 20% glycerol (final concentration) at -80°C . For lipolytic activity screening, clones were replicated with a 96-pin replicator onto LB agar medium containing 1% tributyrin and 12.5 $\mu\text{g mL}^{-1}$ chloramphenicol. Cells were grown at

37°C for 48 h and colonies with a clear hydrolysis halo were selected.

Subcloning and sequence analysis of the esterase gene

Fosmid DNA from a positive clone was extracted by alkaline lysis methods as described by Sambrook et al.²⁴ and digested with *Hind* III. Purified DNA fragments were ligated into *Hind* III-linearized pUC118 and transformed into *E. coli* DH5 α . LB agar medium with 100 $\mu\text{g mL}^{-1}$ ampicillin and 1% tributyrin was used to select the secondary library. One positive recombinant, pUC118-H9Est was purified for DNA sequencing. The open reading frame (ORF) was identified via the ORF Finder program of the National Centre for Biotechnology Information. Similar ORFs were identified by protein homology using complete nonredundant protein databases (www.ncbi.nlm.nih.gov) and the BLAST program.²⁵ Multiple sequence alignment was performed using ClustalW (default parameters). Phylogenetic analysis was conducted with the neighbor-joining method with 500 bootstrap replications using MEGA version 5.0.²⁶

Expression and purification of the recombinant esterase

The H9Est gene (GenBank accession number KF994924) was amplified by PCR using the following primers: forward primer 5'-GCGGGATCCATGACTGTGAATCCTC-3' with *Bam* HI site underlined and reverse primer 5'-GCGGAGCTCGGACTATTTTGTGCCAG-3' with *Sac* I site underlined thus adding to the sequence N-terminal and C-terminal His tags. Purified PCR products were inserted into pET28a and a recombinant plasmid pET28a-H9Est was transformed into *E. coli* BL21 (DE3). Expression of recombinant protein was induced with IPTG (1 mM) after 3 h of incubation at 37°C to OD₆₀₀ 0.6–0.8. Cells were harvested by centrifugation after overnight growth with IPTG at 25°C and resuspended in 50 mM Tris-HCl buffer (pH 8.0). After ultrasonic disruption, cell debris was removed by centrifugation (15,500g, 20 min, 4°C). The esterase was purified by nickel affinity chromatography with a His-Bind Purification kit (Novagen) according to the manufacturer's instructions. Protein concentration was measured using the Bio-Rad Protein Assay system, with BSA as a standard. SDS-PAGE was performed using 5% stacking and 10% resolving gels.

Biochemical characterization of purified H9Est

Esterase standard activity was measured by monitoring hydrolysis of *p*-nitrophenyl butyrate (Sigma, St. Louis, MO) in 50 mM Tris-HCl buffer (pH 8.0) at 40°C. Reaction mixtures (1 ml) contained 0.5 mM substrate. The amount of *p*-nitrophenol liberated during the reaction was monitored continuously at 405 nm in a DU800 spectrophotometer (Beckman Coulter Inc., Fullerton, CA, USA) with a temperature control module. One unit of enzyme activity was defined as the amount of enzyme that released 1 μmol of *p*-nitrophenyl from *p*-nitrophenyl ester per min. Substrate specificity was determined using *p*NitroPhenyl-esterified (*p*NP-ester) substrates with different carbon chain lengths: *p*NP-acetate (C2), *p*NP-propionate (C3), *p*NP-butyrate (C4), *p*NP-caprylate (C8), *p*NP-decanoate (C10) and *p*NP-palmitate (C16). The kinetic parameters K_M and k_{cat} were calculated in 50 mM Tris-HCl (pH 8.0) at 40°C with *p*NP-butyrate as substrate. Kinetic analysis by curve fitting (Hyperbola) used GraphPad Prism 5.0 (GraphPad Software). Optimum temperature was

determined in the range of 10–80°C. The thermal stability of H9Est was studied over 10–50°C. Pure enzyme aliquots (0.2 mg mL⁻¹) in 100 mM Tris-HCl pH 8.0 were incubated in 1.5 mL tubes at indicated temperatures. Aliquots were withdrawn at 20, 40, 60, 80, 100, and 120 min and assayed at 40°C using *p*NP-butyrate as substrate. Optimum pH was determined in the range 3.0–10.0 using buffers 50 mM citric acid-sodium citrate (pH 3.0–6.0), 50 mM Phosphate buffered saline (pH 6.0–8.0), 50 mM Tris-HCl (pH 8.0–9.0), and 50 mM Glycyl-NaOH (pH 9.0–10.0). The effect of NaCl was evaluated by increasing the salt concentration from 0 to 2.5 M at 40°C using standard conditions mentioned above. Results were reported as activity relative to values measured without NaCl. The effects of metal ions and inhibitors on enzyme activity were measured by adding metal ions and inhibitors (final concentrations at 1 mM) to standard enzyme assay mixture. H9Est activity in buffers without additions was used as 100%. Enzyme activity was evaluated in increasing concentrations of the organic solvents acetonitrile, dimethyl ether, dimethyl sulfoxide (DMSO), diethyl ether, dimethyl formamide (DMFA) and polyethylene glycol (PEG 200) from 0 to 20% (v/v). Results were reported as activity relative to values measured without solvents. Data reported considered by mean values of triplicate \pm SD. *P*-value between sample and referring controls were calculated with “T test” with the Primer software.

Circular dichroism (CD)

CD spectra were measured on a J-810 spectropolarimeter (Jasco, Tokyo, Japan) equipped with a F25 temperature controller (Julabo, Seelbach, Germany). Molar ellipticity per mean residue, $[\theta]$ in deg cm² dmol⁻¹, was calculated using the equation $[\theta] = [\theta]_{\text{obs}} \text{mrw} (10.1 C)^{-1}$, where $[\theta]_{\text{obs}}$ is the ellipticity measured in degrees, mrw is the mean residue molecular weight (111.5 Da), *C* is the protein concentration in g mL⁻¹, and *l* is the optical path length of the cell in cm. Far-ultraviolet (UV) measurements (190–260 nm) were carried out from 20 to 90°C using a 0.1 cm optical path length cell and a protein concentration of 2.44 $\times 10^{-6}$ M. Pure protein was suspended in 20 mM Na-phosphate buffer at pH 8.0.

CD spectra, recorded with time constant 4 s, 2 nm bandwidth, and scan rate 20 nm min⁻¹ were averaged over at least three scans. Baseline was corrected by subtracting the buffer spectrum. Thermal denaturation curves were recorded from 20 to 90°C and by monitoring the CD signal at 222 nm. All curves were recorded with a scan rate of 0.5°C min⁻¹.

H9Est modeling

H9Est was modeled using four templates: an acetyl esterase from *Salmonella Typhimurium* (3GA7 PDB entry), a carboxylesterase from *Sulfolobus tokodaii* (3AIN), an esterase in the hormone-sensitive lipase (3FAK) subfamily, and a hyperthermophilic carboxylesterase from the archaeon *Archaeoglobus fulgidus* (1JJI). The use of several templates improved the quality of the generated model by introducing more constraints. Similarity extended along all sequences with the exception of the N-terminal portion of H9Est. Therefore, modeling was limited to the H9Est region between residues 38 and 355. To generate the three-dimensional model, multiple alignments between H9Est and sequences of the four templates from HHpred server²⁷ were

submitted to the comparative structural modeling program Modeller 9v11.²⁸ The modeling algorithm was set to generate 100 models. To select the best model, structure validation was carried out by PDBSum pictorial database (<http://www.ebi.ac.uk/thornton-srv/databases/pdbsum/>). A full set of Procheck structural analyses²⁹ was carried out to evaluate the stereochemical quality of the generated structures. The Z-score of the H9Est model was calculated using the web server WhatIf.³⁰ The solvent-accessible surface area of the H9Est model was calculated by the POPS algorithm.³¹ The molecular graphics software VMD³² was used to display the model.

Molecular dynamic (MD)

MD simulations were performed with GROMACS software (v4.5.5).³³ The model was inserted in a cubic box filled with SPC216 water molecules using a GROMOS43a1 all-atom force field. Simulations were carried out by adding 26 sodium ions for a value of zero for the system net electrostatic charge. The system was subjected to several cycles of energy minimizations and position restraints to equilibrate the protein and water molecules around it. The time step was 2 fs and the temperature was kept at 300 K. Simulation time was 20 ns. GROMACS routines were used to analyze trajectories for root-mean square deviation (RMSD), root-mean squared fluctuations (RMSF) and gyration radius.

Results

Sequence analysis of H9Est

A metagenomic library of 10,000 clones was constructed using DNA isolated from Karuola glacier soil. DNA insert sizes determined by *Bam* HI restriction were 35–45 kb with an average size of 38 kb. Approximately 380 Mb of cloned DNA was stored in the fosmid library. By functional screening, five esterase-positive clones were identified. However, only one positive recombinant, pUC118H9, was obtained after subcloning the positive fosmids. Sequence analysis of the insert revealed an ORF (H9Est) of 1071 bp, encoding a polypeptide of 357 amino acids with a deduced molecular mass of 39.9 kDa and pI 8.67.

A homology search revealed that H9Est was similar to several noncharacterized hypothetical esterases (67%–99% amino acid sequence identity) from the recently annotated whole-genome sequences of several *Acinetobacter* species. The closest match to characterized proteins was an esterase from *Acinetobacter lwoffii* (AAM34295, 66.9% identity). Phylogenetic analysis (Figure 1) revealed that H9Est clustered with family IV lipolytic proteins and was similar to family IV members of known structure: 30.8% identity to a carboxylesterase from *S. tokodaii* (BAB65028), 29.8% identity to a lipase from *Pseudomonas* sp. B11-1 (AAC38151), 29.4% identity to an alpha/beta hydrolase from *Alicyclobacillus acidocaldarius* (ACV59879) and 29.1% identity to a carboxylesterase from *A. fulgidus* (AAB89533). Multiple sequence alignments of H9Est with the closest structure-resolved lipolytic enzymes were performed (Figure 2). Alignments revealed that H9Est contained the three conserved sequence motifs of the family IV: the oxyanion hole-forming residues HGG, the pentapeptide GDSAG signature motif with a serine catalytic nucleophile, and a C-terminal conserved HGF motif. The putative catalytic triad residues D294, H324 and the catalytic nucleophile S200 were also

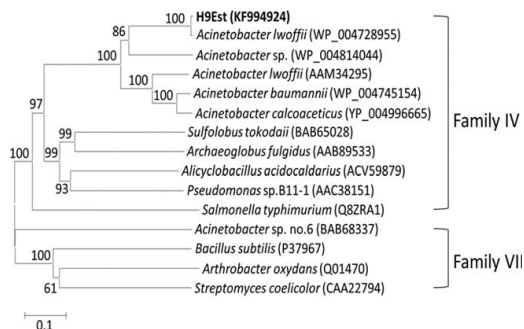


Figure 1. Phylogenetic analysis of H9Est with homologs based on conserved sequence motifs of bacterial lipolytic enzymes.

A phylogenetic tree was constructed using the neighbor-joining method in MEGA 5.0. Protein sequences were retrieved from GenBank (<http://www.ncbi.nlm.nih.gov/>). Scale bar, number of amino acid substitutions per site.

identified. Thus, H9Est from glacier soil was in family IV of bacterial lipolytic enzymes, a family with amino acid sequence similarity to the mammalian hormone-sensitive lipase.¹

Characterization of H9Est

The esterase H9Est gene was expressed in *E. coli* and purified. The molecular mass of H9Est by SDS-PAGE was approximately 40 kDa (Figure 3), the weight as calculated from the amino acid sequence.

H9Est displayed hydrolytic activity towards short chain *p*-nitrophenyl esters with maximal activity for *p*NP-C4 with a specific activity of 0.15 U mg⁻¹ under standard assay conditions. H9Est showed specific hydrolytic activities of 0.04 U mg⁻¹ against *p*NP-C2 and 0.08 U mg⁻¹ against *p*NP-C3 and *p*NP-C8, but no detectable activity towards *p*NP-C10 or *p*NP-C16, confirming that H9Est was an esterase rather than a lipase. The initial reaction velocities of H9Est obeyed Michaelis-Menten kinetics. K_M with *p*NP-C4 was 0.125 mM, k_{cat} was 4.237 s⁻¹, and k_{cat}/K_M was 33.799 s⁻¹ mM⁻¹.

H9Est activity was detected from pH 4.0 to 9.0 with maximum activity at pH 8.0 (Figure 4a). The enzyme retained about 80% of maximum activity at pH 9 with a marked decrease above pH 9. The temperature range of H9Est activity was 10°C to 70°C with an optimum at 40°C (Figure 4b). The enzyme retained at least 20% of maximum activity at 10°C and 10% of the maximum activity at 70°C. Thermal stability experiments revealed that H9Est was stable at temperatures lower than 30°C. H9Est had a 222 min half-life at 10°C and a 152 min half-life at 20°C. The half-life was 72 min at 30°C and 5 min at 40°C. As shown in Figure 4c, little decrease in activity was observed after 2 h of incubation at 10, 20, or 30°C. At 40°C, activity substantially decreased. After 2 h at 40°C, only 5% of enzymatic activity remained. H9Est did not catalyze reactions after 60 min at 50°C.

The effect of NaCl on H9Est activity was evaluated in standard conditions. We observed a substantial increase in the catalytic activity at 1 M NaCl. Higher concentrations of salt gradually decreased H9Est activity, but 60% relative activity remained at 2.5 M NaCl (Figure 4d) indicating good tolerance to high salinity.

The means and standard deviations of the effects of chemicals on enzyme activity are shown in Table 1. Ag⁺ severely inhibited H9Est activity while K⁺, Ca²⁺, Mg²⁺, Fe²⁺, and Fe³⁺ significantly enhanced activity. H9Est activity was inhibited by phenylmethanesulfonyl fluoride (PMSF), suggesting it was a serine esterase as predicted by the Ser catalytic residue. The addition of 1 mM dithiothreitol (DTT) did not influence the enzymatic activity, suggesting that the cysteine was not involved in the catalytic activity.

The effect of organic miscible solvents on H9Est enzymatic activity was evaluated at standard conditions. We observed a similar behavior in the presence of all tested solvents except for polyethylene glycol (Figure 5). Increasing the concentration of organic solvents in the assays led to gradual H9Est inactivation, while the enzyme shown high stability in the presence of polyethylene glycol. In fact 20% polyethylene glycol, the relative retained activity was still 90%.

H9Est model

H9Est three-dimensional homology modeling used the structures of an *S. Typhimurium* acetyl esterase (PDB ID: 3GA 7), an *S. tokodaii* carboxylesterase (3AIN), an esterase in the subfamily of hormone-sensitive lipases (3FAK) and an *A. fulgidus* hyperthermophilic carboxylesterase (1JJJ) as templates. These structures were chosen because they showed substantial structural homology to H9Est as calculated by the HHpred server, despite a low sequence identity of about 30%. The best model (Figure 6a) was selected for energetic and stereochemical quality. In the model, 91.9% of the residues were in the most favored regions of the Ramachandran plot according to the PROCHECK program provided with PDBSum and the model had a WhatIf Z-score of 0.634. These values, when compared with values for the template structures, indicated a good quality model. The H9Est model displayed an alpha-beta structure with ten alpha helices covering 41.5% of the sequence, three 3₁₀ helices (3.1%) and ten beta strands forming two sheets (17%).

As shown in Figure 6b, the catalytic triad of H9Est was formed by S200, D294 and H324; the substrate-binding pocket were formed by G127, G128, A129, D199, S200, A201, N204. The three amino acids forming the catalytic triad were located in three different loops connecting three strands to three helices. S200 was within a conserved motif that included substrate-binding residues; the presence of glycine gave flexibility to this area.

SASA analysis of H9Est model by the POPS algorithm revealed an exposed surface that was more hydrophobic than hydrophilic (59 vs. 41%). This result suggested that the enzyme could adapt to hydrophobic environments such as organic solvents.

Molecular dynamics

To evaluate the stability of the modeled structure, we subjected the best H9Est model to MD simulations. The model reached a stable equilibrated state after 7 ns of simulation; the related RMSD values that measure changes in the three-dimensional structure over time (Figure 7a) were constant in the remaining simulation time. To study variations in the overall size of the system, we computed the gyration radius for all atoms of 346 residues (Figure 7b). The gyration radius trend was similar to the evolution observed in the

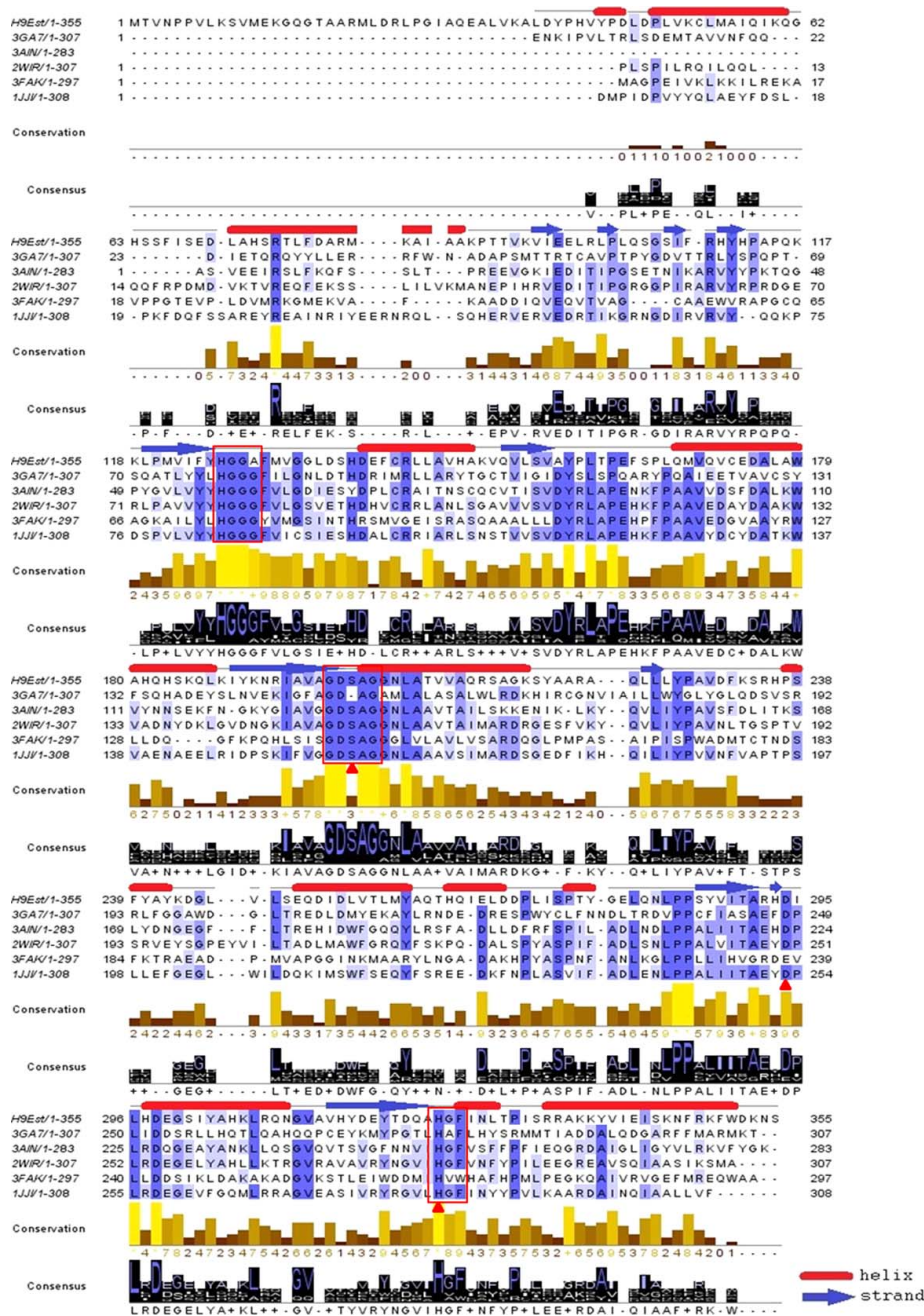


Figure 2. Multiple alignments performed by ClustalW, of H9Est and the five best-scoring templates of known three-dimensional structure.

Blue color scale indicates the conservation level of aminoacids; the most conserved residues are shown in dark blue. Red triangles and red boxes highlight catalytic triad aminoacids within conserved motifs.

RMSD graph with no relevant variation in molecule compactness after 7 ns of simulation. Superposition of RMS fluctuations (Figure 7c) revealed that the residues with a high degree of flexibility were in the loop region. This was

expected for the three residues of the catalytic triad located in loops. Thus, after initial adaption in the first 7 ns, the H9Est structure was unaltered during the MD simulation and the overall stability of H9Est was maintained.

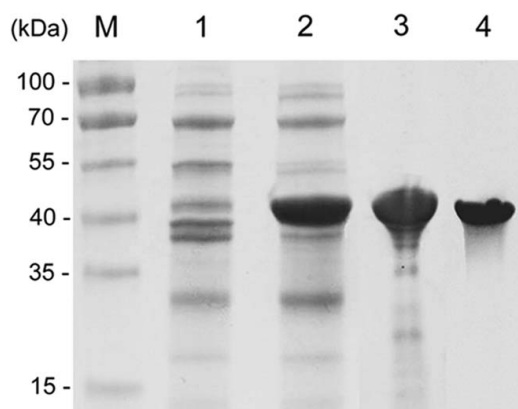


Figure 3. The expression and purification of H9 esterase. (lane M: Marker, Fermentas SM0671; lane 1: negative control: not induced *E. coli* BL21DE3 cells, lane 2: crude enzyme, lane 3: Ni-NTA column purification for the first time, lane 4: Ni-NTA column purification for the second time).

CD of H9Est

The dominant species of H9Est protein was analyzed by CD. In the spectra (Figure 8a), the maximum between 198 and 195 nm and the two minima centered at 208 and 222 nm indicated both α and β secondary structure elements, in line with the predicted structure. Molar ellipticity decreased as tempera-

Table 1. Effects of Chemicals on Enzyme Activity

Inhibitor	Residual activity (%)
None	100.0
Ag ⁺	6.5 ± 0.5
Ca ²⁺	114.5 ± 5.8
Mg ²⁺	137.9 ± 5.1
Fe ²⁺	137.8 ± 10.9
Fe ³⁺	140.5 ± 9.3
K ⁺	137.0 ± 4.4
Li ⁺	83.9 ± 5.3
Cu ²⁺	67.4 ± 6.6
Zn ²⁺	32.3 ± 4
SDS	2.9 ± 0.9
EDTA	88.4 ± 6.3
DTT	86.4 ± 4.4
PMSF	10.2 ± 1.5

All data resulted to be statically significant (*P* value < 0.05).

ture increased, providing evidence for local unfolding of the protein. Thermal denaturation curves at 20–90°C recorded the molar ellipticity at 222 nm (Figure 8b). Far-UV CD spectra at 90°C were typical of random coil. As shown in Figure 8b, thermal denaturation occurred from 35 to 80°C, with a denaturation temperature around 60°C.

Discussion

Using a metagenomic library, we identified a family IV esterase, H9Est, from a Tibetan glacier soil sample. Family IV lipolytic enzymes have been identified from other metagenome libraries and exhibit diverse biochemical

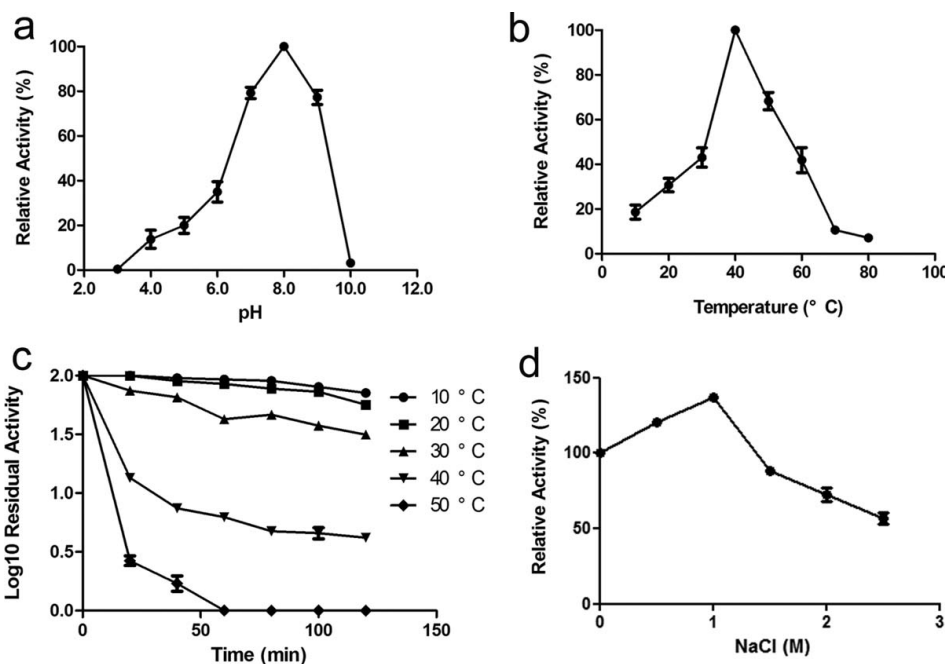


Figure 4. Biochemical features of purified esterase H9Est.

(a) Effect of pH on H9Est activity. Enzyme activity was measured at different pH values at 40°C using *p*NP-C4 as substrate. (b) Effect of temperature. Enzyme activity was determined with *p*-nitrophenyl butyrate as a substrate after 2 min at indicated temperatures and pH 8.0. (c) Thermostability of H9Est at: 10°C (●), 20°C (■), 30°C (▲), 40°C (▼), 50°C (◆). The enzyme was incubated in 50 mM Tris-HCl (pH 8.0) at the indicated temperatures and times. Residual activity was measured at 40°C using *p*NP-C4 as substrate. (d) Effect of NaCl on H9Est activity. Enzyme activity was evaluated in NaCl up to 2.5 M. Residual activity was measured at 40°C using *p*NP-C4 as substrate. 100% relative activity corresponds to 0.15 U mg⁻¹.

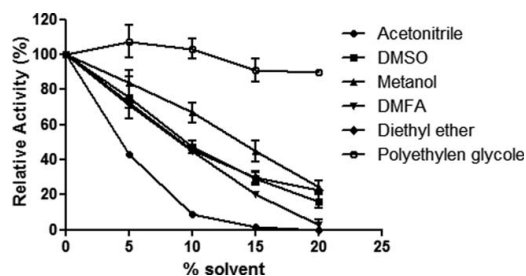


Figure 5. Effect of organic solvents on esterase activity.

Enzyme activity was evaluated in presence of increasing concentrations of acetonitrile (●), DMSO (■), methanol (▲), dimethylformamide (DMFA; ▼), diethyl ether (◆), and polyethylene glycol (○). Residual activity was measured at 40°C using *p*NP-C4 as substrate; 100% relative activity corresponds to 0.35 U mg⁻¹.

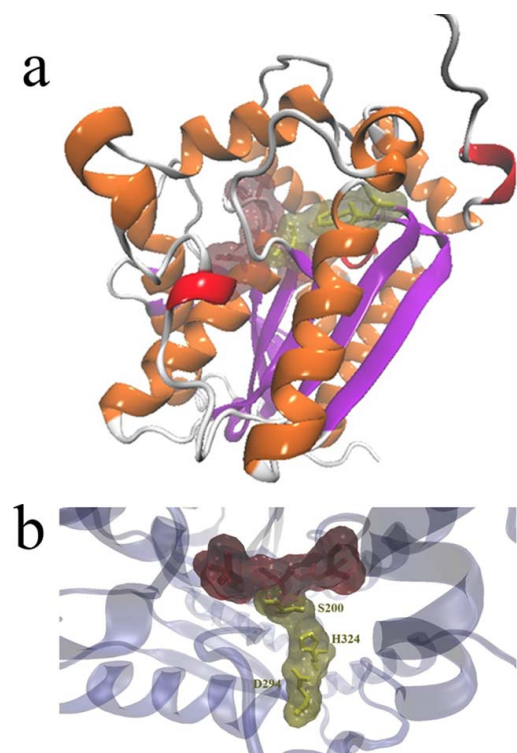


Figure 6. H9Est 3D-model representation.

(a) Orange, α helices; violet, β -strands; red, 3_{10} helices. (b) Yellow, H9Est catalytic triad (S200, D294, and H324); red, substrate binding pocket. The image was obtained with VMD software.

characteristics. Examples include cold-adapted esterases from mountain soil, Arctic sediments and marine sediment,^{34–36} thermophilic esterases from hot springs,³⁷ and alkaliphilic esterase from soil metagenomic libraries.³⁸

Tibetan glaciers areas are constantly cold and could be a good reservoir of novel enzymes active at low temperatures. H9Est is the first characterized esterase from a Tibetan gla-

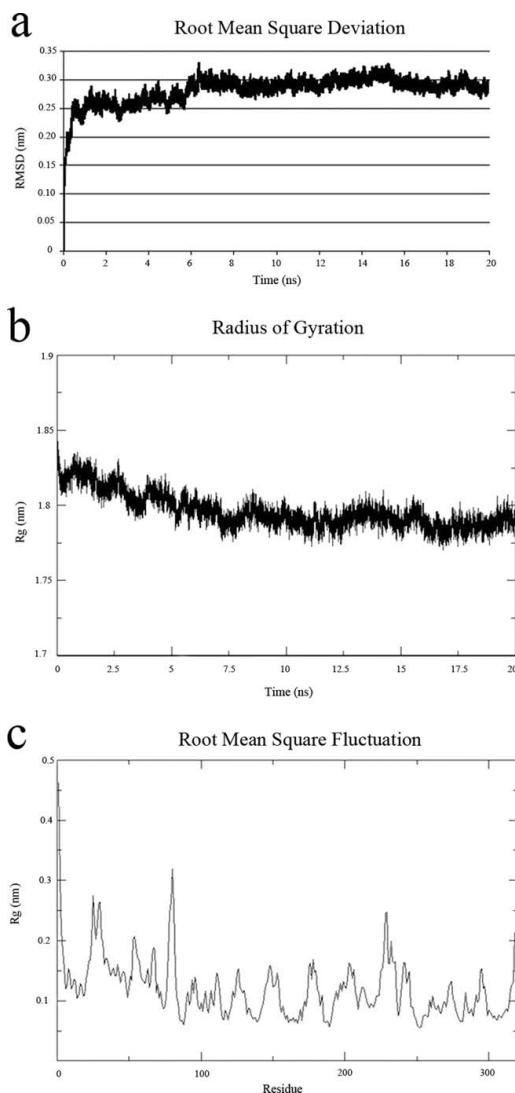


Figure 7. H9Est MD simulation.

(a) Root mean square deviation trend during MD simulation. X-axis, time in ns; y-axis, root mean square deviation in nm. H9Est reached an equilibrated state after 7 ns of MD simulation. (b) Gyration radius trend during MD simulation. X-axis, time in ns; y-axis, radius of gyration in nm. H9Est reached an equilibrated compactness after 7 ns of MD simulation. (c) Root mean square fluctuations at end of MD simulation. X-axis, number of amino acid residues; y-axis, root mean square fluctuation in nm. Peaks, amino acid chain zones with higher fluctuation during the MD simulation.

cier and it catalyzed hydrolysis of substrates with short-chain esters at 10–70°C with maximum at 40°C, retaining 20% of activity at 10°C and 10% of activity at 70°C. Thermal stability analysis further indicated that this esterase had behaviors of a cold-adapted enzyme when compared to previous research articles.^{39–41}

These features of cold adaptation could be related to the structural flexibility of H9Est. Our three-dimensional model

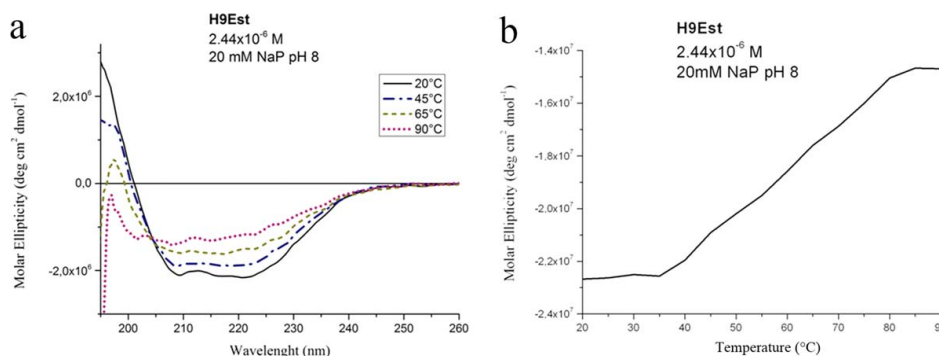


Figure 8. CD spectra of H9Est.

(a) CD spectra in Na-phosphate buffer at different temperatures. X-axis, wavelength in nm; y-axis, molar ellipticity. Spectra became flatter as temperature increased, indicating progressive unfolding of H9Est secondary structures. (b) Thermal denaturation of H9Est. X-axis, temperature in Celsius; y-axis, molar ellipticity at 222 nm. Increase in molar ellipticity indicated progressive protein denaturation.

and MD simulations revealed that the residues with greater fluctuations fell in a loop region, giving H9Est an increased flexibility. This structural feature was probably the reason for the activity H9Est at low temperatures⁴² and suggested an important function for the flexible loops. CD analysis showed that molar ellipticity gradually decreased with increasing temperature as reported for other psychrophilic enzymes.⁴³ Local folding of the protein structure was retained at 35°C to 80°C. This wide denaturation temperature range could indicate different denaturation states that occurred during denaturation, as proposed by D'Amico et al.⁴⁴ In addition to its temperature-related properties, H9Est was active and stable over broad range of NaCl concentrations, despite originating from a non-saline environment. H9Est esterase activity increased with increasing NaCl concentration from 0 to 1.0 M NaCl and retained over 60% residual activity in the presence of 2.5 M NaCl. This result could be explained as salt enhancement of the hydrophobic interactions between enzyme and substrate until the ions in solution bound the charged residue in the active site, leading to decreased activity.

The high tolerance of salinity might classify H9Est as a halotolerant enzyme. So far, only a small number of esterases have been found to be halophilic. Metagenome-derived halotolerant enzymes include EstK7 from tidal flat sediments,⁴⁵ DHAB from a deep sea hypersaline anoxic basin,⁴⁶ Lpc53E1 and EstHE1 from marine sponges¹⁷ and EstA from South China Sea surface water.⁴⁷

The amino acid sequence of H9Est showed 67%–99% identity to hypothetical proteins from several cultured *Acinetobacter* spp., but relatively low similarity to the known proteins (less than 67% identity). *Acinetobacter* spp. has been isolated from clinical specimens and environmental sources such as soil, cotton, activated sludge and wetlands.⁴⁸ High H9Est identity to all lipolytic enzymes from *Acinetobacter* spp. suggested that H9Est originated from an *Acinetobacter* species in Tibetan glacier soil.

The closest characterized protein to H9Est was an esterase (EstA) from *A. lwoffii* (66.9% identity).⁴⁹ EstA exhibited optimal activity at pH 8.0 and 37°C, similar to the activities detected for H9Est. But, H9Est showed different behavior from EstA in the presence of metal ions. Ca²⁺, Mg²⁺ and Fe²⁺ enhanced H9Est activity. Conversely, EstA was strongly inhibited by Ca²⁺, Mg²⁺, Fe²⁺, Cu²⁺, Zn²⁺, Mn²⁺, and Co²⁺.⁵⁰

Esterases are often used in biotransformation of water-insoluble substrates carried out in the presence of organic solvents.^{51–53} H9Est was not sensitive to some miscible organic solvents, retaining more than 60% activity in the presence of methanol or polyethylene glycol. H9Est typically displayed preference or tolerance towards high salinity buffers and was stable in the presence of Ca²⁺, Mg²⁺, Fe²⁺ and Fe³⁺. With these features, H9Est could be a candidate for industrial applications in organic synthesis reactions. Directed evolution studies to improve the catalytic activity are in progress and might help elucidate the relationship between the protein structure and its function.

Conclusions

In the present work, a halotolerant esterolytic enzyme was isolated and identified by functional screening from a glacial soil metagenome. The enzymatic activity profile over a wide range pH, temperature, salt and, nevertheless in the presence of organic solvent and metal ions, make this biocatalyst useful for future applications in basic research and biotechnological processes.

Acknowledgments

This article was supported by the CNR-CAS Cooperation Agreement 2011–2013 entitled: Discovery of new extremozymes and their potential use in biotechnology. This work was also supported by Ministry of Sciences and Technology (MOST) of China Grants (973 Programs: 2011CBA00800 and 2013CBA733900), Chinese Academy of Sciences (Knowledge Innovation Program, KSCX2-EW-G-3).

Literature Cited

1. Arpigny J, Jaeger K. Bacterial lipolytic enzymes: Classification and properties. *Biochem J.* 1999;343:177–183.
2. Wei Y, Schottel JL, Derewenda U, Swenson L, Patkar S, Derewenda ZS. A novel variant of the catalytic triad in the streptomyces scabies esterase. *Nat Struct Biol.* 1995;2:218–223.
3. Charbonneau DM, Beauregard M. Role of key salt bridges in thermostability of *G. Thermodenitrificans* EstGtA2: Distinctive patterns within the new bacterial lipolytic enzyme family XV. *PLoS One.* 2013;8:e76675

4. Bornscheuer UT. Microbial carboxyl esterases: classification, properties and application in biocatalysis. *FEMS Microbiol Rev.* 2002;26:73–81.
5. Akoh CC, Lee GC, Liaw YC, Huang TH, Shaw JF. GDSL family of serine esterases/lipases. *Prog Lipid Res.* 2004;43:534–552.
6. Panda T, Gowrishankar BS. Production and applications of esterases. *Appl Microbiol Biotechnol.* 2005;67:160–169.
7. Manco G, Nucci R, Febbraio F. Use of esterase activities for the detection of chemical neurotoxic agents. *Protein Pept Lett.* 2009;16:1225–1234.
8. Steele HL, Jaeger KE, Daniel R, Streit WR. Advances in recovery of novel biocatalysts from metagenomes. *J Mol Microbiol Biotechnol.* 2009;16:25–37.
9. López-López O, Cerdán ME, González Siso MI. New extremophilic lipases and esterases from metagenomics. *Curr Protein Pept Sci.* 2014;15:445–455.
10. Sang SL, Li G, Hu XP, Liu YH. Molecular cloning, overexpression and characterization of a novel feruloyl esterase from a soil metagenomic library. *J Mol Microbiol Biotechnol.* 2011;20:196–203.
11. Berlemont R, Spee O, Delsaute M, Lara Y, Schuldes J, Schuldes J, Simon C, Power P, Daniel R, Galleni M. Novel organic solvent-tolerant esterase isolated by metagenomics: Insights into the lipase/esterase classification. *Rev Argent Microbiol.* 2012;45:3–12.
12. Khan M, Jithesh K, Mookambikay R. Cloning and characterization of two functionally diverse lipases from soil metagenome. *J Gen Appl Microbiol.* 2013;59:21–31.
13. Liaw RB, Cheng MP, Wu MC, Lee CY. Use of metagenomic approaches to isolate lipolytic genes from activated sludge. *Bioresour Technol.* 2010;101:8323–8329.
14. Hu Y, Fu C, Huang Y, Yin Y, Cheng G, Lei F, Lu N, Li J, Ashforth EJ, Zhang L, Zhu B. Novel lipolytic genes from the microbial metagenomic library of the south china sea marine sediment. *FEMS Microbiol Ecol.* 2010;72:228–237.
15. Jiang X, Xu X, Huo Y, Wu Y, Zhu X, Zhang X, Wu M. Identification and characterization of novel esterases from a deep-sea sediment metagenome. *Arch Microbiol.* 2012;194:207–214.
16. Okamura Y, Kimura T, Yokouchi H, Meneses-Osorio M, Katoh M, Matsunaga T, Takeyama H. Isolation and characterization of a GDSL esterase from the metagenome of a marine sponge-associated bacteria. *Mar Biotechnol (NY).* 2010;12:395–402.
17. Selvin J, Kennedy J, Lejon DP, Kiran GS, Dobson AD. Isolation, identification and biochemical characterization of a novel halo-tolerant lipase from the metagenome of the marine sponge *haliclona simulans*. *Microb Cell Fact.* 2012;11:72.
18. Ranjan R, Grover A, Kapardar RK, Sharma R. Isolation of novel lipolytic genes from uncultured bacteria of pond water. *Biochem Biophys Res Commun.* 2005;335:57–65.
19. Rees HC, Grant S, Jones B, Grant WD, Heaphy S. Detecting cellulase and esterase enzyme activities encoded by novel genes present in environmental DNA libraries. *Extremophiles.* 2003;7:415–421.
20. Martínez-Martínez M, Alcaide M, Tchigvintsev A, Reva O, Polaina J, Bargiela R, Guazzaroni ME, Chicote A, Canet A, Valero F, Rico Eguizabal E, Guerrero Mdel C, Yakunin AF, Ferrer M. Biochemical diversity of carboxyl esterases and lipases from lake arreo (spain): A metagenomic approach. *Appl Environ Microbiol.* 2013;79:3553–3562.
21. Tirawongsaraj P, Sriprang R, Harmpicharnchai P, Thongaram T, Champreda V, Tanapongpipat S, Pootanakit K, Eurwilaichitr L. Novel thermophilic and thermostable lipolytic enzymes from a thailand hot spring metagenomic library. *J Biotechnol.* 2008;133:42–49.
22. Suresh Kumar P, Mrinmoy G, Pulicherla KK, Sambasiva Rao KRS. Cold Active enzymes from the marine psychrophiles: Biotechnological perspective. *Adv Biotech.* 2011;10:43–45.
23. Zhou J, Bruns MA, Tiedje JM. DNA recovery from soils of diverse composition. *Appl Environ Microbiol.* 1996;62:316–322.
24. Sambrook J, Russell D. Molecular cloning: A laboratory manual. Cold Spring Harbor, NY: Cold Spring Harbor Laboratory Press; 2001.
25. Altschul SF, Gish W, Miller W, Myers EW, Lipman DJ. Basic local alignment search tool. *J Mol Biol.* 1990;215:403–410.
26. Tamura K, Peterson D, Peterson N, Stecher G, Nei M, Kumar S. Mega5: Molecular evolutionary genetics analysis using maximum likelihood, evolutionary distance, and maximum parsimony methods. *Mol Biol Evol.* 2011;28:2731–2739.
27. Soding J, Biegert A, Lupas AN. The HHpred interactive server for protein homology detection and structure prediction. *Nucleic Acids Res.* 2005;33:W244–248. 24
28. Sali A, Blundell TL. Comparative protein modelling by satisfaction of spatial restraints. *J Mol Biol.* 1993;234:779–815.
29. Laskowski RA, MacArthur MW, Moss DS, Thornton JM. PROCHECK: A program to check the stereochemical quality of protein structures. *J Appl Crystal.* 1993;26:283–291.
30. Vriend G. WHAT IF: A molecular modeling and drug design program. *J Mol Graphics.* 1990;8:52–56.
31. Cavallo L, Kleijnung J, Fraternali F. POPS: a fast algorithm for solvent accessible surface areas at atomic and residue level. *Nucleic Acids Res.* 2003;31:3364–3366.
32. Humphrey W, Dalke A, Schulten K. VMD: visual molecular dynamics. *J Mol Graphics.* 1996;14:33–38.
33. Hess B, Kutzner C, van der Spoel D, Lindahl E. GROMACS 4: algorithms for highly efficient, Load-balanced, and scalable molecular simulation. *J Chem Theory Comput.* 2008;4:435–447.
34. Ko KC, Rim SO, Han Y, Shin BS, Kim GJ, Choi JH, Song JJ. Identification and characterization of a novel cold-adapted esterase from a metagenomic library of mountain soil. *J Ind Microbiol Biotechnol.* 2012;39:681–689.
35. Jeon JH, Kim JT, Kang SG, Lee JH, Kim SJ. Characterization and its potential application of two esterases derived from the arctic sediment metagenome. *Mar Biotechnol (NY).* 2009;11:307–316.
36. Härdeman F, Sjöling S. Metagenomic approach for the isolation of a novel low-temperature-active lipase from uncultured bacteria of marine sediment. *FEMS Microbiol Ecol.* 2007;59:524–534.
37. Rhee JK, Ahn DG, Kim YG, Oh JW. New thermophilic and thermostable esterase with sequence similarity to the hormone-sensitive lipase family, cloned from a metagenomic library. *Appl Environ Microbiol.* 2005;71:817–825.
38. Choi JE, Kwon MA, Na HY, Hahn DH, Song JK. Isolation and characterization of a metagenome-derived thermoalkaliphilic esterase with high stability over a broad pH range. *Extremophiles.* 2013;17:1013–1021.
39. De Santi C, Tutino ML, Mandrich L, Giuliani M, Parrilli E, Del Vecchio P, de Pascale D. The hormone-sensitive lipase from psychrobacter sp. Ta144: new insight in the structural/functional characterization. *Biochimie.* 2010;92:949–957.
40. Gerday C, Aittaleb M, Bentahir M, Chessa JP, Claverie P, Collins T, D'Amico S, Dumont J, Garsoux G, Georgette D, Hoyoux A, Lonhienne T, Meuwis MA, Feller G. Cold-adapted enzymes: from fundamentals to biotechnology. *Trends Biotechnol.* 2000;18:103–107.
41. Seo S, Lee YS, Yoon SH, Kim SJ, Cho JY, Hahn BS, Koo BS, Lee CM. Characterization of a novel cold-active esterase isolated from swamp sediment metagenome. *World J Microbiol Biotechnol.* 2014;30:879–886.
42. Feller G, Gerday C. Psychrophilic enzymes: molecular basis of cold adaptation. *Cell Mol Life Sci.* 1997;53:830–884.
43. Fu J, Leiros HK, de Pascale D, Johnson KA, Blencke HM, Landfald B. Functional and structural studies of a novel cold-adapted esterase from an arctic intertidal metagenomic library. *Appl Microbiol Biotechnol.* 2013;97:3965–3978.
44. D'Amico S, Marx JC, Gerday C, Feller G. Activity-stability relationships in extremophilic enzymes. *J Biol Chem.* 2003;278:7891–7896.
45. Jeon JH, Lee HS, Kim JT, Kim SJ, Choi SH, Kang SG, Lee JH. Identification of a new subfamily of salt-tolerant esterases from a metagenomic library of tidal flat sediment. *Appl Microbiol Biotechnol.* 2012;93:623–631.
46. Ferrer M, Golyshina OV, Chernikova TN, Khachane AN, Martins Dos Santos VA, Yakimov MM, Timmis KN, Golyshin PN. Microbial enzymes mined from the urania deep-sea hypersaline anoxic basin. *Chem Biol.* 2005;12:895–904.

47. Chu X, He H, Guo C, Sun B. Identification of two novel esterases from a marine metagenomic library derived from South China sea. *Appl Microbiol Biot.* 2008;80:615–625.
48. Anandham R, Weon HY, Kim SJ, Kim YS, Kim BY, Kwon SW. *Acinetobacter brisouii* sp. Nov., isolated from a wetland in Korea. *J Microbiol.* 2010;48:36–39.
49. Kim HE, Lee IS, Kim JH, Hahn KW, Park UJ, Han HS, Park KR. Gene cloning, sequencing, and expression of an esterase from *acinetobacter lwoffii* I6C-1. *Curr Microbiol.* 2003;46:291–295.
50. Kim HE, Park KR. Purification and characterization of an esterase from *acinetobacter lwoffii* I6C-1. *Curr Microbiol.* 2002;44:401–405.
51. Hernández-Rodríguez B, Córdova J, Bárzana E, Favela-Torres E. Effects of organic solvents on activity and stability of lipases produced by thermo tolerant fungi in solid-state fermentation. *J Mol Catal B: Enzym.* 2009;61:136–142.
52. Zaks A, Klivanov AM. Enzymatic catalysis in non-aqueous solvents. *J Biol Chem.* 1988; 263:3194–3201.
53. Rocha JMS, Gil MH, Garcia FAP. Effects of additives on the activity of a covalently immobilised lipase in organic media. *J Biotech.* 1998;66:61–67.

Manuscript received Jan. 23, 2015, and revision received Mar. 23, 2015.

RESEARCH ARTICLE

Investigating the Role of the Host Multidrug Resistance Associated Protein Transporter Family in *Burkholderia cepacia* Complex Pathogenicity Using a *Caenorhabditis elegans* Infection Model

Pietro Tedesco^{1,2}, Marco Visone¹, Ermenegilda Parrilli², Maria Luisa Tutino², Elena Perrin³, Isabel Maida³, Renato Fani³, Francesco Ballestrero⁴, Radleigh Santos⁵, Clemencia Pinilla⁵, Elia Di Schiavi^{6,7}, George Tegos^{5,8,9*}, Donatella de Pascale^{1*}



click for updates

1 Institute of Protein Biochemistry, National Research Council, Via P. Castellino 111, I-80131, Naples, Italy, **2** Department of Chemical Sciences and School of Biotechnological Sciences, University of Naples Federico II, Via Cintia, I-80126, Naples, Italy, **3** Laboratory of Microbial and Molecular Evolution, Department of Biology, University of Florence, Via Madonna del Piano, I-50019, Sesto Fiorentino, Florence, Italy, **4** School of Biotechnology and Biomolecular Sciences and Centre for Marine Bio-Innovation, University of New South Wales, Sydney, 2052, New South Wales, Australia, **5** Torrey Pines Institute of Molecular Studies, Port St. Lucie, FL, United States of America, and San Diego, CA, United States of America, **6** Institute of Bioscience and BioResources, National Research Council, via P. Castellino 111, I-80131, Naples, Italy, **7** Institute of Genetics and Biophysics, National Research Council, via P. Castellino 111, I-80131, Naples, Italy, **8** Wellman Centre for Photomedicine, Massachusetts General Hospital, Boston, MA, United States of America, **9** Department of Dermatology, Harvard Medical School, Boston, MA, United States of America

* d.depascale@ibp.cnr.it (DdP); gtegos@tpims.org (GT)

OPEN ACCESS

Citation: Tedesco P, Visone M, Parrilli E, Tutino ML, Perrin E, Maida I, et al. (2015) Investigating the Role of the Host Multidrug Resistance Associated Protein Transporter Family in *Burkholderia cepacia* Complex Pathogenicity Using a *Caenorhabditis elegans* Infection Model. PLoS ONE 10(11): e0142883. doi:10.1371/journal.pone.0142883

Editor: Denis Dupuy, Inserm U869, FRANCE

Received: July 15, 2015

Accepted: October 28, 2015

Published: November 20, 2015

Copyright: © 2015 Tedesco et al. This is an open access article distributed under the terms of the [Creative Commons Attribution License](https://creativecommons.org/licenses/by/4.0/), which permits unrestricted use, distribution, and reproduction in any medium, provided the original author and source are credited.

Data Availability Statement: Data underlying the findings described in the manuscript are freely available to other researchers and they are in the body of the manuscript.

Funding: This work was supported by the EU-KBBE 2012-2016 project PharmaSea, grant N° 312184. Elena Perrin is financially supported by a "Fondazione Adriano Buzzati-Traverso" fellowship. The funders had no role in study design, data collection and analysis, decision to publish, or preparation of the manuscript.

Abstract

This study investigated the relationship between host efflux system of the non-vertebrate nematode *Caenorhabditis elegans* and *Burkholderia cepacia* complex (Bcc) strain virulence. This is the first comprehensive effort to profile host-transporters within the context of Bcc infection. With this aim, two different toxicity tests were performed: a slow killing assay that monitors mortality of the host by intestinal colonization and a fast killing assay that assesses production of toxins. A Virulence Ranking scheme was defined, that expressed the toxicity of the Bcc panel members, based on the percentage of surviving worms. According to this ranking the 18 Bcc strains were divided in 4 distinct groups. Only the Cystic Fibrosis isolated strains possessed profound nematode killing ability to accumulate in worms' intestines. For the transporter analysis a complete set of isogenic nematode single Multidrug Resistance associated Protein (MRP) efflux mutants and a number of efflux inhibitors were interrogated in the host toxicity assays. The Bcc pathogenicity profile of the 7 isogenic *C. elegans* MRP knock-out strains functionality was classified in two distinct groups. Disabling host transporters enhanced nematode mortality more than 50% in 5 out of 7 mutants when compared to wild type. In particular *mrp-2* was the most susceptible phenotype with increased mortality for 13 out 18 Bcc strains, whereas *mrp-3* and *mrp-4* knock-outs had lower mortality rates, suggesting a different role in toxin-substrate recognition. The

Competing Interests: The authors have declared that no competing interests exist.

use of MRP efflux inhibitors in the assays resulted in substantially increased (>40% on average) mortality of wild-type worms.

Introduction

The *Burkholderia cepacia* complex (Bcc) occupies a critical position among Gram-negative multi-drug resistant bacteria. It consists of at least 20 closely related species inhabiting different ecological niches, including plants and animals [1–5]. Bcc multi drug and pandrug-resistant opportunistic human pathogens cause problematic lung infections in immune-compromised individuals, including cystic fibrosis (CF) patients [6–8]. Bcc members are naturally resistant to antibiotics including cephalosporins, β -lactams, polymyxins and aminoglycosides, rendering Bcc infections challenging to eradicate [9,10]. There is an imminent need to develop new Bcc antimicrobial therapeutic strategies. Dissecting virulence and pathogenicity determinants as well as identifying novel therapeutic targets may be promising approaches. These tasks may be advanced by the exploitation of the non-vertebrate host models *Drosophila melanogaster*, *Galleria mellonella*, and *Caenorhabditis elegans*. Model hosts have been used to evaluate microbial virulence traits involved in mammalian infections and the efficacy of antimicrobial compounds [11–16]. The free-living nematode *C. elegans* is a widespread multicellular organism that is a self-fertilizing hermaphrodite with a rapid generation time. *C. elegans* has been proven cost-effective, ethical, reproducible and genetically powerful infection model despite the obvious reported technical limitations (nematodes have lower optimal growth temperatures when compared with human pathogens; occurrence of host specific virulence factors) [15,17–19]. In fact, there is an extensive body of literature for the utility of the nematode to model infection with a variety of Gram-negative bacteria including *Escherichia coli*, *Burkholderia pseudomallei*, *B. cepacia* complex and *Pseudomonas aeruginosa* [20–23]. The *C. elegans*-Bcc studies in the last decade have shed some light on the complex-nematode interaction, correlating genotypic characteristics of the pathogen with phenotypic changes in the host. These efforts have identified specific virulence factors: the auto inducer dependent Acyl-Homoserine Lactone (*aidA*), the phenazine biosynthesis regulator (*Pbr*), and the host factor phage Q, (*hfq*) [16,24–33].

Recent studies have underlined the importance of efflux systems in infection within the content of host-pathogen interaction [34–36]. The host efflux capability is considered part of a basic defence mechanism. For example the *B. pseudomallei* infection stimulates the overproduction of the ATP Binding Cassette (ABC) transporter *pgp-5* in *C. elegans* [37]. However, the partition of host transporters in the infection process has never been studied in depth. Bcc members produce a variety of metabolites and toxins, potential host efflux substrates. Furthermore, exploring the role of host transporters in pathogenicity may facilitate the design of appropriate tools for toxin identification. Multidrug Resistance associated Proteins (MRPs) are members of the ABC efflux transporter family with broad substrate specificity for the transport of endogenous and xenobiotic anionic substances found in Bacteria, Archaea and Eukarya [38–41]. MRPs play important roles in nematode physiology such as control resistance to anthelmintic (ivermectine) and heavy metals (arsenic) [42–44]. This study emphasizes the contribution of the host MRP efflux subfamily to Bcc virulence, employing a panel of 18 strains representing the up-to-date different acknowledged species and a fully functional seven single *C. elegans* mutant set impaired in MRPs. A Virulence-Ranking (VR) scheme based on comparing host survival rates in two different assays was developed. This scheme provides the tool for a detailed study on the effect of the MRP transporter family on Bcc virulence using as well as selected efflux inhibitors.

Materials and Methods

Bacterial strains, nematode strains and growth conditions

C. elegans Wild-type (WT) Bristol N2, NL147 (*mrp-1(pk89)* X), RB1713 (*mrp-2(ok2157)* X), RB1028 (*mrp-3(ok955)* X), VC712 (*mrp-4(ok1095)* X), VC1599 (*mrp-5(ok2067)/szT1* X), RB1070 (*mrp-6(ok1027)* X) and RB1269 (*mrp-8(ok1360)* III) strains were obtained from the *Caenorhabditis* Genetic Centre (CGC). For strain VC1599, due to *ok2067* mutation lethality in homozygosis, all the experiments were performed assaying heterozygotes worms. All mutants presented identical phenotypic traits in respect to WT: normal larval development (eggs reaching adults state in 72 h as indicated on standard table (www.wormbook.org)), non-impaired reproduction, and survival rate at 100% when fed with *E. coli*. Mutant *mrp-5* in heterozygosis also aligned to those parameters. All strains were recovered from frozen stocks, and routinely kept on NGM (Nematode Growth Medium) plates seeded with *E. coli* OP50 as a food source [45]. The panel of Bcc strains used in this work belongs to the Bcc collection at the University of Gent, Belgium, and is listed in Table 1. Bcc and *E. coli* OP50 cells were routinely grown in Luria-Bertani broth (LB) (10 g/L Bacto-tryptone, 5 g/L Yeast extract, 10 g/L NaCl) at 37°C.

Nematode Toxicity Assays

Slow Killing Assay (SKA) was performed against the *C. elegans* WT strain N and MRP-mutants. 2.5-cm-diameter plates containing 3 ml of NGM agar (Peptone 2.5 g/L, NaCl 2.9 g/L, Bacto-Agar 17 g/L, CaCl₂ 1 mM, Cholesterol 5 µg/mL, KH₂PO₄ 25 mM, MgSO₄ 1 mM) were seeded with 50 µl of the overnight Bcc cultures, normalized to an OD₆₀₀ of 1.7 and incubated for 24 h at 37°C to allow the formation of a bacterial lawn. This was the standard bacterial growth condition unless otherwise stated. *C. elegans* WT strain and MRP-mutants were synchronized by bleaching treatment [46], and 30–40 worms at larval stage 4 (L4), were transferred to each plate and incubated at 20°C for three days. The plates were scored for living worms every 24 h.

Fast Killing assay (FKA) was carried out in 2.5-cm-diameter plates containing 3 ml of Peptone Glucose Sorbitol (PGS) agar medium [25] (Peptone 12 g/L, Glucose 12 g/L, Sorbitol 27.25 g/L, NaCl 12 g/L, Bacto-Agar 17 g/L, CaCl₂ 1 mM, Cholesterol 5 µg/mL, KH₂PO₄ 25 mM, MgSO₄ 1 mM). Plates were prepared as described above for the SKA. Then, L4 worms from WT strain and MRP-mutants were collected from NGM plates, washed with M9 medium (Na₂HPO₄·7H₂O 12.8 g/L, Na₂HPO₄ (anhydrous) 6 g/L, KH₂PO₄ 3 g/L, NaCl 0.5 g/L, NH₄Cl 1 g/L) and 30–40 L4 worms were spotted onto the bacterial lawn. The plates were then incubated at 20°C and scored for living worms every 24 h. In both assays, *E. coli* OP50 was used as a negative control. A worm was considered dead when it no longer responded to touch. For statistical purposes, 5 replicates per trial were carried out with a unique egg preparation. The incubation time was set at 2 days. A pathogenicity scheme (VR) was established by comparing the "infectivity" towards nematodes between *E. coli* OP50 and Bcc isolates.

Microscopy analysis

40–60 WT L4 worms were grown on NGM plates seeded with Bcc or *E. coli* OP50 propagated in standard growth conditions. Plates were incubated at 20°C, and after 4 and 24 h, the nematodes were inspected using a Zeiss Axioskop microscope equipped with Differential Interference Contrast (DIC) employing 10x, 20x, 40x, 63x and 100x objectives and 10X eyepiece. Images were collected with a Zeiss AxioCam MR digital camera.

Table 1. *Burkholderia cepacia* complex used in this work and VR relative to the different killing assays.

Species	Strain	Source	SKA	FKA
<i>Burkholderia cepacia</i>	LMG 1222	Onion	0	3
<i>Burkholderia multivorans</i>	LMG 13010	CF	0	0
<i>Burkholderia cenocepacia</i>	LMG 16656	CF	2	2
<i>Burkholderia stabilis</i>	LMG 14294	CF	3	3
<i>Burkholderia vietnamiensis</i>	LMG 10929	Soil	1	0
<i>Burkholderia dolosa</i>	LMG 18943	CF	0	1
<i>Burkholderia ambifaria</i>	LMG 19182	Soil	0	3
<i>Burkholderia anthina</i>	LMG 20980	Soil	2	1
<i>Burkholderia pyrrocinia</i>	LMG 14191	Soil	0	2
<i>Burkholderia ubonensis</i>	LMG 20358	Soil	2	1
<i>Burkholderia latens</i>	LMG 24064	CF	1	1
<i>Burkholderia diffusa</i>	LMG 24065	CF	2	2
<i>Burkholderia arboris</i>	LMG 24066	Soil	1	1
<i>Burkholderia seminalis</i>	LMG 24067	CF	2	2
<i>Burkholderia metallica</i>	LMG 24068	CF	3	3
<i>Burkholderia lata</i>	LMG 22485	Soil	0	1
<i>Burkholderia contaminans</i>	LMG 23361	AI	1	3
<i>Burkholderia pseudomultivorans</i>	LMG 26883	CF	0	1

Abbreviations: Soil = Soil rhizosphere, AI = Animal Infections, CF = Cystic Fibrosis patients VRs

0 = 100% > Survival worms > 80%

1 = 79% > Survival worms > 50%

2 = 49% > Survival worms > 6%

3 = 5% > Survival worms > 0%

doi:10.1371/journal.pone.0142883.t001

Toxin Diffusion assay

Bcc or *E. coli* OP50 cells were grown under standard growth conditions and spread on sterile 0.22 µm Millipore Nitrocellulose (Darmstadt, Germany) filter disk located onto 2.5-cm-diameter PGS plates [25]. After overnight incubation at 37°C, the filter together with the bacterial lawn was removed and the plates were allowed to cool to room temperature. 30–40 hypochlorite-synchronised WT L4 nematodes were spotted onto the conditioned agar. Paralysis and

mortality of the worms were detected at 4 and 24 h. The experiments were performed in triplicate, and data reported are mean values \pm SD.

Statistical analysis and clustering

All the Kaplan-Meier survival curves were analyzed using the Graph-pad Prism 5 software. Comparisons *vs.* control for both the *C. elegans* and inhibitor experiments were performed using Fisher's exact test to account for possible non-Normality in the data. In particular, as it was observed that replicate means of *C. elegans* percent mortality correlated extremely well to pooled percent mortality ($R^2 > 0.99$ in all cases), counts of *C. elegans* that were alive and dead after 72 h were used to populate the various 2x2 tables onto which the Fisher's exact test was applied. Bonferroni-Holm correction of p-values was used to account for the multiple comparisons performed.

Mutant clustering analysis was performed using hierarchical clustering via Ward's method. Clusters were fixed using a consistency threshold of 1.1, resulting in cophenetic coefficient (correlation between cluster and metric distance) of at least 0.80.

Transporter Inhibitor assays

The MRP transporter inhibitors mometasone furoate, lasalocid A sodium, verapamil hydrochloride were purchased from Sigma-Aldrich, Saint Louis, MO. Compounds were dissolved in DMSO and spread onto NGM plates in different concentration ranges: 25–100 μ M (mometasone and verapamil) and 125–500 nM (lasalocid). DMSO (0,5% w/v) was used as control. Subsequently, Bcc strains (grown in standard conditions) were spotted onto the plates that were incubated overnight at 37°C. After the incubation 30–40 WT L4 worms were spotted onto the bacterial lawn. The plates were then incubated at 20°C for 3 days and scored for living worms every 24 h. The experiments were performed in triplicate, and the data reported are mean values.

Results and Discussion

Killing of *C. elegans* by Bcc strains

To evaluate Bcc virulence determinants and properties, two different assays were performed: i) SKA, performed on a low osmolarity medium (NGM), assigned to correlate worms mortality with intestinal bacterial accumulation/colonisation [24,25]; ii) FKA carried out on a high osmolarity medium (PGS) to demonstrate the secretion of bacterial toxins and evaluate their capacity to paralyse and kill the nematodes [24,25]. A VR was established for the Bcc strains under investigation by comparing the "infectivity" against nematodes between *E. coli* OP50 and Bcc isolates. The VR ranges from 0 to 3 (see Fig 1) and was based on the percentage of surviving worms after the period of observation, which was set at 3 days. A Bcc strain was considered to be non-pathogenic (VR = 0) when no symptom of disease was observed during the course of nematodes infection and the percentage of live worms at the conclusion of the period of observation ranged from 100 to 80%; VR = 1 corresponded to a percentage of alive worms between 79 to 50%; VR = 2 corresponded to a percentage of alive worms between 49 to 6%; finally, the VR was considered 3 when the percentage of surviving worms was \leq 5%.

SKA performed against WT L4 worms revealed diverse pathogenicity capabilities among the 18 Bcc representatives [Table 1]:

- i. 2 Bcc strains (*B. metallica*, *B. stabilis*) displayed high nematocide activity (VR 3). No viable nematodes were detectable in the plates after 3 days of incubation at 20°C.

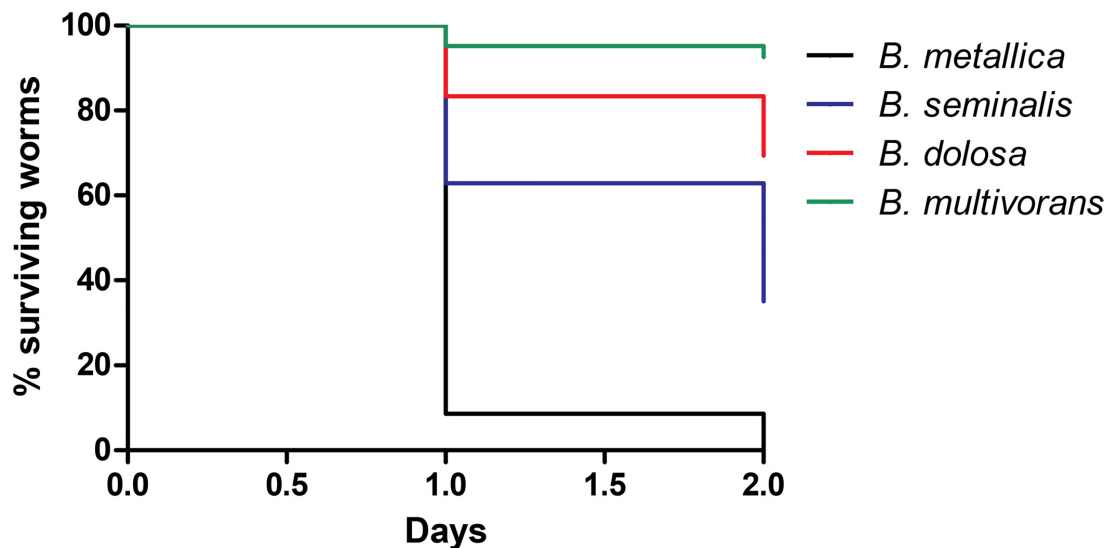


Fig 1. Kaplan-Meier survival plots for L4 N2 worms fed with exemplifying Bcc strains for different VR grown on PGS medium. Worms fed on: *B. metallica* (VR 3; black line; $n = 113$; 0% survival at day 2); *B. seminalis* (VR 2; blue line; $n = 150$; 34% survival at day 2); *B. dolosa* (VR 1; red line; $n = 198$; 69% survival at day 2); *B. multivorans* (VR 0; green line; $n = 120$; 93% survival worms). n : Number of worms at day 0. All p-values, comparing each survival curve between them, resulted to be < 0.0001 , calculated with "Log-rank (Mantel-Cox) Test" with the Graph-pad Prism 5 software.

doi:10.1371/journal.pone.0142883.g001

- ii. Half of the Bcc strains exhibited VR between 1 and 2, showing an intermediate toxicity towards *C. elegans*.
- iii. Seven Bcc strains (*B. ambifaria*, *B. cepacia*, *B. dolosa*, *B. pseudomultivorans*, *B. pyrrocinia*, *B. lata* and *B. multivorans*) were unable to kill worms, and the whole population was viable (VR = 0).

Nematodes killed in the lawn of bacteria took on a ghostly and hollow "shell-like" appearance about 48 h after the L4 were first introduced, and their shells induced by *B. ubonensis*, *B. metallica* and *B. stabilis* were defined as "chalk-mark ghosts". This shape is characteristic of organisms lacking a discernible internal cell structures. Often the ghosts eroded to a mere outline.

The pathogenicity of the 18 Bcc strains was then assessed on FKA. Data obtained are summarised in [Table 1](#). Nematodes death on FKA appeared to be a rapid process as they loose locomotor functions, as shown by the quick onset of lethargy. Motility visibly decreased after exposure for 4 h, and the rate of foraging was similarly affected in the same time frame. In FKA, five strains (*B. ambifaria*, *B. cepacia*, *B. contaminans*, *B. metallica*, *B. stabilis*) demonstrated deep killing ability (VR = 3) against *C. elegans* and only two strains (*B. multivorans* and *B. vietnamiensis*) were completely ineffective in killing worms. For the highly active strains, almost 100% mortality occurred in 24 h, while on SKA 3 days are required for complete killing ([Fig 2](#)).

Nine out of 18 Bcc strains have previously been characterized using SKA [[30,47](#)]. The VR of 7 strains (*B. anthina*, *B. ubonensis*, *B. vietnamiensis*, *B. cenocepacia*, *B. dolosa*, *B. ambifaria*, *B. cepacia*) are consistent with the previously reported SKA ranking. The same comparison revealed a variation for *B. pyrrocinia* and *B. stabilis*, which were found as more and less

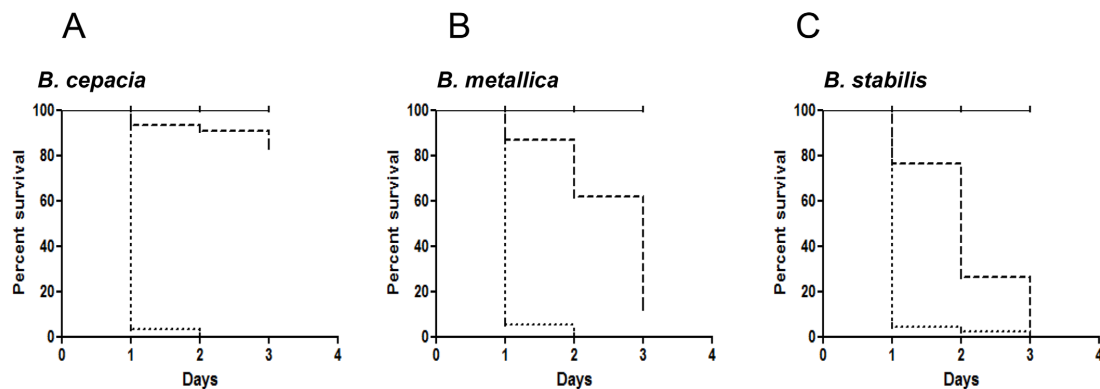


Fig 2. Kaplan-Meier survival plots for L4 stage WT worms fed with: *E. coli* OP50 (solid lines), Bcc strains on NGM (dashed lines), Bcc strains on PGS (dotted lines). n: Number of worms at day 0. A) The pathogenicity of Bcc strain *B. cepacia* on SKA (n = 93) was compared with the ability on FKA (n = 184). **B)** The pathogenicity of Bcc strain *B. metallica* on SKA (n = 80) was compared with the ability on FKA (n = 113). **C)** The pathogenicity of Bcc strain *B. stabilis* on SKA (n = 87) was compared with the ability on FKA (n = 161). P-values were calculated between survival curves on FKA and SKA of each bacteria, and resulted to be < 0.0001 calculated with "Log-rank (Mantel-Cox) Test" with the Graph-pad Prism 5 software.

doi:10.1371/journal.pone.0142883.g002

virulent, respectively. This variability may be due to ranking differences, as the experimental conditions were very reproducible. This is the first report for an indicative pathogenicity ranking for 8 *Burkholderia* species, recently added to Bcc, (*B. latens*, *B. diffusa*, *B. arboris*, *B. seminalis*, *B. metallica*, *B. pseudomultivorans*, *B. lata*, *B. contaminans*). *B. metallica*, *B. stabilis* (both isolated from CF patients) were the most virulent in both assays (Fig 2B and 2C). The comparison of data obtained in the FKA and SKA revealed that, on average, strains isolated from CF patients appeared more virulent than environmental isolates on SKA. In particular, three Bcc strains (*B. ambifaria*, *B. cepacia* and *B. pyrrocinia*) exhibited high nematocidal activity in the FKA, whereas they were unable to kill the worms in the SKA (VR 0 and 1). Therefore we can assume that toxin production is a common virulence mechanism for Bcc members, while CF isolates might have acquired different pathogenic traits that allow them to infect and colonize hosts, as already proposed by Pirone et al. [48]. The only exception is represented by *B. multivorans*, and *B. pseudomultivorans*. These two strains are CF isolates, but were non-virulent towards nematodes. This evidence likely relies on the limitation of the nematode host model, once more indicating that virulence factors are not universal for all hosts [15].

Bacterial intestinal accumulation. The two Bcc strains with VR = 3 in the SKA (*B. stabilis* and *B. metallica*) were then assessed for their ability to accumulate in the *C. elegans* intestine. Worms grown in standard condition were inspected using a compound microscope at different incubation times to evaluate the bacterial accumulation in the intestinal lumen.

Bcc colonization of nematode occurred rapidly. After 4 h of incubation, worms fed with *E. coli* OP50 showed a thin intestinal lumen (Fig 3A and 3B), whereas, when spotted onto *B. metallica* layer, worms already presented deformed intestines (Fig 3E). After 24 h nematodes displayed a full intestinal lumen packed with bacteria (Fig 3F). These data confirmed that Bcc with high VR were able to accumulate within the entire nematode intestine and therefore slow-killing may resemble an infection-like process. On the contrary, nematodes exposed to the strain *B. pseudomultivorans*, which exhibited a low pathogenicity (VR = 0 on SKA), under the same experimental conditions presented a healthy intestine with the presence of bacterial cells only in the first part of the intestine (Fig 3C and 3D). This finding may signify that: i) even non-pathogenic Bcc strains were able to pass intact through the pharynx and occupy the

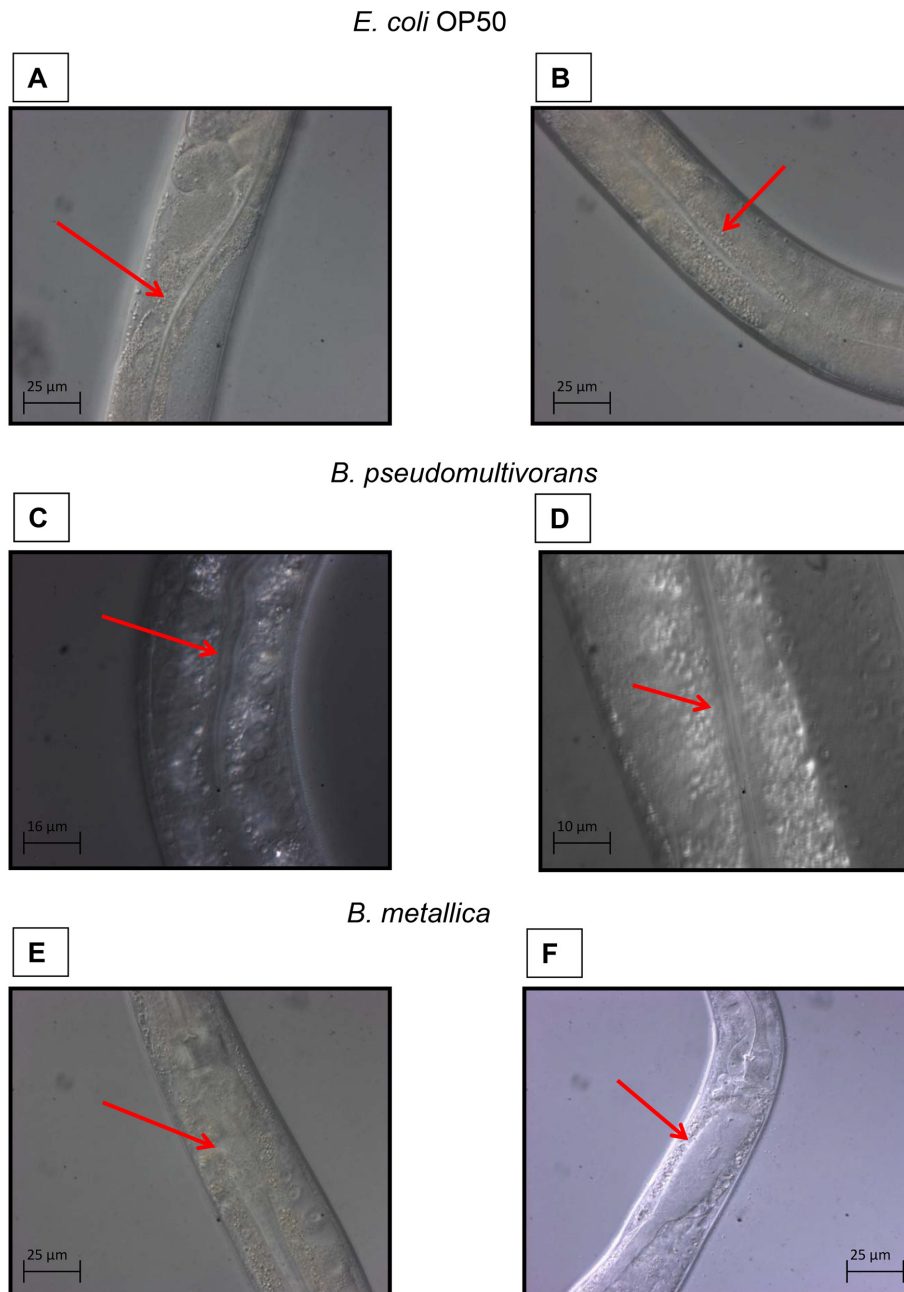


Fig 3. The ability of *Bcc* strains to accumulate in *C. elegans* intestinal lumen was evaluated with microscopy analysis. Red arrows indicate the nematodes intestine. **A)** Intestinal lumen of one L4 stage WT worm after 4 h of incubation on NGM plate spotted with *E. coli* OP50, and **B)** after 24 h of

incubation on the same plate. **C)** Intestinal lumen of one L4 WT after 4 h of incubation on NGM plate spotted with *B. pseudomultivorans* (VR 0 on SKA, and **D)** after 24 h of incubation on the same plate. **E)** Intestinal lumen of one L4 WT after 4 h of incubation on NGM plate spotted with *B. metallica* (VR 3 on SKA, and **F)** after 24 h of incubation on the same plate.

doi:10.1371/journal.pone.0142883.g003

intestine; ii) the accumulation of the Bcc in the whole nematode gut, especially in the last part of the intestine, might be responsible for the worm's death [24].

Toxin Diffusion assay. To evaluate the contribution of diffusible secreted factors (toxins and/or other virulence chemical signalling molecules) to the rapid kinetics of killing on FKA, we performed the toxin diffusion assay [25]. These experiments were carried out on a reduced panel consisting of the five Bcc strains possessing the highest nematocidal activity on FKA (*B. contaminans*, *B. cepacia*, *B. ambifaria*, *B. metallica* and *B. stabilis*). Results shown in Fig 4 revealed that a high percentage of worms were paralyzed after 4 h of incubation on plates, even if they were not in contact with the bacteria. In particular, only 30% of the worms placed on *B. ambifaria* plates were still mobile and active, whereas the remaining nematode population appeared paralysed. On the contrary, worms spotted on plates containing *E. coli* conditioned agar did not present any paralysis or mortality. Among the tested Bcc strains, *B. ambifaria* was the most active toxin producer. Indeed, after 24 h of incubation only 20% of the total number of nematodes was still moving on *B. ambifaria* plates (Fig 4). In the case of *B. stabilis*, it was observed that paralyzed worms at 4 h were able to move again and survive. One plausible explanation for this variation might be related to low stability of the diffusible toxins/virulence determinants produced by those strains that require constant production.

Interestingly, when the toxin filter assay was performed on NGM medium, no paralysis or mortality was detected. This experiment confirms that FKA rapid killing kinetics revealed a role for diffusible toxins as a main component of the infectious process. Thomson and Dennis demonstrated the production by Bcc strains of a haemolytic toxin required for full virulence, synthesized by a non-ribosomal peptide synthase (NRPS) pathway, typical of a complex secondary metabolite [49]. They screened a panel of Bcc strains including *B. cenocepacia*, *B. stabilis*, *B. pyrrocinia* and *B. vietnamiensis* for the presence of this gene cluster. A NRPS cluster was identified in *B. pyrrocinia* and *B. stabilis* with VR = 3 on FKA. Moreover, Bcc strains are known to produce toxins with demonstrated antifungal activity like the cyclic peptides occidiofungins (burkholdines) [50]. Therefore, we cannot *a priori* exclude the possibility that a peptide might represent the toxin active towards *C. elegans*.

Killing of MRPs knock-out *C. elegans* mutants by Bcc member strains

The nematode-Bcc pathogenicity ranking system developed was investigated for its ability to detect and map genotype-specific host responses. We obtained access to a complete, seven MRPs knock-out nematode mutant set, *mrp-1(pk89)*, *mrp-2(ok2157)*, *mrp-3(ok955)*, *mrp-4(ok1095)*, *mrp-5(ok2067)*, *mrp-6(ok1027)* and *mrp-8(ok1360)*, impaired in the corresponding ABC membrane transporters.

These knock-out mutants exhibited identical phenotypic attributes with the WT. The 18 Bcc representative strains were profiled against the 7 mutants in both SKA and FKA. Control mortality was calculated to be the number of dead worms divided by the number of total worms. Pooled mortality counts (alive vs. dead) for each mutant were tested against the WT using Fisher's Exact test. Statistically significant (Bonferroni-Holm corrected p-value < 0.05) differences from WT are shown in Table 2. The mortality rates calculated were highly variable suggesting a Bcc strain-specific effect towards the MRP *C. elegans* mutants. Some trends were detected: *mrp-5* and *mrp-2* had increased mortality rate for several Bcc strains in both SKA and

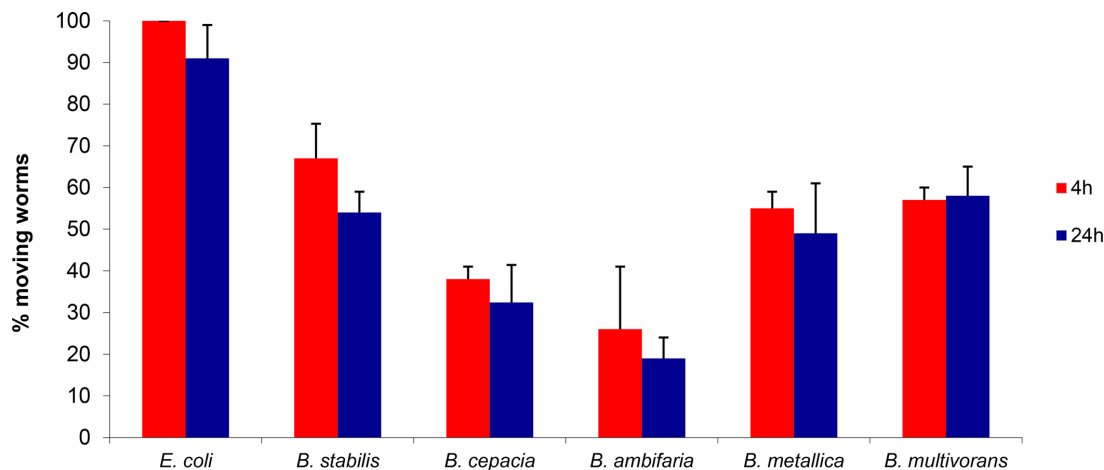


Fig 4. Secreted compounds or toxins mediate fast killing. Data reports paralysis and mortality at 4 and 24 h of worms plated on PGS medium plates treated with Bcc strains or *E. coli* grown on a sterile disk. Data represent mean values of three independent experiments and SD values are reported. P-values were calculated between sample (Bcc) and control (OP50) at the corresponding time, and were always < 0.05 .

doi:10.1371/journal.pone.0142883.g004

FKA. Specifically, 8 Bcc strains in SKA and 9 in FKA showed increased killing towards *mrp-5*, while 8 strains in SKA and 8 in FKA appeared more virulent against *mrp-2*. *C. elegans* mutants *mrp-3* and *mrp-4* displayed lower killing rates when incubated with several Bcc strains. In particular, mutant *mrp-4* exhibited decreased mortality to 8 Bcc species in SKA and to 7 strains in FKA. Regarding the Bcc strains, on SKA *B. ambifaria* displayed increased virulence towards the whole mutant set, with mortality rate compared to the WT higher than 75% and 71% towards, *mrp-5* and *mrp-6* respectively. *B. arboris* demonstrated an increased pathogenic effect towards *mrp-1*, *mrp-2*, *mrp-6*, *mrp-8*, while *B. dolosa* was more lethal against *mrp-2*, *mrp-5*, *mrp-6*, *mrp-8* mutants. On FKA, *B. lata* and *B. multivorans* were the most pathogenic strains with increased mortality rate against all mutants, while *B. diffusa* was more virulent against 6 mutants, and *B. arboris* against 5 mutants.

The complete set of killing results for each Bcc strain generated a unique killing profile in each MRP mutant. To determine whether these profiles constitute a coherent mutant classification pattern, a hierarchical clustering of significant effect sizes vs. each strain (Ward's method, Consistency Threshold 1.1) was performed. This analysis showed different patterns for *mrp-3* and *mrp-4* when compared with the rest of MRP-phenotypes in both FKA and SKA. However, *mrp-3* and *mrp-4* share low sequence identity/similarity among them (data not shown), suggesting that these two transporters do not have similar substrate specificity or function. These MRP-phenotypes were grouped consistently and differentiated from the rest of single knock out strains (Fig 5). This pattern could justify the diverse phenotypic response to Bcc of the MRP knock-out mutants, indicating variation in substrate profile specificity for the 7 MRP efflux systems. The clustering patterns of the other transporters suggest distinct substrate specificity, in agreement with the low degree of sequence identity/similarity shared among them (data not shown). Nevertheless, we can assume that toxins and small molecules are MRP-related substrates, and these transporters play a fundamental role in Bcc defence, with the exception of *mrp-3* and *mrp-4*.

Table 2. MRP knock-out *C. elegans* mutants mortality expressed as percentage of dead worms and comparison between the mutants and the WT. Mutant mrp-5 was tested as heterozygote, due to lethality of the mutation in homozygosis. Statistical significant differences appear highlighted, with negative values indicating statistically significant reductions in mortality from WT, and with positive values indicating statistically significant increases in mortality from WT.

Strain	WT Mortality FKA	Significant Changes in % Mortality						
		mrp-1	mrp-2	mrp-3	mrp-4	mrp-5	mrp-6	mrp-8
<i>B. ambifaria</i>	95	NS	-27	NS	NS	NS	NS	NS
<i>B. anthina</i>	42	45	50	NS	NS	58	NS	NS
<i>B. arboris</i>	28	70	72	21	NS	NS	72	72
<i>B. cenocepacia</i>	64	NS	31	NS	-45	NS	27	NS
<i>B. cepacia</i>	100	-19	NS	NS	-19	NS	-15	-18
<i>B. contaminans</i>	94	NS	NS	-17	-16	NS	NS	NS
<i>B. diffusa</i>	69	NS	NS	NS	NS	NS	NS	-26
<i>B. dolosa</i>	31	33	NS	59	NS	48	49	NS
<i>B. latens</i>	42	NS	NS	-34	NS	38	NS	-28
<i>B. metallica</i>	100	NS	NS	-13	-17	NS	NS	-10
<i>B. pseudomultivorans</i>	20	NS	NS	NS	NS	50	NS	NS
<i>B. pyrrocinia</i>	70	NS	21	-44	-35	26	NS	29
<i>B. seminalis</i>	64	NS	NS	-44	-31	NS	NS	NS
<i>B. stabilis</i>	100	-9	-47	NS	NS	-10	-63%	-77%
<i>B. ubonensis</i>	52	NS	41	NS	-24%	38	NS	32
<i>B. vietnamiensis</i>	14	NS	40	-12%	NS	57	61	35
<i>B. lata</i>	18	38	64	27	42	70	54	53
<i>B. multivorans</i>	7	33	22	21	34	62	28	45
Strain	WT Mortality SKA	mrp-1	mrp-2	mrp-3	mrp-4	mrp-5	mrp-6	mrp-8
<i>B. ambifaria</i>	6	61	67	30	28	75	71	58
<i>B. anthina</i>	91	9	NS	-27	-24	NS	NS	NS
<i>B. arboris</i>	46	53	54	-35	NS	NS	50	51
<i>B. cenocepacia</i>	81	NS	NS	NS	-77	-65	-24	-54
<i>B. cepacia</i>	9	81	75	NS	NS	78	62	45
<i>B. contaminans</i>	47	30	26	49	NS	NS	NS	NS
<i>B. diffusa</i>	88	NS	NS	NS	-25	NS	NS	NS
<i>B. dolosa</i>	13	NS	25	NS	NS	61	61	28
<i>B. latens</i>	22	NS	43	-19	-19	46	NS	42
<i>B. metallica</i>	100	NS	NS	-14%	-8%	NS	NS	NS
<i>B. pseudomultivorans</i>	11	NS	NS	NS	NS	30	NS	NS
<i>B. pyrrocinia</i>	5	53	61	NS	NS	64	57	46
<i>B. seminalis</i>	69	28	NS	-50	-67	NS	NS	NS
<i>B. stabilis</i>	100	-90	-58	NS	NS	-55	-60	-84
<i>B. ubonensis</i>	83	-60	NS	-28	-36	NS	NS	NS
<i>B. vietnamiensis</i>	46	-44	-39	-43	-44	-34	50	-41
<i>B. lata</i>	10	NS	NS	NS	NS	52	NS	NS
<i>B. multivorans</i>	3	NS	22	NS	NS	35	41	NS

NS = Not significant difference

doi:10.1371/journal.pone.0142883.t002

Inhibitor experiments

The Bcc pathogenicity ranking system was used to facilitate testing for a distinct MRP-efflux system substrate profile within the content of infection. Disabling efflux pumps genetically

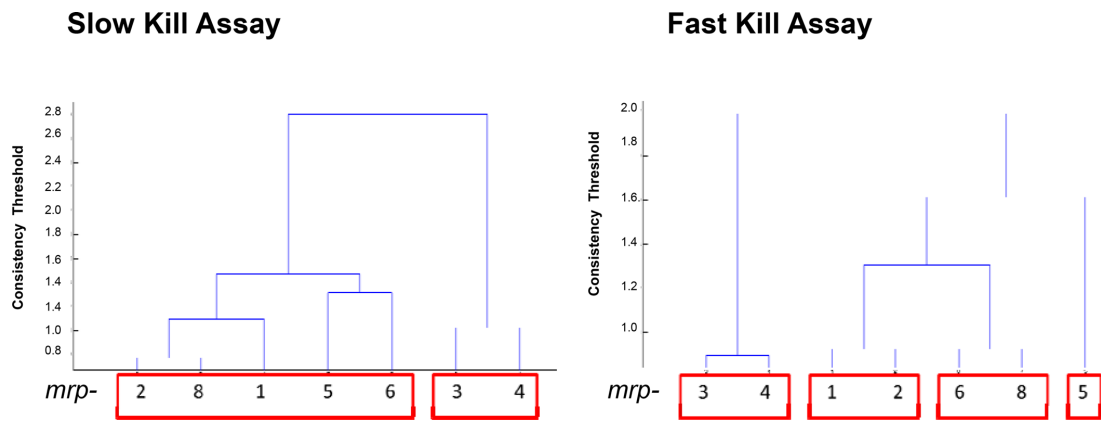


Fig 5. Hierarchical Clusterings. Ward's method with a consistency threshold 1.1 used to cluster mutants based on significant changes in pathogenicity.

doi:10.1371/journal.pone.0142883.g005

(knock-outs) or chemically (small molecules-inhibitors) should have a similar toll on increasing nematode mortality. A pilot analysis was performed utilizing the Bcc strains that exhibited increased *C. elegans* susceptibility in numerous efflux knock-outs on SKA (*B. ambifaria*, *B. arboris*, *B. cepacia*, *B. dolosa*, *B. pyrrocinia*) and the well-characterized mammalian MRP-efflux inhibitors mometasone furoate, lasalocid A and verapamil [51]. All compounds did not affect Bcc or *C. elegans* viability at the concentration used for the assay, (S1 Fig) The compounds were spread in concentration ranges onto NGM plates to perform SKA and DMSO (0.5%) was used as a growth control. Control mortality was calculated to be the number of dead worms divided by the number of total worms. Comparison to solvent control of pooled mortality counts was done using Fisher's Exact test; results were considered significant if Bonferroni-Holm corrected *p*-values were less than 0.05. Statistically significant differences from the WT are shown in Table 3. Reduction in mortality from the controls was not observed. The inhibitor use in the infection system, provided a statistically significant increase of mortality in the presence of at least one inhibitor compared to DMSO controls for 3 Bcc strains, whereas *B. pyrrocinia* and *B. ambifaria* killing rates were not affected.

In particular, the presence of mometasone (100 μM), *B. arboris*, *B. cepacia* and *B. dolosa* enhanced virulence against nematodes with mortality rate of 40% higher than the control. Lasalocid (500 nM) caused an increase in the percentage of dead worms of 34% and 48%

Table 3. Effect of ABC inhibitors during *C. elegans*- Bcc infection on SKA. Nematodes mortality expressed as percentage of dead worms and compared between samples with inhibitors and control with DMSO (0.5%). Statistical significant differences were reported.

Strain	Control Mortality	Significant Changes in % Mortality								
		Verapamil			Mometasone			Lasalocid		
		100 μM	50 μM	25 μM	100 μM	50 μM	25 μM	500 nM	250 nM	125 nM
<i>B. cepacia</i>	17	NS	NS	NS	45	NS	NS	34	NS	NS
<i>B. arboris</i>	20	35	NS	27	45	NS	NS	NS	NS	NS
<i>B. dolosa</i>	32	NS	NS	NS	44	29	NS	48	38	NS

NS = Not significant difference

doi:10.1371/journal.pone.0142883.t003

with *B. cepacia* and *B. dolosa*, respectively. Verapamil (100 μ M) enhanced killing only for *B. arboris*, with a killing rate of 35% higher than the control. These results demonstrated that the inhibitor driven MRP transporter inactivation results in increased mortality at least for two inhibitors, of the nematodes to Bcc strains, supporting the role of these transporters in Bcc infection. Verapamil has been characterized as a competitive inhibitor in ABCB1 malignant cell overexpression [52] as well as a potent ABCC family inhibitor [53]. It is also involved in inhibiting *C. elegans* P-gp1, which is involved in nematode resistance to ivermectine [54]. The present experimental setup differs as it explores verapamil against a number of targets simultaneously not by isolating transporters of interest. This analysis suggests that verapamil very likely works, but the number of interactions leading to a weaker phenotype should be investigated further.

Conclusions

The major aim of this work was to inquire the role of host transporters in the infection developing a nematode virulence ranking system focusing in well-recognized Bcc strains. It is common knowledge that every bacterial species includes member-strains with different pathogenic characteristics. However, the key purpose was to build the model using type strains of each of the 18 currently known Bcc species, a combination of two different killing assays (SKA and FKA), and a set of nematode mutants impaired in MRP efflux transporters. We focused on type strains due to the extensive information known, as many Bcc genomes have been completely sequenced and more will be soon become available. To define Bcc virulence we established a VR scheme, based on the percentage of surviving worms. Both nematocidal assays revealed different pathogenicity profiles for the Bcc species. Strains with high score in the VR system were able to accumulate in the nematodes intestine and produce virulence factors, on SKA and FKA, respectively. Only Bcc CF isolates accumulate within worms, an observation that correlates well with the apparent differences in virulence factors between environmental and CF isolates. This VR scheme was applied to profile Bcc pathogenesis in seven MRP impaired *C. elegans* mutants. MRPs are implicated in distinct nematode cellular processes: MRP1 is involved in heavy metal tolerance and ivermectine resistance [42,43]; MRP4 is central in early-stage differentiation [55]; MRP5 acts as a fundamental heme exporter into embryonic development [56]. Results showed increased nematode mortality for several *C. elegans* mutants grown in the presence of specific Bcc strains compared to WT nematodes. In particular *mrp-2* and *mrp-5* were the most susceptible mutants with increased mortality respectively in 13 and 11 different Bcc strains in the two assays, suggesting an active role of these two efflux transporters in host defense. However strain *mpr-5* was tested only in heterozygosis and this could have affected survival rate. Cluster analysis consistently grouped and separated *mrp-3* and *mrp-4* mutants in both assays from the other MRP-phenotypes. This pattern suggested different substrate specificity for these MRP transporters. To further explore the role of MRP transporters in host defense, inhibitor experiments were carried out on a selected panel of the five most "infectious" Bcc strains against the MRP knock-out mutants (*B. ambifaria*, *B. arboris*, *B. cepacia*, *B. dolosa*, *B. pyrrocinia*). These strains were tested against the WT nematodes in the presence of three well-characterized MRP-inhibitors, with a broad inhibitory activity against MRP transporters [51]. These results suggested that chemically disabling of the MRPs resulted in increased *C. elegans* susceptibility to Bcc strains. The use of mometasone and lasalocid in the infection system increased killing rate when incubated with *B. cepacia* and *B. dolosa*, while verapamil showed a mild effect for *B. arboris*.

In conclusion, this study provided tools to correlate microbial pathogenicity with the host transporters, and highlighted specific efflux systems with a central role in Bcc virulence.

It is worth noting that MRPs share components of a conserved activation mechanism with the Cystic Fibrosis Transmembrane conductance Regulator (CFTR)[57,58]. Therefore, identification of bacterial signalling molecules with substrate specificity in recognizing MRPs CFRT-like efflux transporters involved in host response could be a starting point for the development of novel therapeutic strategies.

Supporting Information

S1 Fig. Bcc strain growth in the presence of inhibitors. For the Bcc strain growth curves in the presence of inhibitors, one single colony of each Bcc strain was placed in a tube containing 3 mL of LB broth. The tubes were then incubated at 37°C overnight in agitation. The overnight cultures were used to inoculate 250 mL flasks containing 50 mL of LB broth plus the inhibitors at an initial concentration of 0.01 OD600/mL. For each strain, a set of 5 flasks was employed: 1) Verapamile 100 µM; 2) Mometasone 100 µM; 3) Lasalocid 500 nM; 4) DMSO 0.5% v/v; 5) control (no inhibitor or DMSO). The flasks were incubated at 37°C in agitation at 220 rpm. Bacterial growth was monitored following OD600 for 36 hours every 2 hours. The experiments were performed in duplicate and the data reported represent mean values. Error bars were omitted for clarity. Results proved that the inhibitors did not interfere with Bcc growth at the concentration used in our assays, as the growth curves obtained for each strain are very similar with no viable effect in growth by any inhibitor.
(DOC)

Acknowledgments

Nematode strains used in this work were provided by the CGC, which is funded by NIH Office of Research Infrastructure Programs (P40 OD010440). *Burkholderia cepacia* complex strains, used in this work, were kindly provided by Prof. Peter Vandamme, University of Gent, Belgium.

This work was supported by the EU-KBBE 2012–2016 project PharmaSea, grant N° 312184.

Elena Perrin is financially supported by a “Fondazione Adriano Buzzati-Traverso” fellowship.

Author Contributions

Conceived and designed the experiments: PT EDS FB GT DdP. Performed the experiments: PT MV DdP. Analyzed the data: PT EP IM RF EDS FB GT MLT EP RS CP DdP. Contributed reagents/materials/analysis tools: EDS DdP. Wrote the paper: PT EP IM RF EDS FB GT MLT EP RS CP DdP.

References

1. Compant S NJ, Coenye T, Clement C, Ait Barka E (2008) Diversity and occurrence of *Burkholderia* spp. in the natural environment. *FEMS Microbiol Rev* 32(4): 607–626. doi: [10.1111/j.1574-6976.2008.00113.x](https://doi.org/10.1111/j.1574-6976.2008.00113.x) PMID: [18422616](https://pubmed.ncbi.nlm.nih.gov/18422616/)
2. Coenye T, Vandamme P (2003) Diversity and significance of *Burkholderia* species occupying diverse ecological niches. *Environ Microbiol* 5: 719–729. PMID: [12919407](https://pubmed.ncbi.nlm.nih.gov/12919407/)
3. Peeters C, Zlosnik JE, Spilker T, Hird TJ, LiPuma JJ, Vandamme P (2013) *Burkholderia pseudomultivorans* sp. nov., a novel *Burkholderia cepacia* complex species from human respiratory samples and the rhizosphere. *Syst Appl Microbiol* 36: 483–489. doi: [10.1016/j.syapm.2013.06.003](https://doi.org/10.1016/j.syapm.2013.06.003) PMID: [23867250](https://pubmed.ncbi.nlm.nih.gov/23867250/)
4. Mahenthiralingam E, Urban TA, Goldberg JB (2005) The multifarious, multireplicon *Burkholderia cepacia* complex. *Nat Rev Microbiol* 3: 144–156. PMID: [15643431](https://pubmed.ncbi.nlm.nih.gov/15643431/)
5. De Smet B, Mayo M, Peeters C, Zlosnik JE, Spilker T, Hird TJ, et al. (2015) *Burkholderia stagnalis* sp. nov. and *Burkholderia territorii* sp. nov., two novel *Burkholderia cepacia* complex species from

- environmental and human sources. *Int J Syst Evol Microbiol* 65: 2265–2271. doi: [10.1099/ijs.0.000251](https://doi.org/10.1099/ijs.0.000251) PMID: [25872960](https://pubmed.ncbi.nlm.nih.gov/25872960/)
6. Ramsay KA, Butler CA, Paynter S, Ware RS, Kidd TJ, Wainwright CE, et al. (2013) Factors influencing acquisition of *Burkholderia cepacia* complex organisms in patients with cystic fibrosis. *J Clin Microbiol* 51: 3975–3980. doi: [10.1128/JCM.01360-13](https://doi.org/10.1128/JCM.01360-13) PMID: [24048536](https://pubmed.ncbi.nlm.nih.gov/24048536/)
 7. Rose H, Baldwin A, Dowson CG, Mahenthiralingam E (2009) Biocide susceptibility of the *Burkholderia cepacia* complex. *J Antimicrob Chemother* 63: 502–510. doi: [10.1093/jac/dkn540](https://doi.org/10.1093/jac/dkn540) PMID: [19153076](https://pubmed.ncbi.nlm.nih.gov/19153076/)
 8. Nash EF, Thomas A, Whitmill R, Rashid R, Barker B, Rayner RJ, et al. (2010) "Cepacia syndrome" associated with *Burkholderia cepacia* (genomovar I) infection in an adolescent with cystic fibrosis. *Pediatr Pulmonol*.
 9. Bazzini S, Udine C, Riccardi G (2011) Molecular approaches to pathogenesis study of *Burkholderia cenocepacia*, an important cystic fibrosis opportunistic bacterium. *Appl Microbiol Biotechnol* 92: 887–895. doi: [10.1007/s00253-011-3616-5](https://doi.org/10.1007/s00253-011-3616-5) PMID: [21997606](https://pubmed.ncbi.nlm.nih.gov/21997606/)
 10. Drevinek P, Mahenthiralingam E (2010) *Burkholderia cenocepacia* in cystic fibrosis: epidemiology and molecular mechanisms of virulence. *Clin Microbiol Infect* 16: 821–830. doi: [10.1111/j.1469-0691.2010.03237.x](https://doi.org/10.1111/j.1469-0691.2010.03237.x) PMID: [20880411](https://pubmed.ncbi.nlm.nih.gov/20880411/)
 11. Fallon JP, Reeves EP, Kavanagh K (2011) The *Aspergillus fumigatus* toxin fumagillin suppresses the immune response of *Galleria mellonella* larvae by inhibiting the action of haemocytes. *Microbiology* 157: 1481–1488. doi: [10.1099/mic.0.043786-0](https://doi.org/10.1099/mic.0.043786-0) PMID: [21349977](https://pubmed.ncbi.nlm.nih.gov/21349977/)
 12. Lionakis MS (2011) *Drosophila* and *Galleria* insect model hosts: new tools for the study of fungal virulence, pharmacology and immunology. *Virulence* 2: 521–527. doi: [10.4161/viru.2.6.18520](https://doi.org/10.4161/viru.2.6.18520) PMID: [22186764](https://pubmed.ncbi.nlm.nih.gov/22186764/)
 13. Abebe E, Abebe-Akele F, Morrison J, Cooper V, Thomas WK (2011) An insect pathogenic symbiosis between a *Caenorhabditis* and *Serratia*. *Virulence* 2: 158–161. PMID: [21389770](https://pubmed.ncbi.nlm.nih.gov/21389770/)
 14. Olsen RJ, Watkins ME, Cantu CC, Beres SB, Musser JM (2011) Virulence of serotype M3 Group A *Streptococcus* strains in wax worms (*Galleria mellonella* larvae). *Virulence* 2: 111–119. PMID: [21258213](https://pubmed.ncbi.nlm.nih.gov/21258213/)
 15. Uehlinger S, Schwager S, Bernier SP, Riedel K, Nguyen DT, Sokol PA, et al. (2009) Identification of specific and universal virulence factors in *Burkholderia cenocepacia* strains by using multiple infection hosts. *Infect Immun* 77: 4102–4110. doi: [10.1128/IAI.00398-09](https://doi.org/10.1128/IAI.00398-09) PMID: [19528212](https://pubmed.ncbi.nlm.nih.gov/19528212/)
 16. Schwager S, Agnoli K, Kothe M, Feldmann F, Givskov M, Carlier A et al. (2013) Identification of *Burkholderia cenocepacia* strain H111 virulence factors using nonmammalian infection hosts. *Infect Immun* 81: 143–153. doi: [10.1128/IAI.00768-12](https://doi.org/10.1128/IAI.00768-12) PMID: [23090963](https://pubmed.ncbi.nlm.nih.gov/23090963/)
 17. Kurz CL, Chauvet S, Andres E, Aurouze M, Vallet I, Michel GP et al. (2003) Virulence factors of the human opportunistic pathogen *Serratia marcescens* identified by in vivo screening. *EMBO J* 22: 1451–1460. PMID: [12660152](https://pubmed.ncbi.nlm.nih.gov/12660152/)
 18. Mylonakis E, Ausubel FM, Tang RJ, Calderwood SB (2003) The art of serendipity: killing of *Caenorhabditis elegans* by human pathogens as a model of bacterial and fungal pathogenesis. *Expert Rev Anti Infect Ther* 1: 167–173. PMID: [15482109](https://pubmed.ncbi.nlm.nih.gov/15482109/)
 19. Tan MW, Ausubel FM (2000) *Caenorhabditis elegans*: a model genetic host to study *Pseudomonas aeruginosa* pathogenesis. *Curr Opin Microbiol* 3: 29–34. PMID: [10679415](https://pubmed.ncbi.nlm.nih.gov/10679415/)
 20. Bhatt S, Anyanful A, Kalman D (2011) CsrA and TnaB coregulate tryptophanase activity to promote exotoxin-induced killing of *Caenorhabditis elegans* by enteropathogenic *Escherichia coli*. *J Bacteriol* 193: 4516–4522. doi: [10.1128/JB.05197-11](https://doi.org/10.1128/JB.05197-11) PMID: [21705596](https://pubmed.ncbi.nlm.nih.gov/21705596/)
 21. Lee SH, Ooi SK, Mahadi NM, Tan MW, Nathan S (2011) Complete killing of *Caenorhabditis elegans* by *Burkholderia pseudomallei* is dependent on prolonged direct association with the viable pathogen. *PLoS One* 6: e16707. doi: [10.1371/journal.pone.0016707](https://doi.org/10.1371/journal.pone.0016707) PMID: [21408228](https://pubmed.ncbi.nlm.nih.gov/21408228/)
 22. O'Quinn AL, Wiegand EM, Jeddelloh JA (2001) *Burkholderia pseudomallei* kills the nematode *Caenorhabditis elegans* using an endotoxin-mediated paralysis. *Cell Microbiol* 3: 381–393. PMID: [11422081](https://pubmed.ncbi.nlm.nih.gov/11422081/)
 23. Lee SH, Wong RR, Chin CY, Lim TY, Eng SA, Kong C et al. (2013) *Burkholderia pseudomallei* suppresses *Caenorhabditis elegans* immunity by specific degradation of a GATA transcription factor. *Proc Natl Acad Sci U S A*.
 24. Huber B, Feldmann F, Kothe M, Vandamme P, Wopperer J, Riedel K, et al. (2004) Identification of a novel virulence factor in *Burkholderia cenocepacia* H111 required for efficient slow killing of *Caenorhabditis elegans*. *Infect Immun* 72: 7220–7230. PMID: [15557647](https://pubmed.ncbi.nlm.nih.gov/15557647/)
 25. Kothe M, Antl M, Huber B, Stoecker K, Ebrecht D, Steinmetz I, et al. (2003) Killing of *Caenorhabditis elegans* by *Burkholderia cepacia* is controlled by the cep quorum-sensing system. *Cell Microbiol* 5: 343–351. PMID: [12713492](https://pubmed.ncbi.nlm.nih.gov/12713492/)

26. Sousa SA, Ramos CG, Leitao JH (2011) Burkholderia cepacia Complex: Emerging Multihost Pathogens Equipped with a Wide Range of Virulence Factors and Determinants. *Int J Microbiol* 2011.
27. Tegos GP, Haynes MK, Schweizer HP (2012) Dissecting novel virulent determinants in the Burkholderia cepacia complex. *Virulence* 3: 234–237. doi: [10.4161/viru.19844](https://doi.org/10.4161/viru.19844) PMID: [22546904](https://pubmed.ncbi.nlm.nih.gov/22546904/)
28. O'Grady EP, Viteri DF, Sokol PA (2012) A unique regulator contributes to quorum sensing and virulence in Burkholderia cenocepacia. *PLoS One* 7: e37611. doi: [10.1371/journal.pone.0037611](https://doi.org/10.1371/journal.pone.0037611) PMID: [22624054](https://pubmed.ncbi.nlm.nih.gov/22624054/)
29. Cooper VS, Carlson WA, Lipuma JJ (2009) Susceptibility of *Caenorhabditis elegans* to Burkholderia infection depends on prior diet and secreted bacterial attractants. *PLoS One* 4: e7961. doi: [10.1371/journal.pone.0007961](https://doi.org/10.1371/journal.pone.0007961) PMID: [19956737](https://pubmed.ncbi.nlm.nih.gov/19956737/)
30. Cardona ST, Wopperer J, Eberl L, Valvano MA (2005) Diverse pathogenicity of Burkholderia cepacia complex strains in the *Caenorhabditis elegans* host model. *FEMS Microbiol Lett* 250: 97–104. PMID: [16043310](https://pubmed.ncbi.nlm.nih.gov/16043310/)
31. Springman AC, Jacobs JL, Somvanshi VS, Sundin GW, Mulks MH, Whittam TS, et al. (2009) Genetic diversity and multihost pathogenicity of clinical and environmental strains of Burkholderia cenocepacia. *Appl Environ Microbiol* 75: 5250–5260. doi: [10.1128/AEM.00877-09](https://doi.org/10.1128/AEM.00877-09) PMID: [19542323](https://pubmed.ncbi.nlm.nih.gov/19542323/)
32. Sousa SA, Ramos CG, Moreira LM, Leitao JH (2010) The hfq gene is required for stress resistance and full virulence of Burkholderia cepacia to the nematode *Caenorhabditis elegans*. *Microbiology* 156: 896–908. PMID: [19942656](https://pubmed.ncbi.nlm.nih.gov/19942656/)
33. Markey KM, Glendinning KJ, Morgan JA, Hart CA, Winstanley C (2006) *Caenorhabditis elegans* killing assay as an infection model to study the role of type III secretion in Burkholderia cenocepacia. *J Med Microbiol* 55: 967–969. PMID: [16772429](https://pubmed.ncbi.nlm.nih.gov/16772429/)
34. Martinez JL, Sanchez MB, Martinez-Solano L, Hernandez A, Garmendia L, Fajardo A, et al. (2009) Functional role of bacterial multidrug efflux pumps in microbial natural ecosystems. *FEMS Microbiol Rev* 33: 430–449. doi: [10.1111/j.1574-6976.2008.00157.x](https://doi.org/10.1111/j.1574-6976.2008.00157.x) PMID: [19207745](https://pubmed.ncbi.nlm.nih.gov/19207745/)
35. Buroni S, Pasca MR, Flannagan RS, Bazzini S, Milano A, Bertani I, et al. (2009) Assessment of three Resistance-Nodulation-Cell Division drug efflux transporters of Burkholderia cenocepacia in intrinsic antibiotic resistance. *BMC Microbiol* 9: 200. doi: [10.1186/1471-2180-9-200](https://doi.org/10.1186/1471-2180-9-200) PMID: [19761586](https://pubmed.ncbi.nlm.nih.gov/19761586/)
36. Feinbaum RL, Urbach JM, Liberati NT, Djonovic S, Adonizio A, Carvunis AR, et al. (2012) Genome-wide identification of *Pseudomonas aeruginosa* virulence-related genes using a *Caenorhabditis elegans* infection model. *PLoS Pathog* 8: e1002813. doi: [10.1371/journal.ppat.1002813](https://doi.org/10.1371/journal.ppat.1002813) PMID: [22911607](https://pubmed.ncbi.nlm.nih.gov/22911607/)
37. Ooi SK, Lim TY, Lee SH, Nathan S (2012) Burkholderia pseudomallei kills *Caenorhabditis elegans* through virulence mechanisms distinct from intestinal lumen colonization. *Virulence* 3: 485–496. doi: [10.4161/viru.21808](https://doi.org/10.4161/viru.21808) PMID: [23076282](https://pubmed.ncbi.nlm.nih.gov/23076282/)
38. Harland DN, Dassa E, Titball RW, Brown KA, Atkins HS (2007) ATP-binding cassette systems in Burkholderia pseudomallei and Burkholderia mallei. *BMC Genomics* 8: 83. PMID: [17391530](https://pubmed.ncbi.nlm.nih.gov/17391530/)
39. Dean M, Rzhetsky A, Allikmets R (2001) The human ATP-binding cassette (ABC) transporter superfamily. *Genome Res* 11: 1156–1166. PMID: [11435397](https://pubmed.ncbi.nlm.nih.gov/11435397/)
40. Sheps JA, Ralph S, Zhao Z, Baillie DL, Ling V (2004) The ABC transporter gene family of *Caenorhabditis elegans* has implications for the evolutionary dynamics of multidrug resistance in eukaryotes. *Genome Biol* 5: R15. PMID: [15003118](https://pubmed.ncbi.nlm.nih.gov/15003118/)
41. Rees D, Johnson E, Lewinson O (2009) ABC transporters: the power to change. *Nat Rev Mol Cell Biol* 10: 218–227. doi: [10.1038/nrm2646](https://doi.org/10.1038/nrm2646) PMID: [19234479](https://pubmed.ncbi.nlm.nih.gov/19234479/)
42. James CE, Davey MW (2009) Increased expression of ABC transport proteins is associated with ivermectin resistance in the model nematode *Caenorhabditis elegans*. *Int J Parasitol* 39: 213–220. doi: [10.1016/j.ijpara.2008.06.009](https://doi.org/10.1016/j.ijpara.2008.06.009) PMID: [18708066](https://pubmed.ncbi.nlm.nih.gov/18708066/)
43. Yan R, Urdaneta-Marquez L, Keller K, James CE, Davey MW, Prichard RK (2012) The role of several ABC transporter genes in ivermectin resistance in *Caenorhabditis elegans*. *Vet Parasitol* 190: 519–529. doi: [10.1016/j.vetpar.2012.06.038](https://doi.org/10.1016/j.vetpar.2012.06.038) PMID: [22840641](https://pubmed.ncbi.nlm.nih.gov/22840641/)
44. Kurz CL, Shapira M, Chen K, Baillie DL, Tan MW (2007) *Caenorhabditis elegans* pgp-5 is involved in resistance to bacterial infection and heavy metal and its regulation requires TIR-1 and a p38 map kinase cascade. *Biochem Biophys Res Commun* 363: 438–443. PMID: [17888400](https://pubmed.ncbi.nlm.nih.gov/17888400/)
45. Brenner S (1974) The genetics of *Caenorhabditis elegans*. *Genetics* 77: 71–94. PMID: [4366476](https://pubmed.ncbi.nlm.nih.gov/4366476/)
46. Stiemagle T (2006) Maintenance of *C. elegans* WormBook, The *C. elegans* Research Community.
47. Wopperer J, Cardona ST, Huber B, Jacobi CA, Valvano MA, Eberl L (2006) A quorum-quenching approach to investigate the conservation of quorum-sensing-regulated functions within the Burkholderia cepacia complex. *Appl Environ Microbiol* 72: 1579–1587. PMID: [16461713](https://pubmed.ncbi.nlm.nih.gov/16461713/)

48. Pirone L, Bragonzi A, Farcomeni A, Paroni M, Auriche C, Conese M, et al. (2008) Burkholderia cenocepacia strains isolated from cystic fibrosis patients are apparently more invasive and more virulent than rhizosphere strains. *Environ Microbiol* 10: 2773–2784. doi: [10.1111/j.1462-2920.2008.01697.x](https://doi.org/10.1111/j.1462-2920.2008.01697.x) PMID: [18643926](https://pubmed.ncbi.nlm.nih.gov/18643926/)
49. Thomson EL, Dennis JJ (2012) A Burkholderia cepacia complex non-ribosomal peptide-synthesized toxin is hemolytic and required for full virulence. *Virulence* 3: 286–298. doi: [10.4161/viru.19355](https://doi.org/10.4161/viru.19355) PMID: [22546908](https://pubmed.ncbi.nlm.nih.gov/22546908/)
50. Lu SE, Novak J, Austin FW, Gu G, Ellis D, Kirk M, et al. (2009) Occidiofungin, a unique antifungal glycopeptide produced by a strain of Burkholderia contaminans. *Biochemistry* 48: 8312–8321. doi: [10.1021/bi900814c](https://doi.org/10.1021/bi900814c) PMID: [19673482](https://pubmed.ncbi.nlm.nih.gov/19673482/)
51. Strouse JJ, Ivniiski-Steele I, Waller A, Young SM, Perez D, Evangelisti AM, et al. (2013) Fluorescent substrates for flow cytometric evaluation of efflux inhibition in ABCB1, ABCC1, and ABCG2 transporters. *Anal Biochem* 437: 77–87. doi: [10.1016/j.ab.2013.02.018](https://doi.org/10.1016/j.ab.2013.02.018) PMID: [23470221](https://pubmed.ncbi.nlm.nih.gov/23470221/)
52. Horger KS, Liu H, Rao DK, Shukla S, Sept D, Ambudkar SV, et al. (2015) Hydrogel-assisted functional reconstitution of human P-glycoprotein (ABCB1) in giant liposomes. *Biochim Biophys Acta* 1848: 643–653. doi: [10.1016/j.bbame.2014.10.023](https://doi.org/10.1016/j.bbame.2014.10.023) PMID: [25450342](https://pubmed.ncbi.nlm.nih.gov/25450342/)
53. Eilers M, Roy U, Mondal D (2008) MRP (ABCC) transporters-mediated efflux of anti-HIV drugs, saquinavir and zidovudine, from human endothelial cells. *Exp Biol Med (Maywood)* 233: 1149–1160.
54. Ardelli BF, Prichard RK (2013) Inhibition of P-glycoprotein enhances sensitivity of Caenorhabditis elegans to ivermectin. *Vet Parasitol* 191: 264–275. doi: [10.1016/j.vetpar.2012.09.021](https://doi.org/10.1016/j.vetpar.2012.09.021) PMID: [23062691](https://pubmed.ncbi.nlm.nih.gov/23062691/)
55. Currie E, King B, Lawrenson AL, Schroeder LK, Kershner AM, Hermann GJ (2007) Role of the Caenorhabditis elegans multidrug resistance gene, mrp-4, in gut granule differentiation. *Genetics* 177: 1569–1582. PMID: [17947407](https://pubmed.ncbi.nlm.nih.gov/17947407/)
56. Korolnek T, Zhang J, Beardsley S, Scheffer GL, Hamza I (2014) Control of metazoan heme homeostasis by a conserved multidrug resistance protein. *Cell Metab* 19: 1008–1019. doi: [10.1016/j.cmet.2014.03.030](https://doi.org/10.1016/j.cmet.2014.03.030) PMID: [24836561](https://pubmed.ncbi.nlm.nih.gov/24836561/)
57. Wei S, Roessler BC, Chauvet S, Guo J, Hartman JLt, Kirk KL (2014) Conserved allosteric hot spots in the transmembrane domains of cystic fibrosis transmembrane conductance regulator (CFTR) channels and multidrug resistance protein (MRP) pumps. *J Biol Chem* 289: 19942–19957. doi: [10.1074/jbc.M114.562116](https://doi.org/10.1074/jbc.M114.562116) PMID: [24876383](https://pubmed.ncbi.nlm.nih.gov/24876383/)
58. Keppler D (2011) Multidrug resistance proteins (MRPs, ABCCs): importance for pathophysiology and drug therapy. *Handb Exp Pharmacol*: 299–323. doi: [10.1007/978-3-642-14541-4_8](https://doi.org/10.1007/978-3-642-14541-4_8) PMID: [21103974](https://pubmed.ncbi.nlm.nih.gov/21103974/)

Article

Antimicrobial activity of monoramnholipids produced by bacterial strains isolated from Ross sea (Antarctica)

Pietro Tedesco¹, Isabel Maida², Fortunato Palma Esposito¹, Emiliana Tortorella¹, Karolina Subko³, Chidinma Christiana Ezeofor³, Ying Zhang³, Jioji Tabudravu³, Marcel Jaspars³, Renato Fani² and Donatella de Pascale^{1*}

¹ Institute of Protein Biochemistry, National Research Council, Via P. Castellino, 111, I-80131 Naples, Italy. p.tedesco@ibp.cnr.it; f.palma@ibp.cnr.it; e.tortorella@ibp.cnr.it; d.depascale@ibp.cnr.it

² Department of Biology, University of Florence, Via Madonna del Piano 6, I-50019 Sesto Fiorentino (FI), Italy. isabel.maida@unifi.it; renato.fani@unifi.it;

³ Marine Biodiscovery Centre, Department of Chemistry University of Aberdeen, Old Aberdeen, AB24 3UE, Scotland, UK. k.subko.11@aberdeen.ac.uk; j.tabudravu@abdn.ac.uk; m.jaspars@abdn.ac.uk; chidinma.christiana.ezeofor.14@aberdeen.ac.uk; ying.zhang.14@aberdeen.ac.uk

* Author to whom correspondence should be addressed: Dr. Donatella de Pascale, IBP-CNR E-Mail: d.depascale@ibp.cnr.it. Tel.: +39 081 6132314; Fax: +39 081 6132277

All the authors belong to the EU-FP7 PharmaSea project, Grant agreement n° 312184

Academic Editor:

Received: / Accepted: / Published:

Abstract:

Microorganisms living in extreme environments represent a huge reservoir of novel antimicrobial compounds and possibly of novel chemical families. Antarctica is one of the most extraordinary places on Earth and exhibits many distinctive features. Antarctic microorganisms are well known producers of valuable secondary metabolites. Specifically, several Antarctic strains have been reported to inhibit opportunistic human pathogens strains belonging to *Burkholderia cepacia* complex (Bcc). Herein, we applied a biodiscovery pipeline for the identification of anti-Bcc compounds. Antarctic sub-sea

sediments were collected from the Ross Sea, and used to isolate 25 microorganisms, which were phylogenetically affiliated to three bacterial genera (*Psychrobacter*, *Arthrobacter*, and *Pseudomonas*) via sequencing and analysis of 16S rRNA genes. They were then subjected to a primary cell-based screening to determine their bioactivity against Bcc strains. Positive isolates were used to produce crude extracts from microbial spent culture media, to perform the secondary screening. Strain *Pseudomonas* BNT1 was then selected for bioassay-guided purification employing SPE and HPLC. Finally, LC-MS and NMR structurally resolved the purified bioactive compounds. With this strategy, we achieved the isolation of 3 Rhamnolipids, two of which were new, embedded with high (MIC < 1 µg/mL) and unreported antimicrobial activity against Bcc strains.

Keywords: Antimicrobials; Rhamnolipids; Antarctic; Bcc; microorganisms

1. Introduction

The alarming rise of Multi-Drug Resistance (MDR) bacteria in the last decades has highlighted the need for novel antimicrobial compounds and for effective drug discovery approaches [1, 2]. Natural products are the largest source of new antibiotic molecules, representing about two-thirds of new antibacterial therapies approved between 1980 and 2010 [3, 4]. Bioprospecting for natural products from unexplored natural environments, such as the marine environment is considered a promising strategy to identify novel compounds. It is increasingly recognized that a huge number of natural products and novel chemical entities exist in these environments, but the overwhelming biological diversity of these environments has so far only been explored to a very limited extent [5, 6]. The Antarctic environment, as well as having incredibly low temperatures, possesses other diverse traits that may have helped to shape the unique way in which Antarctic bacteria have evolved. This extreme environment contains hyper-salinity that exists in sea ice brine channels, a lack of free water due to freezing temperatures, as well as low nutrient availability. Unique light conditions also exist due to the high latitude of the region. Several studies have shown that Antarctic bacteria harvested from Antarctic corals and sponges are promising source of new antimicrobial compounds [7-14]. Specifically, several Antarctic strains belonging to the genus *Pseudoalteromonas*, *Psychrobacter*, *Pseudomonas*, and *Arthrobacter*, were able to inhibit the growth of several strains belonging to the *Burkholderia cepacia* complex (Bcc) [11, 14]. Further studies demonstrated that the antimicrobial activity relies (at least in part) on the production of Volatile Organic Compounds (VOCs)[12, 13, 15]. The Bcc consists of at

least 20 closely related species inhabiting different ecological niches such as water, soil, plants rhizosphere, and plants and animals [16-18]. Bcc are also opportunistic human pathogens that cause lung infections in immune-compromised individuals, including cystic fibrosis (CF) patients [19]. In one-third of infected individuals it causes the “cepacia syndrome” – a form of septic shock, which involves the lungs essentially shutting down resulting in fatality [20-22]. Bcc bacteria have showed to be very resilient and incredibly difficult to combat as they are resistant to almost all known antimicrobial agents and can survive under the most extreme conditions [23]. In this publication we report a complete biodiscovery pipeline aiming at the identification of novel anti-Bcc compounds, starting from the isolation of bacteria from Antarctic sub-sea sediments. Bacteria were tested for their antimicrobial potential and a bioassay-guided purification was performed that yielded 3 bioactive compounds active against Bcc. Structures were then elucidated and 2 compounds have not been reported previously.

2. Results and Discussion

2.1 Isolation of bacteria, typing and phylogenetic analysis

Psychrophilic Antarctic bacteria were isolated from sediments on PYG minimal medium. After 15 days of incubation at 4°C, 25 visible colonies were picked and grown in liquid PYG at 15 °C for 48 hours in agitation, and glycerol stab were stored at -80°C.

In order to check whether the 25 bacterial isolates represented either the same or different strains, a RAPD analysis was carried out using the primers 1253 (5'-GTTTCCGCCC-3') and AP5 (5'-TCACGCTGCG-3'). The RAPD profiles obtained were then compared among them; the comparative analysis obtained with primer 1253 revealed that the 25 Antarctic isolates were split into 18 different RAPD group (hereinafter RAPD haplotypes), most of which represented by just 1 bacterial isolate as summarized in **Table 1**. Two groups embedding more than one isolate were identified: group 1 (RAPD halpotype 1) including strains BTN1, BTN6, BTN 7, BTN8, BTN9 and BTN10 and group 4 (embedding isolates BTN20A, BTN20B, and BTN24). These data were completely confirmed by the RAPD analysis performed with primer AP5.

Genus	Strains	RAPD profile	Accession number
<i>Pseudomonas</i>	BTN1		KT989002
	BTN6		KT989003
	BTN7	1	KT989004
	BTN8		KT989005
	BTN9		KT989006
	BTN10		KT989007
	BTN3	2	KT989009
	BTN19	3	KT989019
	BTN20B	4	KT989021
	BTN24		KT989022
	BTN21	5	KT989025
	BTN23	6	KT989024
	BTN2	7	KT989008
	BTN11	8	KT989011
<i>Psychrobacter</i>	BTN5	9	KT989010
	BTN20A	4	KT989020
	BTN15	10	KT989015
	BTN13	11	KT989012
	BTN14	12	KT989013
	BTN17	13	KT989017
	BTN16	14	KT989016
	BTN18	15	KT989018
	BTN12	16	KT989014
	BTN22	17	KT989023
<i>Arthrobacter</i>	BTN4	18	KT989001

Table 1: list of the strains used in this work, for each strain are reported the genus and the RAPD haplotype.

The phylogenetic affiliation of bacterial isolates was performed through the 16S rRNA genes amplification and analysis. To this purpose the 16S rRNA genes were PCR amplified and the nucleotide sequence of the amplicons determined. Each sequence was used as a query in a BLAST search to retrieve the most similar ones. Sequences were then aligned using the program ClustalW and the alignment was used to construct the phylogenetic trees shown in **Figure S1**, revealing that:

- i) As expected on the basis of the sharing of RAPD profiles, the six strains exhibiting the same RAPD profile (RAPD haplotype 1) share the same 16S rRNA gene sequence and clustered together joining the species *Pseudomonas azotoformans*.
- ii) Strain BTN4 was affiliated to the genus *Arthrobacter*.
- iii) All the other strains were affiliated to the genus *Psychrobacter* and, according to the different RAPD profile they exhibited, joined different *Psychrobacter* clades. The three strains (BTN20A, BTN24 and BTN 20B) sharing the same RAPD profile (RAPD haplotype 4), joined the same *Psychrobacter* cluster.

2.2 Cross-streaking experiments

In order to check the ability of Antarctic bacteria to inhibit the growth of Bcc strains, cross-streaking experiments were performed using representative of each RAPD haplotype as test strain. We used as targets a panel of 84 different Bcc strains belonging to 17 known species (see **Table S1**). Most of the strains had a clinical origin. Data obtained are summarized in **Table S1**, revealing that all BTN strains are able to completely inhibit the growth of Bcc strains. In order to check whether this anti-Bcc activity was due VOCs synthesis, a further cross-streaking experiment was performed using Petri dishes with a central septum, which physically separates the tester (Antarctic) from the target strains. To perform this analysis we selected the 17 Bcc type strains listed in **Table S2**, which are highlighted in red. Data obtained are reported in **Table 2** and revealed that the inhibitory power of the BTN strains decreased in the presence of the central septum. This finding suggested that BTN strains synthesize a combination of volatile and soluble molecules and that the Bcc-inhibitory activity likely might rely principally on the soluble fraction. Thus, we decided to concentrate our efforts on the soluble molecules for this study.

Bcc Strain	S	BTN strain																							C+
		1	2	3	5	11	13	14	4	12	15	16	17	18	19	20 _a	20 _b	21	22	23					
<i>B. ambifaria</i> LMG 19182	W	-	-	-	-	-	-	-	-	-	-	-	-	-	-	-	-	-	-	-	-	-	-	+	
	N	-	-	-	-	-	-	-	-	-	-	-	-	-	-	-	-	-	-	-	-	-	-	-	+
<i>B. anthina</i> LMG 20980	W	-	-	-	-	-	-	-	-	-	-	-	-	-	-	-	-	-	-	-	-	-	-	+	
	N	-	-	-	-	-	-	-	-	-	-	-	-	-	-	-	-	-	-	-	-	-	-	-	+
<i>B. vietnamensis</i> LMG10929	W	-	-	-	-	-	-	-	-	-	-	-	-	-	-	-	-	-	-	-	-	-	-	+	
	N	-	-	-	-	-	-	-	-	-	-	-	-	-	-	-	-	-	-	-	-	-	-	+	
<i>B. cenocepacia</i> LMG 16656	W	±	-	±	±	-	±	-	-	-	-	-	±	±	-	±	±	-	-	-	-	-	-	+	
	N	-	-	-	-	-	-	-	-	-	-	-	-	-	-	-	-	-	-	-	-	-	-	+	
<i>B. cepacia</i> LMG 1222	W	±	±	±	±	±	±	±	±	±	±	±	±	±	±	±	±	±	±	±	±	±	±	+	
	N	-	-	-	-	-	-	-	-	-	-	-	-	-	-	-	-	-	-	-	-	-	-	+	
<i>B. contaminans</i> LMG 23361	W	±	±	±	±	±	±	±	±	±	±	±	±	±	±	±	±	±	±	±	±	±	±	+	
	N	-	-	-	-	-	-	-	-	-	-	-	-	-	-	-	-	-	-	-	-	-	-	+	
<i>B. diffusa</i> LMG 24065	W	±	±	±	±	±	±	±	±	±	±	±	±	±	±	±	±	±	±	±	±	±	±	+	
	N	-	-	-	-	-	-	-	-	-	-	-	-	-	-	-	-	-	-	-	-	-	-	+	
<i>B. dolosa</i> LMG 18943	W	±	±	±	±	±	±	±	±	±	±	±	±	±	±	±	±	±	±	±	±	±	±	+	
	N	-	-	-	-	-	-	-	-	-	-	-	-	-	-	-	-	-	-	-	-	-	-	+	
<i>B. lata</i> LMG 22485	W	±	±	±	±	±	±	±	-	±	±	±	±	±	±	±	±	±	±	±	±	±	±	+	
	N	-	-	-	-	-	-	-	-	-	-	-	-	-	-	-	-	-	-	-	-	-	-	+	
<i>B. latens</i> LMG 24064	W	-	-	±	±	±	-	-	-	-	±	±	±	±	-	±	±	-	-	-	-	-	-	+	
	N	-	-	-	-	-	-	-	-	-	-	-	-	-	-	-	-	-	-	-	-	-	-	+	
<i>B. metallica</i> LMG 24068	W	±	±	±	±	±	±	±	±	±	±	±	±	±	±	±	±	±	±	±	±	±	±	+	
	N	-	-	-	-	-	-	-	-	-	-	-	-	-	-	-	-	-	-	-	-	-	-	+	
<i>B. multivorans</i> LMG 13010	W	-	±	±	±	±	±	±	-	±	±	±	±	±	±	±	±	±	±	±	±	±	±	+	
	N	-	-	-	-	-	-	-	-	-	-	-	-	-	-	-	-	-	-	-	-	-	-	+	
<i>B. pseudomultivorans</i> LMG 26883	W	±	±	±	±	±	±	±	±	±	±	±	±	±	±	±	±	±	±	±	±	±	±	+	
	N	-	-	-	-	-	-	-	-	-	-	-	-	-	-	-	-	-	-	-	-	-	-	+	
<i>B. pyrrocinia</i> LMG 14191	W	±	±	±	±	±	±	±	±	±	±	±	±	±	±	±	±	±	±	±	±	±	±	+	
	N	-	-	-	-	-	-	-	-	-	-	-	-	-	-	-	-	-	-	-	-	-	-	+	
<i>B. seminalis</i> LMG 24067	W	-	±	±	±	±	±	±	-	±	-	±	±	±	±	±	±	-	±	±	±	±	±	+	
	N	-	-	-	-	-	-	-	-	-	-	-	-	-	-	-	-	-	-	-	-	-	-	+	
<i>B. stabilis</i> LMG 14294	W	±	±	±	±	±	±	±	±	±	±	±	±	±	±	±	±	-	±	±	±	±	±	+	
	N	-	-	-	-	-	-	-	-	-	-	-	-	-	-	-	-	-	-	-	-	-	-	+	
<i>B. uborrensis</i> LMG 20358	W	-	-	±	±	±	±	±	-	±	±	±	±	±	-	±	±	±	±	±	±	±	±	+	
	N	-	-	-	-	-	-	-	-	-	-	-	-	-	-	-	-	-	-	-	-	-	-	+	

Table 2: Growth of Bcc strains in cross-streaking experiment carried out using Petri dishes either with (W) or without (N) a central septum (S). Symbols: +, growth; ±, reduced growth; -, no growth.

2.3 Extracts antimicrobial assay

Eight of the most active Antarctic strains belonging to the three different genera (*Pseudomonas*, *Psychrobacter*, and *Arthrobacter*) were selected and used to produce extracts, which were then tested against a reduced panel of Bcc type-strains isolated from CF patients. The MIC assays were carried out as described in Materials and Methods. **Table 3** reports the antimicrobial activity as percentage of Bcc growth inhibition in the presence of each extract at a concentration of 1 mg/mL.

Species	Strain	<i>Pseudomonas</i>	<i>Psychrobacter</i>						<i>Arthrobacter</i>
		BTN 1	BTN 2	BTN 15	BTN 3	BTN 19	BTN 21	BTN 5	BTN 4
<i>B. diffusa</i>	LMG 24065	100 ± 0	75 ± 3	77 ± 3	43 ± 7	45 ± 11	70 ± 4	77 ± 9	63 ± 3
<i>B. metallica</i>	LMG 24068	92 ± 4	70 ± 5	71 ± 3	32 ± 2	30 ± 3	53 ± 5	77 ± 4	64 ± 9
<i>B. cenocepacia</i>	LMG 16656	100 ± 0	78 ± 2	87 ± 1	84 ± 6	64 ± 4	45 ± 1	84 ± 2	57 ± 1
<i>B. latens</i>	LMG 24064	100 ± 0	53 ± 11	75 ± 2	55 ± 6	43 ± 3	65 ± 2	56 ± 3	41 ± 2
<i>B. seminalis</i>	LMG 24067	100 ± 0	43 ± 6	67 ± 5	73 ± 8	45 ± 6	78 ± 11	40 ± 3	56 ± 3

Table 3: Antimicrobial activity of BTN cell extracts reported as % of inhibition of Bcc strains treated with 1 mg/mL of BTN extracts. .

Data obtained revealed that the extracts were differentially active against the selected Bcc strains. Three Antarctic bacterial strains, i.e. BTN2, BTN15, and BTN5, were able to inhibit at least three of the five Bcc strains more than 70 % of growth. However, the extract from *Pseudomonas* BTN1 exhibited the best anti-Bcc activity; indeed, it was able to almost completely inhibit the growth of all the target strains at the concentration used. For this reason, this strain was selected for further scale-up and extract purification.

2.4 Bioassay-guided purification of BTN1 extract

Pseudomonas sp. BTN1 strain was grown in 3L TYP medium for 5 days at 20°C, then the culture broth was extracted with ethyl acetate. Subsequently, the crude extract (1 g) was fractionated with a SPE C18 Cartridge. Elution was performed stepwise with an increasing methanol concentration. The 4 eluted fractions were collected, dried and dissolved in DMSO to perform bioassay at a stock concentration of 50 mg/mL. The fraction eluted at 100% methanol was shown to be the most active one against *B. cenocepacia* LMG 16656 with a MIC of 50 µg/mL and was subjected to HPLC separation. HPLC chromatograms extracted from 200 to 400 nm presented 11 different peaks, which were separated, dried and dissolved in DMSO at a stock concentration of 10 mg/mL to perform MIC

assay. Data obtained revealed promising inhibitory activity against *B. cenocepacia* strain LMG 16656 of three compounds, hereinafter referred to as Compound **1**, **2** and **3**, respectively.

2.5 Compound structure elucidation

The molecular formula of compound **1** was established as C₂₈H₅₂O₉ by HRESIMS (555.35141 Δ 0.92 ppm [M+Na]⁺). Dereplication of this compound based on 1D, 2D NMR and LCMS data indicated that the primary structure of **1** was similar to a known rhamnolipid [24], but differed in terms of the relative configuration of the sugar moiety. The relative configuration of the sugar unit of compound **1** was identified as β -L-rhamnopyranose as compared to α -L-rhamnopyranose for the known compound based on analysis of coupling constants and proton chemical shifts and by comparing with literature values (ref).

The molecular formula of Compound **2** was established as C₂₈H₅₀O₉ by high-resolution electrospray ionization mass spectrometry (HRESIMS) (553.33429 Δ -0.75 ppm [M+Na]⁺) and subsequent dereplication suggested it was new. The molecular formula suggested 4 degrees of unsaturation. The ¹H, ¹³C NMR data (Table 1) in CD₃OD of **2** revealed one ester (δ_C 173.4 ppm), one carboxylic acid group (δ_C 171.40) ppm, two olefinic carbons (δ_C 132.8, 123.7 ppm), and an anomeric carbon (δ_C 98.47 ppm) of a sugar unit. This analysis accounted for 3 of the double bond equivalents, suggesting that the sugar unit was present as a ring. The structure was elucidated based on 2D NMR correlation experiments. Data clearly showed three distinctive spin systems. There were COSY correlations observed between the anomeric proton and the adjacent protons of the sugar unit. There was a strong observed COSY correlation between the methyl group at δ_H 1.27 ppm and the proton at δ_H 3.38 ppm placing the methyl group at position C5. The proposed structure was fully supported by HMBC correlations (Table 4) indicating that compound **2** is a rhamnolipid with the A and B chains having 10 and 12 carbons respectively, and a single unsaturation at position B5. The sugar moiety in compound **2** was identified as β -L-rhamnopyranose based on the chemical shift of the anomeric proton, δ_H 4.86 ppm as compared to δ_H 5.11 ppm for α -L-rhamnopyranose sugars, and similarities of proton chemical shifts with β -L-rhamnopyranose sugars (Ref). Because of overlap of the water peak and the anomeric proton in the ¹H NMR spectrum of **2** in CD₃OD it was remeasured in DMSO-d₆. It showed the anomeric proton as a broad singlet suggesting that the sugar was linked in an equatorial position to the lipid chain giving rise to a very small coupling constant with H-2 (³J(1,2)). All the other coupling constants (³J(2,3), 3.5 Hz), (³J(3,4), 9.5 Hz), (³J(4,5), 9.8 Hz) agreed with the published data for β -L-rhamnopyranose sugars (ref).

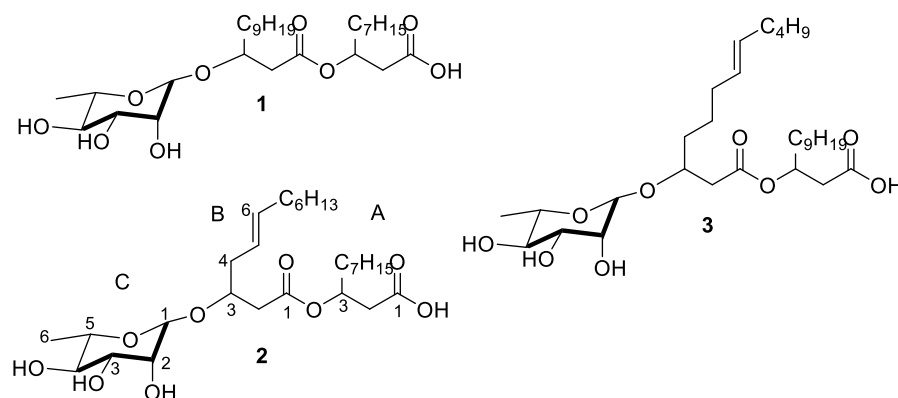


Figure 1. Structures of the 3 rhamnolipids isolated from *Pseudomonas* BTN1.

The molecular formula of compound **3** was established as $C_{30}H_{54}O_9$ by HRESIMS 581.36490 Δ 1.72 ppm $[M+Na]^+$. Based on 1D and 2D NMR data compound **3** was similar to **2**, the difference being an additional C_2H_4 unit. However, careful interpretation of the data indicated that both the lipid chains A and B were C12 carbons with a single unsaturation at position B7 instead of C10 and C12 carbons and an unsaturation position at B5 in **2**. The relative configuration of the sugar unit was similar to that of compound **2** based on analysis of chemical shifts and proton coupling constants.

		2				3			
	Position	δ_C /ppm	δ_H /ppm (m, J in Hz)	COSY $^1H-^1H$	HMBC H \rightarrow C	δ_C /ppm	δ_H /ppm (m, J in Hz)	COSY $^1H-^1H$	HMBC H \rightarrow C
A	1	173.4				175.5			
	2	38.9	2.58, dd, 7.1, 6.0	A3	A1	40.9	2.55, m; 2.53, m	A3	A1
	3	71.1	5.27, quintet, 6.70	A2, A3	A1, A2	72.7	5.29, quintet	A2, A4	A1, A2
	4	33.8	1.64, m	A3	A3	34.9	1.63, bm	A3	A3
	5	24.9	1.35, overlap			26.0	1.35, overlap		
	6	29.3	1.31, overlap			30.5	1.37, overlap		
	7	29.3	1.31, overlap			30.1	1.32, overlap		
	8	31.6	1.31, overlap			29.8	1.33, overlap		
	9	22.3	1.33, overlap	A10	A10	30.2	1.36, overlap	A10	A10
	10	13.1	0.92, m	A9	A9	32.7	1.31, overlap	A9	A9
	11					23.4	1.33, overlap		
	12					14.1	0.92, m		
B	1	171.4				172.3			
	2	39.5	2.53, dd, 8.0, 7.09	B3	B1	41.0	2.59, m; 2.50, m	B3	B1
	3	72.9	4.16, quintet, 5.76	B2, B4	B1, B5	74.8	4.10, quintet, 5.87	B2, B4	B1, B5

	4	30.4	2.39, m	B3, B5	B3, B5	33.5	1.58, bm	B3, B5	B3, B5
	5	123.7	5.40, m	B4, B6	B3, B4, B6, B7	25.7	1.43, overlap	B4, B6	
	6	132.8	5.55, m	B5, B7	B5, B8	27.8	2.08, overlap	B5, B7	
	7	27.1	2.08, quartet	B6	B5, B6	130.0	5.37, m	B6, B8	B8, B9
	8	29.3	1.31, overlap			131.2	5.39, m	B7	B7
	9	28.9	1.33, overlap	B7		32.7	1.31, overlap	B8	
	10	31.6	1.31, overlap			32.7	1.31, overlap		
	11	22.3	1.33, overlap		B12	23.4	1.33, overlap	B12	
	12	13.1	0.92, m		B11	14.1	0.92, m	B11	
C	1	98.5	4.86, overlap	C2	B3, C2	100.0	4.80, d, 1.44	C2	B3, C2
	2	71.2	3.77, dd, 3.45, 1.70	C1, C3	C3, C4	72.4	3.76, dd, 3.42, 1.66	C1, C3	C3, C4
	3	70.9	3.64, dd, 9.46, 3.46	C2, C4	C5	71.9	3.66, dd, 9.70, 3.46	C2, C4	C5
	4	72.7	3.38, dd, 9.81, 9.78	C3, C5	C3	73.8	3.35, dd, 9.94, 8.84	C3, C5	C3
	5	68.7	3.67, m	C4, C6	C4, C6	69.8	3.68, m	C4, C6	C4, C6
	6	16.7	1.27, d, 6.22	C5	C5	17.6	1.27, d, 6.33	C5	C5

Table 4. NMR data of 2 and 3 in CD₃OD. ^a150 MHz; ^b600 MHz

Compound 2. [α]_D -53.4° (*c* 0.001 MeOH; UV(MeOH) λ_{\max} (log ϵ) 202 (3.55) nm; IR (film) ν_{\max} 3361, 2925, 2855, 1735, 1671, 1575, 1455, 1380, 1314, 1207, 1161, 1126, 1037, 983, cm⁻¹; ¹H, ¹³C, HMBC NMR data see Table 1; HRESIMS *m/z* 553.33429 Δ -0.75 ppm [M+Na]⁺ calculated for C₂₈H₅₀O₉.

Compound 3. [α]_D +49.3° (*c* 0.001 MeOH. UV(MeOH) λ_{\max} (log ϵ) 202 (3.78) nm; IR (film) ν_{\max} 3387, 2926, 2855, 1667, 1587, 1402, 1316, 1204, 1130, 1072, 1049, 983 cm⁻¹; ¹H, ¹³C, HMBC NMR data see Table 1; HRESIMS *m/z* 581.36490 Δ 1.72 ppm [M+Na]⁺ calculated for C₃₀H₅₄O₉.

2.6 Antimicrobial activity of BTNI pure compounds

The three monorhamnolipids isolated from strain BTNI were tested against a selected panel of Bcc strains isolated from CF patients and *S. aureus*. MIC and MBC values are reported in Table 5. It is worth noticing that the 3 compounds have identical MIC and MBC values indicating a bactericidal effect against the target bacteria, as reported for several natural biosurfactants [25, 26]. Compounds 2 and 1 were the most active compounds as they were effective against all the tested stains, with the only exception of *B. diffusa*. Specifically, compounds 2 and 1 had the lowest MBC values against *B. cenocepacia* (3.12 μ g/mL) and *S. aureus* (respectively 3.12 and 1.56 μ g/mL). Compound 3 had antimicrobial effect only against *S. aureus* with a MBC value of 100 μ g/mL, while resulted to ineffective towards Bcc strains. Rhamnolipids (RLs) are well-known secondary metabolites

synthesized by members of different Gram-negative species, particularly from bacteria belonging to the genus *Pseudomonas*. They perform several potential functions in bacteria: as powerful biosurfactants they are involved in the uptake and biodegradation of poorly soluble substrates and are essential for surface motility and biofilm development [27]. Recently, they have emerged as potential antimicrobials against a broad range of pathogens such as *Staphylococcus*, *Mycobacterium*, and *Bacillus*, and significant activity against a number of Gram-negative species, including *Serratia marcescens*, *Enterobacter aerogenes*, and *Klebsiella pneumoniae* [28-30]. RLs act like synthetic surfactants and their proposed mechanism of action consists of intercalation into biological membranes and destruction by their permeabilising effect leading to cell death [31].

Antimicrobial activity ($\mu\text{g/mL}$)												
	<i>B. cenocepacia</i> LMG 16656		<i>B. metallica</i> LMG 24068		<i>B. seminalis</i> LMG 24067		<i>B. diffusa</i> LMG 24065		<i>B. latens</i> LMG 24064		<i>S. aureus</i> 6538P	
	MIC	MBC	MIC	MBC	MIC	MBC	MIC	MBC	MIC	MBC	MIC	MBC
C1	3.12	3.12	50	50	12.5	12.5	>200	>200	12.5	12.5	1.56	1.56
C2	3.12	3.12	25	25	3.12	3.12	200	200	12.5	12.5	3.12	3.12
C3	200	200	>200	>200	>200	>200	>200	>200	>200	>200	100	100

Table 5. MIC and MBC values of the 3 mono-rhamnolipids isolated in this study.

3. Experimental Section

3.1 Isolation of bacterial strains

The Antarctic bacterial strains used in this study were isolated from environmental samples collected at -20 m of depth (sub-sea sediments) near the Mario Zucchelli Station, Baia Terranova, Ross sea, Antarctica (74.6936° S, 164.1117° E). 1 gr of sediments was mixed with 20 mL of M9 salts solution (KH_2PO_4 3.0 g/L, Na_2HPO_4 6.0 g/L, NaCl 0.5 g/L, NH_4Cl 1.0 g/L) in a 50 mL Falcon tube and gently mixed; the supernatant was serially diluted in sterile M9 buffer and plated on PYG medium (Peptone 5.0 g/L, Yeast extract 4.0 g/L, Glucose 1.0 g/L, CaCl_2 0.2 g/L, $\text{MgSO}_4 \cdot 7\text{H}_2\text{O}$ 0.4 g/L, K_2HPO_4 1.0 g/L, KH_2PO_4 1.0 g/L, NaHCO_3 10.0 g/L NaCl 2.0 g/L and 17 g/L). After 15 days of incubation 24 visible colonies were picked, grown in liquid PYG and stored at -80°C.

3.2 Target strains and growth conditions

Bcc strains used in this work are listed in **Table 2** and **Table S1**. Bcc and *S. aureus* 6538P were routinely grown on Luria-Bertani broth (LB) (Tryptone 10 g/L, Yeast extract 5 g/L, NaCl 10 g/L) at 37 °C. BTN isolated Antarctic strains were routinely grown in TYP medium (Bacto-tryptone 16 g/L, 16 g/L Yeast extract, 10 g/L NaCl) and Marine Broth (MB) at 21 °C. To allow bacterial growth on solid media, 17 g/L of bacteriological agar were added to each medium.

3.3 RAPD analysis

Typing of bacterial isolates was performed using the Random Amplified Polymorphic DNA (RAPD) technique performed on cell lysates [32-34]; to this purpose, Antarctic bacterial colonies grown overnight at 21°C on MA plates were suspended in 25 µl of sterile distilled water, heated to 95°C for 10 min, and cooled on ice for 5min. RAPD analysis was carried out in a total volume of 25µl containing 1X Reaction Buffer, 300 µM MgCl₂, 200 µM of each deoxynucleoside triphosphate, 0.5 U of Polytaq DNA polymerase (Polymed, Florence, Italy), 10 µM of primer 1253 (5' GTTCCGCC 3') or primer AP5 (5' TCACGCTGCG 3') and 2 µl of lysate cell suspension [34]. PCR were performed using MasterCycle Personal Thermal Cycler (Eppendorf, Hamburg, Germany). After incubation at 90°C for 1 min and 95°C for 1.5 min, the reaction mixtures were cycled 45 times through the following temperature profile: 95°C for 30 s, 36°C for 1 min, and 75°C for 1 min. Samples were then incubated at 60°C for 10 min, and finally at 5° C for 10 min. Amplification products were then stored at -20°C. Reaction products were analyzed by agarose (2.5 % w/v) gel electrophoresis in TAE buffer containing 0.5 µg/ml (w/v) of ethidium bromide.

3.4 Phylogenetic affiliation of BTN strains

Two µl of each cell lysate were used for the amplification *via* PCR of 16S rRNA genes. PCR were carried out in a total volume of 50 µl containing 1X Reaction Buffer, 150 µM MgCl₂, 250 µM of each deoxynucleoside triphosphate, and 2.0 U of Polytaq DNA polymerase and 0.6 µM of primer P0 (5' GAGAGTTTGATCCTGGCTCAG) and P6 (5' CTACGGCTACCTTGTTACGA)[35]. The reaction conditions used were: 1 cycle (95° C for 90 s), 30 cycles (95° C 30 s, 50° C 30 s, and 72° C 1 min), with a final extension of 10 min at 72 °C. Amplicons corresponding to the 16S rRNA genes (observed under UV light, 312 nm) were excised from the gel and purified using the "QIAquick" gel extraction kit (QiAgen, Chatsworth, CA) according to manufacturer's instructions. Direct sequencing was performed on both DNA strands using an ABI PRISM 310 Genetic Analyzer (Applied Biosystems,

Forster City, CA) and the chemical dye terminator [36]. Each 16S rRNA gene sequence was submitted to GenBank and assigned the accession number shown in Table 1. BLAST probing of DNA databases was performed with the BLASTn option of the BLAST program using default parameters [37]. Nucleotide sequences were retrieved from RDP databases. The ClustalW program was used to align the 16S rRNA gene sequences obtained with the most similar ones retrieved from the databases [38]. Each alignment was checked manually, corrected, and then analysed. The evolutionary history was inferred using the Neighbor-Joining method according to the model of Kimura 2-parameter distances [39, 40]. The percentage of replicate trees where the associated taxa clustered together in the bootstrap test (1000 replicates) is shown next to the branches [41].

3.4 Cross streaking

Cross-streaking experiments were carried out as previously described [11]. Petri dishes with or without a septum separating two hemi-cycles were used. Plates with a central septum allowed the growth of tester and target strains without any physical contact. Antarctic strains (tester strains) were grown on MA for four days at 21°C; then they were streaked on TYP and incubated at 21°C for four days. Bcc strains (target strains) were perpendicularly streaked to the initial streak and plates were further incubated at 21°C for two days and at 37°C for two additional days. The experiments were conducted in parallel with a positive control to verify the viability of Bcc cells.

3.5 Extract preparation

A single colony of a bacterial isolate was used to inoculate 3 mL of liquid TYP media in sterile bacteriological tube. After 48 h of incubation at 21°C at 200 rpm the pre-inoculum was used to inoculate 100 mL of TYP medium in a 500 mL flask, at an initial cell concentration of 0.01-OD₆₀₀/mL. The flasks were incubated up to 5 days at 21°C at 200 rpm. The cultures were then centrifuged at 6800 x g at 4°C for 30', and the exhausted culture broths were collected and stored at -20°C. The exhausted culture broths were subjected to organic extraction using 3 volume of ethyl acetate in a 500 mL separatory funnel. The organic phase collected was evaporated using a Laborota 4000 rotary evaporator (Heidolph, Schwabach, Germany), and the extracts were weight, dissolved in 100% DMSO at 50 or 100 mg/mL and stored at -20°C.

3.6 Antimicrobial assays

3.6.1 Minimal inhibitory concentration assay (MIC)

To evaluate the antimicrobial potential of Antarctic extracts, samples were placed into each well of a 96-well microtiter plate at an initial concentration of 2% (v/v) and serially diluted using LB medium. Wells containing no compound represented the negative control. DMSO was used as control to determine the effect of solvent on cell growth. A single colony of a Bcc strain was used to inoculate 3 mL of liquid LB media in sterile bacteriological tube. After 6-8 h of incubation, growth was measured by monitoring the absorbance at 600 nm and about 40000 CFU were dispensed in each well of the prepared plate. Plates were incubated at 37°C for 24h and growth was measured with a Cytation3 Plate Reader (Biotek, Winoosky, VT) by monitoring the absorbance at 600 nm.

3.6.2 Minimal bactericidal concentration (MBC) assay

To determine the MBC, the dilution representing the MIC and two of the more concentrated test product dilutions were plated on LB agar plates and enumerated to determine CFU/ml. An aliquot of the positive control was plated and used to establish a baseline concentration of the microorganism used.

3.7 Purification of ethyl-acetate crude extract

Crude extract of 3L BTN1 fermentation, prepared as described above, was subjected to fractionation using Chromabond SPE C18 column cartridges (Macherey-Nagel, Duren, Germany) The sample was dissolved in methanol and loaded on the top of the column. Elution was performed at step increasing methanol concentration (25%-50%-100%-100%+TFA). HPLC separations were carried out using a VP 250/10 Nucleodur C18 HTec, 5 µm, (Macherey-Nagel Duren, Germany) connected to a Ultimate 3000 HPLC Chromatograph with a Ultimate 3000 Diode Array detector and in-line degasser (Dionex, Sunnyvale, CA). Detection was achieved on-line through a scan of wavelengths from 200 to 400 nm.

3.8 NMR- LCMS experiments

NMR data, both 1D and 2D were recorded on a spectrometer (Bruker, Billerica, MA) at 600 and 150 MHz for ¹H and ¹³C respectively using an ID cryoprobe in methanol-d₄ as solvent. Chemical shifts are reported in parts per million (δ/ppm) downfield relative to residual CD₃OD at 3.31 ppm for protons and 49.0 ppm for carbons. High-resolution mass spectrometry and fragmentation data were recorded

using a LTQ Orbitrap system (ThermoScientific, Whaltman, MA) coupled to an 1290 Infinity HPLC system (Agilent, Santa Clara, CA). The following conditions were used: capillary voltage 45 V, capillary temperature 320°C, auxiliary gas flow rate 10-20 arbitrary units, sheath gas flow rate 40-50 arbitrary units, spray voltage 4.5 kV, mass range 100-2000 amu (maximum resolution 30,000). Optical rotation measurements were recorded using a Perkin Elmer, Model 343 Polarimeter at 589 nm (Perkin Elmer, Whaltman, MA). The UV spectrum was recorded on a UV-Vis spectrophotometer model S10 (Spectromlab, Barcelona, Spain). The IR was recorded on a PerkinElmer FTIR Spectrum Two instrument (Perkin Elmer, Whaltman, MA).

4. Conclusions

Exploiting a bioassay-driven purification approach, 3 RLs (one of which was novel) with antimicrobial activity against Bcc strains, were isolated from *Pseudomonas* sp. BTN1, recovered from Antarctic sediments. RLs represent a promising class of biosurfactants as antimicrobials or in combination with antibiotics. A recent study suggested the use of RLs as an additive in the formulation of antibiotic and other antimicrobial agents for enhancing the effectiveness of chemotherapeutics [42]. Moreover, the possibility of RLs production by the fermentation of organic waste (such as waste oils), make this products economically appealing [43]. To the best of our knowledge, this is the first report of antimicrobial activity of RLs against Bcc strains, and it prompts future studies aimed at RLs exploitation as drugs to counteract these hazardous opportunistic human pathogens.

Acknowledgments

This work was supported by the EU FP7 KBBE 2012-2016 project PharmaSea, grant N° 312184 and from the Italian Cystic Fibrosis Research foundation (Grant FFC#12/2011).

Author Contribution

PT, IM, RF, JT, MJ and DDP conceived and designed the experiments; PT, IM, FPE, ET, JT, KS, CCE, YZ performed the experiments; PT, IM, FPE, KS, CCE, YZ RF, JT, and DDP analyzed the data; RF, MJ and DDP contributed reagents/materials/analysis tools; PT, IM, FPE, JT, RF, MJ and DDP wrote the paper.

Conflict of Interest

The authors declare no conflict of interest.

References and Notes

1. Berdy, J., Thoughts and facts about antibiotics: where we are now and where we are heading. *The Journal of antibiotics* **2012**, *65*, (8), 385-95.
2. Tegos, G. P.; Hamblin, M. R., Disruptive innovations: new anti-infectives in the age of resistance. *Current opinion in pharmacology* **2013**, *13*, (5), 673-7.
3. Newman, D. J.; Cragg, G. M., Natural products as sources of new drugs over the 30 years from 1981 to 2010. *Journal of natural products* **2012**, *75*, (3), 311-35.
4. Bologna, C. G.; Ursu, O.; Oprea, T. I.; Melancon, C. E., 3rd; Tegos, G. P., Emerging trends in the discovery of natural product antibacterials. *Current opinion in pharmacology* **2013**, *13*, (5), 678-87.
5. Zhu, F.; Ma, X. H.; Qin, C.; Tao, L.; Liu, X.; Shi, Z.; Zhang, C. L.; Tan, C. Y.; Chen, Y. Z.; Jiang, Y. Y., Drug discovery prospect from untapped species: indications from approved natural product drugs. *PloS one* **2012**, *7*, (7), e39782.
6. Jaspars, M.; Challis, G., Microbiology: a talented genus. *Nature* **2014**, *506*, (7486), 38-9.
7. von Salm, J. L.; Wilson, N. G.; Vesely, B. A.; Kyle, D. E.; Cuce, J.; Baker, B. J., Shagenes A and B, new tricyclic sesquiterpenes produced by an undescribed Antarctic octocoral. *Organic letters* **2014**, *16*, (10), 2630-3.
8. Godinho, V. M.; Goncalves, V. N.; Santiago, I. F.; Figueredo, H. M.; Vitoreli, G. A.; Schaefer, C. E.; Barbosa, E. C.; Oliveira, J. G.; Alves, T. M.; Zani, C. L.; Junior, P. A.; Murta, S. M.; Romanha, A. J.; Kroon, E. G.; Cantrell, C. L.; Wedge, D. E.; Duke, S. O.; Ali, A.; Rosa, C. A.; Rosa, L. H., Diversity and bioprospection of fungal community present in oligotrophic soil of continental Antarctica. *Extremophiles : life under extreme conditions* **2015**, *19*, (3), 585-96.
9. Lee, L. H.; Cheah, Y. K.; Nurul Syakima, A. M.; Shiran, M. S.; Tang, Y. L.; Lin, H. P.; Hong, K., Analysis of Antarctic proteobacteria by PCR fingerprinting and screening for antimicrobial secondary metabolites. *Genetics and molecular research : GMR* **2012**, *11*, (2), 1627-41.
10. Papa, R.; Parrilli, E.; Sannino, F.; Barbato, G.; Tutino, M. L.; Artini, M.; Selan, L., Anti-biofilm activity of the Antarctic marine bacterium *Pseudoalteromonas haloplanktis* TAC125. *Research in microbiology* **2013**, *164*, (5), 450-6.
11. Papaleo, M. C.; Fondi, M.; Maida, I.; Perrin, E.; Lo Giudice, A.; Michaud, L.; Mangano, S.; Bartolucci, G.; Romoli, R.; Fani, R., Sponge-associated microbial Antarctic communities exhibiting antimicrobial activity against *Burkholderia cepacia* complex bacteria. *Biotechnology advances* **2012**, *30*, (1), 272-93.
12. Papaleo, M. C.; Romoli, R.; Bartolucci, G.; Maida, I.; Perrin, E.; Fondi, M.; Orlandini, V.; Mengoni, A.; Emiliani, G.; Tutino, M. L.; Parrilli, E.; de Pascale, D.; Michaud, L.; Lo Giudice, A.; Fani, R., Bioactive volatile organic compounds from Antarctic (sponges) bacteria. *New biotechnology* **2013**.
13. Romoli, R.; Papaleo, M. C.; de Pascale, D.; Tutino, M. L.; Michaud, L.; LoGiudice, A.; Fani, R.; Bartolucci, G., Characterization of the volatile profile of Antarctic bacteria by using solid-phase microextraction-gas chromatography-mass spectrometry. *Journal of mass spectrometry : JMS* **2011**, *46*, (10), 1051-9.
14. Maida I., B. E., Fondi M., Perrin E., Orlandini V., Papaleo M.C., Mengoni A., de Pascale D., Tutino M.L., Michaud L., Lo Giudice A. and Fani R., Antimicrobial activity of *Pseudoalteromonas* strains isolated from the Ross Sea (Antarctica) vs Cystic Fibrosis opportunistic pathogens. *Hydrobiologia* **2015**, Accepted for publication.
15. Romoli, R.; Papaleo, M. C.; de Pascale, D.; Tutino, M. L.; Michaud, L.; Lo Giudice, A.; Fani, R.; Bartolucci, G., GC-MS Volatolomic Approach to Study the Antimicrobial Activity of the Antarctic Bacterium *Pseudoalteromonas* sp.TB41. *Metabolomics* **2013**, *10*, 42-51.
16. Coenye, T.; Vandamme, P., Diversity and significance of *Burkholderia* species occupying diverse ecological niches. *Environmental microbiology* **2003**, *5*, (9), 719-29.

17. Compant S, N. J., Coenye T, Clement C, Ait Barka E, Diversity and occurrence of Burkholderia spp. in the natural environment. *FEMS Microbiol Rev* **2008**, *32*(4), 607-626.
18. De Smet, B.; Mayo, M.; Peeters, C.; Zlosnik, J. E.; Spilker, T.; Hird, T. J.; LiPuma, J. J.; Kidd, T. J.; Kaestli, M.; Ginther, J. L.; Wagner, D. M.; Keim, P.; Bell, S. C.; Jacobs, J. A.; Currie, B. J.; Vandamme, P., Burkholderia stagnalis sp. nov. and Burkholderia territorii sp. nov., two novel Burkholderia cepacia complex species from environmental and human sources. *International journal of systematic and evolutionary microbiology* **2015**, *65*, (7), 2265-71.
19. Drevinek, P.; Mahenthiralingam, E., Burkholderia cenocepacia in cystic fibrosis: epidemiology and molecular mechanisms of virulence. *Clinical microbiology and infection : the official publication of the European Society of Clinical Microbiology and Infectious Diseases* **2010**, *16*, (7), 821-30.
20. Ramsay, K. A.; Butler, C. A.; Paynter, S.; Ware, R. S.; Kidd, T. J.; Wainwright, C. E.; Bell, S. C., Factors influencing acquisition of Burkholderia cepacia complex organisms in patients with cystic fibrosis. *Journal of clinical microbiology* **2013**, *51*, (12), 3975-80.
21. Rose, H.; Baldwin, A.; Dowson, C. G.; Mahenthiralingam, E., Biocide susceptibility of the Burkholderia cepacia complex. *The Journal of antimicrobial chemotherapy* **2009**, *63*, (3), 502-10.
22. Nash, E. F.; Thomas, A.; Whitmill, R.; Rashid, R.; Barker, B.; Rayner, R. J.; Whitehouse, J. L.; Honeybourne, D., "Cepacia syndrome" associated with Burkholderia cepacia (genomovar I) infection in an adolescent with cystic fibrosis. *Pediatric pulmonology* **2010**.
23. Tegos, G. P.; Haynes, M. K.; Schweizer, H. P., Dissecting novel virulent determinants in the Burkholderia cepacia complex. *Virulence* **2012**, *3*, (3), 234-7.
24. Sharma, A.; Jansen, R.; Nimtz, M.; Johri, B. N.; Wray, V., Rhamnolipids from the rhizosphere bacterium Pseudomonas sp. GRP(3) that reduces damping-off disease in Chilli and tomato nurseries. *Journal of natural products* **2007**, *70*, (6), 941-7.
25. Das, P.; Mukherjee, S.; Sen, R., Antimicrobial potential of a lipopeptide biosurfactant derived from a marine Bacillus circulans. *Journal of applied microbiology* **2008**, *104*, (6), 1675-84.
26. Das, P.; Yang, X. P.; Ma, L. Z., Analysis of biosurfactants from industrially viable Pseudomonas strain isolated from crude oil suggests how rhamnolipids congeners affect emulsification property and antimicrobial activity. *Frontiers in microbiology* **2014**, *5*, 696.
27. Abdel-Mawgoud, A. M.; Lepine, F.; Deziel, E., Rhamnolipids: diversity of structures, microbial origins and roles. *Applied microbiology and biotechnology* **2010**, *86*, (5), 1323-36.
28. Haba, E.; Pinazo, A.; Jauregui, O.; Espuny, M. J.; Infante, M. R.; Manresa, A., Physicochemical characterization and antimicrobial properties of rhamnolipids produced by Pseudomonas aeruginosa 47T2 NCBIM 40044. *Biotechnology and bioengineering* **2003**, *81*, (3), 316-22.
29. Benincasa, M.; Abalos, A.; Oliveira, I.; Manresa, A., Chemical structure, surface properties and biological activities of the biosurfactant produced by Pseudomonas aeruginosa LBI from soapstock. *Antonie van Leeuwenhoek* **2004**, *85*, (1), 1-8.
30. Haba, E.; Bouhdid, S.; Torrego-Solana, N.; Marques, A. M.; Espuny, M. J.; Garcia-Celma, M. J.; Manresa, A., Rhamnolipids as emulsifying agents for essential oil formulations: antimicrobial effect against Candida albicans and methicillin-resistant Staphylococcus aureus. *International journal of pharmaceutics* **2014**, *476*, (1-2), 134-41.
31. Sotirova, A. V.; Spasova, D. I.; Galabova, D. N.; Karpenko, E.; Shulga, A., Rhamnolipid-biosurfactant permeabilizing effects on gram-positive and gram-negative bacterial strains. *Current microbiology* **2008**, *56*, (6), 639-44.
32. Williams, J. G.; Kubelik, A. R.; Livak, K. J.; Rafalski, J. A.; Tingey, S. V., DNA polymorphisms amplified by arbitrary primers are useful as genetic markers. *Nucleic acids research* **1990**, *18*, (22), 6531-5.
33. Welsh, J.; McClelland, M., Fingerprinting genomes using PCR with arbitrary primers. *Nucleic acids research* **1990**, *18*, (24), 7213-8.

34. Mori, E.; Lio, P.; Daly, S.; Damiani, G.; Perito, B.; Fani, R., Molecular nature of RAPD markers from *Haemophilus influenzae* Rd genome. *Research in microbiology* **1999**, *150*, (2), 83-93.
35. Grifoni, A.; Bazzicalupo, M.; Di Serio, C.; Fancelli, S.; Fani, R., Identification of *Azospirillum* strains by restriction fragment length polymorphism of the 16S rDNA and of the histidine operon. *FEMS microbiology letters* **1995**, *127*, (1-2), 85-91.
36. Sanger, F.; Nicklen, S.; Coulson, A. R., DNA sequencing with chain-terminating inhibitors. *Proceedings of the National Academy of Sciences of the United States of America* **1977**, *74*, (12), 5463-7.
37. Altschul, S. F.; Madden, T. L.; Schaffer, A. A.; Zhang, J.; Zhang, Z.; Miller, W.; Lipman, D. J., Gapped BLAST and PSI-BLAST: a new generation of protein database search programs. *Nucleic acids research* **1997**, *25*, (17), 3389-402.
38. Thompson, J. D.; Higgins, D. G.; Gibson, T. J., CLUSTAL W: improving the sensitivity of progressive multiple sequence alignment through sequence weighting, position-specific gap penalties and weight matrix choice. *Nucleic acids research* **1994**, *22*, (22), 4673-80.
39. Saitou, N.; Nei, M., The neighbor-joining method: a new method for reconstructing phylogenetic trees. *Molecular biology and evolution* **1987**, *4*, (4), 406-25.
40. Kimura, M., A simple method for estimating evolutionary rates of base substitutions through comparative studies of nucleotide sequences. *Journal of molecular evolution* **1980**, *16*, (2), 111-20.
41. Felsenstein, J., Confidence Limits on Phylogenies: An Approach Using the Bootstrap. *Evolution* **1985**, *39*, (4), 783-791.
42. Bharali, P.; Saikia, J. P.; Ray, A.; Konwar, B. K., Rhamnolipid (RL) from *Pseudomonas aeruginosa* OBP1: a novel chemotaxis and antibacterial agent. *Colloids and surfaces. B, Biointerfaces* **2013**, *103*, 502-9.
43. Dobler, L.; Vilela, L. F.; Almeida, R. V.; Neves, B. C., Rhamnolipids in perspective: gene regulatory pathways, metabolic engineering, production and technological forecasting. *New biotechnology* **2016**, *33*, (1), 123-35.